MODELING AND EVALUATION OF TRACTOR WHEEL TRAFFIC COMPACTION EFFECT ON SUBSOILING DRAFT IN THE AGRICULTURAL FARM OF EGERTON UNIVERSITY, KENYA

SAMUEL OTIENO ABICH

A Thesis Submitted to the Graduate School in Partial Fulfilment of the Requirements for the Doctor of Philosophy Degree in Agricultural Engineering of Egerton University

EGERTON UNIVERSITY

OCTOBER, 2023

DECLARATION AND RECOMMENDATION

Declaration

I hereby declare that this thesis is my original work and has not been presented to this University or any other for the award of a degree.

Signature.. otienoabich ..... Date.....**19th Sept. 2023**.....

Samuel Otieno Abich, MSc

BD11/22010/18

Recommendation

This thesis has been presented with our recommendation as University supervisors.

Signature..... ..... Date ……**19. 09. 2023**……

Prof. Daudi M. Nyaanga, PhD

Department of Agricultural Engineering,

Egerton University.

Signature..... ..... Date ……**19th September 2023**……

Eng. Prof. Ayub N. Gitau, PhD

Department of Environmental and Biosystems Engineering,

University of Nairobi.

COPY RIGHT

DEDICATION

This work is dedicated to Dorine, Alspencer, Veronica, Marvine, Leshamta and Tatyana.

ACKNOWLEDGEMENTS

I am grateful to God for the gift of life. My sincere gratitude to African Development Bank (AfDB) for the scholarship to undertake my studies and to Egerton University for granting me a tuition fee waiver and a fully paid study leave. I owe the Faculty of Engineering and Technology a huge debt of gratitude for letting me use their laboratories, workshop, and experimental site for my coursework and research.

I sincerely thank Prof. Daudi Nyaanga and Prof. (Eng.) Ayub Gitau, who I had the honor of working with as my research supervisors. Their direction ensured I finished this research thesis on schedule and to a higher standard. Their constant encouragement and availability for consultations is highly appreciated. I am grateful to Prof. Eng. Japheth Onyando, Dr. Samuel Nyakach, Dr. Romulus Okwany and Mr. Aggrey Muyera for technical support.

Finally, may I also express my gratitude to Mr. Boniface Muliro and Mr. Simon Thuku from the Department of Environmental and Biosystems Engineering, University of Nairobi for their guidance during field investigations and to Fredrick Okinda, Edwin Amisi and Samuel Kinyanjui for assistance in conducting laboratory tests.

ABSTRACT

Soil performance is vital for the survival of human civilizations since it ensures provision of food for the human population. Soil compaction has impacted about 45% of agricultural soil and degraded an estimated 83 Mha of agriculture therefore reducing agricultural productivity. The objective of this study was to model and evaluate the compaction effect of tractor wheel traffic on sub soiling draft for soils in the agricultural farm of Egerton University, Kenya. Tractor wheel traffic experiments were conducted on the selected plots with varying levels of compaction. A dynamometer attached to the subsoiling equipment was used to measure the draft requirements during subsoiling. Soil samples were collected at various depths before and after tractor wheel passes and analyzed for physical properties (bulk density, moisture content, porosity, infiltration rate and saturated hydraulic conductivity) and mechanical properties (penetration resistance, cohesion, angle of internal friction and shear strength) were determined. The study employed a factorial experiment with a Completely Random Block design to look at the effects of five wheel passes (1, 2, 3, 4, 5) on soil properties at depths of 0 - 20, 20 - 30, and 30 - 40 cm with three replications. The wheel passes were equivalent to vertical loads of 26, 51, 77, 102 and 128 kN respectively. Increasing the number of wheel passes and the depth caused a significant increase in the soil's bulk density (from 1256 to 1593 kg m^{-3}), penetration resistance (642 to 1539 kPa), strength (121.20 to 156.97 kPa), internal angle of friction (29 to 35^o), and cohesion (6.84 to 8.42 kPa), while decreasing the moisture content (from 41 to 33%), infiltration rate (15.30 to 3.35 mm h^{-1}), porosity (34 to 5%) and saturated hydraulic conductivity (5.63 to 0.54 to mm h^{-1}). The draft requirement for subsoiling increased from 1.40 kN for the no pass at the 0 - 20 cm depth to 10.68 kN for five wheel passes in the 30 – 40 cm depth. Subsoiling draft was modeled as a function of soil depth, bulk density, penetration resistance, shear strength, angle of internal friction and cohesion. The R^2 for Multiple Linear Regression (MLR), Dimensional Analysis, Adaptive Neuro Fuzzy Inference System (ANFIS) and Artificial Neural Networks (ANN) were 0.9838, 0.8722, 0.9999 and 0.9941 respectively. The t-test revealed that there was no significand difference between the measured and predicted draft for the MLR (t = 0.13), Dimensional Analysis (t = 0.15), the ANN (t = 0.12) and ANFIS (t = 0.19) models. Conclusions of this study emphasize the significant influence of tractor wheel passes on soil properties and draft requirements. Recommendations include the promotion of optimized subsoiling strategies. This research contributes to promoting sustainable agricultural practices and soil management strategies.

TABLE OF CONTENTS

LIST OF FIGURES

LIST OF TABLES

LIST OF ABBREVIATIONS AND ACRONYMS

ANN	Artificial Neural Networks
ANFIS	Adaptive Neuro Fuzzy Inference System
ANOVA	Analysis Of Variance
ASABE	American Society of Agricultural and Biological Engineers
CFD	Computational Fluid Dynamics
CTF	Controlled Traffic Farming
DEM	Discrete Element Method
df	Degrees of Freedom
FEM	Finite Element Methods
FIS	Fuzzy Inference System
FL	Fuzzy Logic
GPS	Global Positioning System
LOM	Largest Of Maxima
LSD	Least Significant Difference
MAE	Mean Absolute Error
MAPE	Mean Absolute Percentage Error
MAX	Maximum
MF	Membership Function
MIN	Minimum
MLR	Multiple Linear Regressions
MOM	Mean of Maxima
RMSE	Root Mean Square Error
RTF	Random Traffic Farming
SOM	Smallest Of Maxima
SPH	Smoothed Particle Hydrodynamics
p	*p* value
MSS	Mean Sums od Squares
TSK	Takagi-Sugeno-Kang
UN	United Nations

LIST OF SYMBOLS

α	Rake angle (º)
A	Premise of a fuzzy rule
A_0	Tool surface area (m^2)
β	tool tilt angle (º)
$\beta_0, \beta_1, \beta_2, \beta_n$	Regression constants
ε	Error term of a model
ϕ	Angle of soil internal friction (º)
ρ	Density (kg m^{-3}).
δ	Soil-metal friction angle
σ	Shear strength (kPa)
B	Consequent parts of a fuzzy rule
C	Cohesion (kPa)
C_a	Adhesion strength (kPa)
d	Tillage depth (m)
F	Draft force (kN)
FC	Fuel consumption (l h^{-1})
f_n	Transfer function
F_t	Implement draft due to preceding traffic (kN)
F_r	Rolling resistance (N)
g	Acceleration due to gravity (m s^{-2})
m	Mass of implement (kg)
N	Normal force (N)
P	Penetration resistance (kPa)
p, q, r, s	Constants
R_f	Tractor front wheel reaction (N)
R_r	Rear wheel reaction (N)
S	Wheel slip (%)
T_d	Unloaded overall tyre diameter (m)
T_p	Implement draft with no traffic (kN)
T_w	Width of unloaded tyre section (m)

v	Operation speed (m s^{-1})
v_c	Volume of the soil cores
w_{ij}	The connection weight between node i and j
w	Width of cut (m)
w_d	Dynamic wheel load (N)
w_{ik}	Connection weight between i^{th} layer of input and k^{th} neuron of hidden layer
x_1	Perpendicular distance from the rear axle of a tractor to its centre of gravity
x_2	Wheelbase
X	Input
$x_{1\ldots..}\ x_n$	Independent variables
Y	Predicted value of output

CHAPTER ONE
INTRODUCTION

1.1 Background to the study

Soil performance is vital for the survival of human civilizations since it ensures provision of food for the human population, as well as feed and fodder for animals (Hillel, 2009, Songül, 2021). Soil compaction is a cause of productive agriculture degradation. It has impacted about 45% of agricultural soil and degraded an estimated 83 Mha of the soil (Brus & van den Akker, 2018). Since soil degradation is rapid and its regeneration slow, it is important to use the soil sustainably in dealing with the problems of food security, energy demand, biodiversity and climate change (Grigorev et al., 2020; Lal, 2009; Nawaz et al., 2013). Soil compaction is the process of densification of the soil and distortion of the soil structure which results in deterioration or loss of the functions of the soil (Yang et al., 2022). Compaction of soil modifies structure of the soil irreversibly (Pagliai et al. 2003; Shaheb et al., 2021), affects ecological functions of soil (Seehusen et al., 2014), decreases aeration and leads to higher emissions of nitrous oxide and methane gas from the soil (Batey, 2009; Bengough et. al, 2011).

Soils that are compacted have high bulk density and strength, few macro pores and a high tortuosity causing low water infiltration rate and hydraulic conductivity (Yang et al., 2022). These in turn increases the risks of run off, erosion and temporal water logging (Keller et al., 2013). Compacted soils limit crop development and soil nutrient uptake because they prevent root elongation and growth, which results in lower yield (Horn, 2015; Martínez et al., 2008; Yang et al., 2022). Van Camp et al. (2004) noted that soil compaction is a global threat that requires attention.

According to Kremers and Boosten (2018), compaction affects the soil to depths of about 0.75 m. By crushing the soil aggregates and combining them into large units, soil compaction affects the soil structure and increases the soil bulk density and penetration resistance (Shaheb et al., 2021). Compaction affects soil nitrogen and carbon cycling, soil water dynamics, crop growth and cultivation draft requirements (Songül, 2021).

A variability of factors affects the magnitude of compaction of the soil and its distribution within the soil mass therefore making it a complex phenomenon (Rodriguez et al., 2012). Since soil compaction occurs below the surface, it is a challenge to find. Soil compaction occurs in

conventional and no-tillage systems due to forces of compression applied by machinery wheels to soil (Garcia-Tomillo et al., 2018).

For conventional tillage, Kroulik et al. (2011) demonstrated that at least one wheel pass tracked 85% of a field. The compacted soil can recover within two years after the first wheel pass if no further impacts are exerted. Subsequent wheel passes will induce additional soil compaction. At the moment complete avoidance of machinery use, and therefore wheel traffic, is not possible since very few farm operations can be undertaken without use of machines (Shaheb et al., 2021).

Because of increased mechanization of tillage operations to meet food demand, agricultural traffic causes the majority of soil compaction (Seehusen et al., 2014; Songül, 2021). The compaction of soil due to wheel passes depend on the spread of vibrations in the soil, soil shear forces and the tyre pressure (Grigorev et al., 2020). Wheel traffic increases soil strength, resulting in higher tillage draft requirement (Keller et al., 2004). The higher energy consumption in primary tillage is aggravated by the rapidly escalating fuel cost leading to higher cost of production to the farmer (Raper & Bergtold, 2007).

Subsoiling can help to alleviate soil compaction. However, the alleviation of soil compaction using this method is energy consuming. Although many studies have been undertaken on soil compaction, not much has been documented on subsoiling draft requirements and prediction for silt loam soils in Kenya. This study modeled subsoiling draft in a silt loam soil using four modeling approaches of Dimensional Analysis, Artificial Neural Networks (ANN), Multiple Linear Regression (MLR) and Adaptive Neuro-Fuzzy Inference System (ANFIS). These modeling techniques were chosen because MLR is a simple linear modeling technique, Dimensional Analysis offers a theoretical framework, ANFIS combines neural networks and fuzzy logic for nonlinearity and interpretability, while ANN excels in capturing complex relationships.

1.2 Statement of the problem

In modern agricultural practices, the use of heavy machinery, particularly tractors, is essential for efficient soil preparation and cultivation. However, the repeated passage of tractor wheels over agricultural fields can lead to compaction of the soil, resulting in altered soil properties such as increased bulk density, cone index, moisture content, and changes in soil strength, cohesion, and

angle of internal friction. This compaction, in turn, affects the draft requirements for subsoiling operations, crucial for soil improvement and crop growth.

Despite the evident significance of wheel traffic compaction in agricultural operations, there is a notable gap in comprehensive modeling approaches that quantitatively assess the complex interplay between wheel traffic, soil properties, and subsoiling draft requirements. Consequently, there was a need to investigate and model the effects of tractor wheel passes on soil properties, elucidate the impact of varying levels of wheel traffic compaction on the draft requirement for subsoiling, and develop predictive models that could accurately estimate subsoiler draft requirements based on soil properties.

This research aimed to fill this gap by employing multiple modeling techniques, including Multiple Linear Regression, Dimensional Analysis, Artificial Neural Networks (ANN), and Adaptive Neuro-Fuzzy Inference Systems (ANFIS), to provide a holistic understanding of how wheel traffic compaction influences the tillage draft required for subsoiling in silt loam soils. By doing so, this study intends to contribute valuable insights to optimize agricultural practices, enhance soil health, and increase crop productivity while minimizing energy consumption and environmental impact.

1.3 Objectives

The broad objective of this study was to model and evaluate the compaction effect of tractor wheel traffic on sub soiling draft for soils in the agricultural farm of Egerton University, Kenya

1.3.1 Specific objectives

The specific objectives of the study were to:

i. Evaluate the effect of tractor wheel passes on soil physical and mechanical properties;
ii. Determine how different levels of wheel traffic compaction affect draft requirement for subsoiling;
iii. Model subsoiler draft requirements based on selected soil properties using MLR, Dimensional Analysis, ANFIS and ANN modeling techniques.

1.3.2 Research questions

The research questions were:

i. How do the soil physical and mechanical properties change due to wheel traffic compaction?
ii. How does the draft requirement for subsoiling equipment change with varying levels of wheel traffic compaction?
iii. How does the prediction accuracy of the MLR, Dimensional Analysis, ANFIS and ANN subsoiling daft models compare?

1.4 Justification

Soil compaction induced by tractor wheel passes not only reduces soil quality but also diminishes crop yields. By rigorously assessing the effect of wheel traffic on soil physical and mechanical properties, this research sought to unveil the intricacies of soil behavior under compaction. In doing so, it contributes directly to sustainable soil management, aiding in the preservation of this finite and essential resource for future generations.

Moreover, the study's exploration of how varying levels of wheel traffic compaction impact the draft requirements for subsoiling is invaluable to both farmers and agricultural practitioners. With knowledge of how compaction affects draft needs, they can optimize their tillage practices, saving on fuel costs, and reducing the environmental footprint of farming operations. This efficiency is not just economically advantageous but also aligns with the global call for responsible resource utilization.

The study employs various modeling techniques such as Multiple Linear Regression (MLR), Dimensional Analysis, Artificial Neural Networks (ANN), and Adaptive Neuro-Fuzzy Inference Systems (ANFIS). These modeling approaches are widely applicable in agricultural research and can potentially be adapted for optimization problems.

Beneficiaries of this study encompass a diverse spectrum of stakeholders. Farmers stand to gain through enhanced knowledge and practices that can augment crop productivity and financial returns. Agricultural researchers will find a valuable foundation for further exploration in soil science, while agricultural machinery manufacturers can innovate equipment tailored to address compaction challenges. Environmentalists and policymakers can leverage the study's insights to advocate for sustainable agricultural policies, safeguarding both soil health and the environment.

This study contributes to SDG 2 by aiming to optimize agricultural practices through better understanding of soil compaction. By improving subsoiling techniques, it can help increase agricultural productivity, reduce soil degradation, and ultimately contribute to food security. By modeling and evaluating the compaction effect of tractor wheel traffic on subsoiling draft, the study supports sustainable and efficient agricultural production practices of SDG 12. It helps reduce unnecessary resource consumption, such as fuel and machinery wear and tear, aligning with the principles of responsible production and consumption.

Reducing unnecessary tractor wheel traffic and optimizing draft requirements for subsoiling can lead to lower greenhouse gas emissions. The study promotes climate-resilient agricultural practices, aligning with the objectives of SDG 13. In line with SDG 9, the study's use of advanced modeling techniques (ANFIS, and ANN) reflects innovation in agricultural research and infrastructure development. These techniques can lead to more efficient machinery and improved farming practices (UN, 2015).

1.5 Scope and limitation

1.5.1 Scope

The research sought to evaluate the effect of wheel traffic on soil bulk density, cone index (penetration resistance), shear stress, saturated hydraulic conductivity, infiltration rate, angle of internal friction and cohesion on the topsoil to a depth of 40 cm The effects on soil biological and chemical properties were not considered. The changes in soil conditions resulting from wheel traffic application were limited to the time between application of wheel traffic and immediately after. This study did not take into account how tillage type, or tire pressure affected soil compaction, and this can be considered for further work.

1.5.2 Limitations

The tractor used in this study was a Massey Ferguson Extra 455. The experiments were performed on a silt loam soil with moisture content ranging between 33% and 41% dry basis. The sampling depth was limited to the top 40 cm of soil. The modeling techniques analyzed were Multiple Linear Regression, Dimensional Analysis, Artificial Neural Networks and Adaptive Neuro Fuzzy Inference System.

1.6 Definition of terms

Adaptive neuro-fuzzy inference system: This is a kind of artificial neural network that is based on Takagi–Sugeno fuzzy inference system.

Analysis of Variance Is a statistical method used to test differences between two or more means.

Angle of internal friction (friction angle): This is measurement of the soil's capacity to endure shear stress. When failure only results from a shearing stress (σ), the angle (φ), measured between the normal force and resultant force, is obtained.

Artificial neural network: This is a computing system created to mimic how the human brain processes and evaluates data, handles issues that, by statistical criteria, would be deemed intractable or challenging.

Bulk density: This is the proportion of the soil's dry bulk to its overall volume.

Cohesion: This is the soil's shear strength at zero compressive loads.

Conceptual framework: This is a textual or visual depiction of a relationship between variables that is anticipated.

Data analysis: This is the procedure for cleansing, converting, and modeling data in order to draw out relevant information and make decisions based on the data analysis.

Defuzzification: In this method, a single number is extracted from the output of the aggregated fuzzy set. It is used to convert the outcome of a fuzzy inference into a clear output

Dimensional analysis: Dimensional analysis is a mathematical technique used in physics and engineering to analyze and simplify complex physical problems by examining the relationships between the various physical quantities involved. It is particularly useful for understanding the fundamental principles governing physical systems, scaling laws, and the behavior of systems under different conditions without having to solve detailed equations.

Discrete element method: s a numerical technique used for simulating and analyzing the behavior of granular materials, particles, and discrete objects in various physical and engineering systems.

Unlike continuous methods like the Finite Element Method (FEM), DEM treats the materials or particles as distinct entities with individual properties and interactions.

Draft: This is the force necessary to move an object in the desired direction.

Finite element method: This is a numerical technique used for solving complex engineering and mathematical problems involving physical phenomena like heat transfer, fluid flow, structural mechanics, and electromagnetic interactions. FEM divides a complex system into smaller, simpler subdomains called "finite elements" to approximate the behavior of the entire system.

Fuzzification: Fuzzification is a process in fuzzy logic and fuzzy systems where crisp or precise input data is transformed into fuzzy sets or linguistic variables.

Fuzzy inference system (FIS): A Fuzzy Inference System (FIS) is a computational framework used for modeling and simulating complex systems where traditional binary, crisp logic or numerical methods may not be appropriate due to uncertainty or vagueness in the input data or problem domain.

Fuzzy logic: Fuzzy logic is a branch of artificial intelligence and mathematical logic that deals with reasoning under uncertainty and imprecision.

Generalization: Describes how well a model will perform when faced with novel, unforeseen data that comes from the same distribution as the model's initial data.

Hitch: This is the part of a tool that is used to attach it to a power source.

Iinfiltration rate: This refers to the rate at which water enters the soil surface and moves into the soil profile.

Internal angle of friction (φ): The soil's internal angle of friction is a fundamental geotechnical property that characterizes the shear strength and resistance to sliding or deformation of a soil mass.

Least significant difference: This is the value at a certain degree of statistical probability that is exceeded by the difference between two means.

Linear regression: Linear regression is a statistical method used to model the relationship between a dependent variable (or target) and one or more independent variables (or predictors) by fitting a linear equation to the observed data**.**

Mathematical model: Mathematical modeling is a process used in science, engineering, economics, and social sciences to describe and analyze real-world phenomena using mathematical equations, relationships, and abstract representations.

Mechanical stability of the soil: This reflects the soil's level of deformation resistance.

Modeling: Modeling is the process of creating a simplified representation or abstraction of a real-world system using mathematical, physical, or conceptual techniques.

Model calibration: This is an iterative process where the model is compared to the actual system and modified as necessary until the model is acceptable.

Model validation: This procedure verifies that the model serves the required goal. This entails proving that the model is accurate under the circumstances of its intended use.

Moisture content of soil: This is the proportion of water mass to total mass of solids in a sample.

Multiple linear regression: This is a statistical technique that uses several explanatory variables to predict the outcome of a response variable.

Operating width: This is the horizontal range within which an implement functions as intended, measured perpendicular to the direction of motion.

Penetration resistance: This soil penetration resistance, also known as soil compaction resistance or soil cone index, is a measure of the resistance or force required to penetrate a probe or cone into the soil at a specific depth.

Pi theorem: The pi- theorem asserts that if there are n variables that can be defined in terms of m dimensional units, then they may be combined in $(n - m)$ dimensionless terms known as π-*terms*.

Porosity: Soil porosity refers to the volume of pore space or voids within a soil mass relative to its total volume.

Rake Angle: This is a forward angle formed by the tool's face and the horizontal soil surface.

Saturated hydraulic conductivity: This is a measurement of how well a saturated soil transmits water under a hydraulic gradient.

Shear strength: This is a measurement of the soil's resistance to deformation caused by the continual movement of individual soil particles.

Soil biodiversity: Soil biodiversity refers to the variety and abundance of living organisms in the soil, including bacteria, fungi, protozoa, nematodes, earthworms, arthropods, and other microorganisms and macroorganisms.

Soil compaction: Soil compaction is the process of increasing the density and reducing the volume of soil through the application of mechanical energy.

Soil failure: Soil failure refers to the condition where soil loses its ability to support an applied load or external forces, leading to deformation, settlement, or even collapse.

Soil hydrological properties: Soil hydrological properties refer to a set of physical characteristics of soil that influence its ability to retain, transmit, and manage water.

Soil mechanical properties Soil mechanical properties refer to the physical characteristics of soil that relate to its behavior under applied forces or loads.

Soil physical properties: Soil physical properties are the characteristics of soil related to its physical structure and composition.

Soil strength: This refers to a soil's capacity to withstand an applied force.

Soil-tool geometry: This refers to the relationship between the shape, design, and characteristics of a soil cultivation tool and how it interacts with the soil during various agricultural operations.

Specific draft: This is the draft force in a tilled cross section per unit of area.

Student's *t*-test: The t-test is a statistical hypothesis test that is used to determine whether there is a significant difference between the means of two groups or samples.

Sub-soiling: Sub-soiling is a farming practice that involves loosening or breaking up the soil in the lower layers of the ground, typically below the depth of normal plowing or cultivation. This is done to alleviate soil compaction, improve soil aeration, and promote better root growth for crops

Tillage depth: This is the vertical distance between the tool's point of penetration and the soil's surface.

Tillage: This involves mechanically modifying the soil's properties to improve crop output.

Tool width: This is the largest horizontal tool projection, measured perpendicular to the tool's direction of action, into the ground.

Transfer function: This mathematical function hypothetically simulates the outcome of the system for each potential input.

Variance: This is statistical analysis of the variation in numbers within a data collection.

CHAPTER TWO
LITERATURE REVIEW

2.1 Soil compaction

The global population is rapidly increasing, and it is expected to reach 9 600 million by 2050. This will lead to increased demand for food leading to the challenge of sustainable agricultural production, minimizing environmental damage, and ensuring nutrition and food security. The development and utilization of agricultural machinery has transformed food output and sustainability (Shaheb et al., 2021).

The performance of multiple field operations like cultivation, spraying, planting, and harvesting require varying load demands from farm machinery (Pitla et al., 2016). Soil compaction is defined as a decrease in total and air-filled porosity that occurs because of soil densification and distortion, which damages or eliminates one or more soil functions (Liu et al., 2022). The additional weight of these machines causes greater wheel loads, which increases the danger of soil compaction (Chamen, 2015; Chamen et al., 2015; Głąb, 2014; Keller et al., 2019; Van den Akker, 2008; Van den Akker & Schjønning, 2004). In addition, new methods of tillage and implements for farm operations have increased tillage draft needs (Zadeh, 2006). Soil compaction is a concern for many countries around the globe (Jones et al., 2003).

Soil compaction affects about 68,000,000 ha of soils worldwide (Nawaz et al., 2013) with The European Union reporting that it has affected 32% of soils in Europe. Given its invisible nature, there is a possibility of soil compaction affecting greater area than is documented. There is a likelihood of further increase in the damage to the soils of developing countries by soil compaction (Jones et al., 2003).

Soil compaction occurs when the tension applied to the soil exceeds the soil strength, according to (Keller et al. 2019). These forces are distributed to various soil depths via the footprint formed by the earth and tyre (Figure 2.1). Compaction has environmental and agronomic consequences. It rearranges soil grains decreasing void spaces and increasing bulk density. This procedure is accompanied by the removal of soil air and the densification of the soil (Defossez & Richard, 2002).

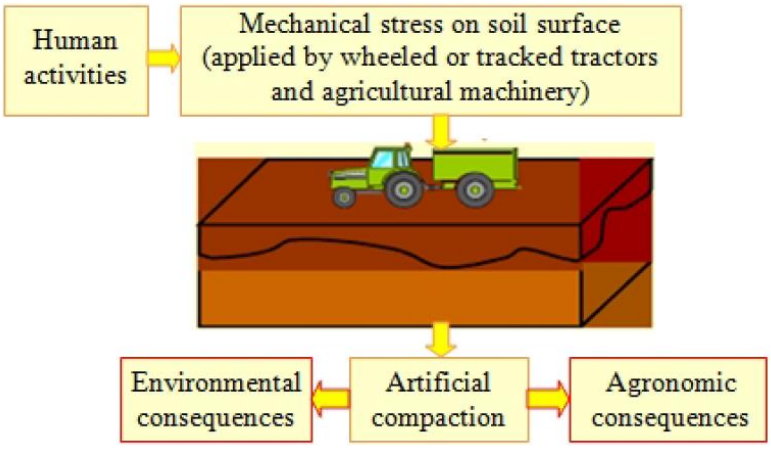

Figure 2.1: Basic mechanism of soil compaction

Compaction degrades land and impacts adversely on the environment and agronomic productivity (Barbero-Sierra et al., 2015; Pagliai et al., 2003) and is a cause of erosion and flooding (Keller, 2004). Therefore, remedying soil compaction will lead to enhanced sustainable use of soils for food security (Berisso et al., 2013; Chamen et al., 2015; Nawaz et al., 2013).

2.2 Compaction effect of tractor wheel traffic intensity on physical and mechanical properties of soil

The susceptibility of a soil to compaction is dependent on soil structure, texture, water content and organic matter. Compaction is more likely in soils with a weak structure and a greater clay concentration (Nawaz et al., 2013; Schjønning et al., 2015). It is dependent on interaction of machine, soil-water status, soil structure and organic matter content (McGarry, 2001). Climate, soil type, farm management practices, crop type and agricultural machinery influence soil compaction (Tenu et al., 2012). The type of equipment, wheel passes, tyre pressure, axle load and soil-tyre interaction affect the degree of soil compaction (Berisso et al., 2012, Chamen, 2017).

Compaction can be caused by soil consolidation or external pressure applied to the soil, as well as by human-induced factors (machineries, tillage practice and livestock trampling) or natural causes (tree root and precipitation). Natural causes of soil compaction are less harmful in comparison to anthropogenic causes (Nawaz et al., 2012).

2.2.1 Repeated tillage at same depth

Crusting is caused by tillage that breaks down the soil aggregates on the soil surface. However, repeated tillage orients soil particles in the same direction causing a layer of compacted soil to form beneath the tilled area. On the other hand, hardpan occurs just below the tillage depth due to repeated cultivation at the same depth (Nawaz et al., 2012). This is because the weight of the tillage implements causes soil contact between the soil and the tool to compress and smear. Tillage pan can therefore be eased by altering tillage ploughing depth across seasons (Hamza & Anderson, 2005).

2.2.2 Soil moisture content

The stability of soil aggregates and their tensile strength is determined by soil moisture content. Whereas dry soil particles are tightly bound, water loosens these bonds (Hillel, 2003; Nawaz et al., 2013). According to Hamza and Anderson (2002), increased soil moisture content lowered the load bearing capacity of the soil and caused compaction to penetrate further into the soil profile. It has also been reported that moisture increases soil deformation (Hakansson & Lipiec, 2000). Drier soils have low stress transformation, and their structure is deformed less (Batey, 2009).

When soil moisture content is increased, soil compaction increases up to an optimum water content above which soil compaction decreases with increased moisture content under a given load. Also, as traffic frequency reduces, soil compaction diminishes more quickly in a dry soil than it does in a wet one (Hamza & Anderson, 2005).

Soil moisture content influences penetration resistance and soil susceptibility to compaction (Lipiec et al., 2002). Shah et al. (2017) reported a smaller difference in soil resistance between uncompacted and compacted soils at high moisture content. Therefore, soil moisture is an important consideration when scheduling farm operations to minimize compaction.

2.2.3 Mechanized operations

Tillage is done to optimize germination conditions, seedling establishment, crop growth (Sahay, 2008) and to improve soil hydro-physical properties (Gachene & Kimaru, 2003). The use of tractors to reduce drudgery in farm operations causes soil compaction (Agele et al., 2016). The use of heavy machinery in tillage has been reported to induce subsoil compaction (Mosaddeghi et al., 2000). Tullberg (2000) observed that over 30% of zero tillage systems is trafficked by the tyres.

Trafficking exposes the soil to surface loads that destroy soil structure (Lamande & Schjonning, 2011). Traffic intensity affects the extent of soil compaction (Mujdeci et al., 2017) and result compaction along the wheel tracks and on the headlands (Balbuena et al., 2000).

Soil strength is determined by soil parameters, but soil stress is determined by wheel load, the number of wheel passes, wheel size, and tyre inflation pressure (Horn et al., 2003; Keller & Arvindson, 2004; Lamandé et al., 2007). Figure 2.2 presents the factors that influence wheel traffic compaction.

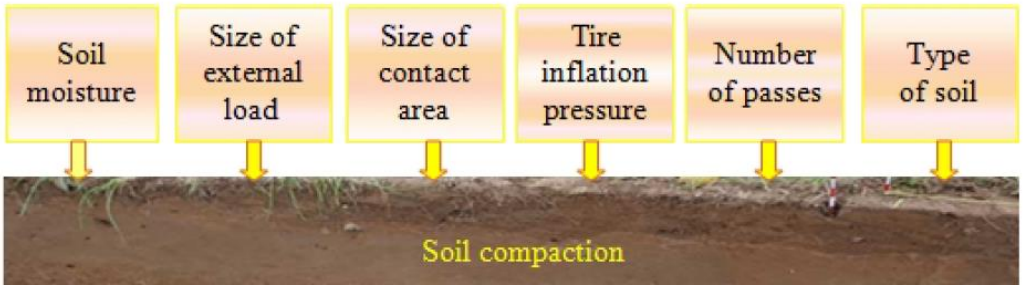

Figure 2.2: Factors that influence the machine induced soil compaction (Keller & Arvindson, 2004)

Different studies have reported that wheel load influence subsoil compaction, while and inflation pressure and tyre contact area affect the topsoil (Botta et al., 2009). Therefore, wheel traffic intensity can be defined by wheel load and the number of wheel passes (Augustin et al., 2020).

As illustrated in Figure 2.3, the depth of stress distribution and the volume of soil impacted by compaction increase for the same vehicle as the number of passes on the same track rises.Wheel load influences stress transmission to lower soil layers (Berisso et al., 2012).

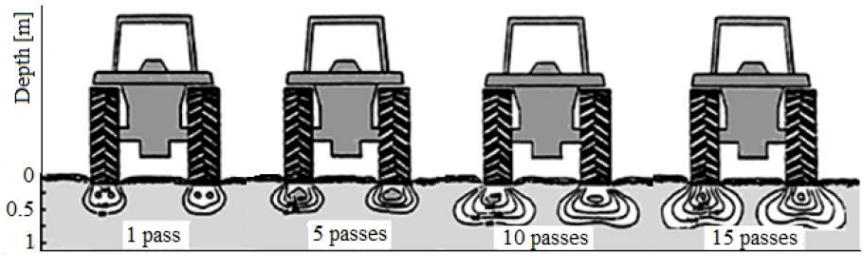

Figure 2.3: Distribution of stress in soil depth as affected by wheel passes (Duiker, 2004)

Soil structure and texture (Jones et al., 2003), soil moisture content (Yavuzcan et al., 2005), speed of the tractor, dynamic load of compressing wheel (Aksakal & Oztaş, 2010; Javadi & Spoor, 2006), and number of tractors passes (Botta et al., 2006) affect the severity of soil compaction. Hakansson and Lipiec (2000) reported that the number of passes of agricultural machinery increased the deformation on the soil. Botta et al. (2009) observed that soil compaction is increased by repeated passes of agricultural machinery over the same location.

The bulk density increased to a depth of 15 cm due to equipment usage, according to Balbuena et al. (2000), who also noted penetration resistance increases of 16 to 76% in the first 0.40 m of the surface layer. Yet in a case including grassland, there were no discernible differences between the impacts of heavy and light loads on the topsoil.

The consequences of soil compaction are particularly noticeable in turning lanes and tyre tracks, as well as on top soil (Balbuena et al., 2000). The soil vulnerability to compaction is reported to be due to an interaction of soil physical properties and tractor wheel passes (Hamza & Anderson 2005; Shah et al., 2017). According to Duiker (2004), the first pass of a wheel does the most compaction with studies showing that the first pass accounts for around 75% of the increase in soil density and 90% of wheel sinking.

Topsoil compaction occurs within the cultivated horizon while subsoil compaction occurs below the cultivated horizon (Botta et al., 2002). High wheel loads of agricultural machines induce high pressure to the ground (Shah et al., 2017) and damage the structure of soil (Defossez & Richard, 2002). Wheel loads exert pressure vertically in course textured soils while transmission is multidirectional in soils with fine textures (Smith et al. 2000).

The front wheel reaction can be determined using the equation:

$$R_f = mg\frac{X_2}{X_1} \tag{2.1}$$

where R_f is the front wheel reaction (N);

g is acceleration due to gravity (m s^{-2});

m is mass of the tractor (kg);

X_1 is perpendicular distance from the rear axle to the centre of gravity (m);

X_2 is the wheelbase (m).

The rear wheel reaction is given by:

$$R_r = mg - R_f \quad (2.2)$$

where R_r is the rear wheel reaction (N);

R_f is the front wheel reaction (N).

In comparison to a tractor with more wheels, a tractor with fewer wheels puts more pressure on the ground. Therefore single-tyre farm implements cause greater compaction compared to multi-tyre farm machines (Shah et al., 2017; Schäfer-Landefeld et al. 2004). Studies have shown that for the same axle load, single tyres have more impact on subsoil compaction compared to dual tyre (Hamza & Anderson, 2005).

Soil-tyre interaction is influenced by dynamic axle load, tyre geometry, lug design, tyre type, and inflation pressure (Defossez & Richard, 2002). Due to tyre stiffness, tire inflation pressure controls the amount of soil compaction (Saffih-Hdadi et al., 2009). Pytka (2005) reported that soil-tyre interface pressure and rutting effect were altered by lowering inflation pressure.

It was observed that the first wheel pass induced compaction to a greater degree compared to subsequent passes (Hamza & Anderson, 2005). Botta et al. (2006) observed that many passes of a 1 Mg wheel load tractor prevented seedling emergence in a direct drilled topsoil. Compaction effects reached 0.6 m deep in the soil profile with 10 to 12 passes of this tractor.

2.3 Consequences of soil compaction

2.3.1 Soil physical and hydrological properties

The kind of soil determines how soil compaction affects soil functions. Sandy soils are less susceptible to soil compaction because they have larger soil particles and larger pores. In contrast, silt clay loam soils have small particles making them more susceptible to compaction especially when moist (Hargreaves et al., 2019).

The capacity and intensity of the soil characteristics are used to quantify the impact of soil compaction. The composition of a certain volume of soil is defined by a capacity parameter, but its internal structure or functions are not. Examples of capacity parameters are bulk density, pore size distribution, grain size distribution, plant available water capacity and texture (Horn & Kutilek, 2009).

Intensity parameters define dynamic elements over space and time and the measurement of the processes within the soil. These parameters include hydraulic conductivity, air permeability, soil strength, as well as the pore continuity (Bergamin et al., 2015; Horn & Kutilek, 2009; Sahu & Raheman, 2006). Depending on crop yield, parameters used to detect adverse changes of the soil can have high or low indication. Parameters with low indication include penetration resistance, bulk density, and shear resistance. On the other hand, air capacity, saturated hydraulic conductivity and infiltration have high indication on crop yield (Horn & Fleige, 2009).

The soil's capacity to support plant and animal life and preserve the quality of the water depends on its quality (Bergamin et al., 2015). Penetration resistance, bulk density, shear resistance, infiltration rate, air capacity and saturated hydraulic conductivity are used as indicators of soil quality. Indicators of soil compaction include soil strength, moisture content (Hamza & Anderson, 2005), plant growth, and yield (Batey, 2009).

Lipiec et al. (2003) reported that the spatial variability of compaction is higher in topsoil and plough pans than in sub soils, in pastures than in cropped soils, and for permeability than for bulk density. For this reason, Alaoui et al. (2011) cautioned that it is useful to express compaction effects relative to reference levels to assess the compaction severity for a given soil. Studies on soil compaction therefore require many replicates before valid conclusions can be drawn (Ball et al., 2016; Batey, 2009; Ewetola et al., 2022; Keller, 2004).

a) **Bulk density**

Bulk density is defined as the ratio of the dried weight of the soil to its total volume (Han et al., 2016; Naghdi & Solgi, 2014) and is given by:

$$\text{Bulk density, } \rho = \frac{W_d}{V_c} \tag{2.3}$$

where w_d is mass of the dry soil (kg);

v_c is volume of the soil cores (m^{-3}).

Bulk density of soil is correlated to other soil biological, chemical and physical properties (Gao et al., 2016). It indicates soil porosity (Casanova et al., 2016) and provides information on soil stress

and soil penetration resistance (Al-Shammary & Al-Sadoon, 2014). The bulk density of a soil can be used to evaluate how susceptible it is to compaction (McGarry, 2001).

Erbach (2006) observed that bulk density of agricultural soils varied between 9000 and 1800 Kg m^{-3}. Soils with bulk densities above 1400 kg m^{-3} can withstand compaction (Powers et al., 2005). Since bulk densities of volcanic soils are less than 1000 kg m^{-3}, these soils are susceptible to compaction (Parker, 2007).

The diffusion of oxygen into the soil is restricted by increase in bulk density. According to Tracy et al. (2011) and Batey (2009), soil compaction changes root development, decreases soil nutrient absorption, and diminishes soil hydraulic conductivity.

Because of biotic activity and organic matter, which produce a well-developed crumb structure, soils of forested land have low bulk density in the upper layers (Corti et al., 2002). Agricultural soil compaction appears as widespread or localized compaction that extends below the surface with bulk densities of between 1500 to 1800 kg m^{-3} (Spoor et al., 2003). The overall compaction brought on by the frequent passing of large tractors penetrates deeper, with dry bulk densities between 1900 and 2000 kg m^{-3} (Batey & McKenzie, 2006).

The first pass is responsible for around 75% of the increase in soil density and 90% of wheel sinking (Duiker, 2004). A soil resists further compaction once compacted because of it has more micropores than macropores (Ampoorter et al., 2012). Soil bulk density is increased with increase in wheel passes (Balbuena et al., 2000). Botta et al. (2004) reported that eight wheel passes of a 1400 kg tractor on a fine clay soil increased its bulk density from 1870 to 1970 kg m^{-3} in the depth 0 - 0.60 m.

Ahad et al. (2015) observed a positive relationship between bulk density and soil texture, mineral content and organic matter content. However, a negative relationship with optimum moisture content and porosity was observed. Krebstein et al. (2014) reported that compaction did not have a significant effect on bulk density of sandy loam soil. Ahmadi and Ghaur (2015) observed a change in bulk density of 13% for a clay loam soil when wheel passes were increased from 0 to 4.

A study was conducted by Patel and Mani (2011) on sandy loam soil to determine the effect of wheel passes on compaction. The bulk density increased continuously with frequency of wheel

passes. The highest bulk density of 1.66 Mg m^{-3} was caused by a normal load of 8.40 kN after 16 wheel passes.

A study by Defossez and Richard (2002) determined soil bulk densities of untrafficked and trafficked soil up to 0.60 m deep. The study indicated that bulk densities of non-wheeled area near the top of the soil were 200 kg m–3 less than trafficked area up to 0.25 m deep. These bulk density differences decreased to a depth of 0.45 m where there were no observable differences.

Chan et al. (2010) compared bulk density of soils under random and controlled traffic. They observed the bulk density for random traffic was higher than that for controlled traffic by 7.2% after two years. Between 0.10 and 0.20 m soil layer, random traffic showed higher bulk density than controlled traffic by 8.3%. n the remaining soil layers, there was no discernible difference between the treatments.

Although dry density has been used to quantify soil compaction, Alaoui and Helbling (2005) observed that it is limited when comparing the degree of compaction between different soil types. Alaoui et al. (2011) noted that although bulk density accounted for total soil volume, it did not account for pore distribution or connectivity. Bulk density of gravelly soils is difficult to measure (Webb, 2002). It does not account for shearing and dynamic damages on the pore system (Chamen et al., 2015; Nawaz et al., 2013). Therefore, Lipiec and Hatano (2003) noted that ss a measure of soil compaction, soil bulk density alone is insufficient. They recommended that other soil properties such as moisture content, aeration and strength should equally be assessed.

b) Porosity

Tractor wheel passes on soils result in external physical loading that deforms pores and reduces pore space (Alaoui et al., 2011; Ewetola et al., 2022). Soil porosity may be calculated from particle density and bulk density using the bulk density data according to the formula (Tanveera et al., 2016):

$$\text{Total porosity} = 1 - \frac{\rho_b}{\rho_s} \quad (2.5)$$

where ρ_b is the bulk density (kg m^{-3});

ρ_s is the average particle density (kg m^{-3}).

The volume, size distribution, shape, and connectivity of pores are altered by soil compaction (Keller, 2004; Mossadeghi-Björklund et al., 2016). It fragments and homogenize pores (Alaoui et al., 2011). When soils are compacted, the volume of pore decreases, causing the aggregates to shatter and create smaller inter-aggregate pores. The macropores are destroyed by compaction and become smaller pores (Alaoui & Helbling, 2006; Nawaz et al., 2013). Animal trampling reduces the micropores whereas vehicular traffic affects the macropores and their connectivity (Boivin et al., 2006). Mechanical operations reduce soil porosity (Silva et al., 2008). Soil compaction affects the continuity of burrow networks (Jégou et al.,2002).

Vertical, cylindrical pores offer greater resistance to vertical compression in comparison to horizontal, planar pores (Alaoui et al., 2011; Lipiec et al., 2003). Schwen et al. (2011) observed that compaction distorted connectivity of many macropores thereby reducing hydraulic conductivity. Water retention properties and pore size distribution are altered by compaction (Dexter, 2004; Mossadeghi-Björklund et al., 2016). In coarse-texture soils, macroporosity is texture-dependent, so compaction increases grain-to-grain contacts (Alaoui et al., 2011). Total porosity is less sensitive to compaction than macroporosity (Li & Zhang, 2009). In comparison to soils with horizontal pores, coarse-textured soils with vertical pores are less prone to compaction (Schäffer et al., 2008).

The topsoil has an anisotropic soil pore structure with enlarged pores that are parallel to the ground surface because of machinery wheel passes (Pagliai et al., 2003). Traffic-induced compaction creates structural pores (Alaoui & Helbling, 2006; Dexter et al., 2008; Keller, 2004). Macropores are sensitive to compaction. Increased soil compaction from wheel traffic reduces the volume of the macrospores (Alaoui & Helbling, 2006). A decrease in pore space makes it more difficult for water and air to pass through the soil. Compaction limits root penetration in the soil and decreases the soil's ability to store water (Osunbitan et al., 2005).

Alaoui and Helbling (2006) observed that macropores comprise 0.2 to 2% of the soil volume. Less vertical infiltration due to macropore volume might result in higher surface runoff (Alaoui, 2015). Infiltration may be reduced, nevertheless, if the connection between the top surface and the subsurface macropores is severed (Alaoui, 2015; Jégou et al., 2002).

Ramezani et al. (2017) investigated water flow path in loamy clay soil by comparing five treatments consisting of 0 (no traffic), 1, 3, 4 and 8 passes. According to the study, the number of pores decreased as compaction levels increased. The number of pores was higher when there was no traffic, but it was lower when the tractor made eight runs over the area. The number of big and medium pores was lower after one wheel pass than it was compared to the control treatment by 16.5 and 13%, respectively. In comparison to one wheel pass, Zink et al. (2011) found that the subsurface pore space decreased after ten wheel passes.

c) Soil water content

Moisture content influences tillage soil resistance (Gitau et al., 2006). Tillage is inefficient at reducing soil compaction if soil moisture content is not at its ideal level, and following traffic might result in even more compaction (Spoor, 2006). Increased soil moisture raises the risk of compaction and structural deformation of the soil (Hamza & Anderson, 2005).

The moisture content is determined using the equation below (Nkakini & Vurasi, 2015):

$$w = \frac{m_w - m_d}{m_d} \tag{2.6}$$

where w is moisture content db (%);

m_w is the moist sample's mass (kg);

m_d is the oven-dried soil's mass (kg).

Soil compaction in wet conditions induces soil deformation and therefore affects soil structural characteristics (Zink et al., 2011). In a clay loam soil, Ahmadi and Ghaur (2015) examined the relationship between the amount of wheel traffic and the soil's moisture content. Gradual increase in the moisture content was observed to result in increased soil bulk density.

Dry soils display interlocking, frictional resistance to deformation, and a greater degree of particle-to-particle interaction. Increased soil moisture reduces the frictional forces between soil particles, which lowers the soil's bearing capacity (Han et al., 2006). This renders the soil extremely vulnerable to soil compaction. More pores in a soil with a higher moisture content are filled with water that cannot be crushed (Importer et al., 2012). Rut development results from machine-

induced pressures placed on the soil when the moisture content rises over a specific threshold point (Williamson & Neilsen, 2000).

Odey et al. (2014) examined the impact of tractor wheel traffic on soil moisture content both before and during cropping. One week before to field preparation, the field moisture contents were 11, 12, and 14% (dry basis) at depths of 0 - 0.15 m, 0.16 - 30 m, and 0.31 - 0.45 m, respectively. After six weeks after planting, the average moisture content for harrowed and ploughed plots rose from 15 to 16, and 18% for the corresponding depths.

Compaction decreases water storage and root proliferation (Whitmore et al., 2010). This affects the water use efficiency and the irrigation demands. In a vertisol that had been compacted by a 6000- and 10 000-kg axle load, Radford et al. (2001) examined the water consumption efficiency of maize. In comparison to the 6000 kg axle load, it was found that the 10,000 kg axle load reduced water usage efficiency from 14.3 to 9.7 kg ha^{-1}. According to Chamen (2011), infiltration rose by 84 to 400% in the absence of wheel traffic compaction, increasing the amount of water that is available to plants.

d) Infiltration rate

Water infiltrates much slower in structureless soils than in uncompacted soils (Batey, 2009; Ewetola et al., 2022; Hamza & Anderson, 2003). Traffic intensity negatively affects the soil infiltration (Raper & Kirby, 2006). Chamen (2011) observed that uncompacted soil had five times higher infiltration rate than a compacted one. Higher rates of water infiltration of between 29 and 73% have been reported on untrafficked soils compared to trafficked soil (Chyba, 2012).

Li et al. (2001) compared wheeled and non–wheeled areas in a controlled traffic farming (CTF) experiment using a 4 Mg tractor. Infiltration rates between 50 and 100 mm h^{-1} were observed for noncompacted soils while infiltration rates between 10 and 25 mm h^{-1} were noted for compacted areas. Infiltration rates were reduced by 50 to 90% in compacted soils as compared to non-compacted soil. They concluded that soil compaction had a bigger impact on water infiltration than cultivation.

The mean infiltration rates between 1.32 and 5.70 cm h^{-1} were observed on a loamy sand soil by Chen et al. (2010). The controlled traffic showed higher infiltration ability rate than random traffic

by Al-Ghazal (2002) using five tractor passes **(**0, 2, 4, 6 and 8). The four-pass treatment reduced infiltration rate by 69%, whereas the eight-pass treatment reduced it by 77%.

Chyba et al. (2017) investigated the impact of tractor wheel passes on soil infiltration rate. Infiltration ate was observed to decrease with increase in number of wheel passes from zero to three. The untrafficked soil had a high rate of soil infiltration with a value of 22.43 mm h^{-1}, which decreased by 82% after the first pass. It decreased further by 16% to 0.4 mm h^{-1} after the third pass. Compaction avoidance has been shown to lower flooding risk in wet situations and drought risk in dry ones (Chamen et al., 2015).

e) Saturated hydraulic conductivity

Saturated hydraulic conductivity depicts the movement of water through a saturated soil (Chapuis, 2004). It regulates the rate and course of water transport through wet soil (Horgan & Ball, 2005). The hydraulic conductivity of surface soil layers at saturation governs the partitioning between groundwater recharge and surface runoff (Lin, 2010). Since saturated hydraulic conductivity is connected to soil structure, transport mechanisms, and oxygen diffusion, it is one of the best predictors of physical quality (Lipiec & Hatano, 2003; Van den Akker, 2008).

Saturated hydraulic conductivity can be calculated according to Thuku (2018):

$$K_{sat} = \frac{QL}{At\Delta H} \quad (2.7)$$

Where K_{sat} is the saturated hydraulic conductivity (mm hr^{-1});

Q is water volume flowing out (m^3);

L is length of the soil column (m);

A is the area of cross-section (m^2);

ΔH is difference in head at inlet and outlet (m);

t is time (h).

When the soil pores are filled with water, water moves through the soil in a saturated state; when the bigger soil pores are filled with air, water moves through the soil in an unsaturated state. In dry soils, a vapor movement occurs when vapor moves from a region of high vapor pressure to one of lower vapor pressure (Oluwafemi et al., 2019).

Krebstein et al. (2014) observed a reduction in saturated hydraulic conductivity of 26.6% in the top soil (0 – 0.10 m) and 12.5% in lower layers of the soil (10 – 20 cm) because of compaction, According to Schwen et al. (2011), soil compaction reduces saturated hydraulic conductivity because it distorts the connectivity, structural flow pathways, and hydraulic efficiency of several macropores. Vehicle traffic lowered saturated hydraulic conductivity by nearly three times in a silt loam soil (Blanco-Canqui et al., 2004).

According to Zhang et al. (2006), saturated hydraulic conductivity varied in Calcic Cambisols for all levels of soil compaction at depths of 0 – 10 and 10 – 15 cm. Servadio et al. (2005) reported that hydraulic conductivity for single tyres of one and four passes were 2.8 to 1.6 mm h^{-1}, respectively.

Small bulk density increases have been reported to cause large decrease in hydraulic conductivity and is dependent on the soil porosity and its saturation degree (Oluwafemi et al., 2019). Saturated hydraulic conductivity results show high variability in time and space (Głąb, 2014; Reynolds et al., 2009). Although field measurements of saturated hydraulic conductivity are more realistic and less time-consuming (Alaoui & Helbling, 2006), they are less controlled than laboratory methods (Rezaei et al., 2016).

f) Penetration resistance

Soil strength reflects soil resistance to a tillage tool moving through it (Hamza & Anderson, 2003) and is measured using a cone penetrometer (ASABE, 2006). Penetration resistance can be calculated as (ASABE, 2006):

$$PR = \frac{C_s I}{A_c} x100 \quad (2.4)$$

where PR is penetration resistance (N m^{-2});

I is the impression on the scale (m);

Cs is the spring constant (N m^{-1});

A_C is the area of the cone (m^2).

In contrast to bulk density data, data on penetration resistance measurement from an entire soil profile may be collected automatically (Raper, 2005). Penetration resistance affects performance

of tractors, water infiltration and tillage draft (Botta et al., 2006; Manuwa & Ademosun, 2007; Mari et al., 2006).

Penetration resistance has been reported to increase by 76% for loam, 45% for clay and 92% for silt due to soil compaction (Pagliai, 2003; Stenitzer & Murer, 2003). Patel and Mani (2011) working on sandy loam soil reported increase of penetration resistance in the 0 – 15 cm soil layer with increase inf wheel passes. For soil depths of 0 - 5, 5 - 10 and 10 - 15 cm, a load of 8.40 kN and 16 wheel passes produced penetration resistance of 2750, 3873 and 4243 J m^{-1}, respectively.

The influence of wheel traffic on soil compaction in a clay loam soil were investigated by Capello et al. (2018). In controlled grass treatments, the penetration resistance along the profile varied between 1500 and 3700 kPa and from 2500 to 4300 kPa in no-track and in track positions, respectively. The penetration resistance increased to 9500 kPa in the first 0.20 m of soil profile with a maximum value of 25000 kPa at 0.07 m depth after 5 passages.

Chyba et al. (2017) reported that penetration resistance increased thought the soil profile with increase in wheel passes. Naderi-Boldaji et al. (2018) and Botta et al. (2009) reported linear increase in penetration resistance with the number of subsequent wheel passes on the soil. Taghavifar and Mardani (2014a) observed highest penetration resistance of 0.260 MPa at a depth of 0.21 m at the third pass and wheel load of 3.00 kN. The least penetration resistance of 121 kPa was observed at the first pass with a wheel load of 1.00 kN.

Jabro et al. (2009) observed that penetration resistance increased with depth for a sandy loam soil. They reported a mean penetration resistance of 640 kPa from 0 to 5 cm, 1840 kPa from 5 to 10 cm and 2270 kPa from 10 to 15 cm depths. Field tests were conducted by Servadio et al. (2015) to compare the compaction effects of one to four wheel passes of two different tyre configurations. The mean values of penetration resistance were 2.02MPa for the one-tyre tractor and 1.86 MPa for the two-tyres tractor in the top 0.20 m of soil. A mean penetration resistance of 2.72 MPa for the single tyres tractor and 1.72 MPa for the two-tyre tractor were recorded in the 0.21 to 0.35 m layer.

Chan et al. (2010) compared the penetration resistance of soils under random and controlled traffic in 0 to 40 cm soil layer. The results indicated that the penetration resistance for controlled and random traffic were 1.051 MPa and 1.487 MPa after two years of experiment, respectively.

Controlled traffic was reported to reduce penetration resistance by 29.3% compared with random traffic treatment.

It may be difficult to detect compacted soil layers if penetration resistance is measured under high soil moisture contents because penetration resistance reduces with increased moisture content at a faster rate in higher bulk densities (Vaz et al., 2011). Furthermore, penetration resistance is affected by soil type, organic matter content, soil texture, soil compressibility and metal-soil friction (Sun et al., 2012). Being a point measurement and not a bulk soil measurement, penetration resistance varies spatially (Alaoui & Helbling, 2006; Lipiec and Hatano, 2003; Nawaz et al., 2013; Van den Akker, 2008). Therefore, used alone as compaction indicator, penetration resistance can give a misleading picture about soil compaction (Batey, 2009).

g) Shear strength

The capacity of a given soil to withstand an applied load is known as soil strength. When an external stress exceeds the mechanical stability of soil, compaction occurs (Nawaz et al., 2003). Mechanically or hydraulically applied stress causes soil deformation. Whereas soil stress propagation depends on both soil strength and soil deformation, soil deformation depends on both soil stress and soil strength (Keller et al., 2013).

The greatest stress a soil has ever experienced before to loading is called precompression stress. Deformation has been found to be elastic for stresses below precompression stress and plastic for stresses above precompression stress (Schäffer et al., 2007). Krebstein et al. (2014) observed an increase in the precompression stress of a sandy loam soil of 12.6% in the upper soil layer (0 to 0.1 m) and 15.2% at a depth of 0.1 to 0.2 m because of soil compaction.

Compaction occurs at stresses greater than precompression stress and increases its value irreversibly (Lipiec et al., 2003). Although precompression stress directly relates soil strength to soil stress, the concept relates to equilibrium conditions and laterally confined expansion (Abu-Hamdeh & Reeder, 2003). Schaffer et al. (2007) cautioned that the soil's water content and drainage parameters affect precompression stress.

A critical level of stress is reached when a tillage tool is dragged into the soil, creating failure planes in the ground. When Mohr's circle meets the failure envelope, the critical normal and shear

stress that results in soil failure is achieved (Ahmadi, 2016). As shown in Figure 2.4, a straight line with an intercept (soil cohesion, C) and an angle with the horizontal (soil internal friction, φ) characterizes the soil failure zone (Kasisira & du Plessis, 2006).

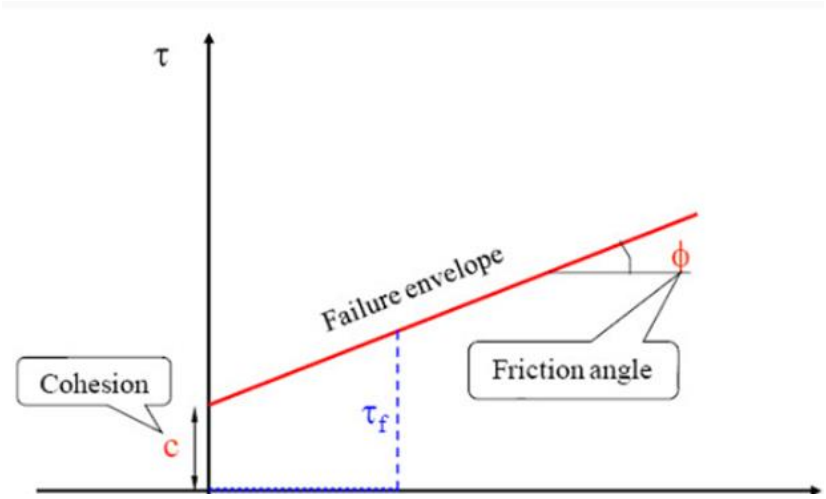

Figure 2.4: Mohr-Coulomb failure criterion and failure envelope (Kasisira & du Plessis, 2006)

According to the Mohr-Coulomb criteria, soil cohesion and internal friction affect soil shear strength. Only the links between nearby soil particles can cause soil cohesion, which is the maximal shear stress at zero normal stress (Zadeh, 2006). Cohesion is the binding force between particles of the soil per unit area. It is affected by pore space, soil type and moisture content and is independent of the applied force.

Depending on the kind of soil and the moisture content, the soil cohesion rises as the soil bulk density increases. In comparison to fine-grained soils, coarse-grained soils showed larger internal friction angles (Gitau et al., 2006).

Wang et al. (2022) carried out a field experiment to investigate the stress transfer by several passes with various tractors. The findings demonstrated that tractors with small axle-loads produced greater soil extra stress from 0 to 20 cm depth at each number of passes, whereas tractors with big axle-loads produced higher soil additional stress at 20 to 80 cm depth.

According to research by Battiato et al. (2013), more wheel passes on the same track on mineral soils result in deeper stress distribution and more compaction-affected soil volume. Pytka and Szymaniak (2005) demonstrated that the first two wheel passes of a tractor induce the most soil

deformation, which diminishes in subsequent passes. According to Schjnning et al. (2012), the greatest stress in the tyre-soil contact region is more than twice as high for narrow, high-pressure tires and almost comparable to the ground pressure for big, low-pressure tires. Berisso et al. (2013) indicated that soil pore continuity was affected by deviatoric stresses.

Pytka and Szymaniak (2004) determined the stress distribution under multiple passes of a 29-kW tractor of mass 2480 kg. They reported a significantly higher increase in maximum stress between the first two passes, than between the second and third pass. They ascribed the difference in stresses detected between the second and third wheel passes to soil consolidation

The interlocking of uneven soil particles causes internal friction in the soil, which is influenced by the typical load applied (Gitau et al., 2006; Marenya, 2009). The angle of internal friction reveals whether soil granules are in contact with one another. It is affected by normal stress, water content, soil porosity and grain size distribution. Increased soil moisture content and density have been reported to increase angle of internal friction and cohesion of coarse-grained soils (Zadeh, 2006).

According to some reports, the rate of shear has no effect on the internal angle of friction. In comparison to sandy soils, clay soils have a smaller internal friction angle. Depending on the kind of soil, this angle can range from 25° for loose, fine-textured moist soils to around 45° for thick, coarse-textured dry soils (Zadeh, 2006). The adhesion between soil and metal surfaces when they come into contact is known as soil-metal friction. It occurs when the cohesive forces of the soil aggregate are less than the frictional and adhesive binding forces between the soil and the metal surfaces in contact (Ren et al., 2001). Because of this, equipment design must consider soil-metal friction (Sahu & Raheman, 2006).

2.3.3 Crop yield

The increased contact between soil particles and roots caused by compaction results in a fast exchange of ions. Nevertheless, soil compaction reduces root penetration ability since it increases soil strength (Hamza & Anderson 2005; Kirby & Bengough, 2002). The turgor pressure within the elongating zone of the root provides the force required to push the root cap through the soil. If this pressure is insufficient to overcome soil resistance, the root tip growth ends (Odey et al., 2014).

Topsoil compaction limits root development more so than subsurface compaction (Botta et al., 2006). Rooting depth and length are reduced because of soil compaction (Kristoffersen & Riley, 2005). Since roots can't grow as widely in compacted soils, there is less availability to nutrients (Miransari et al., 2009: Nawaz et al., 2012). Root penetration was reported to be limited by compaction of calcareous loamy soils with 5% organic matter at depths greater than 0.20 m. (Bouwman & Arts, 2000). According to Saqib et al. (2004a), wheat plant root density decreased when a sandy clay loam soil was compacted from 11210 to 1650 kg m^{-3}.

Because the roots of plants extend less slowly in compacted soils, they have limited access to soil nutrients (Miransari et al., 2009). Significant soil compaction might lead to stunted plant shoot development (Nawaz et al., 2012). Seedling emergence is also negatively impacted by soil compaction (Shaheb et al., 2021). Low germination rate, late germination, and high mortality rate are some additional impacts of soil compaction (Nawaz et al., 2012). In a greenhouse experiment, Jordan et al. (2003) noted a rise in the bulk density of a dry soil from 1300 to 1800 kg m^{-3}. Oak seedlings emerged later because of this. Young seedlings' reduced height was also seen. Silva et al. (2008), however, found no correlation between soil compaction and plant height.

Chamen et al. (2015) observed that lower revenue and high production costs and are imposed by soil compaction. Lower revenues arise from lower yields and additional fertilizer use (Saqib et al., 2004a) while decreased yield result from the reduced accessibility of nutrients (Chamen et al., 2015). The impacts of soil compaction on crop productivity are doubled by salinity (Koch et al., 2008; Saqib et al., 2004a; Whalley et al., 2008).

For some crops, light compaction of the soil has been proven to be beneficial. Alameda and Villar (2009) reported that compacting sandy soils moderately can enhance the growth of woody plant species seedlings growth. A loamy sand soil was subjected to different loads by Bouwman and Arts (2000). They found that after five years, a moderate degree of compaction gave the highest crop yield.

Håkansson (2005) analyzed yield reductions against degree of compactness for different crops in terms of soil density. According to the study's findings, less compaction is preferable for oil seed, whereas more compaction is better for cereal crops. High soil compaction reduced potassium

absorption and barley output in clay loam, silt and loam soils with relative compactness levels of 75 and 90% of the typical level (Kristoffersen & Riley, 2005).

2.3.4 Environmental impacts

The wheel traffic-induced soil compaction affects the environment in various ways as summarized in Figure 2.5.

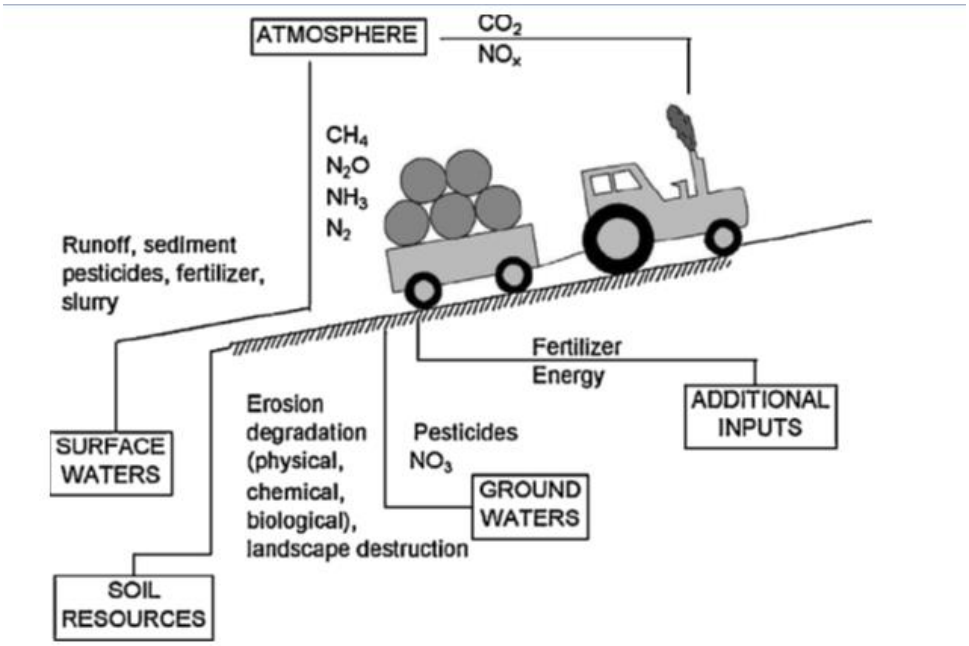

Figure 2.5: Implications of compaction to the environment **(**Chamen et al., 2015**)**

Soil compaction causes emissions of N_2O (Ball et al., 2008; Hansen et al., 2008; Vermeulen & Mosquera, 2009) and increase denitrification rate and emissions of N_2O by 400 to 500% (Nawaz et al., 2012). In the absence of traffic, Vermeulen and Mosquera (2009) observed a 50% reduction in N_2O emissions. Milne et al. (2011) predicted N_2O emissions from soil using water-filled pore space and nitrate. The primary parameters influencing N_2O emissions from arable soils were found as water-filled pore space and temperature (Dobbie & Smith, 2003; Milne et al., 2011). Lower efflux of CO_2 has been observed when soil is compacted (Silveira et al., 2010).

Increased anaerobic soil conditions brought on by soil compaction lead to an increase in methanogenic bacteria and a decrease in methanotrophic bacteria. This results in the lower oxidation rate than its production rate of CH_4 (Nawaz et al., 2012). Furthermore, anaerobic soil conditions might lead to higher leaching and less pesticide breakdown (Alletto et al., 2010).

2.3.5 Soil biodiversity

The microbial biomass of the soil is affected adversely by soil compaction Beylich et al., 2010; Frey et al., 2009; Pupin et al., 2009; Shestak & Busse, 2005). Due to soil compaction, air-filled porosity was reduced by 13 to 36%, which led to a decrease in microbial biomass carbon and nitrogen (Tan & Chang, 2007). The amount of nitrogen available to plants can be reduced by microbial processes occurring in compacted, waterlogged soils (Chamen et al., 2015; Tan et al., 2008).

Stresses in the soil have an impact on enzyatic activity. The activities of amidase, dehydrogenase phosphatase, and urease are decreased because of soil compaction (Tan et al., 2008;) while the activity of phosphatase increased (Pupin et al., 2009). Comparing compacted and non-compacted soils, researchers have shown that the former had greater methanogen levels and lower eukaryotic/prokaryotic ratios (Jordan et al., 2003; Schnurr-Putz et al., 2006).

Compaction reduces macro pores affecting the movements of the soil fauna (Bouwman & Arts, 2000; Radford et al., 2001). Larger soil fauna in interstitial spaces in the soil influence decomposition of soil organic matter. Compaction also reduces the population of nematodes (Chan & Barchia, 2007). In highly compacted soils, there has been a documented rise in herbivore nematodes and a decline in bacterivore and omnivore nematodes (Bouwman & Arts, 2000). However. Beylich et al. (2010) reported that compaction of the soil had no impact on the soil's biota or biological processes. Ground flora is important in revegetation, water and nutrient cycling and aesthetics (Zenner et al., 2006). Some plant species can recover after severe soil degradation (Demir et al., 2008).

2.4 Alleviation of soil compaction

Avoidance of compaction is more effective and less costly than remediation. The strategies to reduce compaction caused by agricultural operations depend on climate, soil type, and land use (Chamen et al., 2015). Biological activity, natural weathering and agronomic measures are ineffective in amelioration of compaction (Spoor et al., 2003) necessitating the use of mechanical measures to hasten the recovery of the compacted soil (Radford et al., 2007; Spoor, 2006).

2.4.1 Controlled traffic

According to Antille et al. (2015), controlled traffic farming (CTF) is a mechanized system where machinery have the same track width to restrict traffic to lowest possible regions covered by permanent traffic lanes. This restriction of wheeling to permanent traffic lanes improves tractive efficiency (Alakukku et al., 2003). Controlled traffic improves soil conditions for both crops and tyres (Hamza & Anderson, 2015). The system slows down recompaction of cultivated soil reduces slipping and enhances water penetration in the soil (Li et al., 2001). It reduces run-off, improves soil structure, minimizes nitrogen losses, and increases soil moisture (Li et al., 2000). Chamen (2003) reported yield improvements of up to 35% for CTF systems.

Bulinski and Niemczyk (2001) reported that the soil bulk density in CTF system was higher by up to 39% compared to cropped area outside the traffic lanes. Hamza and Anderson (2015) observed that up to 79% less energy for disc ploughing was used up in controlled traffic. Nikolic et al. (2001) approximated this saved energy to be between 20 and 25%. Chen and Yang (2015) reported that CTF systems increased soil compaction in traffic lanes thus reducing it in crop zone. They added that the system reduced fuel consumption by 24%.

Up to 86% of the field in random traffic farming (RTF) has tyres on it in a season (Kroulik, 2009) with 95% of the field experiencing at least a wheel pass (Kroulík et al., 2011). This percentage reduced to 45% when a one-pass system of cultivation was used (Chamen et al., 2015). According to Kingwell and Fuchsbichler (2011), the productivity of sandy loam soils improved by 53% under CTF systems. Chamen (2011) reported that CTF increased yields by 8% on silt, 19% on clay, 20% for root crops and 22% on loam.

Because of the high entry cost and the difficulties of matching axle and implement widths, CTF adoption has been delayed (Chamen et al., 2015). Although CTF is achievable because of the usage of auto steering systems and Global Positioning System (GPS), definite field layouts and machinery operating width are necessary.

2.4.2 Tyres with low ground pressure

These who are a preventative measure that only work on topsoil for tyres and on subsoil for tracked vehicles (Ansorge & Godwin, 2008). Lower inflation pressure spreads the load across a larger region, lowering ground pressure and enhancing pressure distribution uniformity (Alakukku et al.,

2003). Bigger tyres with low inflation pressures lessen the possibility for soil compaction (Hetz, 2001).

Using 1000 kg loads to compare rubber tracks and tyres, Pagliai et al. (2003) concluded that the tracks confined compaction to the surface layers. Similar findings were reported by Ansorge and Godwin (2007) with weights of 12000 kg. Lamandé and Schjønning (2011) postulated that stresses in the topsoil increased with contact pressures whereas those at lower depths rise with load. They observed that in a silty clay loam, the maximum stress was correlated with the mean ground pressure at 0.30 m depth, whereas the stress was correlated with wheel load at 0.90 m deep.

2.4.3 Deep ripping

Tillage can reduce topsoil compaction's negative impacts (Berisso et al., 2012). According to Schjønning et al. (2016), subsoil compaction occurs below 25 cm depth and cannot be removed by conventional tillage. Hard pans form at soil layers between 15 and 36 cm deep (Alakukku et al., 2003; Kumar & Thakur, 2005). Chisel plough, subsoilers, and cultivators are used in deep tillage operations to reduce soil compaction (ASABE Standards, 2009). Deep ripping ameliorates hard setting soils and destroys hard pans (Hamza & Anderson, 2003; Torella et al., 2001). It is employed to break up the compacted soil horizons below the topsoil that limits the infiltration of water and penetration of roots (Bateman & Chanasyk, 2001).

Improved soil health can result from deeply ripping compacted soil (Laker, 2001). Deep loosening of soil overcomes friction, shear resistance and soil adsorption force (Sahu & Raheman, 2008). According to Hamza and Anderson (2002), the impact of ripping on water infiltration decreased drastically in the second year, indicating that the soil re-compacted. Ripping enhances water and nutrient infiltration as well as plant root development (Borghei et al., 2008). At depths ranging from 0.25 - 0.90 m, a subsoiler splits up compacted strata of soil to form continuous grooves created by shanks drawn into the soil (Kees, 2008).

Subsoiler shanks are of different shapes and may be straight or parabolic shaped, having wings or with no wings. Parabolic shanks require less power to pull them than straight shanks. Winged parabolic or straight shanks require more power to pull them (Li et al., 2012;).

To improve drainage and root penetration, Spoor et al. (2003) advised cutting cracks across the compacted regions. Chamen (2011) reported that subsoiling increased infiltration by around 1.7 times on clay and sandy loam soil. Allen and Musick (2001) reported a similar observation on infiltration in watered furrows, which rose by 28% owing to subsoiling. According to Said (2003), subsoiling enhanced overall porosity, macropores, and movement of water vertically in the soil profile.

Working on a sandy loam soil, Chamen (2011) reported no response from winter wheat despite loosening the soil to 0.35 m depth. Two tractor passes afterwards restored the soil to its previous strength. Olesen and Munkholm (2007) investigated the effect of subsoiling on a sandy loam and loamy sand and concluded that loosening the subsoil was ineffective in reducing subsoil compaction. Ripping should be undertaken at an optimum moisture content to reduce cost (Hamza & Penny,2002; Lacey et al., 2001). The depth of ripping for breaking the hard pan layer is greater for deeper cultivations.

2.4.4 Using lighter machinery

Less soil compaction is attained by using lighter equipment. When two tractors of different masses with a similar contact pressure are compared, the larger tractor will result in a higher rise in bulk density for the same number of wheel passes. More passes with the lighter tractor might result in just as much compaction (Chamen et al., 2015).

Botta et al. (2006) showed that numerous wheel passes with a 1000 kg tractor rendered direct drilled topsoil unsuitable for seedling emergence. During 10 to 12 passes of this tractor, the effects of soil compaction reached a depth of 0.60 m in the same profile.

2.4.5 Cover crops

Soil compaction increases mechanical resistance to the growth of roots and changes pore space configuration and their extent (Hamza & Anderson, 2005). Plant species with deep tap root can be used in soil compaction alleviation (Rosolem et al., 2002). Biological tillage is whereby deep-rooted crops penetrate through compacted soils and causes the soil to fragment (Chen & Weil, 2010). The force required to push the root cap through the resisting soil is provided by the turgor pressure within the elongating region of the root.

According to Hamza et al. (2001), lupin (Lupinus spp.) and radish (Raphanus spp.) roots have a brief reduction in diameter when transpiration begins, followed by a brief rise. This diurnal oscillation destabilizes and loosens the soil. Cover crop leaves also generate a thick mat of biomass on the ground that supplies organic matter and conserves moisture, increasing earthworm activity in the soil and resulting in lower soil bulk density (Weil & Williams, 2004).

2.4.6 Organic matter in the soil

Retaining sufficient organic matter improves soil stability and resistance to deterioration. Organic matter bind soil mineral particles together and therefore influence soil compatibility. This influence is related to C/N ratio, degree of resistance to decomposition, organic matter, soil type, moisture, and temperature (Sainju et al., 2007)

Cover crops were reported to improve carbon sequestration in irrigated crops. Since organic materials have higher porosity and less bulk density than soils, integrating organic matter with soil increases soil porosity and bulk density. The organic matter's elasticity restricts the passage of forces to the subsoil, functioning as a buffer to lessen the effect of agricultural equipment on the soil. The demand for N, P, and K nutrients decreases as a result of bacterial activity and other activities on organic matter increasing the amount of nutrients in soil (Cuttle et al., 2003).

The effects of sheep manure and vermicompost at values of 0, 2, 4, 6, and 8% on soil compaction in loam and clay loam were studied by Shahgoli and Jnatkhah (2018). It was reported that both organic matter applications at all levels significantly reduced soil compaction. Application of 8% organic matter resulted in a 9.3% decrease in soil compaction. With 8% organic matter added, the smallest bulk density of 1.48 g cm^{-3} was reached, resulting in a 10% drop in compaction.

Morvan et al. (2018) investigated the impact of organic farming on the physical parameters of silty soils in France's Brie region. They found no statistically significant variations in saturated hydraulic conductivity or bulk density. Mosaddeghi et al. (2000) observed that mixing 50 and 100 Mg ha^{-1} of livestock dung into silty clay loam topsoil decreased the compaction impact of two tractor runs of 48.5 kW. According to Hamza and Anderson (2005), applying 10 Mg ha^{-1} of green leaf manure resulted in a drop in bulk density of 20 kg m^{-3} and an increase in sol strength of 11800 kPa for sandy loam soil, while increasing infiltration rate by 40 mm h^{-1}.

Growing green manure crops, keeping previous crop remains on the soil's surface, and adding animal manures or sludge are all ways to absorb organic manure into the soil. Hence, soil structure is strengthened (Cuttle et al., 2003). The susceptibility of soils to compaction was found by Diaz-Zorita and Grosso (2000) to reduce when organic carbon levels were raised for clay loam. For sand and clay soils, Kumar et al. (2009) reported a similar finding. The efficiency of various techniques of incorporating organic matter into the soil varies. Powlson et al. (2011) disproved the notion that incorporating straw into the soil improved organic matter levels in less than ten years.

2.4.7 Conservation tillage

Conservation tillage decreases the requirement for soil cultivation and reduces the amount of soil compaction caused by vehicle activity. Low tillage measures assist to decrease soil crusting and improve the soil's organic matter content by retaining residues on the surface of the ground. As it rains, the residue on the soil surface absorbs the impact of water droplets.

Petersen et al. (2004) reported that reducing secondary tillage lowered the susceptibility of soils to compaction, hence retaining soil aggregates. Over tilling disrupted the natural soil structure, leaving the soil more prone to compaction and crusting. According to Powlson et al. (2012), reduced tillage has the potential to increase nitrous oxide emissions.

2.4.8 Crop rotations and management

Crop rotations should include crops that vary in depth and zone of rooting. They should be combined with agronomic management practices which promotes plant roots to grow through and shatter soils that are compacted, enhance soil structure, water infiltration organic matter content and biological diversity (Bavin et al., 2009).

2.5 Compaction effect of tractor wheel traffic intensity on subsoiling draft

Draft is the amount of force needed to move a tillage tool in the tractor's forward motion (ASABE, 2006). It is the portion of the pulling power that is created horizontally by the tractor when pulling an implement during ploughing (Olatunji et al., 2009). Tillage causes soil failure by tension, shear, compression, and plastic flow (Zadeh, 2006). While wheel activity increases soil strength and the need for tillage draft, tillage diminishes soil strength (Tullberg, 2000).

A portion of tillage energy requirement is used to overcome the soil particles that are interlocked. Increased draft leads to significant energy consumption with attendant economic and environmental challenges (Godwin, 2007; Nawaz et al., 2012). According to Tullberg et al. (2003), the compacting and decompacting of the tractor's own wheel tracks uses up half of the tractor's overall power output. According to Moitzi et al. (2006), 20% of ploughing fuel usage is utilized to drag the plough through the soil. The remainder of the fuel usage is attributable to efficiency losses in the gearbox, engine, and wheel-oil contact.

Draft measurements are needed for determination of tractive performance and energy requirement of a tractor (Chen et al., 2008; Kathirvel et al., 2001; Mamkagh, 2016). According to Arslan et al. (2015), compared to non-trafficked areas, tyre tracks needed 47% and 49% more draft during tillage operations for RTF and CTF, respectively. The draft needs for deep tillage for CTF and RTF treatments, respectively, were 39% and 13% less in the non-compacted zone.

2.5.1 Soil parameters

Soil properties affecting draft include soil strength, bulk density, soil texture and structure, and moisture content (Alimardani et al., 2009). Changes of soil bulk density during tillage operations affect mechanical behavior of soil. Chamen et al. (2015) observed that a compacted soil resulted in more energy consumption to pull tools through it. They observed a draft reduction of 25% in non-compacted loam and clay soils. Gasso et al. (2013) concluded that non-compacted soil requires less tillage energy than compacted soils. Higher traction force has been reported for chisel plough in soils of higher bulk density (Dahab & Mutwalli, 2002).

According to Mouazen and Ramon (2002), implement draft rose as penetration resistance increased. Manuwa and Ademosun (2007) found similar results, noting that the rate of draft increased sharply when penetration resistance rose from roughly 200 to 850 kPa. Increase of moisture content reduces soil cohesion and friction angle resulting in reduced strength. Elevated moisture content reduces soil shear strength, weakens the inter-particle bonds, reduces internal friction, and increases the workability and compatibility of the soil. Mouazen et al. (2003) showed that draft decreased with increasing moisture content. Reduced moisture lowers soil−metal sliding friction leading to less subsoiler energy consumption. Raper and Sharma (2004), on the other hand,

advised that certain soils attach to metals with increasing moisture content in the soil, leading to greater draft.

Bulk density is a pertinent variable in draft considerations since draft increases when the density of soil is increased. Nkakini and Vurasi (2015) reported that when bulk density increased, so did the power needs of a disc plough. Manuwa and Ademosun (2007) found that increasing the soil bulk density of a fine sandy loam from 1680 to 1830 kg m^{-3} resulted in a 15 to 35% increase in draft. This was attributed to the fact that more soil mass is moved by the plough if the soil is dense than if it were less dense, for the same width and depth of cut. An increase in draft is therefore needed to counteract for the larger soil mass's acceleration (Kawuyo, 2011).

Adhesion is affected by the tool characteristics and physical properties of the soil (Sharifat & Kushwaha, 2000). Soil properties affecting adhesion include void ratio, water content, organic matter content, clay content and grain size distribution while the properties of the tool include tool geometry, 0perating speed and surface roughness (Ren et al., 2001). Adhesion of soil increases fuel consumption, leading to higher draft and reduced efficiency (Birch et al., 2016).

The draft force of subsoiler was observed by Mouazen and Ramon (2002) to decrease with moisture content linearly and to be a cubic function of dry density and a quadratic function of wet bulk density. Tong and Moayad (2006) found that the draft increased with increasing soil bulk density from field experiments with a chisel plough.

Khan et al. (2010) showed that certain soils exhibited their best adhesion at water contents between 22 and 32%. Satomi et al. (2012) observed that when void ratio rose, the adhesion reduced. According to Birch et al. (2016), compaction effort had a substantial impact on the angle of internal friction and the adhesion constant. They ascribed the greater adhesion value in clay soils to the increased surface area formed at the soil-metal contact and the fineness of the particles.

Raper and Sharma (2004) subsoiled at a depth of 33 cm with soil water content of 6.1, 6.5, 9.9, and 11.2%. The findings indicated that the lowest moisture content (6.1%) produced the greatest draft and vertical forces. At a moisture level of 6.5%, when draft forces were reduced by 25% to 32%, the soil was at its most conducive for subsoiling.

Arvidsson et al. (2004) measured draft during tillage at depths of 0.13, 0.17 and 0.21 m with a mould board and a chisel plough. The mould board plough had higher specific draft than chisel plough. The specific draft rose as the moisture content dropped. This rise in specific draft with decrease in soil moisture was larger for the chisel than for mould board plough.

2.5.2 Tool parameters

Rake angle, aspect ratio, shape, soil-metal sliding friction, tool type, share sharpness, attachments, and furrow width are some of the elements that affect tool design (Odey et al., 2018; Tong & Moayad, 2006). Cutting forces rose nonlinearly when the cutting breadth was increased (Abo-Elnor et al., 2004). However, Zadeh (2006) reported that draft and tool width had a linear relationship. Differences in the specific drafts of chisel, mouldboard, and disc harrow were reported by Arvidson et al. (2004). The chisel plough was observed to have higher specific draft than the disc harrow and the mouldboard plough. They attributed the difference to the geometric differences of implements and the mode of break-up of the soil.

Draft of a subsoiler is affected by shank shapes. Shank shapes include straight shank, no-wing type, swept shank, curved shank, parabolic shank, winged type, non-vibration type, vibration and rotary types (Raper & Sharma, 2004). In sandy soil, straight shanks that are vertically inclined give reduced draft compared to curved subsoiler (Raper & Bergtold, 2007). A moldboard plough and field cultivator have drafts that are approximately 2.1 and 1.8 times that of a chisel plough and disc harrow, respectively. This means that utilizing energy-efficient tillage equipment can result in significant energy savings (Askari & Khalifahamzehghasem, 2013).

2.5.3 Operational parameters

Operational parameters include tillage depth, width of cut and implement travel speed (Naderloo et al., 2009; Shafaei et al., 2018a). The connection between speed and draft has been described as exponential, parabolic, linear, and polynomial. These discrepancies are attributable to the influence of shear rate on soil-metal friction, the effect of shear rate on soil shear strength, and the inertia required to accelerate soil (Zadeh, 2006).

When the speed of a tillage implement increases and the fresh mass of soil disturbed accelerates, dynamic effects on the cutting force prevail. In sandy soils, soil strength does not vary much with shear rate (Gitau et al., 2006; Olatunji et al., 2015). When speed rises, inertial forces are engaged

in accelerating the soil. Clay soils exhibit increases in shear strength at higher speeds, with rising shear rate outweighing inertial forces (Zadeh, 2006).

Increase in draft with speed was suggested by Zadeh (2006) to be due to wave propagation effect in which tillage draft requirements decrease when the tillage tool speed exceeds a certain optimum limit. This may be explained by the fact that the plastic zone of soil in front of the tool is reduced when the tool's speed is higher than the speed of wave of soil stress propagation lowering soil cutting resistance (Al-Suhaibani, 2010).

Askari et al. (2017) investigated the influence of tine type, operating depth, and forward speed on subsurface tillage tine draft demands in a clay loam soil. Three subsoil tillage tines, four speeds (1.8, 2.3, 2.9, and 3.5 km h^{-1}), and three depths were applied (30, 40 and 50 cm). They found that tine type and depth had a greater influence on tine draft than speed. They noticed an increase in draft as their speed and depth increased.

Metwalli et al. (2002) showed that ploughing depth and inflation pressure had significant effect on draft in clay loam soil. Draft was observed to increase linearly with depth in non-cohesive soils, whereas this relationship was quadratic in highly cohesive soil. Zadeh (2006) reported that draft force increased with depth of operation. The impact of the weight of the disc plough and the depth of the tilling on the draft needs was examined by Olatunji et al. in 2009. Increasing velocity and soil moisture content were observed to increase the draft demand. Aday et al. (2001) found that the draft requirement dropped by 6% when speed rose from 0.28 to 0.77 m s^{-1}.

According to Sahu and Raheman (2006), the reason why the draft increased with speed and depth was because greater soil volume was handled as depth increased and therefore accelerating the soil mass at a faster speed needed more effort due to higher soil resistance. Although Aday and Nassir (2009) reported an increase in specific energy of chisel plough with forward speed, they observed a reduction of the specific energy with reduced ploughing depth.

Ploughing depth and speed were reported by Al-Janobi et al. (2002) to affect the horizontal force required to pull chisel plough. According to Khader (2008), as ploughing speed was raised from 0.89 to 1.92 m s^{-1}, the energy used by a chisel plough to pulverize soil increased from 0.080 to

0.108 MJ m^{-3}. Mileusnic et al. (2010) reported that zero tillage used between 80 and 284 MJ ha^{-1} of fuel energy, while conventional tillage used between 412 and 740 MJ ha^{-1}.

According to Košutić et al. (2005), a conservation system with a chisel plough required 37.5% less energy than a conventional tillage system. Compared to traditional tillage, which had a fuel efficiency of 0.27 ha h^{-1} and a fuel use of 54 L ha^{-1}, direct drilling used 8.9 L ha^{-1} of fuel per hectare (Yalcin et al., 2005).

2.6 Modeling of compaction effect of tractor wheel traffic on sub soiling draft

A model is a scaled replica and a simplified representation of a complex system (Yusuf, 2015). A model is an abstract, mental, physical, and/or mathematical representation of a system (Putri et al., 2020); a system comprises of interrelated elements, while simulation involves the utilization of computer models to imitate a process or a condition (de Wit et al., 2019).

Models can be classified as deterministic or stochastic, static or dynamic, iconic or analog, discrete, or continuous, and mathematical or conceptual (Makange et al., 2021). Mathematical models are sets of equations representing interconnections in a system. Conceptual models are a set of mathematical expression that explain causes and effects in the system; a set of general laws or theoretical principles governing the operation of the units or the entire process in the system (Nyaanga, 2000). Most models for draft prediction characterize compaction from bulk density, penetration resistance and water content (Stenitzer & Murer, 2003). Cohesion is the primary characteristic used in foundation engineering models to describe soil strength (Arvidsson & Keller, 2011).

The approaches used in modeling soil-tool interaction include numerical methods, empirical, dimensional analysis, and analytical methods (Karmakar, 2005). Researchers use empirical models to develop an understanding of a system through parametric studies (Nyaanga, 2000). The variables are fitted into a curve and the curve of best fit is drawn and an appropriate model developed (Karmakar & Kushwaha, 2006). Since data is very varied due to the non-homogeneous nature of soil, empirical approaches for analyzing the interaction between soil and tools are useful but have poor accuracy. Complex processes cannot be explained using empirical approaches, and extrapolating the findings to all field circumstances is not easy (Ucgul, 2014).

Soil-tool interactions can be simulated using continuum or dis-continuum approaches (Makange et al., 2021). Continuum methods include Finite Element Method (FEM) and Computational Fluid Dynamics (CFD) while dis-continuum methods include Smoothed Particle Hydrodynamics (SPH) and Discrete Element Method (DEM) (Lysych, 2019). These methods are illustrated in Figure 2.6.

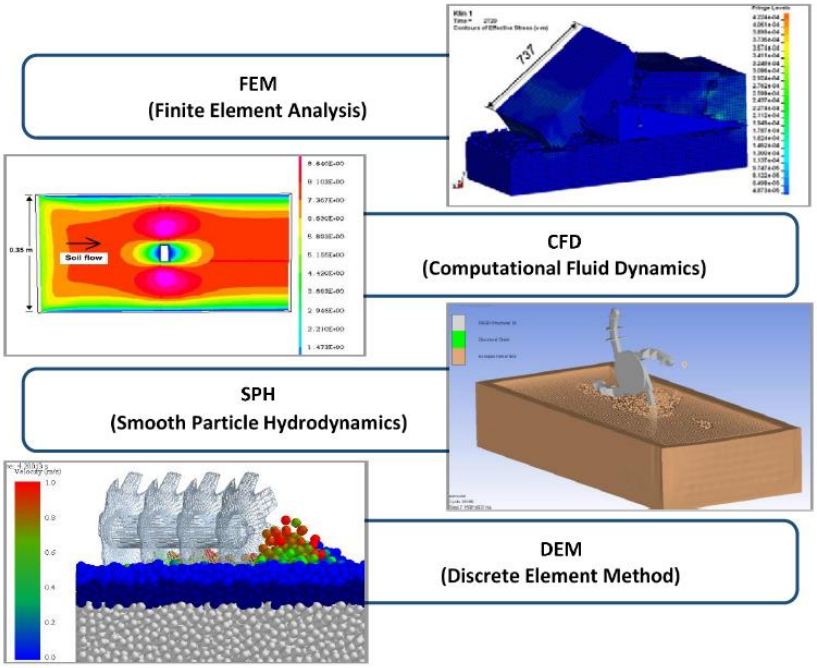

Figure 2.6. Numerical techniques for simulating interactions between soil and tillage tools (Lysych, 2019)

Modeling process involves model construction, verification and validation. Model construction involves making simplifying assumptions, identifying the boundary conditions, defining the range of model applicability formulating the mathematical function linking the decision variables, calibrating the model and validation of the model (Figure 2.7).

The model is continually compared to the real system during development and the feedback is used to adjust the assumptions accordingly. Changes made to the model during these stages may necessitate repeating the other stages iteratively (Yusuf, 2015).

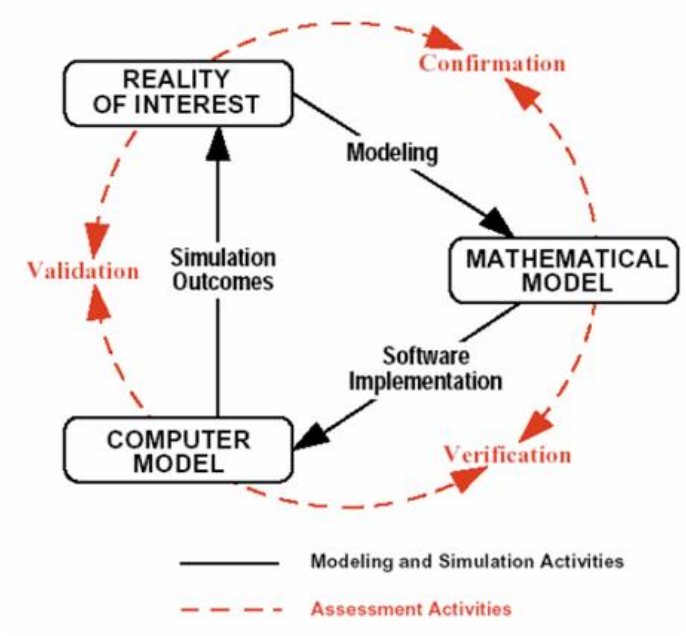

Figure 2.7: The general model verification and validation process

2.6.1 Linear regressions

Regression analysis is done to understand how a dependent variable change if any independent variables is changed, with the other variables fixed. A function is specified using a set number of unknown variables that are computed from independent variables in a parametric approach known as linear regression. The goal of linear regression is to minimize the sum of the squared prediction errors to identify the line that best fits a given set of data (Montgomery et al., 2007).

To predict the value of a dependent variable, a basic linear regression employs one independent variable. Simple linear regression is of the form:

$$Y = \beta_0 + \beta_1 X_1 \tag{2.8}$$

Where Y is the dependent variable;

β_0 is the intercept term;

β_0 is the slope;

X_1 is the independent variable.

Multiple linear regressions (MLR) are used to build linear connections between the independent variables and the dependent variable (Sheehy et al., 2006). The independent variable is used to

estimate values for the dependent variables. MLR is a form of linear regression involving multiple regressor variables (Anwar & Miyami, 2011):

$$y = a_0 + a_1x_1 + a_2x_2 + a_3x_3 + \ldots\ldots + a_nx_n + \varepsilon \quad (2.9)$$

Where y is the dependent variable;

$a_0, a_1, a_2, \ldots\ldots a_n$ are the regression coefficients;

$x_1, x_2 \ldots\ldots x_n$ are the variables of the regression model;

ε is the model error.

Training a linear regression model is quicker that other models such as neural networks. In addition, the strength of the relationship between the dependent variable and the independent variables may be determined using linear regression. Moreover, it may be used to detect independent variables with no relationship to the dependent variable and variables with unnecessary information about the dependent variable (Nyaanga, 2000).

The relationship between the explanatory and dependent variables must be linear for the linear regression modeling technique to be applied. The residuals must have a normal distribution, and the residuals in the dependent variable observations must not influence one another. There should be homoscedasticity among the samples and no multicollinearity among the explanatory factors (Anwar & Mikami, 201l). By incorporating several independent variables that have a substantial impact on the dependent variable, a linear regression model's prediction accuracy can be improved. However, too many independent variables will result in existence of independent variables with very little significance on the dependent variable. This reduces the prediction accuracy (Li & Wang, 2019).

Manuwa (2009) calculated specific coefficients for subsoiling in a sandy clay loam soil at depths of 35, 70, 150, 200, and 200 mm at 11.5% moisture content. The following relationship was obtained for a 0.50 m wide flat plate travelling at 2.5 m $s^{-1,}$ at a rake angle of 90º:

$$F = 82.991e^{0.0091d} \quad (2.10)$$

where F is the implement draft (N);

d is tillage depth (cm).

Using the soil bulk density, moisture content, and depth, Mouazen and Ramon (2006) calculated the draft force on a straightforward deep loosening tine and established the following equation:

$$F = 3.16\rho^3 - 21.36w + 73.39d^2 \quad (2.11)$$

Where w moisture content;

F is the implement draft (N);

d is tillage depth (m);

ρ is bulk density (kg m^{-3}).

Gitau et al. (2006) studied the mechanical characteristics of the compacting chromic luvisols to improve the design of tillage equipment. They employed critical state soil mechanics to analyze the stress-strain behavior of the luvisols using triaxial testing in a lab environment. Randomly selected samples of undisturbed soil were taken from the field and tested in three dimensions utilizing triaxial shearing and isotropic consolidation and compression. Deviatoric stress versus axial strain plots were established to assess soil shear strengths at critical states at different soil moisture levels and two soil depths of 0 - 20 cm for the plough layers and 20 - 40 cm for the hard pan layers, respectively. The trends were successfully estimated using an exponential model that was utilized to match the deviatoric stress-axial strain test results. The shear strength, cohesiveness, the mechanical behavior of the luvisols were all considerably impacted by soil water. The established regression equations demonstrated that the correlations between soil water and internal angle of friction and cohesion are quadratic.

The relationship between depth, speed of operation, and the draft for a mould board plough was modeled by Godwin et al. (2007) as:

$$F = (pd^2 + qd)v^2 + (rd^2 + sd) \quad (2.12)$$

Where F is draft (kN);

d is tool depth (m);

v is working speed (m s^{-1}).

2.6.2 The ASABE model

The ASABE draft prediction equation is given by:

$$F = F_i wd[(p + qv + rv^2)] \quad (213)$$

where, F is draft (N);

F_i is soil texture adjustment parameter;

p, q, and r are parameters that are machine dependent;

v is operation speed (km h^{-1});

w is width of the implement (m);

d is depth of tillage (cm).

All tillage implements, apart from moldboard ploughs, subsoilers, and manure injectors, have a zero coefficient for velocity (ASABE Standards, 2009).

The draft force of farming tools has been predicted using the ASABE model in a variety of soil types (Askari & Khalifahamzehghasem, 2013). However, the standard has inadequate ability in prediction of the draft of specific tools in specific soils (Sahu & Raheman, 2006). Although the ASABE model provide reliable results, its assumptions change when the input variables are changed (Shafaei et al., 2018a).

2.6.3 Dimensional analysis

Dimensional analysis is an approach involving equations that are dimensionally homogeneous, independent of fundamental units (Kawuyo, 2011). Dimensional analysis, according to Simonyan et al. (2006), is an effective technique for building predictive model for a range of systems. The basis of dimensional analysis is the idea that a system may be described by a valid dimensional equation among relevant variables (Karparvarfard & Rahmanian-Koushkaki, 2014).

The foundation of dimensional analysis is the idea that the systems must be qualitatively comparable for absolute numerical equality of quantities to exist and that the magnitude difference between two quantities is independent of the units employed to measure them. It is used to develop prediction equation using the relationship existing among variables and reduces the number of variables in a problem (Srivastava et al., 2006). Yusuf (2015) reported that although several possible combinations of the π-terms exist, only a few reflect the physical phenomena modeled by the terms.

Nkakini et al. (2019) used dimensional analysis and the Buckingham π-theorem to create a model for estimating fuel usage during harrowing on a loamy sand soil. A coefficient of determination of 0.96 was found between the measured and predicted equation results. Kawuyo (2011) developed a draft prediction model for an animal drawn moldboard plough. The mode obtained was:

$$F = v^2 d^2 \left[0.6667\left(\frac{m}{d^3}\right) + 11600\rho M - 0.000626\rho\right] \quad (2.14)$$

Where F is draft (N);

v is operating speed (m s^{-1});

d is soil depth (m);

m is mass of implement (kg);

M is moisture content (%);

ρ is density (g cm^{-3}).

The developed model predicted experimental data reasonably well with a high degree of agreement between expected and observed values (R^2 = 0.92).

Karparvarfard and Rahmanian-Koushkaki (2014) measured fuel consumption and tillage draft for chiseling a clay loam soil. The developed model was reported as:

$$\frac{FC}{Q} = k\left[\left(\frac{v_a}{g^{0.5}w^{0.5}}\right)^{0.54}\left(\frac{d}{w}\right)^{0.0034}\left(\frac{P\rightleftarrows T_w T_d}{w_d}\right)^{-3.5072}\left(\frac{F}{w_d}\right)^{0.0618}(S)^{-0.1509}\left(\frac{F_r}{w_d}\right)^{1.2637}\right]^N \quad (2.15)$$

Where P is the soil penetration resistance (kPa);

d is the working depth (m);

FC is fuel consumed (l h^{-1});

F is draft (N);

F_r is the rolling resistance (N),

g is gravitational acceleration (m s^{-2});

k is the logarithmic line intercept (constant);

N is slope of logarithmic line (constant);

` Q is hourly fuel consumed (l h^{-1});

` S is the slip of the driving wheel (%);

T_w is width of tyre section while unloaded (m);

T_d is overall diameter of unloaded tyre (m);

w_d is dynamic wheel load (N);

w is blade width (m).

Results indicated the predicted fuel consumption rates were 26 to 53% lower than those predicted by the ASABE tillage draft model.

Dimensional analysis was used by Hosseini and Karparvarfard (2011) to develop equations to predict vertical and draft forces on a tine of a chisel as a function of rake angle, forward velocity and tine aspect ratio. The results showed no significant differences between values of intercept of the measured and predicted values plot and the slope.

Moinar and Shahgholi (2018) modeled tractive efficiency of chiseling a silty sandy soil. It was observed that tractive efficiency increased with increase of rake angle and tillage depth. Travel velocity did not show significant effect on tractive efficiency. They obtained the following draft prediction equation:

$$F = 0.0082\left[(v^2 w\gamma)\left(\frac{C}{v^2\gamma}\right)^{0.84}\left(\frac{d}{w}\right)^{1.46}(\sin\alpha)^{2.6}\right] \quad (2.16)$$

Where F is draft (kN);

v is velocity (m s^{-1})

d is the soil depth (m);

w is width of cut (m);

γ is bulk density (kg m^3)

α is the rake angle (^{o})

C is cohesion (kPa);

A mathematical model was formulated by Kabri et al. (2019) for predicting the draft of animal-drawn ridger. Dimensional analysis using Buckingham's π-theorem was used to develop the animal draft output model. They model was given as:

$$F = vd^2\left[0.5585\left(\frac{m}{d^3}\right) + 23266\rho w + 118089.87\rho\right] \quad (2.17)$$

Where F is draft (N);

v is operation speed (m s^{-1})

d is operation depth (cm);

m is mass of implement (kg);

w is moisture content (%);

ρ is density (g cm^{-3}).

The predicted model correlated well with the experimental results with R^2 value of 0.979.

Nkakini et al. (2019) created the following equation for estimating fuel use during harrowing operations using Dimensional analysis:

$$C = 0.00003\left(\frac{FvdM}{Pw}\right) + 0.000002 \quad (2.18)$$

Where F is draft (N);

C is the fuel consumption (l s^{-1});

v is operation speed (m s^{-1})

d is harrowing depth (m);

w is width of cut (m);

P is penetration resistance (N m^{-2});

M is moisture content (%);

ρ is density (g cm^{-3})

The outcome revealed fair agreement, with a coefficient of determination (R^2) of 0.9624.

A mathematical model for predicting tillage energy requirement using dimensional analysis was developed by Yusuf (2015). Test variables were speed, tillage depth, penetration resistance, shear strength and width of cut. The following model was obtained:

$$E = 6vd^2\rho w + 1261.2Pvd^2 + 30.93\sigma d - 120.57v^2d^3\rho \quad (2.19)$$

Where E is energy (MJ ha^{-1});

w is tool width (m);

v is operation velocity (m s^{-1});

d is tillage depth (m);

σ is shear strength (kg m^{-1} s^{-2});

P is penetration resistance (N m^{-2});

ρ is bulk density (kg m^{-3}).

A strong relationship between measured and anticipated results was found during the validation of the model ($R^2 = 0.95$).

Different variables of a system are represented by π-terms in dimensional analysis modeling methodologies, and relationships between the variables are developed. The completeness of the variables determines the effectiveness of a similitude model. Therefore. inaccurate scaling of variables may result in distorted models (Karmakar, 2005).

2.6.4 Analytical models in soil-tool interaction

The concept of passive pressures and the premise that soil fails along a certain path from the cutting tool's point to a location at the soil surface some distance in front of the tool are the basis of analytical models (Murray, 2016). The process of soil fracturing begins with the application of a compressive force by the cutting tool to the soil medium, which creates radial and vertical compressive stresses. The tool blade's bottom is where a plane of shear failure begins. The external stresses from the blade and the soil acts on the sheared segment. The soil segment is ruptured radially outward from the cross-sectional center by the tensile forces that have formed inside it (Karmakar, 2005).

The Mohr-Coulomb criterion has been used to form universal earth moving equation. The equation predicts the tool's draft and the area of the soil it disturbs as a function of the soil's cohesion, the failure wedge's weight, the internal friction of the soil, the rake angle, the soil-tool adhesion, and the tool's working breadth (Murray, 2016). The forces generated by the interactions between the soil and the tillage tool can be divided into interface, acceleration of gravitational forces, and soil strength forces. The interface forces include soil-metal friction angle and adhesion. Soil-tool friction is developed when soil moves on the tool surface. The surface roughness affects the coefficient of friction between soil and the tool surface. The angle of friction between the tool and soil is less than angle of internal friction (Zadeh, 2006).

Since in most applications it is not possible to differentiate between adhesion force and friction, Afify et al. (2020) proposed the following model:

$$F = A_0\, C_a + N \tan \varphi \qquad (2.20)$$

Where A_0 is tool surface area (m^2);

Ca is soil adhesion strength (kN);

N is the normal force (kN);

φ is angle of internal friction (°).

Cohesion is the force required to remove the soil slice from the shear failure surface by outweighing the soil's internal force. When a tool applies pressure to the soil and compresses it, the failure surface creates an angle (β) with the horizontal. This angle is determined from Mohr`s circle using the equation:

$$\beta = \frac{1}{2}(90 - \varphi) \tag{2.21}$$

where φ is angle of internal friction (°)

When the tool's force is greater than the cohesive force, the soil slice is severed.

Soil strength is a function of cohesion and angle ofinternal friction expressed as:

$$\tau = C + \sigma \tan \varphi \tag{2.22}$$

Where τ is soil shear stress (Pa);

σ is normal stress (kPa).

There is an accelerating force produced as the soil mass is forced to move along the tool surface (Afify et al., 2020). This force is expressed as:

$$B = \frac{\gamma}{g}\ b\ d\ V_0^{\,2}\ \frac{\sin\delta}{\sin(\delta+\beta)} \tag{2.23}$$

Where B is force accelerating the soil (kN);

γ is the bulk density (kg m^{-3});

g is the acceleration due to gravity (m s^{-2});

d is depth of cut (m);

b is the tool width (m);

V_0 is the soil velocity (m s^{-1});

β is the angle of the forward failure surface (°);

δ is the rake angle (°).

The weight of soil causes the gravitational force. The volume of the soil is determined by the tool's surface area and tool width. It is expressed using:

$$W = \gamma b A_0 \tag{2.24}$$

Where W is weight of soil (kg);

γ is bulk density (kg m^{-3});

A_0 is area of forward shear failure surface (m^2);

b is the tool width (m).

Figure 2.8 illustrates a free body diagram of a soil section reacting to an approaching tillage tool. By adding together the pressures created by soil-tool interactions in both the horizontal and vertical axes and equating them to zero, equation 2.26 is created (Afify et al., 2020).

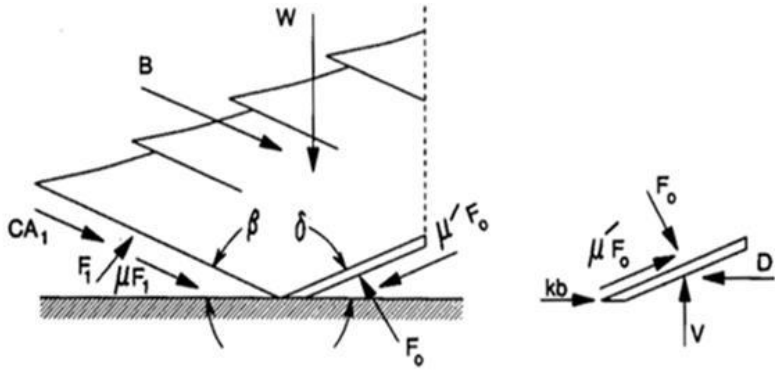

Figure 2.8: Free body diagram of soil segment to an advancing tool (Afify et al., 2020)

$$F = \frac{W}{Z} + \frac{C\ A_1 + B}{Z(\sin\beta + \mu\cos\beta)} + \frac{C_a A_0}{Z(\sin\delta + \mu''\cos\delta)} \tag{2.25}$$

Where W is weight of the soil (kg)

$$Z = \frac{\cos\delta\ \ \mu'\sin\delta}{\sin\delta + \mu'\cos\delta} + \frac{\cos\beta - \mu\sin\beta}{\sin\beta + \mu\cos\beta} \tag{2.26}$$

A_1 is the area of forward shear failure surface (m^2);

β is the angle of the forward failure surface (°);

B is the soil acceleration force (kN);

δ is the rake angle (°);

μ’ is the coefficient of external friction angle;

μ is coefficient of internal friction angle.

The failure plane areas and tool surface for the soil shear reactions forces is determined by:

$$A_1 = \frac{b\ d}{\sin \beta} \tag{2.27}$$

$$A_0 = b\ d' \left[\frac{L_0 + L_2}{2}\right] \tag{2.28}$$

Where L_0 is tool length, (m);

L_2 = d tan δ;

d is cut depth (m);

b is the tool width (m);

β is angle of forward failure surface (°);

δ is rake angle (°).

According to Afify et al. (2020), the adhesion rose from 0.6 to 8.3 kPa as the soil bulk density and moisture levels rose from 1.3 Mg m^{-3} and 11% to 1.49 Mg m^{-3} and 19%, respectively. However, there were no matching changes in the soil's contact friction angle. Consequently, the equation used to determine the draft force of tillage tools was modified to:

$$F = \frac{W}{Z} + \frac{C\ A_1 + B}{Z(\sin \beta + \mu \cos \beta)} \tag{2.29}$$

Where Fis the draft force, (N)

$$Z = \frac{\cos \delta \quad \mu' \sin \delta}{\sin \delta + \mu' \cos \delta} + \frac{\cos \beta - \mu \sin \beta}{\sin \beta + \mu \cos \beta}$$

C is the soil cohesion strength (kPa);

A_1 is the area of forward shear failure surface (m^2);

B is the soil acceleration force (N);

β is the angle of the forward failure surface (°);

μ is the rake angle (°).

Almost all proposed analytical models use simplifying assumptions and the influence of each factor affecting draft must be determined separately (Zadeh, 2006). Analytical models are not able to fully simulate a real system completely (Ucgul, 2014). Also, because the soil structure is not uniform, it is not practical to build a single governing equation to predict the tillage forces. These methods are only suitable for simple tools, for example blades (Murray, 2016). Also, analytical models only look at soil failure and not soil movement because of their dynamic or quasi-static condition assumptions (Ucgul, 2014).

2.6.5 Artificial neural network

Machine learning techniques have enabled great improvement on development of models (Droutsas et al., 2019; Folberth et al., 2019). Christian (2020) showed that machine learning algorithms-based models successfully simulate biophysical systems. Machine learning techniques include decision tree, Bayesian regression, support vector regression, autoregressive integrated moving average, linear regression models, recurrent, feedforward and convolutional neural networks, random forest, and agricultural deep learning (Chakraborty & Joseph, 2017). ANN has recently gained widespread acceptance in crop modeling as a robust computer-based non - linear empirical model (Poznyak et al., 2019). Given the benefits of ANN, many scientists have used it to mimic diverse aspects of agricultural systems.

Artificial Neural Networks is used to model non-linear variables with unknown interactions (Hagan et al., 2002). ANNs can learn from experience and history, generalize on knowledge, perform abstraction, and make errors (Wang & Leng, 2016). ANNs are easy to use and flexible (Al-Janobi et al., 2020). ANN is made up of input, hidden and output layers (Figure 2.9). The study's variables are represented by the number of neurons in the input layer, and the number of neurons in the hidden layer(s) is chosen to enhance forecasts (Demuth et al., 2009).

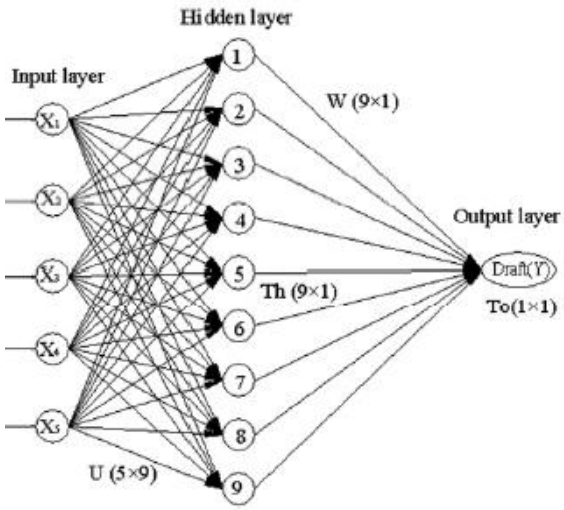

Figure 2.9: Basic structure of an ANN

A neuron is a processing node with synaptic input connections and an output (Jebaraj & Iniyan, 2006) (Figure 2.10). Each processing element receives an input pattern which stimulates it to reach some level of activity. A single output signal is generated by the processing element and transmitted through inter-connections to other processing elements (Khuntia, 2014). Weights are attached to the input connections.

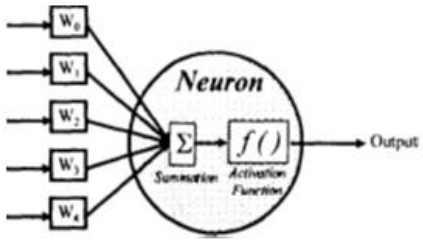

Figure 2.10:A neuron (Khuntia, 2014)

The weighted inputs are added along with the bias to create the net input signal:

$$X = b_j + \sum_{j=1}^{n} w_{ij} x_j \qquad (2.30)$$

where: X is the net input signal;

n is the number of inputs;

x is the input from node j;

w_{ij} is weight of the connection between two nodes;

b_j is bias of node j.

An activation (transfer) function receives the input signal and computes the processing element's output signal as:

$$O_j = f_n(X) \tag{2.31}$$

Where Oj is the output signal from the processing element;

f_n is transfer function;

X is input signal to processing element.

The output is determined by the transfer function employed (Kumar et al., 2002). For hidden and output layers, the sigmoidal function is a typical transfer function. The input layer frequently employs a linear transfer function. A linear function accepts all values, including those outside the range of 1 to +1, but a sigmoid function limits the output to a narrow range (Khuntia, 2014).

(i) Pureline (linear)

$$f(x) = x \tag{2.32}$$

Where x is net input

(ii) Sigmoidal function

a) Logistic function:

$$f(x) = \frac{1}{1 + e^{-x}} \tag{2.33}$$

b) Hyperbolic tangent:

$$f(x) = \frac{e^{x} - e^{-x}}{e^{x} + e^{-x}} \tag{2.34}$$

A model equation is created using the weights from a trained neural network model (Khuntia, 2014). The equation that relates the input parameters to output parameter is written as:

$$Y = f_n\left\{b_0 + \sum_{k=1}^{n}\left[w_{kj} f_n\left(b_{hk} + \sum_{i=1}^{m} w_{ik} X_i\right)\right]\right\} \tag{2.35}$$

where Y is the output;

f_n is transfer function;

w_k is connection weight between k^{th} hidden layer neuron and output neuron;

h is the number of neurons in hidden layer;

Xi is input;

m is number of input variables;

b_0 is the bias at the output layer;

w_{ik} is connection weight between i^{th} layer of input and k^{th} neuron of hidden layer;

b_{hk} is the bias at the k^{th} neuron of hidden layer.

A validation set is used to assess the neural network model's performance after it has been developed using a training dataset (Houshyar et al., 2010). Training is done to select the best performing network (Khuntia, 2014). The output error is distributed back to all the hidden layer neurons during training and used to adjust the weights until there is convergence of the network and output error is minimized. Model validation is done to confirm if the model performs within the limits of the training data.

Model optimization is undertaken to improve the connection weights to find a global solution for a non-linear optimization problem. The backpropagation learning algorithm searches an error surface using gradient descent (Sekhar & Meghana, 2020). The concept behind gradient descent learning is that, knowing which way is up, moving in the opposite direction will get you to the minimum. Step components find the minima by taking steps in the direction estimated. It will take too long to reach it if the steps are too little. A divergence may occur if the steps are excessively big and overshoot the bottom (Litta et al., 2013).

Momentum algorithms use inertia imposed by a momentum parameter to provide gradient descent. The greater the momentum, the smoother the gradient estimation. However, if the momentum is too high, oscillations may occur. Weights are used by the Conjugate Gradient algorithms to identify which direction to shift the weights to reduce error (Hassan et al., 2022). The weight update is determined using second-order methods using the Hessian (Litta et al., 2013).

The Levenberg-Marquadt algorithm combines the steepest-descent algorithm and the Gauss-Newton technique. The Quick Propagation technique computes the derivatives in the direction of

each weight under the assumption that the error surface is a parabola (Kadam & Al-Ibrahimee, 2022). If the present and previous weight updates have the same sign, the learning rate is raised linearly via the Delta-Bar-Delta method. Updates with various signs indicate that the weight has been shifted too far (Litta et al., 2013).

Early saturation of neurons in the network can be prevented by normalization of the data by placing the data in the sigmoid linear range. Data is normalized using the equation:

$$X_n = 2\left[\frac{X_r - X_{min}}{X_{max}}\right] \quad (2.36)$$

where:

X_r is raw in-put variable;

X_n is normalized input variable;

X_{max} is maximum input variable;

X_{min} is minimum input variable.

Complexity, nonlinearity, and uncertainty are three challenging issues that can be solved effectively by using ANN models in engineering. In comparison to other empirical models, ANNs are less sensitive to noise (Zaki et al., 2022).

Abbaspour-Gilandeh et al. (2020) employed ANN to forecast the chisel cultivator's required draft based on the depth of tillage, soil cone index, soil moisture content, and velocity. The scaled conjugate gradient descent technique was utilized to create the ANNs, which outperformed networks created using other approaches. For the simulation's prediction of a chisel cultivator's draft force, the average correlation coefficient and simulation accuracy were 0.945 and 99.83%, respectively.

The draft force of a moldboard plough was modeled by Al-Janobi et al. (2020) based on soil texture index (consisted of clay, silt and sand) and field working index (a combination of ploughing depth, soil bulk density, plough width, ploughing speed, soil moisture content, and tractor power). The coefficient of determination obtained was 0.8602 for draft requirements. Between the observed values and the values predicted by the ANN model, there was a mean absolute error of 0.99 kN.

The draft needs of two-winged share tillage implements in a loam soil were forecasted by Akbarnia et al. (2014) using a 3-7-1 ANN model with a back propagation learning strategy. The inputs were operating speed, working depth and share width while draft requirement was the output. In estimating the draft needs of the winged share tillage tools, the created model had a mean relative error of 0.56 and a mean square error of 0.049.

Alimardani et al. (2009) constructed a preliminary prediction model using soil characteristics, soil physical qualities (% of sand and clay, soil electrical conductivity, soil moisture content, cone index), tractor travel speed, and tillage depth as input parameters. The best method, according to them, was Levenberg-Marquardt, which had a prediction accuracy of 95.8%. In network testing, they obtained an R^2 of 0.987 between the real and projected data from ANN.

Al-Janobi et al. (2001) created a multi-layer perceptron network with an error back propagation learning method to predict the draft of a chisel plough utilizing plowing depths, soil characteristics, and forward operating speeds as input factors and specific draft as the output parameter. The ANN model employed has a sigmoid transfer function in hidden layers and was 4 - 24 - 12 - 1. They noticed that the correlation between the measured and projected draft force was 0.987, and the MSE was 0.1445.

A great quantity of data may be handled by ANNs, and they can distinguish between nonlinear independent and dependent connections as well as the relative relevance of various input factors. Nevertheless, they have drawbacks such as network over- or under-fitting, being a black box, and experimental nature of model construction (Al-Janobi et al., 2020).

2.6.6 Finite element methods

Particles with continuous bonding between them are considered as continuum and can be analyzed using Finite Element Methods (FEM) (Ucgul, 2014). Finite element methods do not require prior assumptions on soil failure patterns to be used for modeling tillage activities of various tools (Kasisira, 2004). The assumption of continuity is not valid when using FEM for force prediction where soil structure changes (Asaf et al., 2007).

If constitutive relation for the soil is known, FEM has an advantage over analytical methods. However, Marenya (2009) observed that FEM applicability in modeling tools is limited because uncertainty exists about the constitutive relationship for agricultural soils.

2.6.7 Computational fluid dynamics

Using the Bingham model for computational fluid dynamics (CFD), Karmakar (2005) modeled soil failure to show soil plastic failure with regard to the yield stress. A CFD model for a narrow tillage tool was verified by Karmakar et al. (2009), who found that it overpredicted the draft force. Also, it was shown that CFD projections for deep tillage and faster operating speeds deviated greatly from the experimental results.

2.6.8 Smoothed particle hydrodynamics

Smoothed Particle Hydrodynamics (SPH) is a continuum simulation approach using a mesh-free algorithm. Urbán et al. (2002) evaluated the SPH method's usefulness in the soil-tool interaction simulation. According to reports, configuring and running a simulation using SPH takes less time and computing power. Yet it was shown that SPH consistently overestimated tillage forces.

2.6.9 Discrete element methods

The discrete (distinct) element technique is a discrete numerical method for analyzing granular materials. It is based on element displacements provided by the equations of motion (Shahgholi et al., 2019). DEM presents the mechanical behavior of an assemblage of discs (2D) and spheres (3D) described as discrete particles with connections between particles guided by certain rules (Murray, 2016).

Several studies have used DEM to simulate soil loosening and disturbance (Chen et al., 2013; Fielke et al., 2013; Tamás et al., 2013; Tanaka et al., 2007). The modeling of the interaction between soil and soil-engaging equipment has been done using DEM (Sadek & Chen, 2015). A study on subsoiler soil-tool interaction model by van der Linde (2007) reported that the DEM explained why a vibratory subsoiler required low draft requirement.

Makange et al. (2021) predicted precise subsoiling using DEM to explain cutting forces and changes in the soil profile caused by a subsoiler. The experimental results acquired in the soil bin

trolley with force sensors were used. They found DEM to be useful in simulating precision subsoiling.

To predic draft forces during tillage at a speed of 12 km h^{-1}, Sadek et al. (2021) created a discrete element model. With the use of a soil bin and a sandy loam soil, draft forces for separately installed discs were measured. Relative errors in their findings ranged from 8% to 14%.

For two different soil types, Mak et al. (2012) developed and calibrated a soil-blade model using DEM. The soil's inherent stresses were used to determine the model's normal stress, bond, and shear strength parameters. The universal earth movement equations accurately predicted the soil cutting forces, which were in good agreement with the simulation results.

Mak and Chen (2014) examined the draft forces of a sweep in a loamy sand soil at various tool travel speeds and depths. The observations were utilized to assess a DEM model that would recreate the soil-cutting process of the sweep. Soil particles were classified as spherical particles having connections. The observed draft forces corresponded well with the predicted ones, with a correlation value of 0.80.

Ndisya et al. (2015) utilized DEM to simulate the draft need of ripping sandy clay soil using tines at various rake angles. The model was calibrated using the results of soil physical tests for moisture content, bulk density, cone index, sieve analysis, angle of repose, and shear strength. The observed and predicted values were not significantly different.

Soil cover depth and soil surface roughness were simulated by Gao et al. (2015) using DEM. To emulate the dynamic soil qualities of a hoe-style seed opener, they created a model. A paired-row hoe-opener tested in a sandy loam soil at a depth of 0.40 m and a speed of 7 km h^{-1} was used to verify the model. Relative errors of under 10% were found in the test findings for soil cover depth, soil roughness, and draft force of the opener.

Shmulevich et al. (2007) used DEM to study the interaction between soil and a broad cutting blade. It was observed that there was a strong connection between the experimental and discrete element simulation findings. They noticed that the soil movement under the blade tip had an impact on the vertical force delivered to the blade.

Linde (2007) created a DEM model to optimise the performance of a vibratory subsoiler and to calculate the decrease in draft caused by the vibrating mechanism. The DEM successfully modeled the vibratory subsoiler mechanism. Obermayr et al. (2011) developed a DEM model for calculating soil-cutting forces in cohesionless granular material. Okayasu et al. (2012) discovered that soil characteristics, tillage depth, and tillage speed influenced plough soil cutting behavior.

Li et al. (2016) used DEM to model how a subsoiler might operate. The draft force of subsoilers was compared at four different places using the validated model. Findings showed that various points produced various draft forces. The subsoiler with a short chisel produced the least draft force (2885 N), but the point with a short face and wings produced the maximum force (4474 N). The simulated results had relative errors of less than 4%.

DEM may be applied to improve tillage machinery and model interactions between soil and tools as well as nonlinear soil dynamics. Mak et al. (2012) pointed out that the research that have been done so far on DEM models are for cohesionless soils and do not include the choice of variables and model calibration.

2.6.10 Fuzzy Inference Systems

Fuzzy logic (FL) mechanizes the human capabilities of reasoning and performing mental tasks. In contrast to previous modeling techniques, FL may link a single output in dynamic and uncertain processes to a set of fuzzy and non-uniform input variables. A nonlinear mapping is done by a fuzzy inference system (FIS) by fuzzy IF - THEN rules from its inputs to output (Mohammadi et al., 2012).

The antecedent of a rule defines the fuzzy area in the input space, and the consequent of the rule specifies the output in the fuzzy region (Bajpal & Mandal, 2015). FIS is used in situations where accurate modeling is challenging (Safa & Samarasinghe, 2011).

i. Steps of fuzzy reasoning

According to Bajpal and Mandal (2015) and Solyali (2020), the steps of fuzzy reasoning performed by FIS are:

a) **Fuzzification**

Fuzzification is transformation of the inputs in a a nonlinear manner. The degree of associated membership functions (triangular, trapezoidal, Gaussian or bell shaped) is used to define linguistic variables of the fuzzy rules.

b) Aggregation

The logical operators AND and OR are used to combine each linguistic assertion once it has been graded for degree. These linguistic assertions are combined using the logical t-norm and the t-conorm operator. The MAX and MIN operators are used in classification tasks.

c) **Activation**

The degree of rule fulfillment determines how much the rules are activated in the output.

d) **Accumulation (Aggregation)**

A fuzzy output results from joining together the output activations of all the rules. Methods of aggregating the outputs include probor (probabilistic OR), max (maximum) and sum (sum of each rule's output set).

e) **Defuzzification**

The final fuzzy output is defuzzified to give a crisp value. Methods of defuzzification include mean of maximum (MOM), largest of maximum (LOM), center of gravity, bisector of area, and smallest of maximum (SOM).

ii. The FIS rule base

According to Bajpal and Mandal (2015), Fuzzy if-then rules are expressed as:

IF x is A THEN y is B (2.37)

Where x is the input;

y is the linguistic output;

A is the premise;

B is the consequent parts of the rule

iii. Types of FIS

a) Mamdani fuzzy system

The Mamdani fuzzy inference system maps input membership functions from input variables, input membership functions into rules, and rules to output features, output membership functions are mapped from output characteristics, and a single-valued output is mapped from output membership functions (Buragohain, 2008; Hayati et al., 2011; Solyali, 2020).

The mean of maxima (MOM), largest of maxima (LOM), and smallest of maxima (SOM) are Mamdani defuzzification strategies. These algorithms choose the mean, greatest, and lowest output values for inputs with the highest membership value (Arlindo et al., 2018). The MOM is used to determine the final output, Z, by determining the mean of a group of output values with the maximum possibility degree, M, using the following equation (Mogharreban & DiLalla, 2006):

$$Z = \sum_{j=1}^{l} \frac{x_j}{l} j \in M \tag{2.38}$$

Other widely utilized defuzzification techniques are the center of gravity (COG) and center of area (COA)/bisector methods (Arlindo et al., 2018). The COG (centroid) approach determines a crisp output by calculating the center of gravity of the output possibilities distribution. The output (Z) of continuous variables is calculated using the equation below (Mogharreban & DiLalla, 2006):

$$Z = \frac{\int_{\mu} \mu(x) x dx}{\int_{\mu} \mu(x) dx} \tag{2.39}$$

Centre of Area calculates the point below the curve where the areas of both sides are equal as (Mogharreban & DiLalla, 2006):

$$\int_{z} \mu(x)\, dx = \int \mu(x)\, dx \tag{2.40}$$

According to Egaji et al. (2015), the COG yields better results than COA.

b) Singleton fuzzy system

In this system, the output to a singleton membership function is restricted to a single value. No integration is carried out therefore computational demand for learning is reduced (Buragohain, 2008).

c) Takagi-Sugeno fuzzy system

A crisp output is computed by the Takagi-Sugeno-Kang (Sugeno) FIS using weighted average. The initial two stages of the fuzzy inference process are comparable for both approaches (Buragohain, 2008). If the function is a constant, a singleton fuzzy system result from a Sugeno fuzzy system.

A Sugeno fuzzy model has a rule in the form (Arlindo et al., 2018):

IF input 1 = r and input 2 = s, THEN Output is z = ar + bs + c (2.41)

The output z is a constant for a zero-order Sugeno model, (a = b = 0). The firing strength w_i of the rule weights the output, z_i of each rule. The final output is given by (Bajpal & Mandal, 2015):

$$\text{Final output} = \frac{\sum_{i=1}^{N} w_i z_i}{\sum_{i=1}^{N} w_i} \quad (2.42)$$

Where $w_i = \prod_k {x_i}^k$

z_i is the output.

Any system's inputs, outputs, membership functions, and rules are the same for both the Sugeno and Mamdani FIS. The output of the Mamdani consists of membership functions, whereas the output of the Sugeno is linear or constant. A dataset is used to train the Sugeno, but Mamdani relies on expert knowledge and does not require a data set (Egaji et al., 2015).

Although the Mamdani FIS employs the method of defuzzification of a fuzzy output, the Sugeno FIS uses weighted average to produce a crisp output. As a result, Mamdani FIS contains output membership functions whereas Sugeno FIS lacks such features (Bajpal & Mandal, 2015). In terms of system architecture, the Sugeno FIS is more adaptable than the Mamdani FIS (Kaur & Kaur, 2012).

A FIS model with 24 rules was developed by Mohammadi et al. (2012) for share tillage tools to predict draft requirements in a loam soil. The input variables of the FIS were depth, speed and share width with draft requirement as the output. The Root Mean Squares of Errors (RMSE) of 0.33 and the coefficient of determination of .92 were found for the relationship.

2.6.11 Adaptive Neuro-Fuzzy Inference System

Fuzzy inference is a technique that interprets the values in the input vector and assigns values to the output vector based on a set of rules. The fuzzy model, fuzzy system, and fuzzy expert system are other names for the FIS (Bajpal & Mandal, 2015). The adaptive neuro-fuzzy inference system (ANFIS) blends both ANN and fuzzy systems. The ANN is used to derive the fuzzy IF-THEN rules while appropriate membership functions are used for inference (Akbarzadeh et al., 2009).

Five functional blocks comprise the FIS as shown in Figure 2.11. The ANFIS is a fuzzy inference system where the parameters governing the membership structure are changed either solely or in conjunction with a least-squares-type approach and the back-propagation method. The fuzzy layer is the top layer in this architecture.

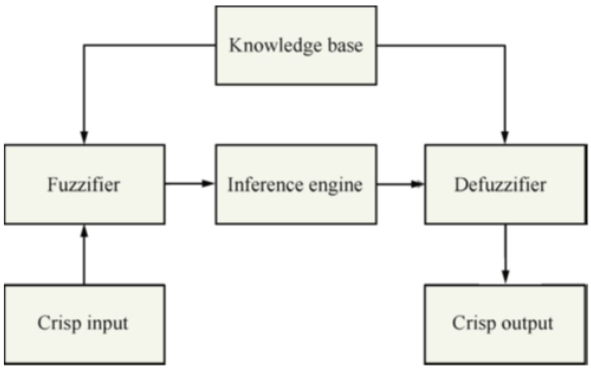

Figure 2.11: A basic FIS

Each node in layer 1 is adaptive and has a node function (Solyali, 2020):

$$O_i^1 = \mu_{A_i} x \tag{2.43}$$

where x is the input;

A_i is linguistic label for node i;

O_i^1 is membership function of A_i.

Bell-shaped membership functions have a minimum of 0 and a maximum of 1 (Khoshnevisan et al., 2014) and is calculated using:

$$\mu(x) = \frac{1}{1 + \left(\frac{x-c}{a}\right)^{2b}} \tag{2.44}$$

where x is the input to node i

According to Khoshnevisan et al. (2014), layer 2 consists of a fixed node whose output is the sum of all incoming signals (T-norm operation):

$$O_i^{\,2} = w_1 = \mu_{Ai}(x)x\mu_{Bi}(x) \quad i = 1,2,3.. \tag{2.45}$$

Where x is input to node i

w_i is weight of node i

Layer 3 variables are modified as a result to decrease the error between experimental observations and ANFIS output. The i^{th} node computes the ratio of the firing strength of the i^{th} rule to the sum of the firing strengths of all rules. The layer's outputs are indicated as normalized firing strengths:

$$O_1^{\,3} = \overline{w_i} = \frac{w_i}{w_2+w_1} \quad i = 1,2,3.... \tag{2.46}$$

where x is input to node i;

w_i is weight of node i;

$\overline{w_i}$ is normalized weight for node i.

Each node in layer 4 adds all the incoming signals to compute the overall output:

$$O_i^{\,4} = \overline{w_i}(p_i(x) + q_i(y) + r_i) \qquad i = 1,2,3.. \tag{2.47}$$

Where $O_i^{\,4}$ is the output of layer 3;

p_i, q_i and r_i are consequent parameters.

The fixed single node in layer 5 computes the overall output as sum of all incoming signals:

$$O_i^{\,5} = \frac{\sum_{i=1}^{2}[\omega_i(p_i(x))+q_i(x)+r_i]}{\sum_{i=1}^{2}\omega_i} \tag{2.48}$$

The network calculates the membership function parameter by combining the least squares approach with back-propagation. In the forward pass, node outputs are carried forward to layer 3, with the resulting variables determined using the least squares approach. In the backward pass, error signals flow backwards, updating the premise variables (Khoshnevisan et al., 2014).

ANFIS can only support the Sugeno-type systems of zeroth or first order with a single output using the same type of output membership functions (constant or linear) having no sharing of rules and having unit weight for each rule (Moinar & Shahgholi, 2019). To increase the accuracy of the ANFIS model and reduce errors, types of input membership functions (triangular, Gaussian, sigmoid, bell-shaped, and trapezoidal), the number of membership functions, optimization methods (back propagation or hybrid), and types of output membership functions (linear and constant), the number of epochs can be varied (Naderloo et al., 2012). The membership function employed is determined by the situation and is based on experience (Mogharreban & DiLalla, 2006).

Taghavifar and Mardani (2014b) conducted research to forecast energy efficiency metrics using ANFIS. Wheel load, speed, and slip were all input factors. The findings of this investigation exhibited great prediction accuracy, with an MSE of 0.0166 and an R^2 of 0.98. Ghadernejad et al. (2018) used the ANFIS model to estimate soil compaction beneath tractor wheels in their investigation. Manure, number of passes, wetness, and depth were all inputs into the FIS. This study's findings predicted soil density with more accuracy than the regression model.

Shafaei et al. (2018b) evaluated the effective chisel plough draft force for farming in a clay loam soil. The input variables were ploughing speed and depth while the output parameter was the draft force in Takagi-Sugeno-Kang type of ANFIS model of the first order. According to the findings, the best ANFIS model has an R^2 of 0.994 and an RMSE of 0.722 (kN). The ANFIS model was found to be more accurate as compared to ASABE draft model. Using ANFIS, Moinar and Shahgholi (2019) predicted rolling resistance with test parameters being tractor speeds, tyre inflation pressure, ballast weight and draft. They found that ANFIS was good for prediction of rolling resistance (R^2 = 0.989).

Al-Dosary et al. (2020) examined the ANFIS approach to determine draft requirements of a disk plough. Depth, speed, initial soil moisture content, soil texture index, initial soil bulk density, disk angle, disk diameter, and disk tilt angle were the input variables, while draft was the output variable. The triangular membership function outperformed all other functions. A comparison of the MLR and ANFIS models revealed that the draft demands of the disk plough could be properly calculated using ANFIS (R^2 = 0.939) compared to MLR (R^2 = 0.561).

The fundamental drawback of the ANFIS model is that if there are more inputs than five, the number of rules and calculation time would grow. ANFIS won't thus simulate the outcome in relation to the inputs (Khoshnevisan et al., 2014).

2.7 Model calibration and validation

Verification of a model is the process of determining that a model meets specifications and fulfills its intended purpose and does not contain errors. The accuracy of the model can be statistically tested by computing draft requirements using known tillage operation parameters and the result compared with draft requirements computed from field measurement. The t-test can be used to reveal the level of accuracy and reliability of the model (Anwar & Miyami, 2011). Verification is done to evaluate whether the model complies with the conceptual specifications.

A model's validity is evaluated by determining how closely the model and the data it uses reflect the real world. Validation is used to show that the model reproduces the behaviors of the real-world system. Model validation aims to make the model address the right problem (Yusuf, 2015). Validation is a quality control procedure to confirm that the model achieves its goal (Nyaanga, 2000). Root mean square error (RMSE) and mean absolute percentage error (MAPE) and coefficient of determination (R^2) are statistical techniques to gauge how accurately a model captures the actual system.

Once a model is accepted, the real system and the model are compared iteratively in a process known as model calibration (validated). The process of confirming that the model implementation effectively reflects the conceptual specification is known as model verification. On the other hand, model validation is the process of evaluating how well the model and the data it uses resemble the real world (United States Department of Defense, 2009).

The optimal models are decided based on minimizing the error. Evaluation of the derived models' prediction accuracy was done using the following indicators:

i. Mean squared error

Mean Squared Error (MSE) determines how well, given a specific input, a true output matches predicted output (Shafaei et al., 2018a). The mean squared error is calculated as:

$$\mathrm{MSE} = \frac{1}{n}\sum(X_i - X_o)^2 \quad (2.49)$$

Where, X_i is the measured draft (kN);

X_0 is the predicted draft (kN);

A high MSE value implies that the prediction is not near the true value while a low value means the predicted value is fairly accurate.

ii. Root mean square error

Root mean square error (RMSE) is measured in the same units as the target variable (Khuntia, 2014) and is calculated as:

$$\mathrm{RMSE} = \sqrt{\frac{1}{n}\sum(X_i - X_o)^2} \quad (2.50)$$

Where X_i is the measured draft (kN);

X_0 is the predicted draft (kN).

iii. Mean absolute error

The average of all observed absolute errors, known as the mean absolute error (MAE) (Khuntia, 2014) and is given by:

$$\mathrm{MAE} = \frac{1}{n}\sum|X_i - X_o| \quad (2.51)$$

Where X_i is the measured draft (kN);

X_0 is the predicted draft (kN).

iv. Mean absolute percentage error

A measure of the closeness of predicted to actual value is known as the mean absolute percentage error (MAPE) (Shafaei et al., 2018a) and is calculated as:

$$\mathrm{MAPE} = \frac{100}{n}\sum\left|\frac{X_i - X_o}{X_i}\right| \quad (2.52)$$

Where X_i is the measured draft (kN);

X_0 is the predicted draft (kN)

v. Coefficient of determination

Coefficient of determination (R^2) measures the linear relationship between the predicted and the observed values. The RMSE measures the average magnitude of the error between model simulations and observations. It ranges from 0 to 1, with 1 indicating that every point on the regression line fits the data perfectly. The coefficient of determination is calculated as:

$$R^2 = 1 - \frac{\sum_{i=1}^{n}(X_i - X_0)^2}{\sum_{i=1}^{n}(X_i - \overline{X})^2} \quad (2.53)$$

Where X_i is the measured draft (kN);

X_0 is the predicted draft (kN);

n is number of turns;

$\overline{X}$ is average draft (kN).

2.7 Summary of the literature reviewed and research gap

Soil compaction affects the following soil properties: porosity, bulk density, water infiltration rate, and soil strength (Horn & Kutilek, 2009). From the reviewed work, not much has been done to quantify to what extent wheel traffic induction affects these properties in silt loam soils in Kenya. Most soil compaction studies have documented how penetration resistance and bulk density are affected by soil compaction with minimal reporting on the effect of wheel traffic compaction on the dynamic soil properties of cohesion, soil strength and angle of internal friction. Similarly, few studies have been undertaken on the effect of these dynamic soil properties on subsoiling draft.

Soil-tool interactions have been modeled using analytical, empirical and numerical modeling approaches. Because of the non-homogeneous character of soils, most empirical models are inaccurate. On the numerical modeling approaches commonly applied, few attempts have been made to model subsoiler draft using ANN and ANFIS. Mak et al. (2012) noted that DEM cannot accurately represent the complex interaction between soil particles and machinery wheels, leading to limitations in predicting subsoiling draft accurately. In a study by Marenya (2009), it was highlighted that FEM might not effectively capture the dynamic and nonlinear behaviour of the soil-tractor interaction during subsoiling, leading to challenges in representing draft requirements.

Among the strengths of MLR, simplicity, interpretability, suitable for linear relationships. Its limitations include being limited to linear relationships and not capable of capturing complex interactions. Dimensional analysis models are based on fundamental principles and give the potential for insightful relationships. However, they are based on rigid assumption of dimensionless groups and might oversimplify complex phenomena (Yusuf, 2015).

ANFIS can capture non-linear relationships and provide interpretability through fuzzy logic. However, their weakness includes complex parameter tuning and the challenge of balancing accuracy and interpretability. ANNs can handle complex patterns, non-linear relationships, and interactions. They are, however, prone to overfitting, are data-intensive, lacks transparency in decision-making (Al-Janobi et al., 2020).

The choice of MLR, Dimensional Analysis, ANN and ANFIS models was made to ensure a comprehensive analysis of the subsoiling draft requirements considering various aspects. MLR and Dimensional Analysis address linear and fundamental relationships. ANFIS and ANN were chosen to capture non-linear complexities and predictive accuracy. This combination offered a holistic understanding of the interplay between soil properties and subsoiling draft.

Observations of soil structure deterioration due to repeated tractor wheel passes are widespread. Studies have shown that soil compaction can lead to decreased water infiltration, increased surface runoff, and soil erosion. These soil structural changes have negative consequences for both agriculture and the environment.

From the literature reviewed, various studies have documented instances where crop yields were significantly lower in areas with high levels of soil compaction caused by wheel traffic. Farmers have experienced decreased productivity and profitability due to this phenomenon. Studies have also revealed that agricultural machinery requires more fuel to operate in compacted soils. This increased fuel consumption leads to higher production costs. Empirical data on fuel consumption in compacted soils supports the need for more efficient tillage practices.

The literature reviewed revealed that the problem of soil compaction caused by wheel traffic is not just a theoretical concern but a practical and widespread issue affecting agricultural productivity, sustainability, and profitability.

While there is existing research on soil compaction and its effects on agriculture, there is a gap in the development of comprehensive predictive models that can accurately quantify the impact of wheel traffic compaction on subsoiling draft requirements. This study aimed to fill this gap by utilizing multiple modeling techniques (MLR, Dimensional Analysis, ANFIS, and ANN) to provide a more holistic understanding of this relationship.

Previous studies have often focused on individual soil properties or compaction levels in isolation. However, there is a need to integrate multiple soil properties, including physical and mechanical properties, into a unified model that can better explain the variations in subsoiling draft requirements. This study addressed this gap by considering a broader range of soil characteristics in the modeling process.

Additionally, while empirical evidence of soil compaction exists, there is a gap in providing data-driven solutions that can enable farmers to make informed decisions regarding subsoiling. This study aimed to offer data-driven modeling solutions that can assist farmers in optimizing their tillage practices and machinery usage.

2.8 Conceptual framework

The conceptual framework of the study (Fig 2.12) provides a visual representation and theoretical foundation for understanding the relationships between the independent variables (depth, bulk density, penetration resistance, moisture content, shear strength, and cohesion) and the dependent variable (subsoiling draft) in the context of the effect of wheel traffic on subsoiling draft requirements in a silt loam soil. The framework outlines the process by which the various modeling techniques (MLR, Dimensional Analysis, ANFIS, and ANN) are applied to capture and analyse these relationships.

The six independent variables that represent key soil properties (depth, bulk density, penetration resistance, moisture content, shear strength, and cohesion) collectively contribute to the mechanical behaviour of the soil and are influenced by wheel traffic. Wheel traffic has a direct impact on soil properties due to compaction and disturbance caused by the machinery. It leads to changes in bulk density, penetration resistance, moisture content, cohesion and shear strength.

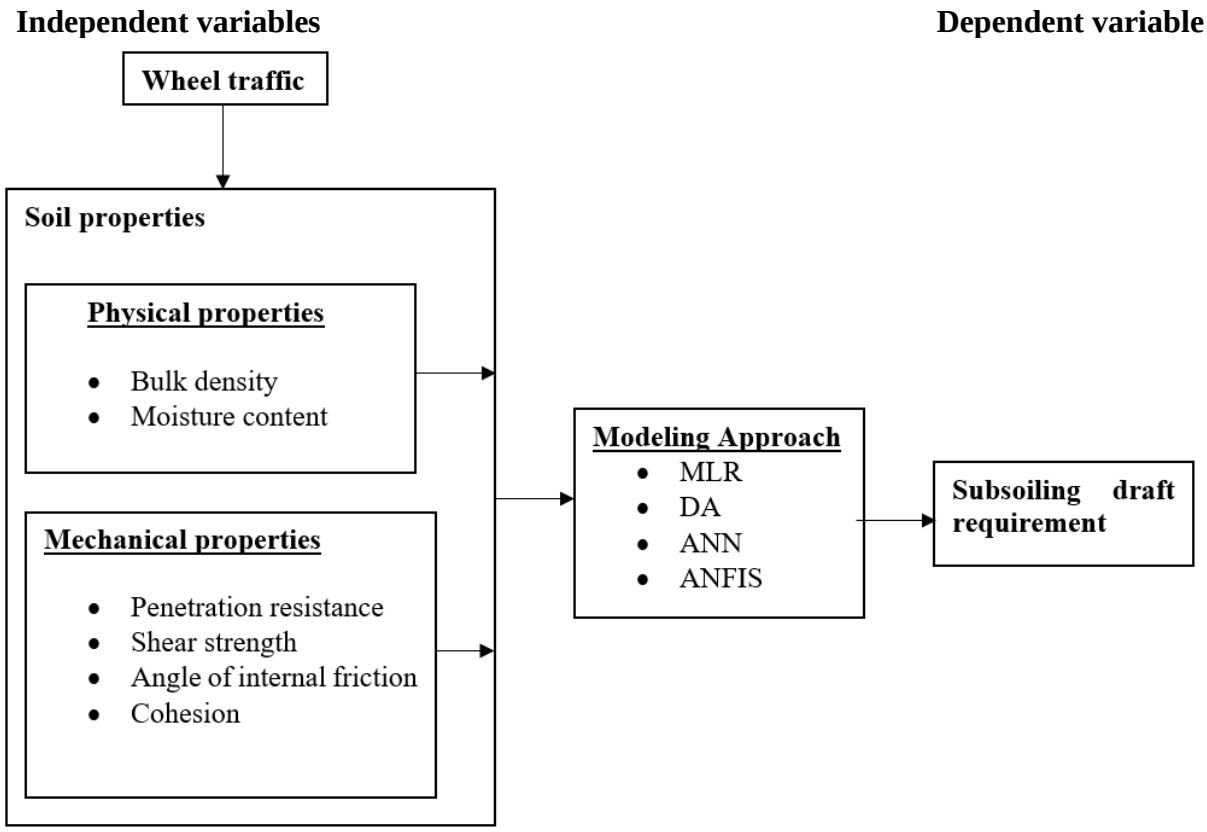

Figure 2.12: Conceptual framework of wheel traffic soil compaction

The dependent variable, subsoiling draft, is a measure of the force required to pull a subsoiling implement through the soil. Subsoiling draft is influenced by soil properties that determine the resistance encountered during subsoiling.

CHAPTER THREE
MATERIALS AND METHODS

3.1 Experimental site and set up

The experiments were carried out in Egerton University, Kenya (Figure 3.1) during the short rains season of August to October 2020. The test farm is located at longitude 35° 35' East, latitude 0° 23' South, and is 2,238 m above the mean sea level. The rainfall in the study area is not uniformly distributed with a mean of 1,000 mm. The minimum temperatures range from 5 °C to 8 °C while the maximum range from 19 °C to 22 °C.

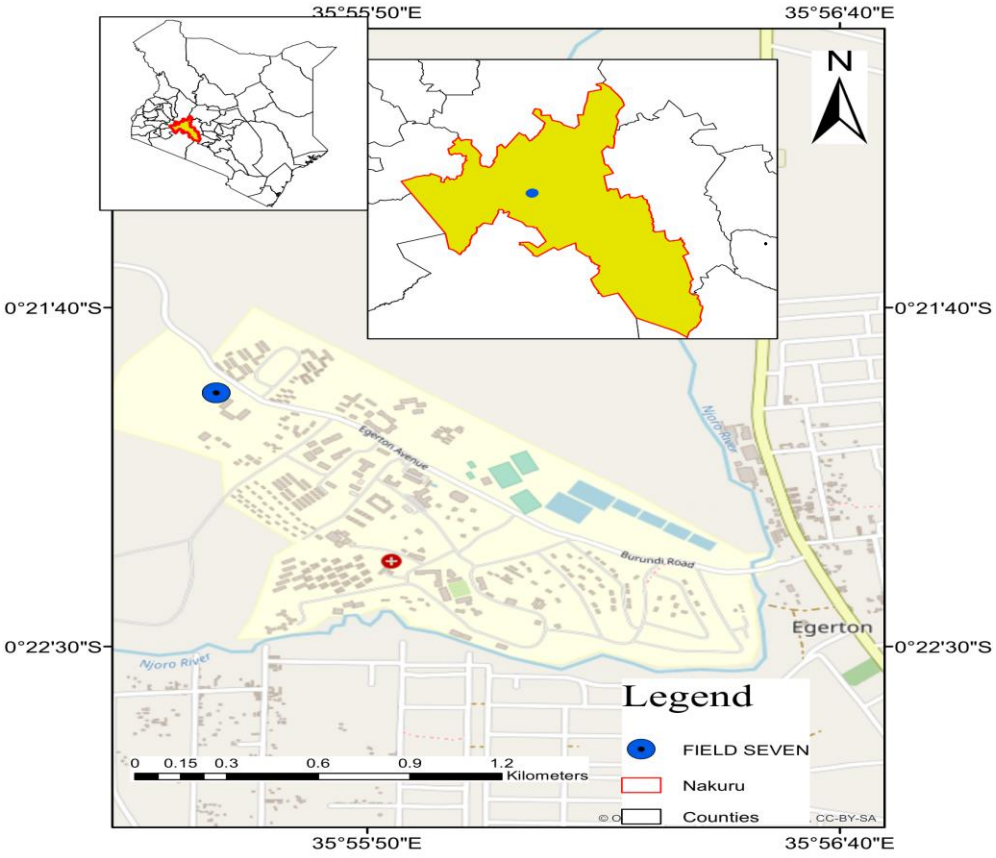

Figure 3.1: Map of experimental site

The test site is relatively level (0 to 1% slope) and has been used for several years with conventional tillage. The topsoil at the experimental site was evaluated by sieve analysis to consist

of 12%, 51% and 37% of clay, silt and sand, respectively. Based on the textural classification of soils technique, this soil was therefore classified as silt loam.

Figure 3.2 gives the layout of 18 experimental plots used in the study. Each plot had a length of 30 m and was 15 m wide with a 5 m wide buffer between adjacent plots. Each treatment plot included three randomly chosen sites (marked 1 to 54 in Fig. 3.1) where soil samples were taken at depths of 0 - 20 cm (plough layer), 20 - 30 cm (hardpan layer), and 30 - 40 cm (subsoil layer) after the pass.

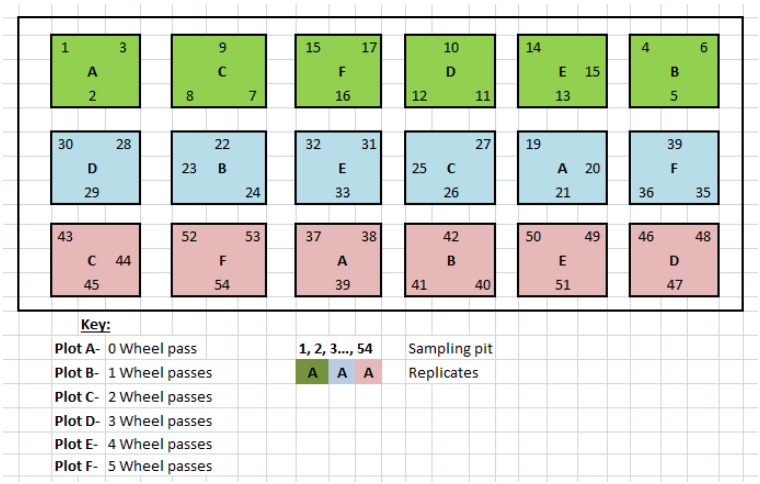

Figure 3 2: Experimental plots layout

3.2 Compaction effect of tractor wheel traffic intensity on physical and mechanical properties of soil

To assess the effect of tractor wheel passes on soil physical and mechanical properties, the following data collection methods were employed:

i. Wheel traffic data

Tractor wheel traffic experiments were conducted on the selected plots with varying levels of compaction. Different numbers of wheel passes were applied to induce varying compaction levels. Information on number of passes was crucial for correlating soil changes with tractor traffic. The specifications of the tractor used to apply wheel passes are given in Table 3.1.

The tractor had a rear axle fitted with two 16 x 38 R1 tread bias-ply tyres. The tractor's front and rear wheel reactions were determined using equations 2.1 and 2.2. Since the mass of the tractor

was 4070 kg and taking gravitational acceleration as 9.81 m s^{-2}; each pass of the Massey Ferguson 455 *xtra* tractor was determined to impart 25.56 kN to the soil.

Table 3.1: Tractor specifications

Specification	Unit
Model	Massey Fergusson 455 *xtra*
Tractor length	4.30 m
Tractor width	2.00 m
Rear tyre width	65 cm
Rear tyre pressure	1.5 bar
Front tyre pressure	1.5 bar
Tractor weight	4070 kg
Perpendicular distance from rear axle to centre of gravity	154 cm
Wheelbase	236 cm
Maximum static load of front axle	49.40 kg

.

.

ii. Soil sampling

Soil samples were collected at various depths before and after tractor wheel passes using standard soil sampling equipment. These samples were analyzed for physical properties (bulk density,

moisture content, porosity, infiltration rate and saturated hydraulic conductivity) and mechanical properties (penetration resistance, cohesion, angle of internal friction and shear strength).

a) Bulk density

The core sampler and its contents were weighed and dried for 24 hours at 105 °C in an oven to achieve a constant mass (Figure 3.3). An electronic balance was used to determine the mass of oven dried soil. Equation 2.3 was used to determine bulk density. The results are presented and discussed in Section 4.1.

b) Porosity

Equation 2.5 was used to calculate the porosity from bulk density and particle density data of the soil. The results of porosity experiments are presented and discussed in Section 4.1.

Figure 3.3: Drying oven

c) Moisture content

The samples' moisture content was calculated using equation 2.6 after the score sample was weighed, dried in an oven at 105 ˚C for 24 hours, and reweighed. The results of moisture content experiments are presented and discussed in Section 4.1.

d) Infiltration rate

Water infiltration rate was measured using metal tubes (150 mm height, 152 mm diameter and 2 mm thickness) before and after wheel traffic treatments for each depth. The soil was penetrated vertically with the tubes (Figure 3.4). A specific volume of water was poured into the tube, and over the course of five minutes, the amount of water that soaked into the soil was calculated. The volume of water infiltrating into the soil per unit time was divided by the tube cross-sectional area to give the rate of infiltration. The results of infiltration rate experiments are presented and discussed in Section 4.1.

Figure 3.4: Double ring infiltrometer

e) Saturated hydraulic conductivity

Soil samples were taken at using a 69 mm diameter, 65 mm height core sampler. The samples were saturated by placing them on perforated disks covered with cloth in a 25 mm deep tray containing water. A rubber tubing was used to connect the saturated soil sample in the core to another core that was placed on top to allow ponding of water on the surface of the sample. Siphons connected to a constant head device were used to apply a thin water layer on the top of the specimen and a constant head of 50 mm maintained above the soil column. At certain time intervals, measurements of the amount of water percolating through the sample were taken. Equation 2.7 was used to get the sample's saturated hydraulic conductivity. The results of hydraulic conductivity experiments are presented and discussed in Section 4.1.

Figure 3.5: Constant head permeameter

f) Penetration resistance

An Eijkelkamp analogue cone penetrometer measuring penetration resistance using a compressed spring was used in this study (Figure 3.6). Readings were collected by pushing the penetrometer vertically into the ground. A slip ring on a graduated scale was slid along as the spring was compressed, indicating the maximum compression measured. The results of penetration resistance experiments are discussed in Section 4.1.

Figure 3.6: Cone penetrometer

g) Shear strength, cohesion and internal angle of friction

Before and after wheel traffic treatment, three undisturbed soil samples were obtained from each plot by pressing sharp, thin-walled stainless steel tubes with an internal diameter of 38 mm and a

length of 200 mm to the necessary depth. To limit water loss, the rings were taken off, the soil was cut, and then the lids were put on top and sealed. The sample was forced out of the tubes using a piston and an extruder. In around the middle of the 200 mm sample, a sample measuring 76 mm in height was removed (Gitau, 2004). Analysis was done in the University of Nairobi Soil Laboratory by tri-axial testing (Figure 2.8) as outlined by Gitau et al. (2008).

Mohr circles and the Mohr-Coulomb equation were used to determine the soil angle of internal friction and cohesion of the soils graphically. The results of soil strength experiments are presented and discussed in Section 4.1

Figure 3.7: Triaxial test apparatus

3.3 Compaction effect of tractor wheel traffic intensity on subsoiling draft

A dynamometer attached to the subsoiling equipment was used to measure the draft requirements during subsoiling. These measurements were recorded for each experimental condition. The dynamometer was attached using shackles between the towing and the towed tractor, as shown in Figure 3.8. The towed tractor's three-point hitch held the subsoiler in place. A data logger made up of an MSI 7300 digital dynamometer (Figure 3.9) that communicated remotely with an MSI 8000 remote display was used to capture subsoiler draft data. The subsoiler's deepest penetration point was used to determine the depth of ploughing, which was measured vertically from the top of the undisturbed soil surface.

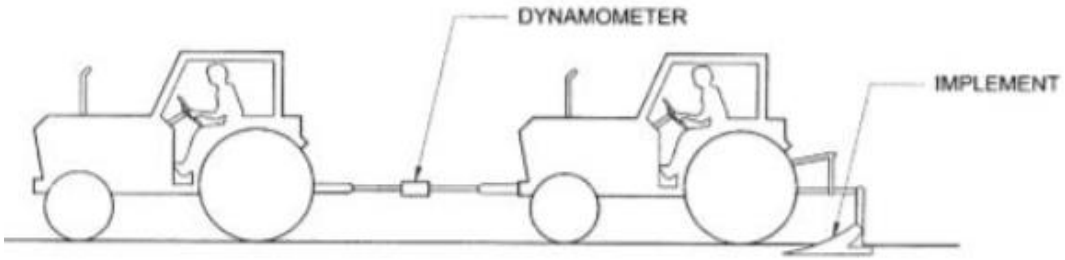

Figure 3.8: Draft measurement

With the implement set in operational position, the towed tractor was put in neutral gear. It travelled for 30 meters at a speed of 2.5 km h^{-1} (0.69 m^{-1}). To record the idle draft as read from the dynamometer in the field, the subsoiler was raised out of the ground and the back tractor was dragged. The difference determined the draft of the tool needed to cut and disrupt the soil. This was repeated three times for each wheel traffic treatment. The results of draft and specific draft calculations are presented and discussed in Section 4.2.

Figure 3.9: Dynamometer used in the study

3.4 Modeling and validation of compaction effect of tractor wheel traffic on sub soiling draft

a) Selection of Soil Properties

The following soil properties were considered to model subsoiler draft:

i. Bulk density
ii. Moisture content
iii. Penetration resistance
iv. Shear strength
v. Soil cohesion

vi. Depth

These variables are summarized in Figure 3.10. It was assumed that there were no variations in soil conditions between time of wheel traffic application and subsoiling. Similarly, the tested soil properties were assumed to have little temporal variations and the variations that occurred were due to wheel traffic effects only.

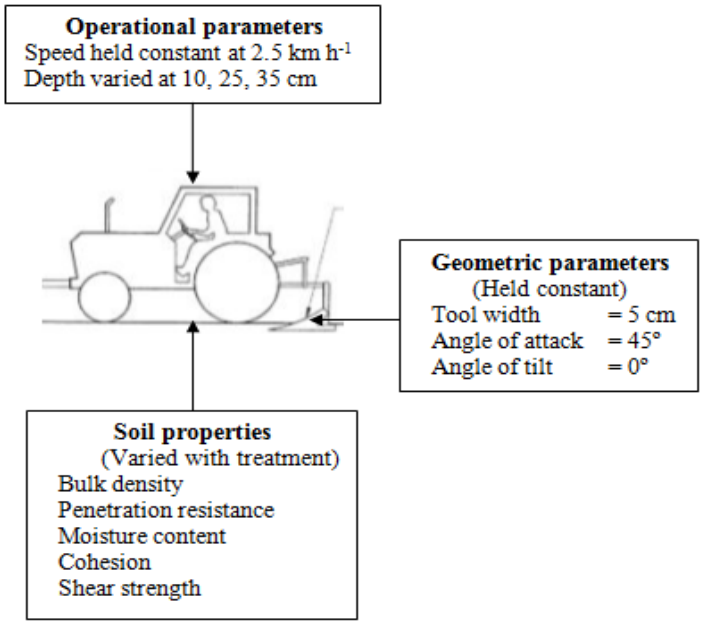

Figure 3.10: Variables used in the study

The following modeling techniques were employed to develop predictive models for subsoiler draft requirements:

i. **Multiple Linear Regression:** MLR was used to establish linear relationships between subsoiler draft and selected soil properties. This technique provides insights into the direct influence of each property on draft.

ii. **Dimensional Analysis:** Dimensional analysis was applied to derive dimensionless groups that describe the soil-tractor interaction. These groups were then used to formulate empirical equations for draft prediction.

iii. **Adaptive Neuro-Fuzzy Inference Systems:** ANFIS was utilized to capture complex relationships between soil properties and draft. It offers the advantage of adaptively adjusting its model structure to the data.

iv. **Artificial Neural Networks (ANN):** ANN modeling was employed to uncover non-linear patterns and interactions between soil properties and draft. Neural networks have the capability to handle complex, non-linear relationships.

3.4.1 Multiple linear regression

Pearson's correlation coefficients were determined between the various variables to check the existence of multicollinearity among the independent variables to be used in the draft model. The regression model was determined using SAS software in terms of the depth of subsoiling, penetration resistance, bulk density, soil cohesion, moisture content, soil strength and draft force. In the model, depth, moisture content, penetration resistance, bulk density, soil cohesion and soil strength were independent variables while draft force was the dependent variable.

All the measured raw data were preprocessed for use in the development and verification of the model. By selecting random values between the minimum and maximum values of the data, the data were split into two portions: 75% for calibration and 25% for validation. The regression model was developed using the calibration data while verification of the developed regression model was done using the validation set. The general regression model of the output and input variables were developed according to equation 3.1 (Anwar & Miyami, 2011).

$$y = a_0 + a_1x_1 + a_2x_2 + a_3x_3 + \ldots\ldots + a_nx_n + \varepsilon \quad (3.1)$$

Where y is the dependent variable;

$a_0, a_1, a_2, \ldots\ldots a_n$ are the coefficients of the multiple regression;

$x_1, x_2 \ldots\ldots x_n$ are the regression model variables;

ε is the error of the model

The formulation and validation of the draft model are described in Section 4.3.2 (a).

3.4.2 Dimensional Analysis

For analyzing any phenomena, a dependent variable is typically a function of several independent variables (Srivastava *et al*., 2006):

$$X_1 = f(X_2, X_3, X_4, \ldots . X_n) \quad (3.2)$$

Where X_1 is dependent variable;

X_2, X_3…..X_n are independent variables.

These n variables involve one or more dimensions of force, length, time or mass. These variables may be categorized into a variety of dimensionless quantities (pi terms) using dimensional analysis (Yusuf, 2015). A functional equation can be written as:

$$\pi_1 = f(\pi_2, \pi_3, \pi_4, \ldots . \pi_n) \quad (3.3)$$

i. Modeling approach

The tool shape, speed, operating depth, and soil conditions all influence the draft needed to draw a subsoiler. Draft varies with the soil penetration resistance, shear strength, bulk density, soil-metal friction, speed of tractor, rake angle of the implement, depth of the subsoiler, soil cohesion, width of cut, adhesion, soil moisture content and soil internal friction (Yusuf, 2015). Thus, the relationship between the pertinent parameters may be summarized in the following form:

$$F = f(d, v, \alpha, \beta, \delta, \rho, w, \sigma, P, C, C_a) \quad (3.4)$$

Where:

F is draft (kN);

d is depth of operation (m);

α is the rake angle (◦);

β is the tilt angle (◦);

ρ is soil bulk density (kg m^{-3});

δ is the soil – metal friction angle (◦);

w is soil moisture content (%);

P is penetration resistance (kPa);

σ is soil shear strength (kPa);

C is cohesion (kPa).

ii. Assumptions used in the model development

The following assumptions were utilized in the model development to reduce the variables involved in draft determination:

a) Soils in the test plots are homogenous,
b) The angles of attack and tilt were zero,
c) Soil adhesion and soil metal friction angle were assumed negligible,
d) The operators are skilled in carrying out field operations.

A set of independent quantities which affect the dependent variable were identified. Dimensions of the independent variables and dependent variable were listed. The quantities were grouped into dimensionally independent subsets. The product of these subsets was reassembled in the form of dimensionless terms to be tested experimentally (Yusuf, 2015).

According to Buckingham π-theorem, the number of dimensionless quantities necessary to represent a connection between variables in a system is equal to the number of quantities involved minus the quantity's fundamental dimensions (Simonyan *et al.*, 2006). The following steps as outlined by Kawuyo (2011) were used to derive a relationship between various physical quantities:

a) The *n* physical quantities and the number of fundamental dimensions *(k)* were listed. Therefore, there are *(n-k)* π-terms. Selection of *k* of these quantities was done ensuring they were dimensionless, and the *k* quantities retained as repeating variables (Table 3.2).
b) The first π-term was expressed as the product of the chosen quantity to unknown exponent, and one other quantity to a known power;
c) One of the remaining variables was picked using the repeated variables to establish the next π-term. This step was repeated for the successive π-terms;
d) The unknown exponents for each π-term were solved by dimensional analysis.

Table 3.2: Pertinent variables affecting tillage draft

Symbol	Variable	Unit	Basic dimensions
F	Draft	kN	MLT^{-2}
$\boldsymbol{\rho}$	Bulk density	kg m^{-3}	ML^{-3}
C	Cohesion	kPa	$ML^{-1}T^{-2}$
$\boldsymbol{\sigma}$	Shear strength	kPa	$ML^{-1}T^{-2}$

W	Moisture content	%	-
P	Penetration resistance	kPa	$ML^{-1}T^{-2}$
D	Depth of cut	M	L

The formulation and validation of the dimensional analysis draft model are described in Section 4.3.2 (b).

3.4.3 Artificial Neural Networks

The ANN modeling was completed With MATLAB R2016a's environment. An input layer, a hidden layer and an output layer make up the three-layer structure that was chosen. Training was undertaken for networks for a specific number of epochs. A trial-and-error method was utilized to determine the ideal number of hidden layer neurons by modifying the network architecture and performing the training process numerous times until a satisfactory performance is reached,

Scaled conjugate gradient training techniques, gradient descent with momentum, and Levenberg-Marquardt were utilized to train the data gathered for this investigation. Of the total data, 70% were used to train the network, 15% to validate the model, and 15% to test the network.

If the hidden layer's number of neurons is sufficient, multilayer networks operate well. This is so because networks' performance is dependent on how many neurons are present in the hidden layer. Few neurons cause mismatch while many neurons result in overfitting which makes the network to lose its capability of generalization.

The network layers were connected using the linear, sigmoid, and hyperbolic tangent activation functions. The training of the network was stopped when no significant improvement in the performance was noted. The network that resulted in maximum efficiency and minimum error was selected as the final form of multilayer perceptron during training.

Normalization of the data was done using equation 2.35 to prevent the network from quick saturation of neurons. The ANN model formulation and validation are presented in Section 4.3.2.

3.4.4 Adaptive Neuro-Fuzzy Inference System

The ANFIS to simulate the draft force of the subsoiler during tillage was developed using the ANFIS toolbox of MATLAB R2016b software (The MathWorks Inc., 2012). Subsoiling depth,

bulk density, soil moisture content, cohesion, and soil strength were used as the factors influencing subsoiling draft. Grid partition structure was used to build the network.

Triangular, trapezoidal, generalized bell membership and Gaussian functions were used in representing the inputs. For every input, three membership functions were employed (high, medium and low) to reduce number of rules. A few of these rules based on the Takagi-Sugeno-Kang (TSK) fuzzy type are presented in Table 3.3.

A hybrid optimization strategy was used for network learning. The mean of the anticipated values was determined using the linear functions of each rule, and the model's final output was weighted according to these values. The minimum degree of membership of the inputs was equal to the weight of each rule.

Table 3.3: Selected rules in the draft prediction model

Inputs						**Output**
Depth	**Bulk Density**	**Cone index**	**Moisture content**	**Cohesion**	**Soil strength**	**Draft**
Low	Medium	Low	Medium	Low	Low	Low
Medium	Medium	Medium	High	High	High	High
High	Low	High	Medium	Medium	Medium	Medium
Medium	Low	Medium	Low	High	High	High
High	High	Low	Medium	High	High	High

Five levels made up the newly created ANFIS structure (Fig. 3.11). The model’s first layer was for the input variables (depth, moisture content, penetration resistance, bulk density, cohesion, and soil strength) membership functions.

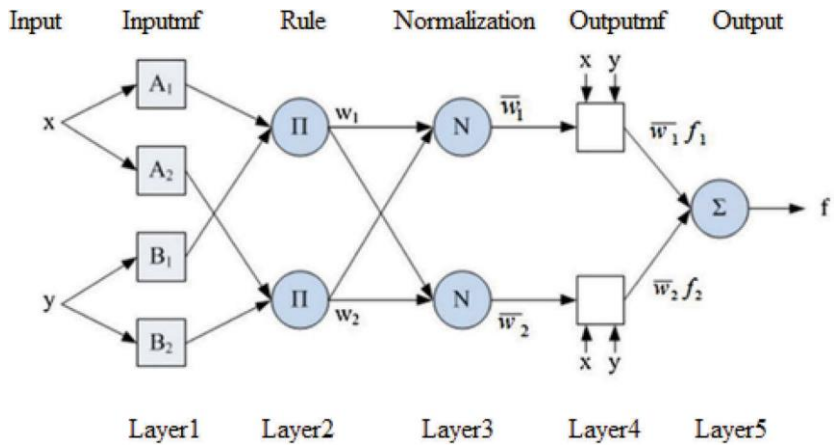

Figure 3.11: A typical structure of the Takagi-Sugeno model (Taşan & Demir, 2020)

The fuzzification layer (layer 2) contained 15 nodes and determined the weights for each MF. The fuzzy rule matching was done by the layer that contains the antecedent rules (layer 3). The fourth layer (consequent rule layer) that followed used the rules' inference to produce the output values. The backpropagation algorithm was used to determine the consequent rules.

Layer 5 was the output (inference rule) layer of subsoiling draft requirements. It merged the inputs and turned the classification's fuzzy output into a binary one. The linear functions of each rule calculated the average of the predicted values to provide the final output value of the model. Figure 3.12 illustrates the framework of the suggested ANFIS.

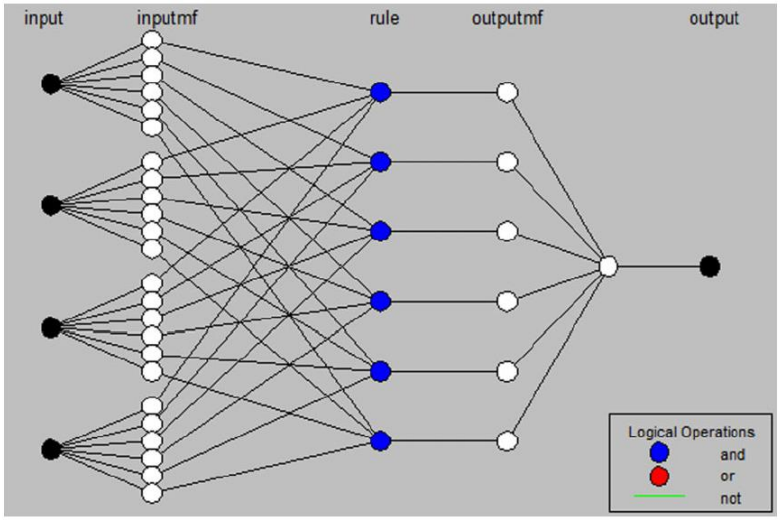

Figure 3.12: Configuration of the Sugeno type of ANFIS model used in the study

The model properties are presented in Table 3.4.

Table 3.4. Specifications of the developed ANFIS model

Parameter	Description
FIS structure	Sugeno
Number of inputs	7
Number of outputs	1
Accept ratio	0. 5
Reject ratio	0.15
Membership functions	4,4,4,4
Optimization method	Hybrid

Numerical ranges were used for depth (0 - 40 cm), bulk density (1256.76 – 1593.04 kg m^{-3}), soil moisture content (39.8 – 47.4%), penetration resistance (642.24 – 1538.64 kPa), cohesion (6.74 – 8.52 kPa), soil strength (121.10 – 157.07 kPa) and draft (1.30 – 10.78 kN). The data were divided into 15% for testing, 15% for validating, and 70% for training. The data and results of ANFIS modeling are presented in Section 4.3.2 (d).

3.4.5 Training

Training refers to the process of teaching a model to make predictions or decisions based on data. It's a crucial step in the development of machine learning algorithms and involved several key components:

i. **Data Preprocessing:** Raw data was preprocessed by data cleaning (removing duplicates or outliers), feature engineering (creating or transforming features to make them more informative), and data splitting (dividing the dataset into training, validation, and test sets).

ii. **Model Selection:** An appropriate machine learning algorithm or model architecture was selected depending on the nature of the problem and the characteristics of the data.

iii. **Training Data:** The training data was used to teach the model to make predictions. During training, the model learns the underlying patterns and relationships in the data. It iteratively adjusts its internal parameters to minimize a defined loss function, which measures the difference between its predictions and the actual target values.

iv. **Training Process:** The training process involved feeding the training data into the model, making predictions, and updating the model's parameters based on the calculated loss. This process continued for multiple iterations or epochs until the model's performance converged to an acceptable level.

v. **Hyperparameter Tuning:** ANN and ANFIS have hyperparameters (parameters that are not learned during training but are set before training begins). Hyperparameter tuning involved finding the best combination of hyperparameters to optimize the model's performance. Techniques like grid search, random search, and Bayesian optimization were commonly used.

3.4.6 Model validation, data analysis and model generalization

After training, the model's performance was assessed using a separate validation dataset. Various evaluation metrics were used to measure how well the model generalizes to unseen data. The optimal models were decided based on minimizing the error between model output and the measured data. Evaluation of predictive ability of the developed models were done using statistical parameters between measured and predicted draft through mean square error (MSE), root mean square error (RMSE), mean absolute error (MAE), mean absolute percentage error (MAPE) and the coefficient of determination (R^2).

The MSE was calculated according to equation 2.49 while the RMSE was determined by equation 2.50. The MAE was determined using equation 2.51 and the MAPE was calculated according to equation 2.52. The coefficient of determination (R^2) was determined using equation 2.53 and *Microsoft Excel*.

The data obtained were tested for normality. Analysis of variance for the datasets was conducted for experiments in a complete randomized factorial design. For pairwise comparisons at the 0.05 level of significance, Fisher's Least Significant Difference (LSD) was applied. To compare the measured and predicted drafts, a paired t-test was employed.

Once the model performs well on the validation set, it is evaluated on a separate test dataset that it has never seen before. This provides a final assessment of the model's generalization performance. Model generalization refers to the ability of a model to perform well on unseen data, beyond the

examples it was trained on. A model that generalizes well can make accurate predictions or classifications on new, previously unseen data that it hasn't encountered during its training phase.

CHAPTER FOUR
RESULTS AND DISCUSSION

4.1 Compaction effect of tractor wheel traffic intensity on soil properties

The studies conducted to ascertain the impact of wheel traffic-induced soil compaction on a subsoiler's draft requirements at plough depth (0 – 20 cm), hardpan layer (20 – 30 cm) and subsoil depth (30 – 40 cm) resulted to the findings and discussion in this chapter. The impact of wheel passes on soil properties and subsoiling draft was assessed before and after the runs by tractor. The soil properties were averaged over the three depths independently.

The results of the wheel passes on the pertinent soil properties considered in this study are summarized in Table 4.1 and discussed below Sections 4.1.1 and 4.2.2. From equation 3.1, one pass was estimated to impart a load of 25.6 kN on the soil.

4.1.1 Soil physical properties

a) Bulk density

It was found that the bulk density of the soil increased with increase of frequency of tractor wheel traffic and soil depth. As the number of passes and load increased, an increase in bulk density was seen in the 0 to 20 cm layer (Figure 4.1). For the untrafficked soil, the layer's lowest bulk density was determined to be 1290.67 kg m^{-3}, and its highest amount after five passes was 1579.54 kg m^{-3}. It was observed that 36% of this increase in bulk density was due to the initial wheel pass.

According to this study, bulk density was often greater in the 20 – 30 cm layer than in the 0 – 20 cm layer. With no wheel pass, it rose from 1318.03 to 1583.68 kg m^{-3} after five wheel passes. It was noted that 15% of the overall change in bulk density in this stratum was attributable to the bulk density change caused by the first wheel pass.

Overall, the bulk density of soil in the 30 - 40 cm layer was higher than that of the topsoil. With no wheel traffic, it was observed to rise from 1336.96 to 1592.94 kg m^{-3} after five wheel passes. The change in bulk density brought about by tractor wheel passes was accounted for to 50% by the first wheel pass.

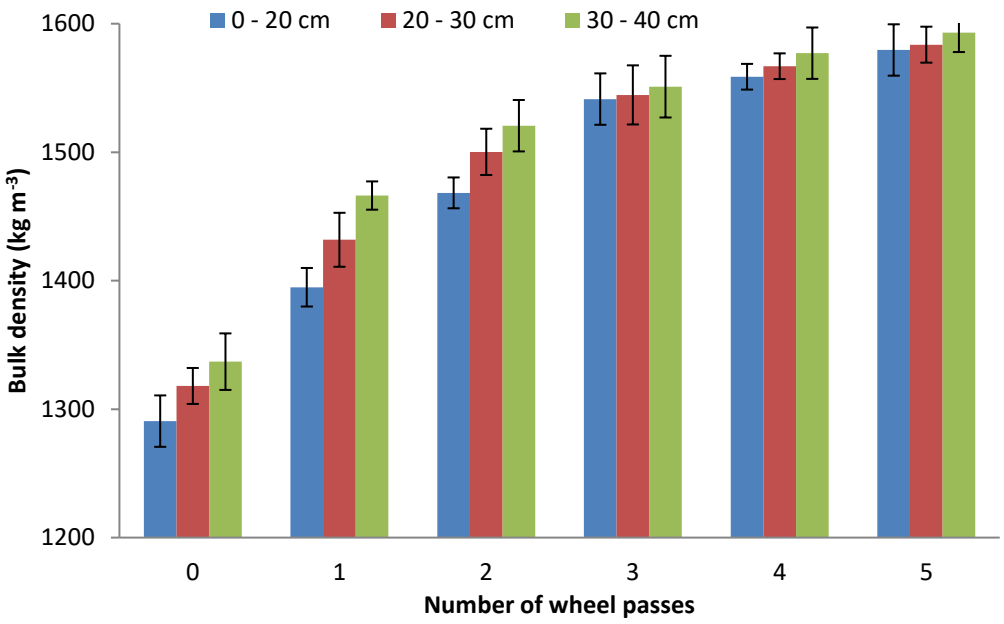

*One wheel pass imparted a vertical normal load of 25.6kN

Figure 4.1: Bulk density as a function of wheel traffic frequency and soil depth

This study found that the number of wheel passes and subsoiling depth affected the degree of soil compaction. The rise in bulk density that was seen as traffic intensity increased revealed that compaction is a dynamic process that fluctuates with the frequency of wheel passes.

Because of the pressing of soil particles closer together and a consequent reduction in pore spaces, many wheel passes result in a decrease in soil volume. The fact that bulk density increased as depth increased suggested that soil compaction is dynamic and is conveyed to lower depths via the soil matrix. These findings agreed with those of Agele et al. (2016), who found a strong correlation between an increase in bulk density and traffic intensity.

Tractor wheel passes, depth of subsoiling, and their interaction were not found to significantly affect bulk density at the 5% level of confidence, according to an analysis of variance (ANOVA) (Table 4.2). It was also shown that further wheel passes did not significantly alter the bulk density.

Table 4.1: Soil properties for various wheel passes and depths

Wheel passes		0	1	2	3	4	5
Normal load (kN)		**0**	**26**	**51**	**77**	**102**	**128**
				Bulk density (kg m^{-3})			
Depth (cm)	0 – 20	1290.67 ±20	1394.87 ± 15	1468.33 ± 12	1541.32 ± 20	1558.71 ± 10	1579.54 ± 20
	20 – 30	1318.03 ± 14	1431.81 ± 21	1500.23± 18	1544.58 ± 23	1566.91 ± 10	1583.68 ± 14
	30 – 40	1336.96 ± 22	1466.24 ± 11	1520.61± 20	1550.99 ± 24	1577.04 ± 20	1592.94 ± 15
				Moisture content (%)			
	0 – 20	41.77 ± 2.58	36.71 ± 1.69	34.37 ± 0.53	32.65 ± 1.05	32.32 ± 0.86	32.92 ± 1.03
	20 – 30	42.79 ± 2.82	37.22 ± 3.30	35.16 ± 2.80	32.89 ± 2.25	32.86 ± 3.02	32.39 ± 3.28
	30 – 40	42.07 ± 1.23	37.78 ± 2.20	36.85 ± 0.54	34.95 ± 1.03	33.56 ± 1.36	33.49 ± 1.41
				Porosity (%)			
	0 – 20	52.57 ± 1054	47.36 ± 1.67	44.59 ± 3.52	42.39 ± 2.14	41.18 ± 2.06	41.28 ± 1.99
	20 – 30	50.26 ± 1.23	45.97 ± 1.40	42.27 ± 1.98	41.88 ± 1.55	40.41 ± 2.00	40.24 ± 2.68
	30 – 40	49.55 ± 1.56	44.67 ± 2.42	41.94 ± 2.52	41.47 ± 2.22	40.49 ± 2.40	39.89 ± 3.31
				Infiltration rate (mm h^{-1})			
	0 – 20	15.30 ± 0.31	10.67 ± 0.22	7.70 ± 0.11	5.67 ± 0.33	6.04 ± 0.84	3.37 ± 0.83
	20 – 30	14.20 ± 0.78	9.10 ± 0.11	6.63 ± 0.37	4.57 ± 0.10	4.14 ± 0.61	2.97 ± 0.29
	30 – 40	13.47 ± 0.30	8.22 ± 0.35	6.07 ± 0.50	4.56 ± 0.13	3.14 ± 0.51	3.35 ± 0.88

		Hydraulic conductivity (mm h^{-1})					
	0 – 20	5.60 ± 0.06	4.70 ± 0.16	3.40 ± 0.14	2.60 ± 0.07	1.80 ± 0.05	0.90 ± 0.11
	20 – 30	3.90 ± 0.17	2.20 ± 0.64	2.20 ± 0.19	1.90 ± 10.05	1.70 ± 0.14	0.60 ± 0.12
	30 – 40	1.80 ± 0.12	1.70 ± 0.25	1.50 ± 0.32	0.50 ± 0.07	0.30 ± 0.09	0.20 ± 0.30

The results show that a higher change of soil bulk density occurs with the first wheel pass, which is consistent with the findings of Wang et al. (2022), Horn et al. (2003), and Ampoorter et al. (2007), but not with Picchio et al. (2012), who reported that soil deformation resulting from multiple wheel passes was greater for the first three runs than for the subsequent ones. Wang et al. (2022) showed that when the number of uninterrupted passes for a heavy axle-load tractor is lower than seven, there was greater rise in soil bulk density.

Table 4.2: ANOVA for bulk density

Source of variation	**Type III *SS***	***df***	***MSS***	***F***	***p***
Model	441.097	18	24.505	7184.007	.201
Wheel passes	1.827	5	0.365	107.106	.234
Depth	0.089	2	0.045	13.078	.029
Wheel passes * Depth	0.024	10	0.002	0.697	.727
Error	0.614	180	0.003		
Total	441.711	198			

It should be cautioned, however, that although the wheel passes subsequent to the first one have a lower effect on bulk density, additional passes may inhibit plant growth and increase tillage draft requirements. Although the findings of this study suggest that compaction mainly affect the top layers of soil that are cultivated, the adverse effects of compaction are usually alleviated by subsoiling. However, soil compaction effects are intensified by repeated wheel passes by the tractor, and the subsoil is affected by the resulting stresses. It is difficult to alleviate subsoil compaction and they persist for longer periods.

b) Moisture content

Figure 4.2 relates moisture content and frequency of tractor wheel traffic at various depths. The initial soil moisture content before wheel traffic application were 42% at 0 – 20 cm depth, 43% at 20 - 30 cm depth and 42% at 30 - 40 cm depth. The moisture content in the three soil layers decreased marginally with wheel traffic intensity but increased with depth. The highest moisture content of 42% was measured at the 30 - 40 cm depth for no traffic conditions whereas the lowest value of 32% was noted on the 0 - 20 cm layer after 4 wheel passes.

After five wheel passes, there was a 10% reduction in the moisture content of the 0 - 20 cm layer, from 42% for untrafficked soil to 32%. Following five wheel passes, the initial wheel pass caused a 40% drop in soil moisture. For any given number of wheel passages, the moisture content was often greater between 20 - 30 cm than the layers above. The moisture content decreased by 10% after 5 passes.

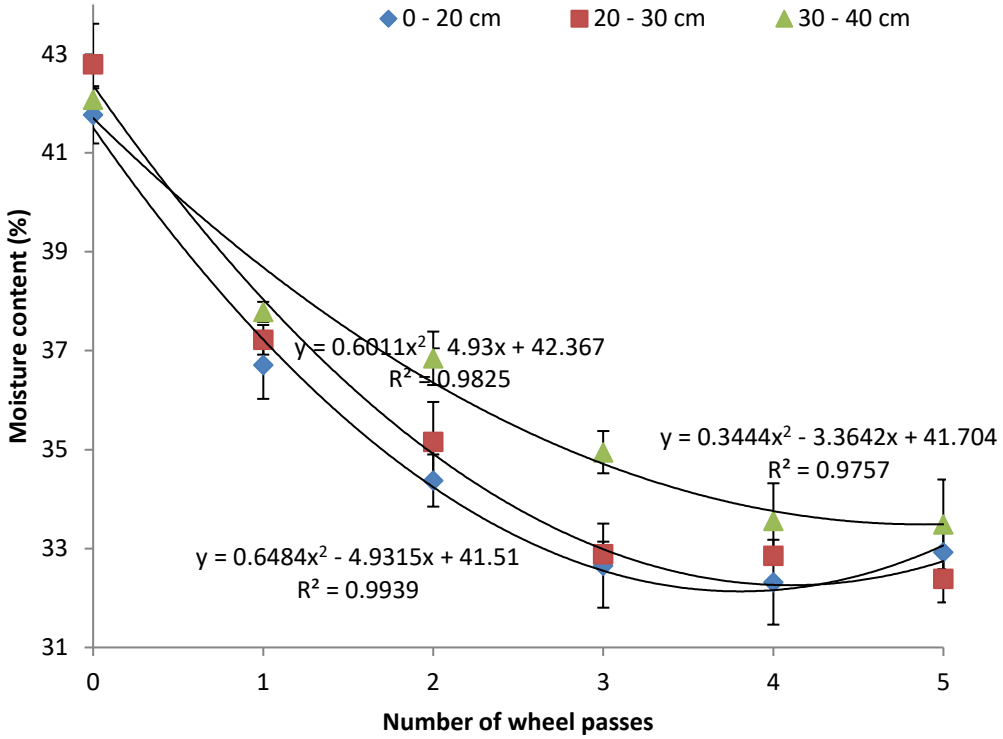

*One wheel pass imparted a vertical normal load of 25.6 kN

Figure 4.2: Soil moisture content variation with wheel passes and soil depth

In the 30 - 40 cm depth layer, moisture content reduced from 42% for the undisturbed soil to 33% after five wheel passes. The 9% decrease in moisture content in this layer was less compared to that of the top layers probably because larger pore spaces were more compressed in the top layer than this layer due to soil compaction.

At the 5% level of confidence, the ANOVA (Table 4.3) showed that both wheel passes and depth had a significant impact on soil moisture content. Nevertheless, the interaction between the number of wheel passes and soil depth was not statistically significant. The outcomes showed a substantial

decrease in water content with the number of passes ($p < 0.05$). This may be attributed to less pore spaces available for water retention in compacted soils.

Table 4.3:ANOVA for moisture content

Source of variation	Type III *SS*	*df*	*MSS*	*F*	*p*
Model	254726.885	18	14151.494	3207.757	.000
Wheel passes	2147.848	5	429.570	97.372	.000
Depth	60.405	2	30.202	6.846	.001
Wheel passes * Depth	37.329	10	3.733	0.846	.585
Error	794.097	180	4.412		
Total	255520.981	198			

The results of this investigation concur with those of Tan et al. (2008) and Acquah and Chen (2022). According to Tan et al. (2008), vehicle traffic compacting forest soil caused an 11% decrease in soil moisture content. The initial wheel pass decreased the moisture level by around 5% in every depth measured. The moisture content was reduced by 17.4% after just one tractor pass in a spring-tine tillage area, according to Acquah and Chen (2022), who conducted their studies in a sandy loam soil.

The rise in soil bulk density which reduces soil porosity and infiltration rate, is what Carter and Shaw (2002) cited as the cause of the drop in moisture content with wheel pass frequency. Once the third wheel passed, it was also seen that the moisture level did not greatly drop. This finding is consistent with those reached by Horn et al. 2004 and Ampoorter et al. (2007), who found that successive wheel passes subsequent to the initial one does not significantly change the status of soil compaction.

c) Porosity

It was observed that when compaction levels and subsoiling depth increased, the porosity decreased (Figure 4.3). For untrafficked soil, the maximum porosity of 53% was found in the 0 - 20 cm layer, whereas the lowest porosity was found in the 30 - 40 cm layer after five wheel passes.

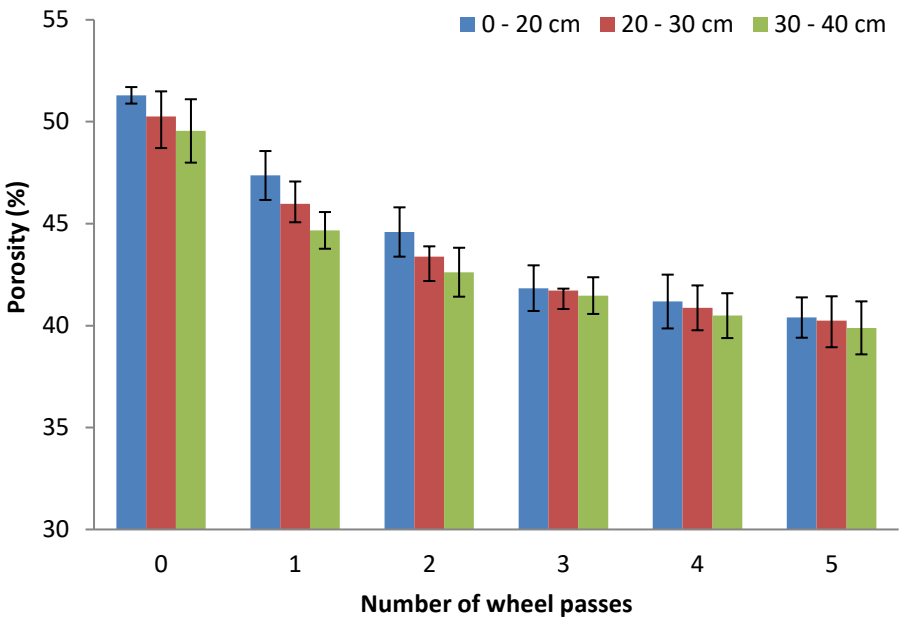

*One wheel pass imparted a vertical normal load of 25.6 kN

Figure 4.3: Porosity as affected by wheel passes and depth

The porosity of the 0 - 20 cm layer was observed to drop from 53% with no wheel pass to 41% after five wheel passes. It was revealed that the first wheel pass contributed 50% of the overall change in porosity brought on by five wheel passes.

For any given number of wheel passes, the porosity of the 20 - 30 cm layer was typically lower than that of the 0 - 20 cm layer. After five wheel passes, the porosity decreased from 50% in no traffic to 40%. It was shown that the initial wheel pass was responsible for 50% of the overall change in porosity in this stratum.

The 30 - 40 cm layer showed a decrease in porosity with increasing wheel passes. The least porosity noted in this layer was 40% after 5 passes while maximum porosity of 50% was noted in the untrafficked soil. As was observed with the upper soil layers, there was negligible reduction in porosity after the third wheel pass.

At the 5% level of confidence, it was determined that the number of wheel passes and soil depth significantly impacted overall porosity. Increasing traffic wheel passes reduced the total porosity significantly ($p < 0.05$) in all the soil depths sampled (Table 4.4). However, the study established

no significant change on the soil porosity after the second wheel passage. Wheel traffic intensity and depth's interaction had no significant influence ($p < 0.05$).

Table 4.4: ANOVA for porosity

Source of variation	Type III *SS*	*df*	*MSS*	*F*	*p*
Model	382623.995	18	21256.889	4376.195	.001
Wheel passes	2601.287	5	520.257	107.106	.000
Depth	127.046	2	63.523	13.078	.002
Wheel passes * Depth	33.838	10	3.384	0.697	.727
Error	874.330	180	4.857		
Total	383498.325	198			

This reduction in porosity due to compaction mainly affects the soil macropores (Ampoorter et al., 2007) and can be attributed to the conversion of the soil macropores to micropores as the wheels press the soil. The reduction has been reported to amount to 50% to 60% in forest soils (Demir et al., 2007; Frey et al., 2009; Solgi & Najafi, 2014). These values are comparable to the change of 40% to 50% obtained in this study.

d) Infiltration rate

The variation of infiltration rate with wheel passes at different depths are presented in Table 4.1. From Figure 4.4, the infiltration rate decreased with increase in wheel pass frequency and the vertical load. However, the decrease was less rapid after the second wheel pass. Infiltration rate was also observed to reduce with increase in depth.

With an increase in wheel traffic intensity, the infiltration rate in the 0 - 20 cm deep zone often decreased. This stratum with no wheel passes had the greatest infiltration rate of 15.30 mm h^{-1} throughout the trial. Five wheel passes later, the infiltration rate was down to 3.37 mm h^{-1} with 39% of the decline in infiltration rate being attributed to the first wheel pass. The infiltration rate dropped by 19% after the third wheel pass.

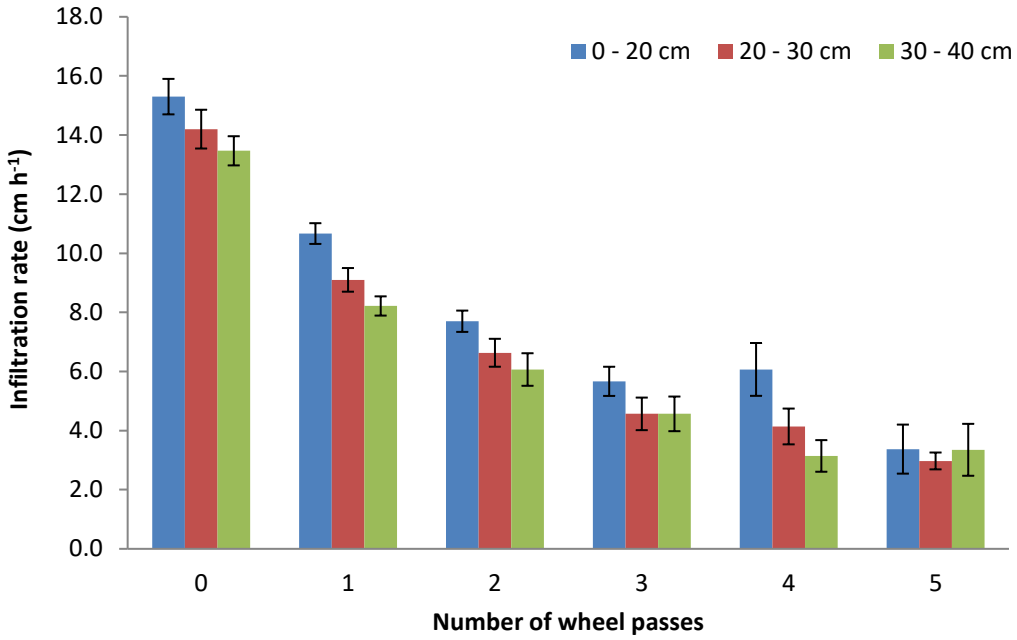

*One wheel pass imparted a vertical normal load of 25.6kN

Figure 4.4: Variation of infiltration rate with wheel passes and soil depth

In the 20 - 30 cm soil depth, the infiltration rate was lower compared to that in the 0 - 20 cm layer for any given wheel pass. It decreased from a high of 14.20 mm h^{-1} at no wheel pass to 2.97 mm h^{-1} after five wheel passes. The first wheel pass caused 19% of the change in infiltration rate.

The infiltration rate in the 30 – 40 cm was generally observed to be lower than the two upper layers. It decreased from 13.47 mm h^{-1} with no wheel pass, to the lowest value of 3.35 mm h^{-1} after five wheel passes. The initial wheel pass was seen to account for 52% of the reduction in infiltration rate.

The ANOVA (Table 4.5) performed on the infiltration rate data revealed that wheel traffic intensity, soil depth and their interactions significantly ($p < 0.05$) affected infiltration rate. The reduced infiltration rate with number of wheel passes and depth of subsoiling could be attributed to the reduction in macropores as the soil is compacted (Zhang et al. 2006).

The findings in this study of 58% reduction in infiltration rate in the top soil layer after the fifth is lower than that observed by Al-Ghazal (2002) of 69%. This could have been due to the different

tractor used in both studies. Ramezani et al. (2017) reached a conclusion that compaction reduced total pore volume thereby reducing infiltration rate.

Table 4.5: ANOVA for infiltration rate

Source of variation	Type III *SS*	*df*	*MSS*	*F*	*p*
Model	789.11	17	46.418	140.13	.001
Wheel passes	754.632	5	150.926	455.62	.001
Depth	26.418	2	13.209	39.88	.001
Wheel passes * Depth	8.0611	10	0.806	2.43	.025
Error	11.925	36	11.925	0.332	
Total	801.036	53	801.036		

e) Saturated hydraulic conductivity

Table 4.2 presents the results of the determination of impact of wheel passes on the saturated hydraulic conductivity at various depths. Figure 4.5 shows that the saturated hydraulic conductivity declined with increasing wheel passes and sample depth. The top soil layer showed the maximum saturated hydraulic conductivity of 5.60 mm h^{-1} with no wheel pass and the lowest value of 0.29 mm h^{-1} with five wheel passes in the layer 30 - 40 cm.

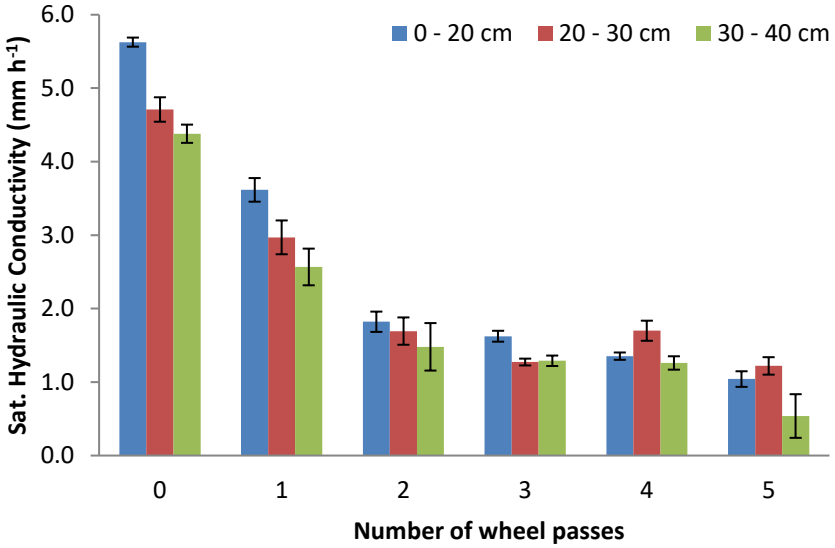

*One wheel pass imparted a vertical normal load of 25.6kN

Figure 4.5: Saturated hydraulic conductivity as affected by wheel passes and depth

The saturated hydraulic conductivity in 0 – 20 cm depth zone was observed to reduce with increase in wheel traffic intensity. The highest saturated hydraulic conductivity recorded in this layer was 5.63 mm h^{-1} observed with no wheel passes while the lowest value was 1.54 mm h^{-1} after five wheel passes. One wheel pass was responsible for 19% of the variation in saturated hydraulic conductivity.

The saturated hydraulic conductivity declined with wheel traffic intensity and was lower in the 20 - 30 cm of soil than it was in the 0 - 20 cm. With no wheel pass, a maximum saturated hydraulic conductivity of 3.90 mm h^{-1} was noted in this stratum. After five wheel passes, this value dropped to 0.60 mm h^{-1}. The initial wheel pass was responsible for 52% of the overall change in hydraulic conductivity in this stratum.

The saturated hydraulic conductivity was lower in 30 - 40 cm layer than the 0 - 20 cm and 20 - 30 cm layers. The saturated hydraulic conductivity decreased with increase in number of wheel passes from 1.80 mm h^{-1} for the no wheel pass treatment to 0.20 mm h^{-1} after five wheel passes.

Wheel passes, soil depth, and their interactions were shown to significantly affect saturated hydraulic conductivity ($p < .05$) using an ANOVA (Table 4.6). Wheel compaction may be the cause of the observed drop in saturated hydraulic conductivity with more wheel passes. According to Zhang et al. (2006), tractor passes reduced the hydraulic conductivity of a soil. This is supported by the results of this investigation.

Table 4.6: Saturated hydraulic conductivity ANOVA

Source of variation	**Type III *SS***	***df***	***MSS***	***F***	***p***
Model	1245.579	15	83.039	1141.463	.002
Wheel passes	330.957	4	82.739	1137.350	.001
Depth	11.904	2	5.952	81.820	.004
Wheel passes * Depth	7.791	8	0.974	13.386	.003
Error	12.003	165	0.073		
Total	1257.582	180			

The reduction in saturated hydraulic conductivity with tractor wheel passes could be attributed to reduced macropores and increased bulk density of the soil with increased wheel intensity. Similar findings were reported by Mossadeghi-Björklund et al. (2016) who observed that compaction reduced saturated hydraulic conductivity of soil by 99% after 8 wheel passes while in this study a reduction of 73% was realized after 5 passes.

4.1.2 Soil mechanical properties

a) Penetration resistance

The results of penetration resistance as affected by wheel traffic in different soil layers are given in Figures 4.6. The initial penetration resistances of the soil before wheel traffic treatments were 0.64 MPa, 0.70 and 0.74 MPa at 0 - 20, 20 - 30 and 30 - 40 cm depths respectively (Table A1). In the 0 - 20 cm layer, the penetration resistance increased from 0.68 MPa in undisturbed soil to 1.23 MPa after five wheel passes. The first wheel pass resulted in a 15% change in soil penetration resistance.

These findings revealed that penetration resistance was often higher in the 20 - 30 cm layer than in the 0 - 20 cm layer. It increased from 0.70 MPa at no wheel pass to 1.09 MPa after five wheel passes, with the first wheel pass accounting for 15% of the overall change in penetration resistance. The soil's penetrating resistance was often stronger in the 30 - 40 cm layer than in the upper levels. It rose from 0.74 MPa when there was no wheel traffic to 1.34 MPa after five wheel passes.

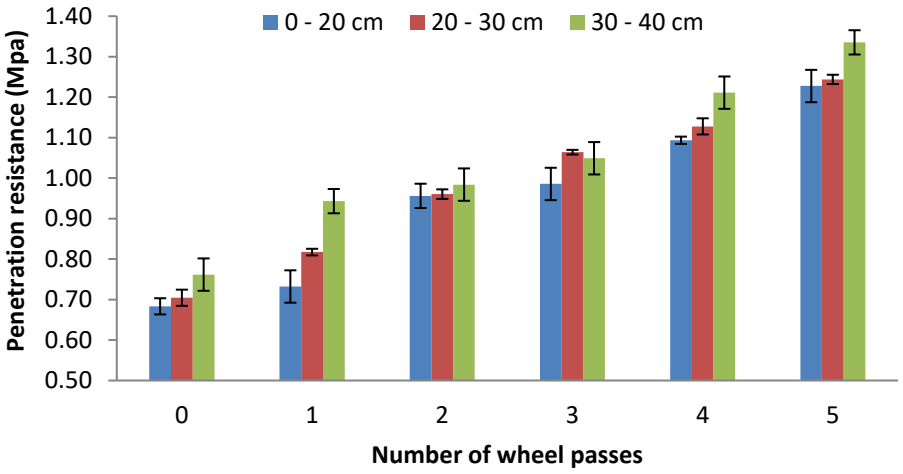

*One wheel pass imparted a vertical normal load of 25.6kN

Figure 4.6: Variation of penetration resistance with depth and wheel passes

Table 4.7: Soil properties for various wheel passes and depths

Wheel passes		**0**	**1**	**2**	**3**	**4**	**5**
Normal load (kN)		**0**	**26**	**51**	**77**	**102**	**128**
		Penetration resistance (MPa)					
Depth (cm)	0 – 20	0.68 ± 0.00	0.73 ± 0.01	0.96 ± 0.01	0.99 ± 0.01	1.09 ± 0.01	1.23 ± 0.01
	20 – 30	0.70 ± 0.02	0.82 ± 0.01	0.96 ± 0.01	1.06 ± 0.01	1.13 ± 0.00	1.24 ± 0.01
	30 – 40	0.76 ± 0.04	0.94 ± 0.01	0.98 ± 0.01	1.05 ± 0.04	1.21 ± 0.00	1.34 ± 0.01
		Cohesion (kPa)					
Depth (cm)	0 – 20	6.84 ± 0.51	7.05 ± 0.29	7.10 ± 0.19	7.28 ± 0.16	7.32 ± 0.26	8.05 ± 0.17
	20 – 30	7.15 ± 0.59	7.14 ± 0.11	7.40 ± 0.33	7.72 ± 0.24	7.77 ± 0.28	8.14 ± 0.11
	30 – 40	7.03 ± 0.20	7.27 ± 0.28	7.29 ± 0.14	7.84 ± 0.13	8.08 ± 0.42	8.42 ± 0.11
		Angle of internal friction					
Depth (cm)	0 – 20	30 ± 0.7	30 ± 1.4	30 ± 0.7	32 ± 0.0	33 ± 1.2	31 ± 1.6
	20 – 30	30 ± 1.0	31 ± 1.1	31 ± 1.5	32 ± 1.2	34 ± 1.6	34 ± 1.5
	30 – 40	31 ± 0.9	32 ± 0.6	32 ± 1.2	33 ± 1.6	34 ± 0.9	35 ± 0.6
		Shear Strength (kPa)					
Depth (cm)	0 – 20	121.20 ± 3.27	125.13 ± 7.37	128.98± 3.77	140.05± 7.99	142.74 ± 5.37	146.86 ± 6.87
	20 – 30	124.58 ± 4.73	131.39 ± 5.58	134.64 ± 7.71	142.29 ± 6.83	148.89± 8.60	149.75± 7.33
	30 – 40	128.60 ± 4.35	136.56 ± 2.91	138.52 ± 6.07	146.32 ± 6.61	154.09 ± 5.17	156.97 ± 3.65

The ANOVA (Table 4.8) showed that at the 5% level of confidence, the change in penetration resistance caused by soil depth, the number of wheel passes, and their interaction were not significant. According to the findings, the penetration resistance was not significantly different across wheel passes after the initial wheel pass.

Table 4.8: ANOVA for penetration resistance

Source of variation	**Type III *SS***	***df***	***MSS***	***F***	***p***
Model	2203446.867	18	122413.715	685.707	.120
Wheel passes	76210.496	5	15242.099	85.379	.261
Depth	4209.589	2	2104.794	11.790	.007
Wheel passes * Depth	1505.839	10	150.584	0.844	.587
Error	35347.361	198	178.522		
Total	2238794.228	216			

Because of the increased penetration resistance at the deeper soils due to earlier land uses, a hard pan may have formed. The greater penetration resistance with soil depth can be attributed to less tillage disturbance. Also, effective stress transfer to the lower depths in compacted soils may have contributed to the rise in penetration resistance with depth. The results corroborate Taghavifar and Mardani's (2014a) assertion that wheel loads and many passes increased soil penetration resistance.

In contrast to Odey (2018), who measured a sandy loam soil's penetration resistance at 4.00 MPa, this study's maximum penetration resistance of 1.34 MPa was lower. It is likely that the field's past cultivation contributed to the reduced penetration resistance found in this research. In many tree species, soil penetration resistance greater than 2.5 MPa limits root development, according to Macr et al. (2017). Five wheel passes were found to be insufficient in this study's findings to significantly increase the silt loam soils' resistance to penetration.

b) Cohesion

It was shown that normal load and traffic intensity caused a progressive increase in soil cohesion (Figures 4.7). The cohesion value ranged from 6.84 kPa in the top 20 cm of soil to 8.42 kPa in the 30 to 40 cm depth during the course of five wheel passes.

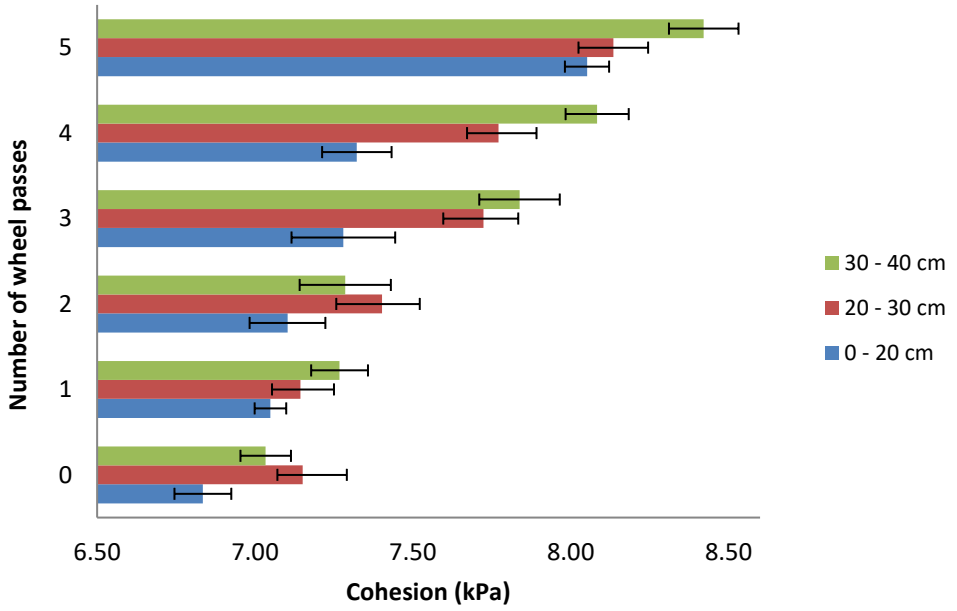

*One wheel pass imparted a vertical normal load of 25.6kN

Figure 4.7: Effect of wheel traffic intensity and depth on soil cohesion

After five wheel passes, the soil's cohesion increased from 6.84 kPa with no wheel activity to 8.05 kPa. The first wheel pass was responsible for 17% of the change in soil cohesion brought on by five wheel passes.

The soil cohesion of the 20 - 30 cm layer was found to be greater than that of the overlying layer. It rose from 7.15 kPa when no wheel passes were made to 8.14 kPa after five wheel passes. Soil cohesion was observed to be greater in the 30 - 40 cm layer than in the two above layers. After five wheel passes, it rose from 7.03 kPa for un-trafficked soil to 8.42 kPa.

The ANOVA found no significant change in soil cohesiveness with depth, traffic intensity, or their interactions at the 5% level of confidence (Table 4.9). The observed rise in soil cohesion with increasing traffic might be ascribed to small particles filling big holes in the soil caused by wheel deformation of larger particles. Gravitational contact between soil particles and water content is the primary source of cohesion.

Table 4.9:ANOVA for cohesion

Source of variation	Type III *SS*	*df*	*MSS*	*F*	*p*
Model	10140.768	18	563.376	6803.155	.123
Wheel passes	29.149	5	5.830	70.398	.158
Depth	4.670	2	2.335	28.196	.237
Wheel passes * Depth	1.950	10	0.195	2.355	.013
Error	13.415	162	0.083		
Total	10154.184	180			

The increase of soil cohesion with depth was also reported by Secco et al. (2013). However, the values of cohesion they observed of 19 kPa to 67 kPa were higher than those observed in this study. This could be ascribed to the difference in the soils used in the two studies.

c) Angle of internal friction

Figure 4.8 present the findings of experiments for determining the angle of internal friction (φ) as impacted by wheel passes (normal load) and subsoiling depth. The undisturbed soil in the 0 - 20 cm layer had the lowest angle of internal friction of 30°. After five wheel passes, the 30 - 40 cm layer had a higher value of 35°.

The angle of internal friction was seen to rise from 30° with no wheel traffic to 31° after five wheel passes in the 0 – 20 cm layer. Hence, the angle of internal resistance was not significantly changed with wheel frequency in this layer. Angles of internal friction in the 20 - 30 cm layer ranged from 30° for untrafficked soil to 34° after five wheel passes, somewhat greater than in the 0 - 20 cm layer. About 25% of the measured change in the soil angle of internal resistance was caused by the first wheel pass.

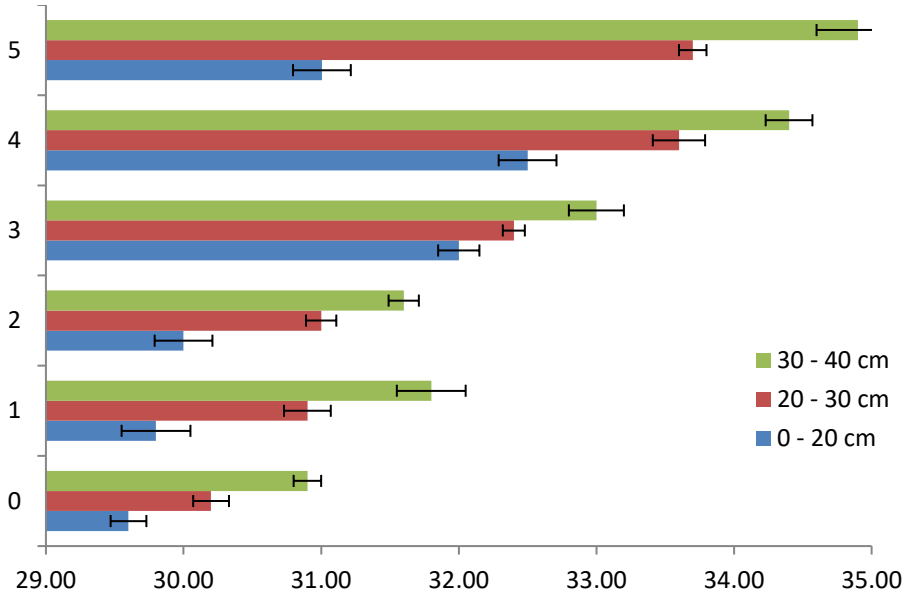

*One wheel pass imparted a vertical normal load of 25.6kN

Figure 4.8: Angle of internal friction variation with number of wheel passes and depth

The internal angle of friction of the 30 - 40 cm layer was greater than that of the two layers above it. The undisturbed soil had a lower value of 31°, whereas the disturbed soil had a value of 35°after five wheel passes. The initial wheel pass caused 25% of the change in internal friction angle.

The angle of internal friction caused by traffic wheel passes, sample depth, and their interactions were not significantly different, according to the ANOVA (Table 4.10).

Table 4.10: ANOVA for angle of internal friction

Source of variation	Type III *SS*	*df*	*MSS*	*F*	*p*
Model	184505.800	18	10250.322	6690.380	.212
Wheel passes	362.978	5	72.596	47.383	.105
Depth	73.644	2	36.822	24.034	.045
Wheel passes * Depth	5.089	10	0.509	0.332	.971
Error	248.200	162	1.532		
Total	184754.000	180			

Because the internal friction angle changes mostly due to clay content and is independent of the structural condition of a soil and does not display spatial variation on the ground, there was a little fluctuation in the angle of internal friction with traffic wheel passes and soil depth.

The results of this study on angle of internal friction are consistent with those of Secco et al. (2013), who found no appreciable difference in angle of internal friction with compaction in the studied soils.

d) Shear strength

Figure 4.9 relates shear strength and frequency of tractor wheel traffic at various depths. The data show that the soil shear strength often increased with depth and wheel passes. Untrafficked soils at a depth of 0 – 20 cm had the lowest shear strength, whereas sub-soils had the highest shear strength, at 157 kPa (30 – 40 cm depth).

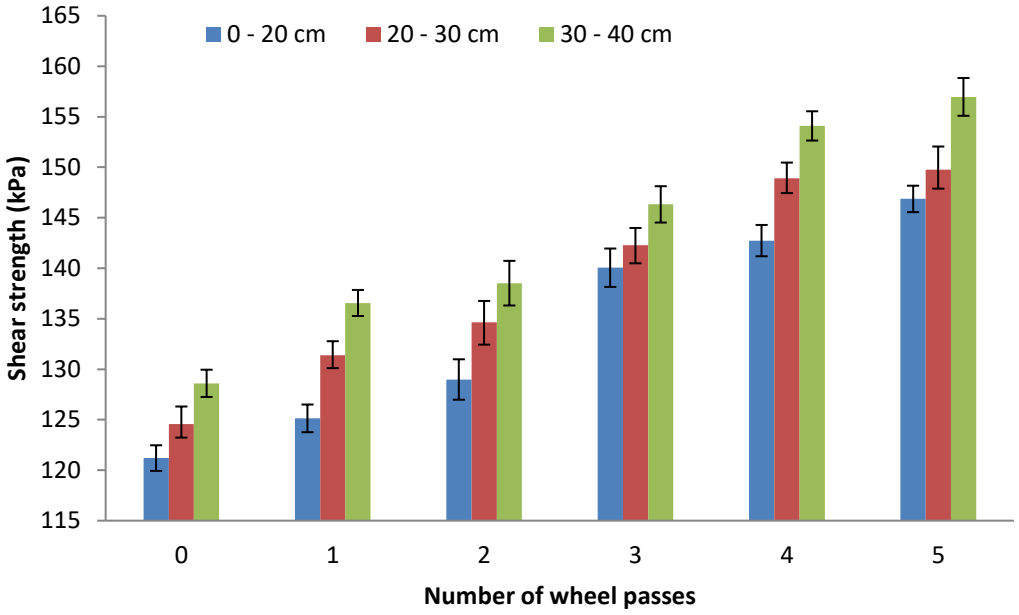

*One wheel pass imparted a vertical normal load of 25.6kN

Figure 4.9: Variations in shear strength with number of wheel passes and depth

The least shear strength in the 0 - 20 cm soil layer was determined to be 121 kPa for the no wheel pass treatment. Soil shear strength rose as wheel traffic intensity increased. After 5 passes, the greatest shear strength measured was 147 kPa. The first wheel pass raised soil shear strength by 15% of the increase observed for five wheel passes.

For any given number of wheel passes, the shear strength of soil in the 20 -30 cm layer was often greater than that in the 0 - 20 cm layer. During no traffic circumstances, a value of 125 kPa was reported as the lowest. With each wheel pass, the soil's strength rose, reaching 150 kPa after five passes.

It was found that the shear strength for the 30 to 40 cm layer was higher than for either the 0 - 20 or 20 - 30 cm levels for any given traffic intensity. After five wheel passes, the soil's shear strength rose from 129 to 157 kPa.

At the 5% level of confidence, the ANOVA (Table 4.11) showed that neither the subsoiling depth, the number of wheel passes, nor their interactions substantially influenced soil shear strength. The fact that stresses are effectively transferred to lower soil layers when soils are compacted may be the cause of the increase in soil strength with depth. Similar findings were reached by Battiato et al. (2013), who demonstrated that increasing the number of wheel passes on the same track enhanced the depth of stress distribution on mineral soils.

Table 4.11: ANOVA for soil strength

Source of variation	**Type III *SS***	***df***	***MSS***	***F***	***p***
Model	19132.94	17	1125.47	31.26	.341
Wheel passes	16352.5	5	3270.49	90.84	.035
Depth	2625.75	2	1312.87	36.47	.429
Wheel passes * Depth	154.734	10	15.4734	0.43	.930
Error	5832.28485	162	36.0018		
Total	24965.2249	179			

4.2 Subsoiling draft as affected by wheel traffic and depth

4.2.1 Effect of wheel traffic soil compaction on subsoiling draft

The results of the net draft requirement of subsoiling as affected by wheel traffic intensity are presented in Table 4.12. The tractor's mean rolling resistance with the subsoiler was found to be 1.17 kN. The study established that the draft requirement of the subsoiler increased with both wheel traffic intensity and depth (Figure 4.10).

The compaction of the 0 - 20 cm layer due to multiple wheel passes resulted in the lowest draft requirement recorded of 1.40 kN for no wheel pass treatment. The draft increased linearly with wheel passes to a maximum of 6.43 kN in the five-wheel pass treatment. The first wheel pass resulted in 68% increase in draft.

Table 4.12: Summary of results on draft and specific draft measurements

	Depth (cm)	**Wheel traffic intensity (passes)**					
		0	**1**	**2**	**3**	**4**	**5**
Draft (kN)	0 – 20	1.40	2.35	3.38	4.60	5.12	6.43
	20 – 30	2.83	5.19	5.73	6.08	7.96	8.09
	30 – 40	4.99	6.00	7.22	8.53	9.83	10.68
Specific draft (kN m^{-2})	0 – 20	43.8	73.4	105.6	143.8	160.0	200.9
	20 – 30	70.8	129.8	143.3	152.0	199.0	202.3
	30 – 40	104.0	125.0	150.4	177.7	204.8	222.5

At any given wheel pass, the subsoiling draft for the 0 - 20 cm layer was often higher than that for the 20 - 30 cm layer. Untrafficked soil had the least draft (2.83 kN), while after a five-wheel pass, draft increased to 8.09 kN.

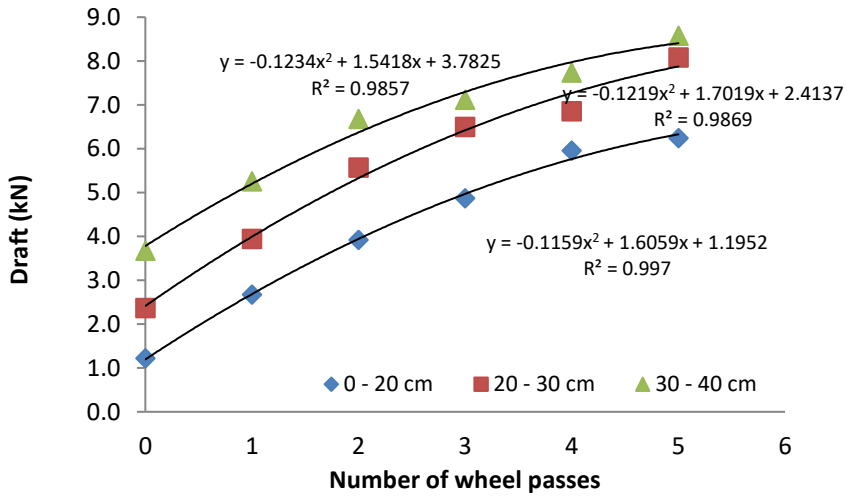

*One wheel pass imparted a vertical normal load of 25.6kN

Figure 4.10: Subsoiling draft as affected by wheel passes and soil depth

The 30 - 40 cm depth required a larger draft than the 0 - 20 cm and 20 - 30 cm layers for any given number of wheel passes. The draft requirement for subsoiling undisturbed soil was recorded as 4.99 kN which increased after five wheel passes to 10.68 kN.

At the 5% level of confidence, the ANOVA revealed that subsoiling depth, wheel passes, and their interactions significantly impacted subsoiling draft (Table 4.13). Draft requirement was noted to significantly increase ($p < .05$) with wheel traffic intensity for all subsoiling depths. The rise in draft with more wheel passes can be ascribed to greater soil strength as wheel compaction intensity increases. The higher draft recorded for subsoiling deeper layers was due to the greater volume of soil mass to be disturbed as the shank got deeper into the soil.

Table 4.13: ANOVA for draft

Source of variation	**Type III *SS***	***df***	***MSS***	***F***	***p***
Model	167671.154	18	9315.064	1740.953	.001
Wheel passes	10323.214	5	2064.643	385.875	.004
Depth	3098.402	2	1549.201	289.540	.002
Wheel passes * Depth	99.408	10	9.941	1.858	.046
Error	16720.479	3125	5.351		
Total	184391.633	3143			

These findings suggest that too much wheeling result in greater draft requirements translating into higher fuel consumption resulting in increased costs. To minimize subsoiling cost, headlands of crop field should permanently be set aside for turning only.

A similar increase in draft with the working depth for chisel ploughs was reported by Naderloo et al. (2009). They observed an increase in draft from 0.7 to 2.4 kN in a clay loam soil which was lower than 1.4 to 4.99 kN obtained in this study with no wheel traffic.

i. Effect of depth on subsoiling draft

In general, there was an almost linear increase in draft with increase in subsoiling depth (Figure 4.11). The subsoiling draft was much lower in 0 - 20 cm depth than draft requirements for 20 - 30 cm and 30 - 40 cm depths. The minimum draft of 3.9 kN was needed to subsoil at.10 cm depth, while a maximum draft of 7.9 kN was required to subsoil 35 cm depths.

Increasing subsoiling depth raised draft by 52%. Draft requirement increased by a further 42% for subsoiling at a depth of 35 cm depth. On average, draft requirements increased with depth at a rate of 0.4 kN cm^{-1}. The draft requirement below the hardpan pan layer (30 – 40 cm) was higher than that obtained within and above the hardpan depth.

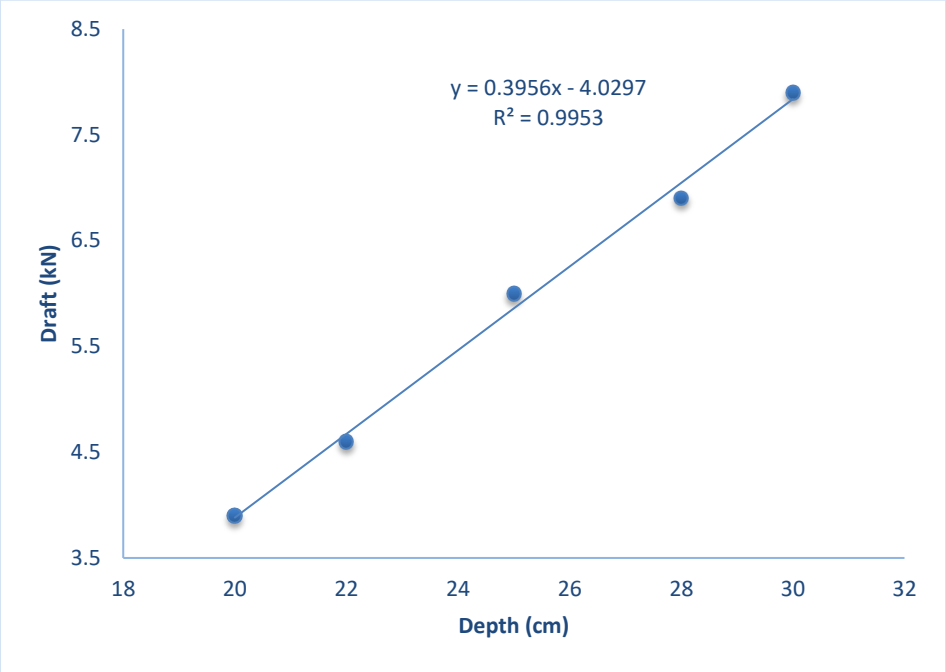

Figure 4.11: Draft variation with soil depth

The increased draft requirement with depth could be because soils at lower depths experience greater confine pressure. This confine pressure prevents the upward movement of the soil, forcing the soil to move forward. The forward movement of the soil is resisted by the undisturbed soil in front of the subsoiler, causing higher draft. Moreover, each increase in ploughing depth results in a rise in the amount of soil that is removed, spread out, and relocated. This means that a higher draft force is required to plough greater soil volume. This finding is in tandem with those of Sahu and Raheman (2006) and Al-Suhaibani and Ghaly (2013).

ii. Effect of bulk density on subsoiling draft

The effect of bulk density on subsoiling draft is illustrated in Figure 4.12. With an increase in bulk density, the draft requirement was shown to rise. The lowest draft requirement of 1.40 kN was

recorded for soil of bulk density 1257 kg m^{-3} while the highest draft requirement of 10.68 kN was needed for subsoiling a soil of bulk density 1593 kg m^{-3}.

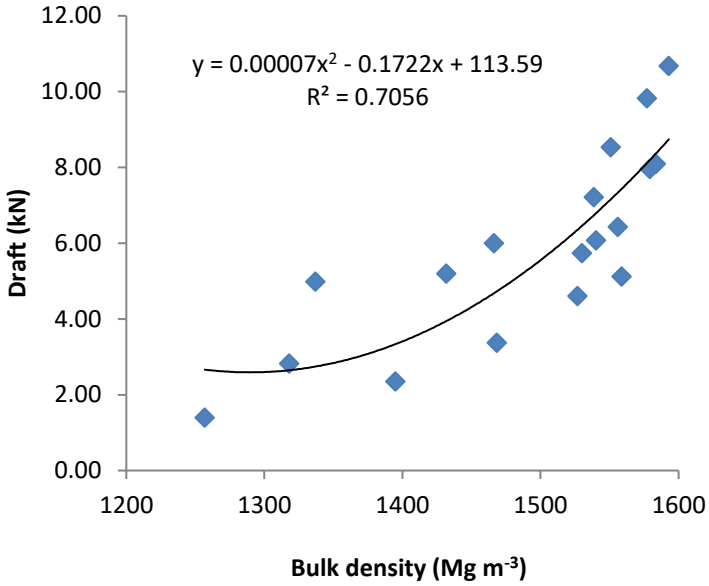

Figure 4.12: Draft variation with soil bulk density

Higher bulk density soils are more compacted, and particles have greater cohesion and therefore more draft is required to rapture the soil. This finding agrees with that of Mouazen and Ramon (2002) who observed.

iii. Subsoiling draft as affected by moisture content

Figure 4.13 shows that as soil moisture content increased, the amount of draft required decreased. Increasing moisture content from 40 to 48% reduced subsoiling draft requirements from 10.68 to 1.40 kN. The reduction in draft was more marked for moisture contents between 40 and 43%.

Increased moisture content causes the soil's interparticle bonding to loosen and internal friction to decrease, making the soil more workable, therefore decreasing draft. In their study, Mouazen et al. (2003) showed that draft decreased with increasing moisture content. Manuwa and Ademosun (2007), however, noted a rise in draft when soil moisture content rose from 11% to 22.5% at a depth of 150 mm.

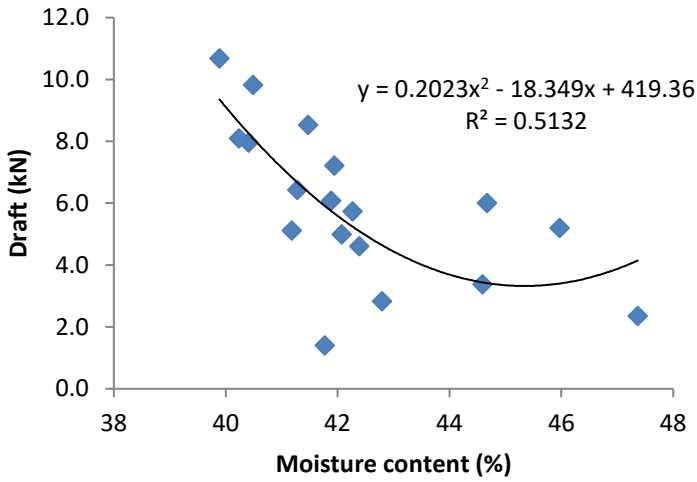

Figure 4 13: Effect of moisture content on subsoiling draft

iv. Effect of penetration resistance on subsoiling draft

The soil penetration resistance and subsoiling draft were shown to be correlated linearly (Figure 4.14). The lowest draft of 1.40 kN was recorded for soil with penetration resistance 642.3 kPa. Increasing penetration resistance to 1335.3 kPa raised draft requirement to maximum of 10.70 kN.

Since soil strength increase with soil penetration resistance, more draft is enquired to break the soil. This result is consistent with that of Gasso et al. (2013) who reached a conclusion that non-compacted soil requires less tillage energy than compacted soils.

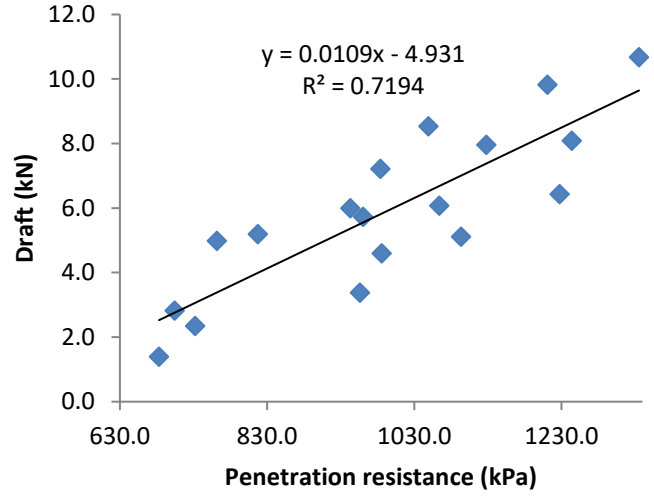

Figure 4.14: Effect of penetration resistance on subsoiling draft

v. Effect of soil cohesion on subsoiling draft

It was established that there was a general positive correlation between subsoiling draft requirements and soil cohesion (Figure 4.15). The lowest draft requirement of 1.40 kN was recorded for soils of cohesion 6.84 kPa. An increase in soil cohesion by 23% to 8.42 kPa increased draft requirement 7 times to 10.68 kN. The higher draft could be attributable to the fact that the bulk density and binding force between soil particles per unit area increase with greater soil cohesion. This finding is consistent with those of Zadeh (2006).

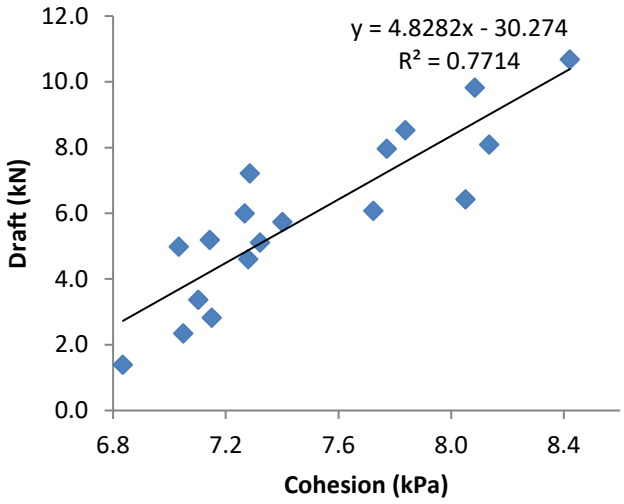

Figure 4.15: Variation of subsoiling draft with cohesion

vi. Subsoiling draft as affected by angle of internal friction

An R^2 of 0.072 was determined for the relationship between angle of internal friction and draft. This signified a weak relationship between angle of internal friction and draft (Figure 4.16). Xue et al. (2022) concluded that increasing the angle of internal fiction leads to more soil inter-particle friction. This leads to greater draft being developed to move the soil particles against each other. A similar observation was made by Zadeh (2006). There exists a weak correlation between draft and angle of internal friction (r = .366).

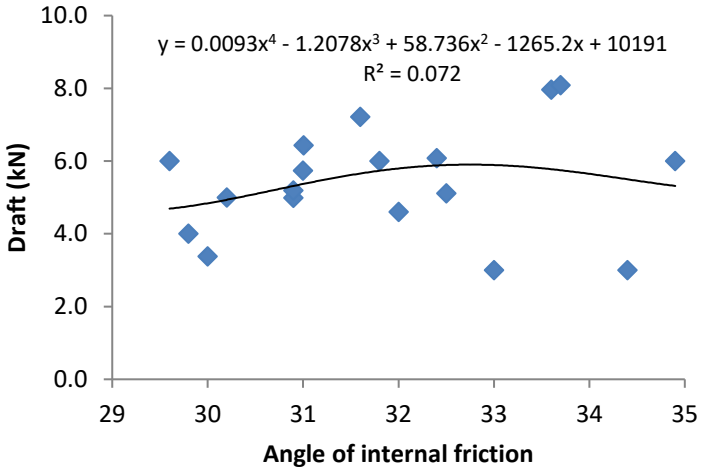

Figure 4.16: Relationship between internal friction and draft

vii. Subsoiling draft as affected by soil shear strength

The capacity of a certain soil to withstand an applied force is known as its strength. A significant positive correlation between soil shear strength and draft was established, as shown in Figure 4.17. The lowest draft requirement of 1.40 kN was recorded for soil shear strength 121.20 kPa which increased to 10.68 kN when the soil shear strength was increased to 188.90 kPa.

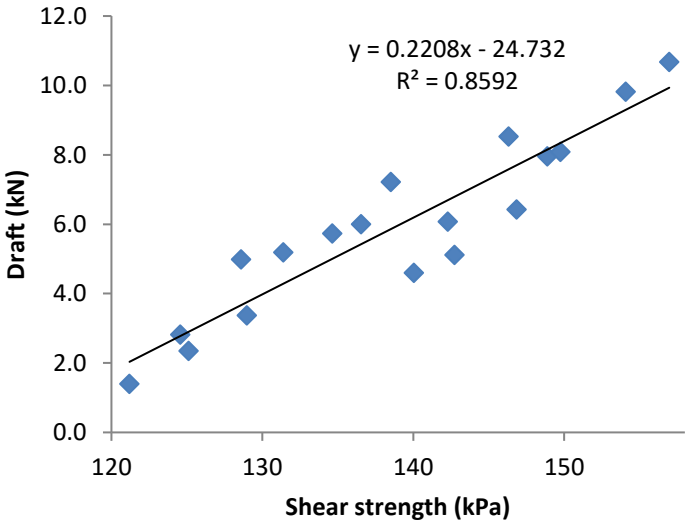

Figure 4.17: Effect of shear strength on subsoiling draft

Overcoming the interlocking force of particles is part of the energy required during subsoiling. Although tillage lowers soil strength and consequent traction efficiency, wheel movement increases soil strength and tillage draft demands (Xue et al., 2022).

4.2.2 Effect of wheel traffic soil compaction on specific draft

Table 4.2 and Figure 4.18 present the findings of a specific draft of subsoiling as influenced by the subsoiling depth and intensity of wheel traffic. There was a general increase in specific draft with number of wheel passes. Maximum specific draft of 222.50 kN m^{-2} was recorded for subsoiling 30- 40 cm layer after five passes while a minimum of 43.8 kN m^{-2} was needed to subsoil the untrafficked 0 – 20 cm layer.

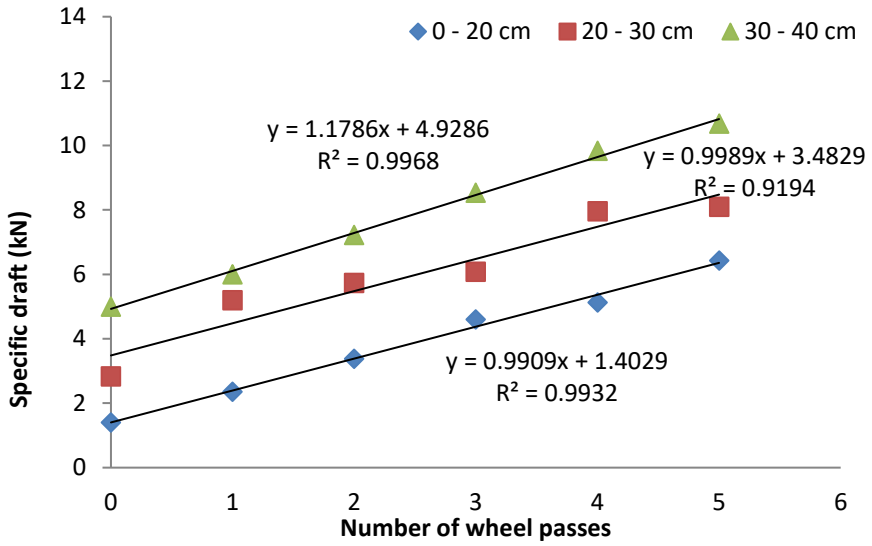

Figure 4 18: Variation of specific draft with wheel passes and depth

Specific draft was seen to rise at the 0 to 20 cm depth, going from 43.8 kN m^{-2} at no wheel pass to 200.9 kN m^{-2} after five wheel passes. Of the overall increase in particular draft, 19% was attributable to the initial wheel pass.

For any wheel pass, the specific draft was often greater in the 20 - 30 cm layer than the 0 - 20 cm layer. The least specific draft in this layer was 70.8 kN m^{-2} for no wheel pass treatment. The specific draft increased with number of wheel passes to 202.3 kN m^{-2} after fiver wheel passes, The first wheel pass accounted for 45% of the increment in specific draft.

For the 30 - 40 cm depth, the observed specific draft was generally higher than the upper layers for any given traffic intensity. The specific draft increased with number of wheel passes from 104.0 kN m^{-2} at no wheel pass to 222.5 kN m^{-2} after five wheel passes.

At the 5% level of confidence, both subsoiling depth and wheel traffic intensity considerably impacted specific draft (Table 4.14). There was no significant change in specific draft across the layers of 20 - 30 and 30 - 40 cm, despite the fact that the specific draft was significantly greater ($p < .05$) for the 0 - 20 cm layer.

Table 4.14: ANOVA for specific draft

Source of variation	Type III *SS*	*df*	*MSS*	*F*	*p*
Model	252671.15	18	9715.064	1740.953	.01
Wheel passes	13328.25	5	5564.652	385.875	.044
Depth	4228.45	2	1899.201	654.540	.003
Wheel passes * Depth	99.408	10	9.941	1.854	.024
Error	17850.425	3125	5.351		
Total	231391.645	3143			

The increased compaction at greater depths could account for the rise in specific draft with depth and wheel traffic intensity. This increases the useful work done per unit volume of the soil cut and moved. Similar observations to these were made by Muhsin (2017) in silt loam soils using a chisel plough. Khadr (2008) also reported a similar trend for mouldboard plough.

4.3 Modeling and validation of compaction effect of tractor wheel passes on subsoiling draft

4.3.1 Correlation analysis of model input variables

Correlation analysis was performed to establish the linear relationship between the dependent and independent variables. Table 4.15 summarizes the findings. According to Wamalwa (2022), correlation measures between variables should be as follows: 0 to 0.4 very weak; 0.4 to less than 0.6, weak; 0.6 to less than 0.8, strong ad 0.8 to 1, very strong or the equivalent negative values as the correlation (r) lies between -1 and 1.

Table 4.15: Correlation matrix of the soil variables under study

	Depth	Bulk density	Penetration resistance	Moisture content	Cohesion	Shear strength	Draft
Depth	1.000						
Bulk density	.212	1.000					
Penetration resistance	.170	0.739	1.000				
Moisture content	-.278	-.488	-.373	1.000			
Cohesion	.352	.775	.478	-.642	1.000		
Shear strength	.367	.900	.536	-.686	.919	1.000	
Draft	.996	.840	.818	-.716	.878	.929	1.000

Subsoiling draft, which was the dependent variable, showed a high correlation with Shear strength (r = .921), bulk density (r = .706) and soil cohesion (r = .869). Moderate correlation existed between subsoiling draft and depth (r = .661) and moisture content (r = -.621). Therefore, from the foregoing analysis, these variables could be used to model subsoiling draft.

4.3.2 Modeling effects of soil compaction on subsoiling draft

a) Multiple Linear Regression draft model

Regressions analyses was performed on the subsoiling draft data using MATLAB R2016a. From the correlation matrix, subsoiler depth, penetration resistance, bulk density, soil cohesion and soil strength were selected as independent variables to be used in modeling draft. The following subsoiler draft model was formulated within the tested range of tillage depth, bulk density, penetration resistance, moisture content and shears strength.

$$F = -26.10 + 0.124d + 0.004\rho + 0.0001P + 0.021w + 0.793C + 0.114\sigma \quad (4.1)$$

Where:

F is draft force (kN);

d is tillage depth (m);

ρ is bulk density (Mg m^{-3});

P is penetration resistance (kPa);

C is cohesion (kPa);

w is moisture content (%);

σ is shear strength (kPa).

From the t-statistic, it was found that moisture content and penetration resistance were not significant in their effect on subsoiler at the 5% confidence level. The observed and predicted subsoiling draft requirement data were compared and tabulated in Table A5.1 and the results plotted in Figure 4.19.

The correlation coefficient of 0.992 (R^2 = 0.984) obtained in this study indicate a close agreement between the observed data and the predicted value by the regression model. The MSE and RMSE were computed as 0.099 $(kN)^2$ and 0.313 kN respectively. The MAE and MAPE were determined as 0.24 kN and 5.41% respectively. The coefficient of determination obtained is comparable to that obtained by Sahu and Raheman (2006) of 0.981 for draft model of tines in a sandy clay loam soil.

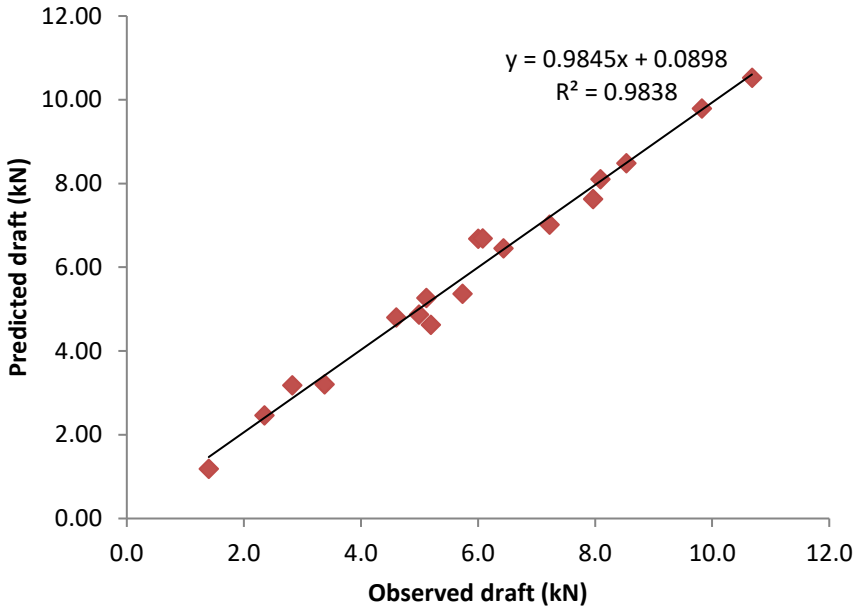

Figure 4.19: Relationship of actual and predicted draft force values

The Student's t-test performed to the predicted and measured data to compare the two means gave t (52) = 0.13, p = .989. Hence it was concluded that the variance of the two samples were the same.

However, the mean of predicted draft was higher than the measured output. This could have been due to errors in measurement of the draft and assumptions on soil homogeneity.

b) Dimensional Analysis modeling

i. Development of π-terms

In this study, the dependent variable was subsoiling draft requirement (F) while the independent variables affecting it were subsoiling depth (d), tractor speed (v), penetration resistance (P), soil bulk density (ρ), moisture content (w), soil shear strength (σ) and cohesion (C). The independent variables were changed by the compaction induced in the soil by tractor wheel passes.

By choosing ρ, d and σ as repeating variables, the π-terms were developed as follows:

For π_1:

$$\pi_1 = k_1(\rho^a d^b v^c F) \tag{4.2}$$

Equating the dimensions:

$$M^0L^0T^0 = [ML^{-3}]^a[L]^b[LT^{-1}]^c[MLT^{-2}] \tag{4.3}$$

$$=M^{a+1}L^{-3a+b-c+1}T^{-2c-2}$$

Solving for exponents:

$$M: 0 = a + 1 \tag{4.4}$$

$$L: 0 = -3a + b + c + 1 \tag{4.5}$$

$$T: 0 = - c - 2 \tag{4.6}$$

From which a = -1 b= -2 and c = -2

$$\pi_1 = k_1(\rho^{-2} d^{-2} v^{-2} F)$$

$$= k_1 \frac{F}{\rho^2 v^2 d^2} \tag{4.7}$$

For π_2:

$$\pi_2 = k_2 w \tag{4.8}$$

For π_3:

$$\pi_3 = k_3(\rho^a d^b v^c P) \tag{4.9}$$

Equating the dimensions:

$$M^0L^0T^0 = [ML^{-3}]^a[L]^b[LT^{-1}]^c[ML^{-1}T^{-2}] \tag{4.10}$$

$$=M^{a+1}L^{-3a+b+c-1}T^{-c-2}$$

Solving for exponents:

M: 0 = a + 1 (4.11)

L: 0 = -3a + b + c- 1 (4.12)

T: 0 = - c - 2 (4.13)

This gives, a = -1, b= 0 and c = -2

Therefore:

$$\pi_3 = k_3(\rho^{-1}v^{-2}P)$$

$$= k_3 \frac{P}{\rho v^2} \quad (4.14)$$

$$\pi_4 = k_4 \frac{C}{\rho v^2} \quad (4.15)$$

Similarly,

$$\pi_5 = k_5 \frac{\sigma}{\rho v^2} \quad (4.16)$$

The π-terms can be reduced further by combining other π-terms to produce a new set of π-terms as follows:

$$\pi_6 = \pi_5 \,.\, \pi_4 \quad (4.17)$$

$$= k_6 \frac{\sigma C}{\rho^2 v^4}$$

Similarly

$$\pi_7 = \pi_4 \,.\, \pi_2 \quad (4.18)$$

$$= k_6 \frac{wP}{\rho v^2}$$

The new π-terms. summarized in Table 4.16, satisfy the requirements for geometric, kinematic and dynamic similarities for the variables in this study.

Table 4.16: Summary of the pi terms

π-term	**Name**	**Remarks**
$\frac{F}{\rho v^2 d^2}$	Operational index	v constant
$\frac{wP}{\rho v^2}$	Soil resistance index	v constant
$\frac{\sigma C}{\rho^2 v^4}$	Soil strength index	v constant

The draft function can then be developed as:

$$\frac{F}{\rho v^2 d^2} = f\left(\frac{wP}{\rho v^2}, \frac{\sigma C}{\rho^2 v^4}\right) \quad (4.19)$$

ii. Formulation of prediction equations

The formation of the prediction equations involved the determination of the functions for the development of the general equation, the determination of the component equations, the mode of combination to form the prediction equations, the value of the constant term for the mode of the combination and formation of the general prediction equation.

The function was determined by keeping one π – term constant and varying others to establish the relationship between them. The procedure was repeated for each of the π-terms in the function to form a general relationship between them. Three component equations were established by plotting π_1 against π_2, π_3, π_4 while holding the others constant. These equations can be expressed as:

$$(\pi_1)_{\overline{3},} = f_1(\pi_2, \overline{\pi_3}) \quad (4.20)$$

$$(\pi_1)_{\overline{2},} = f_2(\overline{\pi_2}, \pi_3) \quad (4.21)$$

The general prediction equation was formed by component equations by multiplication as shown:

$$\pi_1 = c(\pi_1)_{\overline{3}_{,,}}(\pi_1)_{\overline{2}}\pi_1 = c(\pi_1)_{\overline{3}_{,,}}(\pi_1)_{\overline{2}} \quad (4.22)$$

where:

c = constant of multiplication.

The constant C has to be determined in order to determine the necessary and sufficient conditions for valid combination by multiplication of the component equations. This may be done by multiplying the component equations to form the general equation as:

$$F(\pi_2, \pi_3) = f_1(\pi_2, \overline{\pi_3}) f_2(\overline{\pi_2}, \pi_3) F(\pi_2, \pi_3) \quad (4.23)$$

If this is true the set of pi-terms obtained by holding π_2 constant will give the second pi terms with π_3 constant.

$$F(\pi_2, \overline{\pi_3},) = f_1(\pi_2, \overline{\pi_3}) f_2(\overline{\pi_2}, \overline{\pi_3}) f_3(\overline{\pi_2}, \overline{\pi_3}) F(\pi_2, \overline{\pi_3},) \quad (4.24)$$

Therefore

$$f_1(\pi_2, \overline{\pi_3}) = \frac{F(\pi_2, \overline{\pi_3})}{f_2(\overline{\pi_2}, \overline{\pi_3})} \quad (4.25)$$

Similarly, the second pi-term can be obtained by keeping π_2 constant:

$$f_2(\overline{\pi_2}, \pi_3) = \frac{F(\overline{\pi_2}, \pi_3)}{f_1(\overline{\pi_2}, \overline{\pi_3})} \quad (4.26)$$

Therefore

$$F(\pi_2, \pi_3) = \frac{F(\pi_2, \overline{\pi_3})F(\overline{\pi_2}, \pi_3)}{f_1(\overline{\pi_2}, \overline{\pi_3})f_2(\overline{\pi_2}, \overline{\pi_3})} \quad (4.27)$$

But the denominator in equation is obtained by holding π_2 and π_3 constant. Therefore:

$$F(\overline{\pi_2}, \overline{\pi_3}) = f_1(\overline{\pi_2}, \overline{\pi_3})f_2(\overline{\pi_2}, \overline{\pi_3})F(\overline{\pi_2}, \overline{\pi_3}) \quad (4.28)$$

Hence

$$F(\pi_2, \pi_3) = \frac{F(\pi_2, \overline{\pi_3})F(\overline{\pi_2}, \pi_3)F(\overline{\pi_2}, \overline{\pi_3})}{F(\overline{\pi_2}, \overline{\pi_3})} \quad (4.29)$$

From equation above, it can be deduced that

$$c = \frac{1}{F(\overline{\pi_2}, \overline{\pi_3})} \quad (4.30)$$

iii. Formulating prediction equation

The developed π- terms were related by the equation:

$$\pi_1 = k(\pi_2)^a(\pi_3)^b \quad (4.31)$$

Where a and b are constants

Taking logs of both sides:

$$\log \pi_1 = \log k + a \log \pi_2 + b \log \pi_3 \quad (4.32)$$

Dimensionless plots of log π_1 against log π_2 and log π_1 against log π_3 were performed to determine the constants a and b. The relationship between log π_1 against log π_2 is presented in Figure 4.20. From the graph,

$$\log \pi_1 = \log k + a \log \pi_2 \quad (4.33)$$

Therefore $a = 2.584$

$= 2.60$

: $\log k = -9.467$ (4.34)

k-= 0.000000000341

Therefore:

$$\pi_1 = 0.000000000341{\pi_2}^{2.60}$$

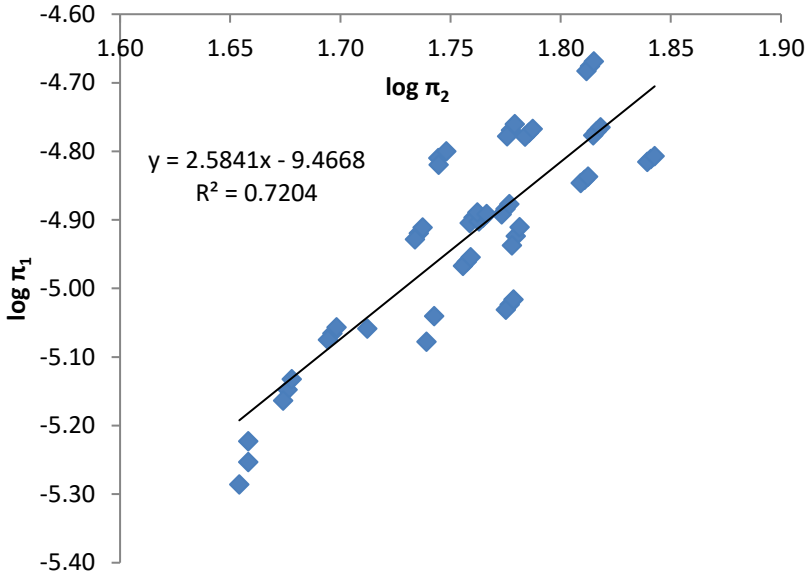

Figure 4.20: Plot of log π_1 against log π_2

Figure 2.21 gives the plot of log π_1 against log π_3.

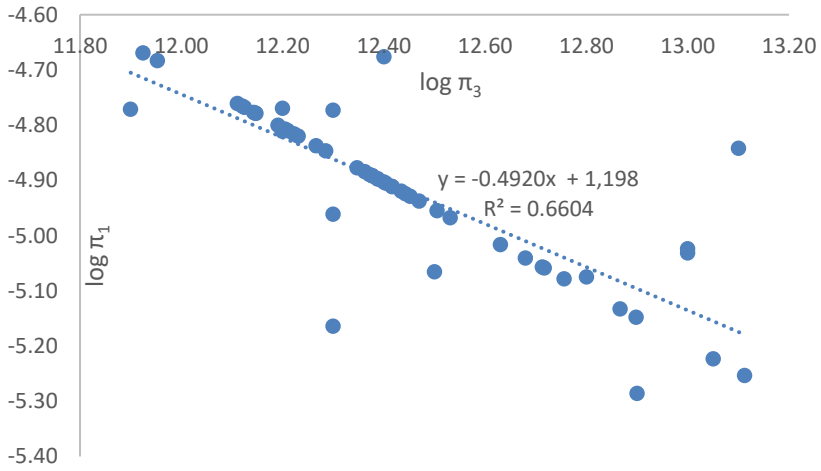

Figure 4.21: Plot of log π_1 against log π_3

From the plot,

$$\log \pi_1 = \log k + b \log \pi_3 \qquad (4.35)$$

From the linear equation,

$$\begin{aligned} b &= -0.492 \\ &= 0.50 \\ \log\ k &= 1.198 \\ k &= 0.0783 \end{aligned} \tag{4.36}$$

Therefore

$$\pi_1 = 0.0783\pi_3{}^{-0.50} \tag{4.37}$$

Combining the above equations:

$$\pi_1 = \frac{1}{1.26\text{x}10^{-11}}(\pi_2)^{2.60}(\pi_3)^{-0.5} \tag{4.38}$$

Therefore,

$$\frac{F}{\rho v^2 d^2} = \frac{1}{1.26\text{x}10^{-11}}\left(\frac{wP}{\rho v^2}\right)^{2.60}\left(\frac{\sigma C}{\rho^2 v^4}\right)^{-0.50} \tag{4.39}$$

From which,

$$F = \frac{\rho v^2 d^2}{1.26\text{x}10^{-11}}\left(\frac{wP}{\rho v^2}\right)^{2.60}\left(\frac{\sigma C}{\rho^2 v^4}\right)^{-0.50} \tag{4.40}$$

iv. Model validation

Comparisons were made between the observed and predicted values of the subsoiling draft (Table A5.1) to assess how effectively the model represents the actual system being predicted (Figure 4.22).

From this graph, R^2 was obtained as 0.872, giving a correlation coefficient of 0.934 between the observed and predicted draft indicating a fair agreement between the two sets of data. The MSE and RMSE for the developed model were computed as 1.271 $(kN)^2$ and 1.128 kN respectively. Similarly, the MAE and MAPE were determined as 1.85 kN and 1.61 % respectively.

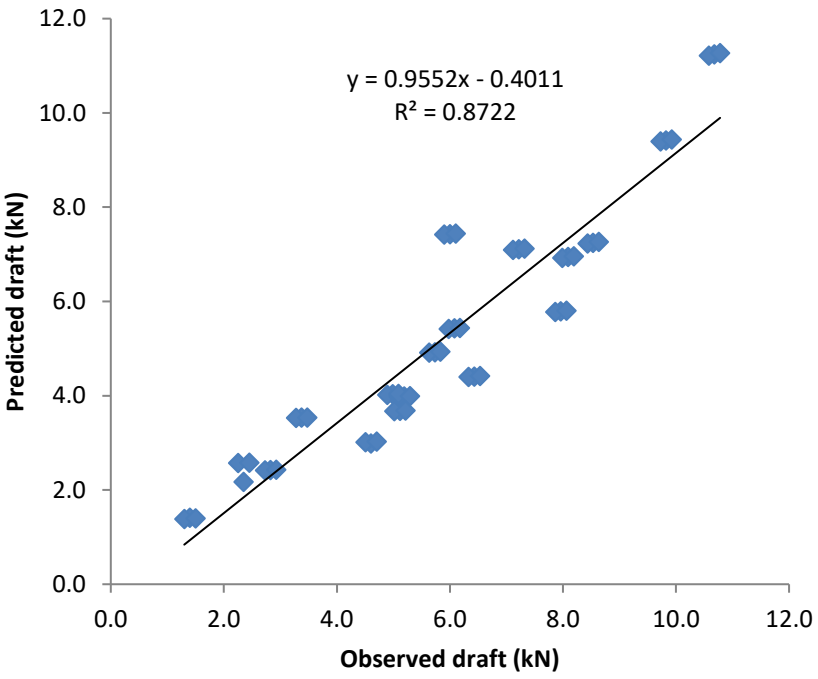

Figure 4.22: Relationship between observed and predicted values of draft

The Student t-test performed to compare the observed and predicted draft gave t (52) = 0.15, p = .910. Hence it was concluded that the variance of the two samples were the same. The predicted draft was found to be 11% less than the observed draft. The discrepancies noted between the two sets of data could be due to the unstable nature of interaction of the soil-tool interface and the assumptions regarding the soil homogeneity. The variations could also have resulted from errors in taking the readings of the dynamometer.

Kawuyo (2011) modeled draft of a ridger using the dimensional analysis technique and obtained an R^2 of 0.97 and RMSE of 0.778. Kabri et al. (2019) foumd a good relationship between observed and predicted draft (R^2 = 0.98).

c) Artificial Neural Networks

Using six neurons in the input layer and one neuron in the output layer, an ANN-based model was created to simulate subsoiling draft. There were 10 neurons in the hidden layer (Roul et al., 2009). The input variables were depth, bulk density, penetration resistance, cohesion, moisture content and shear stress while the output variable was subsoiler draft requirements. The rationale for selecting these independent variables is to capture the multifaceted nature of soil compaction and

its effects on subsoiling draft requirements. By including a combination of soil properties, compaction-related factors, and environmental conditions, the ANN model can learn complex relationships between these variables and predict subsoiling draft requirements accurately.

There were 54 data sets which were divided into 38 for training (70%), 8 for testing (15%) and 8 for validation (15%). Using various training algorithms and hidden layer node numbers, many neural network models were developed. Figure 4.23 depicts the selected ANN's schematic architecture.

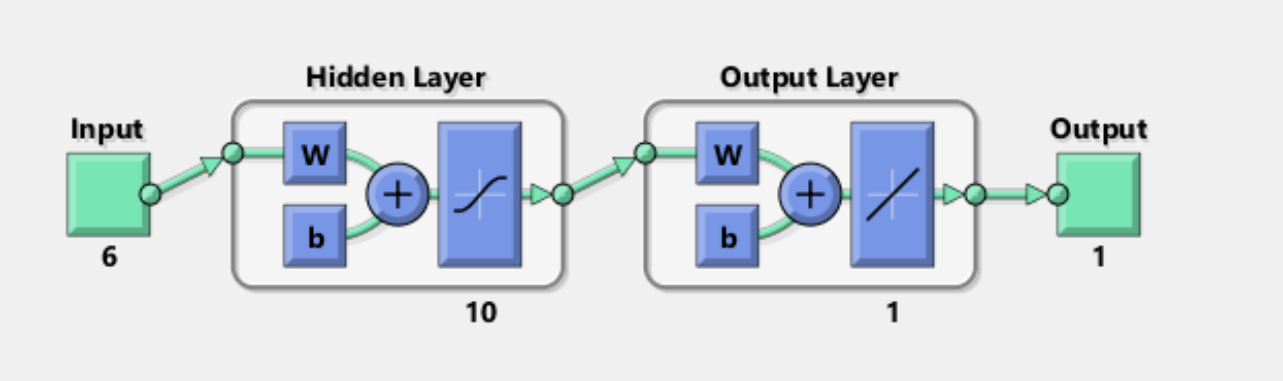

Figure 4.23: The developed ANN architecture

Table 4.13 summarizes the architecture and statistical results of a few different ANN models**.** The MSE chart for the epoch that was used to regulate the network training procedure is shown in Figure 4.24. As seen in the example, the training algorithm was terminated when the training error was acceptable.

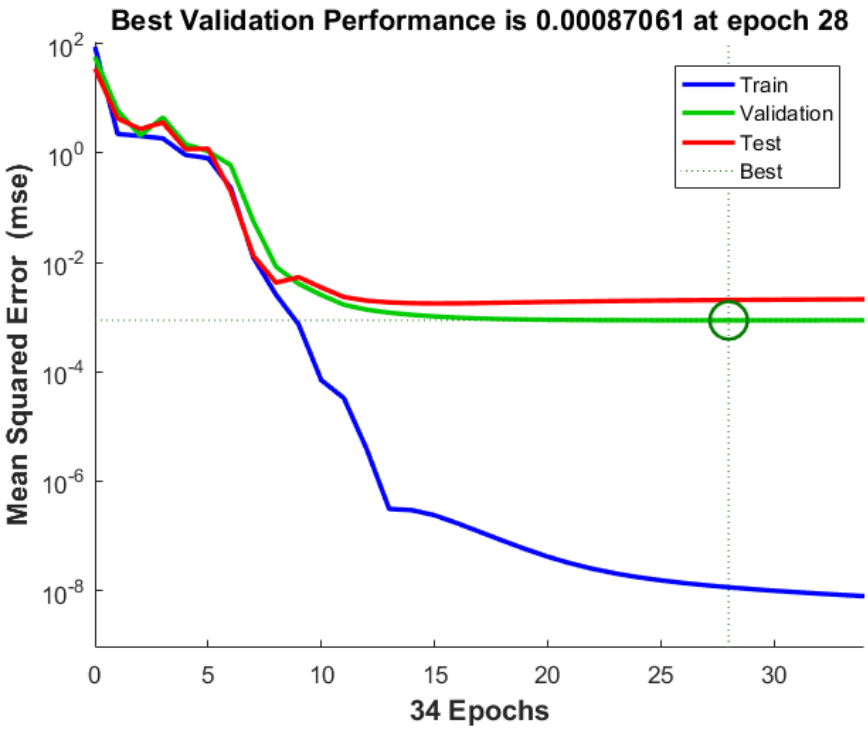

Figure 4.24: Trend of MSE against epochs for trained networks

Table 4.17: Summary of various developed networks evaluated

Network architecture	Learning Algorithm	Input transfer function	Output transfer function	Training		Testing	
				R^2	RSME	R^2	RSME
6-11-1	Gradient descent	Sigmoid	logsig	0.917	0.412	0.904	0.236
6-11-1	Levenberg–Marquardt	Hyperbolic tangent	Linear	0.972	0.114	0.877	1.325
6-10-1	Conjugate gradient	Sigmoid	logsig	0.989	0.075	0.767	1.899
6-10-1	**Levenberg–Marquardt**	**Hyperbolic tangent**	**Sigmoid**	**0.999**	**0.002**	**0.998**	**0.020**
6-3-1	Conjugate gradient	Sigmoid	Logsig	0.968	0.082	0.956	1.234
6-4-1	Levenberg–Marquardt	Hyperbolic tangent	Linear	0.989	0.02	0.899	2.32
6-3-1	Gradient descent	Sigmoid	Sigmoid	0.972	0.412	0.987	1.999
6-3-1	Levenberg–Marquardt	Hyperbolic tangent	Linear	0.972	0.114	0.989	0.365
6-11-1	Gradient descent	Sigmoid	Sigmoid	0.989	0.075	0.889	1.321
6-2-1	Conjugate gradient	Hyperbolic tangent	Linear	0.958	0.399	0.978	1.475
6-5-1	Gradient descent	Sigmoid	Sigmoid	0.968	0.082	0.909	1.544
6-3-1	Levenberg–Marquardt	Hyperbolic tangent	Linear	0.989	0.02	0.991	0.998

The scatter plots of the ANN output versus observed values are given in Figure 4.25. The R^2 obtained was 0.999. The coefficient of determination was 1.000 for the training stage. The evaluation and testing stages' correlation coefficients were 0.999 and 0.998, respectively. The MSE and RMSE for the ANN model were determined as 0.002 $(kN)^2$ and 0.02 kN respectively. The MAE and MAPE were 0.02 and 1.27% respectively.

The little difference in predicted and measured subsoiling draft levels demonstrated the accuracy of ANN in predicting these values. Results from this study and other studies (Al-Hamed et al., 2013; Al-Janobi et al., 2020; Saleh & Ayman, 2013) showed that the ANN model had great predictive ability for estimating tillage draft. Saleh and Ayman (2013) used the error back propagation learning technique to evaluate the performance of straightforward multi-flat plate ploughing tines. Their ANN model demonstrated good agreement with the experimental data with a relative error of 2%.

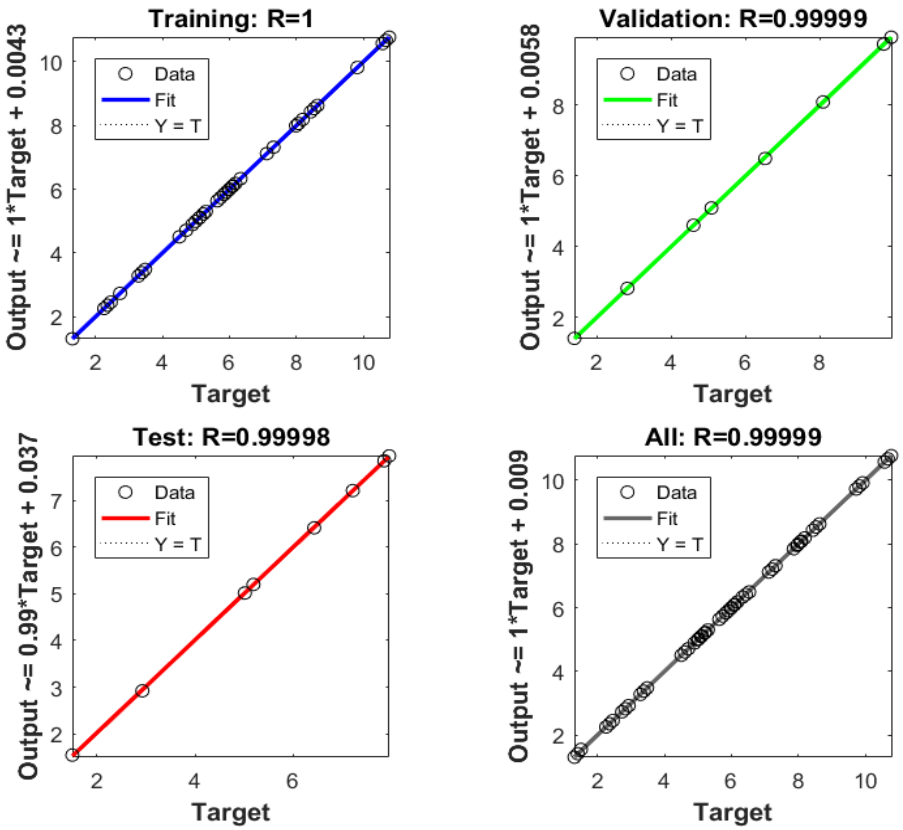

Figure 4.25: Scatter plots of ANN output versus target draft

The t-test performed to the predicted and observed subsoiler data to compare the means gave t (52) = 0.12, p = .989. It was therefore concluded that the variance of the two samples were the same.

d) Adaptive Neuro-Fuzzy Inference System model

Subsoiling depth, bulk density, soil moisture content, cohesion, and soil strength were the input variables while the output variable was subsoiling draft. Grid partition structure was used to build the network. According to Table 4.18, the best ANFIS model included 110 training cycles, three input membership functions for each input, triangular and linear membership functions for input and output, and a weighted sum defuzzification approach. The R^2 was found as 0.994, MSE as 0.039 $(kN)^2$, RMSE as 0.198 kN and MAPE as 0.112%. Figure 4.26 shows plot of observed and predicted draft by outperforming ANFIS model.

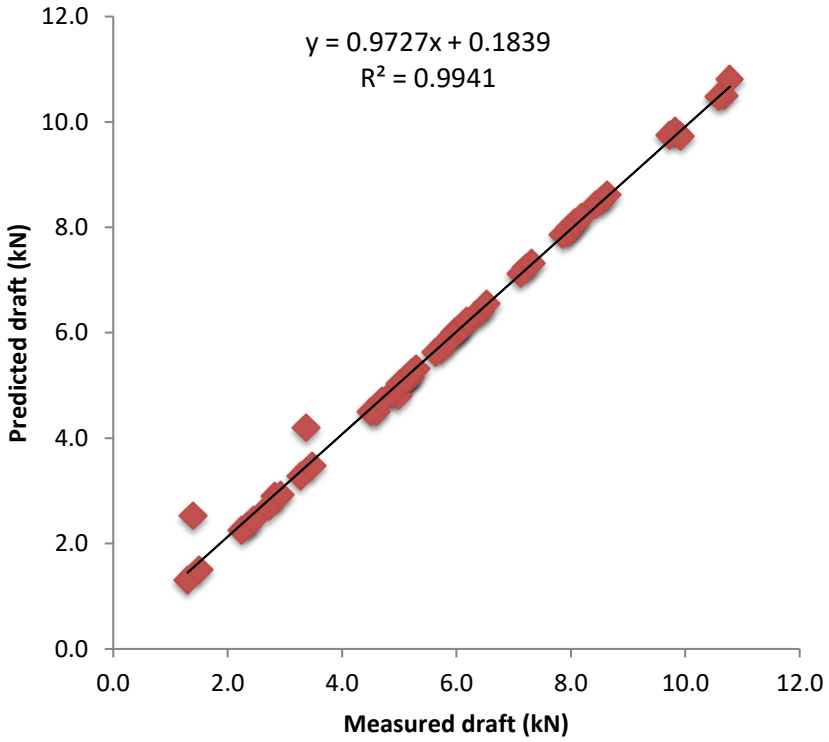

Figure 4.26: Comparison of ANFIS predicted draft and experimental draft

Table 4.18: Structural parameters of selected ANFIS daft prediction models

Number of training cycles	Number of input membership functions	Membership function		Defuzzification method	R^2	RMSE (kN)	MAPE (%)
		Input	Output				
126	4, 3	Gaussian	Constant	Weighted sum	0.999	0.1251	2.412
236	2, 4	Gaussian	Linear	Weighted average	0.986	1.321	1.456
542	3, 4	Pi	Linear	Weighted sum	0.933	1.053	2.145
123	2, 2	Gaussian	Constant	Weighted average	0.994	1.325	3.445
125	3, 2	Pi	Linear	Weighted sum	0.995	1.326	4.321
452	4, 2	Gbell	Linear	Weighted average	0.983	2.343	3.255
110	**3, 4**	**Triangular**	**Linear**	**Weighted sum**	**0.994**	**0.198**	**1.420**
125	2, 3	Gaussian	Constant	Weighted sum	0.845	3.215	3.321
418	3, 3	Pi	Linear	Weighted sum	0.927	2.125	3.222
129	4, 3	Gbell	Constant	Weighted average	0.964	1..165	2.888
111	3, 4	Pi	Linear	Weighted sum	0.934	0.568	1.458
124	3, 2	Gbell	Constant	Weighted average	0.968	1.325	2.452
125	4, 2	Triangular	Linear	Weighted average	0.995	1.326	4.321
452	4, 2	Gaussian	Linear	Weighted sum	0.983	2.343	3.255
174	3, 4	Pi	Constant	Weighted sum	0.958	3.125	2.654
125	2, 2	Gbell	Linear	Weighted sum	0.845	3.215	3.321
418	3, 2	Triangular	Constant	Weighted average	0.927	2.125	3.222

The R^2 for the plot of predicted and observed drat was 0.9841. The MSE and RMSE were determined as 0.039 $(kN)^2$ and 0.198 kN respectively. The MAE and MAPE were 0.06 kN and 7.16% respectively.

The t-test performed to the predicted and observed draft data to compare the means gave t (52) = 0.19, p = .939. This indicated that the variance of the two samples were the same. The best ANFIS model built in this study proved to be reliable enough for predicting subsoiling draft based on changes in selected soil parameters. Like results of the present study, Al-Dosary et al. (2020) examined the ANFIS approach and its performance obtaining a R^2 of 0.939 in prediction of draft. Shafaei et al. (2018b) demonstrated that the best ANFIS model had R^2 of 0.994 and RMSE of 0.722 (kN).

4.3.3 Comparison of the performance of the models

The performance of the MLR, Dimensional Analysis, ANFIS and ANN models is summarized in Table 4.19**.** The forecasting ability of the four models was assessed using MAE, MSE, RMSE, MAPE and R^2.

Table 4.19: Summary of model performance indicators

Model	**MSE $(kN)^2$**	**RMSE (kN)**	**MAE (kN)**	**MAPE (%)**	**R^2**
MLR	0.099	0.313	0.243	5.41	0.984
Dimensional analysis	1.271	1.128	0.946	1.612	0.872
ANN	0.002	0.044	0.02	1.27	0.999
ANFIS	0.039	0.198	0.06	1.42	0.994

The ANN and ANFI IS draft prediction models had lower MSE and RMSE compared to MLR and Dimensional analysis models. The MLR and empirical draft models were observed to have higher MAE and MAPE compared to ANFIS and ANN draft models. ANFIS and ANN draft models showed greater prediction accuracy compared to the MLR and Dimensional Analysis and MLR models.

The ANFIS and ANN draft models were observed to have higher R^2 values compared to MLR and the Dimensional Analysis models. This indicated a greater linear relationship between the

predicted and observed draft for the ANFIS and ANN models than for the MLR and Dimensional Analysis models.

It can be concluded that the best ANFIS and ANN models that were developed in this study were sufficient for prediction of draft force based on variations in subsoiling depth, penetration resistance, shear strength, bulk density, moisture content and cohesion. The results also showed that ANNs and ANFIS could accurately predict subsoiling draft when trained. Mathematical modeling approaches were observed to have lower forecasting ability compared to the artificial intelligence approaches.

4.4 Contribution to knowledge

By assessing the effect of tractor wheel passes on soil physical and mechanical properties, the study contributes to a deeper understanding of how soil compaction occurs in real-world agricultural settings. This insight is crucial for mitigating soil compaction, which can have detrimental effects on soil health and crop productivity.

Determining how different levels of wheel traffic compaction affect draft requirements for subsoiling provides practical guidance to farmers and agricultural practitioners. It helps them make informed decisions about when and how to perform subsoiling operations to minimize compaction and reduce energy consumption.

The study's use of multiple modeling techniques (Multiple Linear Regression, Dimensional Analysis, ANFIS, and ANN) to predict subsoiler draft requirements based on soil properties demonstrates the application of advanced analytical tools in agriculture and soil science. This contributes to the use of innovative methods for optimizing agricultural practices. The study aligns with the principles of sustainable agriculture by focusing on soil health and reduced environmental impact. It provides insights into how to maintain soil quality while using heavy machinery, contributing to long-term sustainability in agriculture.

The development of predictive models for subsoiler draft requirements allows for data-driven decision-making. Farmers can use these models to tailor their farming practices to specific soil conditions, optimizing resource use and crop yields. The study's use of multiple modeling techniques not only contributes to advancing knowledge within the realm of soil behavior and

agricultural practices but also highlights the importance of methodological diversity in scientific research, promoting a more holistic understanding of complex systems.

While conducted at Egerton University, the study's findings and models can be adapted to various agricultural environments with similar soil types and machinery usage patterns. This broadens the applicability of the research beyond the specific study site. The study contributes to the education and training of future agricultural scientists and engineers by demonstrating the application of scientific methods and modeling techniques in solving real-world agricultural problems.

CHAPTER FIVE
CONCLUSIONS AND RECOMMENDATIONS

5.1 Conclusions

The amount of energy consumed during subsoiling and its cost implication affects farm profitability and machine implement matching. A conceptual framework was proposed in which the pertinent variables affecting subsoiler draft were considered. Models for predicting draft required for subsoiling under a silt loam soil were developed.

Arising from the findings of the study, the following conclusions were made:

a) When the wheel traffic frequency was increased from zero to five, an increase was observed in the bulk density (from 1256.76 to 1593.04 kg m^{-3}), penetration resistance (from 642.24 to 1538.64 MPa), shear strength (from 121.20 to 156.97kPa), cohesion (from 6.74 to 8.52 MPa) and angle of internal friction (30 to 35º). However, a reduction was observed in soil porosity (from 53 to 40%), moisture content (from 48 to 40%), infiltration rate (from 15.30 to 2.97 mm h^{-1}). and saturated hydraulic conductivity (from 5.63 to 0.24 mm h^{-1}). These results confirm that wheel traffic soil compaction affect the dynamic soil properties.
b) Different levels of wheel traffic compaction result in varying draft requirements for subsoiling. More compacted soils generally require higher draft forces for subsoiling. An increase in wheel passes and subsoiling depth raised draft (from 1.40 to 4.68 kN). Specific draft increased with number of passes from 103 to 472 kN m^{-2} for the topsoil layer.
c) The relationship between compaction levels and draft requirements can be described through mathematical modeling, allowing for predictions under different scenarios. Multiple Linear Regression, Dimensional Analysis, Adaptive Neuro-Fuzzy Inference Systems, and Artificial Neural Networks are effective modeling techniques for predicting subsoiler draft requirements based on selected soil properties.

5.2 Recommendations

5.2.1 Policy recommendations

a) Develop guidelines for farmers and agricultural practitioners to manage tractor traffic in ways that minimize negative effects on soil properties.

b) Provide guidance to farmers on how to adjust subsoiler settings (e.g., depth and shank spacing) based on soil compaction conditions to optimize draft forces and reduce energy consumption.
c) Develop user-friendly software or apps that integrate the developed models to assist farmers and agricultural advisors in estimating subsoiling draft requirements.

5.2.2 Recommendations for further research

a) Implementation of controlled experiments and monitoring of tractor wheel passes to assess their impact on soil properties under varying conditions.
b) Development of predictive models that incorporate soil compaction levels, equipment specifications, and subsoiling depth to estimate draft requirements accurately.
c) More studies are required in other soils using different types of subsoilers for wider acceptability of the developed draft models.

REFERENCES

Abbaspour-Gilandeh, Y., Fazeli, M., Roshanianfard, A., & Hernández-Hernández, J. L. (2020). Prediction of draft force of a chisel cultivator using artificial neural networks and its comparison with regression model. *Agronomy, 10*(451), 1 - 14. https://doi.org/10.3390/agronomy10040451

Abo-Elnor, M., Hamilton, R., & Boyle, J. T. (2004). Simulation of soil–blade interaction for sandy soil using advanced 3-D finite element analysis. *Soil and Tillage Research*, 75, 61 –73. https://doi.org/10.1016/s0167-1987(03)00156-9

Aboukarima, A. M., Elsoury, H. A., & Menyawi, M. (2015). Artificial Neural Network model for the prediction of the cotton crop leaf area. *International Journal of Plant and Soil Science*, *8*(4), 1-13. https://doi.org/10.9734/ijpss/2015/19686

Abu-Hamdeh, N. H., & Reeder, R. C. (2003). Measuring and predicting stress distribution under tractive devices in undisturbed soils. *Biosystems Engineering*, 85, 493 – 502. https://doi.org/10.1016/s1537-5110(03)00069-2

Acquah, K., & Chen, Y. (2022). Soil compaction from wheel traffic under three tillage systems. *Agriculture, 12*(219), 1 – 13. https://doi.org/10.3390/agriculture12020219

Aday, S. H., Hameed, K. A., & Salman, S. F. (2001). The energy requirement and energy utilization efficiency of two ploughs type for pulverization of heavy soil. *Iraqi Journal of Agric*ulture, *6*(1), 136 - 146.

Aday, S. H., & Nassir, A. J. (2009). Field study of modified chisel plough performance on the specific and equivalent energy. *Basrah Journal of Agricultural Sciences, 22*(1), 95-108.

Afify, M. T., El-Haddad, Z. A., & Lamia, A. A. D. (2020). Modeling the effect of soil-tool interaction on draft force using Visual Basic. *Annals of Agricultural Sciences, Moshtohor*, *58*(2), 223 – 232. https://doi.org/10.21608/assjm.2020.112746

Agele, S., Aiyelari, P., Famuwagun B., & Oluwasola, O. (2016). Effects of tractor wheel passes-induced compaction and organic amendments on soil properties and yield of cowpea (*vigna unguiculata*) in an alfisol of the rainforest zone of Nigeria. *International Journal of Plant and Soil Science, 13*(4), 23 – 29. https://doi.org/10.9734/ijpss/2016/27665

Ahad, T., Kanth, T. A., & Nabi, S. (2015). Soil bulk density as related to texture, organic matter content and porosity in Kandi soils of District Kupwara (Kashmir valley), India. *International Journal of Scientific Research*, 4, 198 – 200.

Ahmad, N., Ul-Hassan, F., & Quadir, G. (2007). Effect of subsurface soil compaction and improvement measures on soil properties. *International Journal of Agriculture and Biology*, *9*(3), 509 – 513.

Ahmadi, I. (2016). Effect of soil, machine, and working state parameters on the required draft force of a subsoiler using a theoretical draft-calculating model. *Soil Research*. https://doi.org/10.1071/sr16193

Ahmadi, I., & Ghaur, H. (2015). Effects of soil moisture content and tractor wheeling intensity on traffic-induced soil compaction. *Journal of Central European Agriculture*, *16*(4), 489 - 502. https://doi.org/10.5513/jcea01/16.4.1657

Akbarnia, A., Mohammadi, A., Farhani, F., & Alimardani, R. (2014). Simulation of draft force of winged share tillage tool using artificial neural network model. *Agricultural Engineering International, CIGR Journal*, *16*(4), 57 - 65.

Akbarzadeh, A., Mehrjardi, R. T., Rouhipour, H., Gorji, M., & Rahimi, H. G. (2009). Estimation of soil erosion covered with rolled erosion control systems using rainfall simulator (neuro-fuzzy and artificial neural network approaches). *Journal of Applied Scientific Research*, 5, 505 – 514.

Aksakal, E. L., & Oztaş, T. (2010). Changes in distribution patterns of soil penetration resistance within a silage corn field following the use of heavy harvesting equipment. *Turkish Journal of Agriculture and Forestry*, 34, 173 - 179. https://doi.org/10.3906/tar-0906-189

Alakukku, L., Weisskopf, P., & Spoor, G. (2003). Prevention strategies for field traffic-induced subsoil compaction, a review. Part 1. Machine/soil interactions. *Soil and Tillage Research*, 73, 145 - 160. https://doi.org/10.1016/s0167-1987(03)00108-9

Alameda, D., & Villar, R. (2009). Moderate soil compaction, implications on growth and architecture in seedlings of 17 woody plant species. *Soil and Tillage Research*, 103, 325–331. https://doi.org/10.1016/j.still.2008.10.029

Alaoui, A. (2015). Modelling susceptibility of grassland soil to macropore flow. *Journal of Hydrology*, 4, 16.

Alaoui, A., & Helbling, A. (2006). Evaluation of soil compaction using hydrodynamic water content variation, comparison between compacted and non-compacted soil. *Geoderma*, 134, 97 – 108. https://doi.org/10.1016/j.geoderma.2005.08.016

Alaoui, A., Lipiec, J., & Gerke, H. (2011). A review of the changes in the soil pore system due to soil deformation, a hydrodynamic perspective. *Soil and Tillage Research,* 115, 1 – 15. https://doi.org/10.1016/j.still.2011.06.002

Al-Dosary, N. M. N., Al-Hamed, S. A., & Aboukarima, A. M. (2020). Application of adaptive neuro-fuzzy inference system to predict draft and energy requirements of a disk plow. *International Journal of Agricultural and Biological Engineering*, *13*(2), 198 – 207. https://doi.org/10.25165/j.ijabe.20201302.4077

Al-Ghazal, A. A. (2002). Effect of tractor wheel compaction on bulk density and infiltration rate of a loamy sand soil in Saudi Arabia. *Emirates Journal of Agricultural Sciences,* 14, 24 – 33. https://doi.org/10.9755/ejfa.v14i1.4982

Al-Hamed, S. A., Wahby, M. F., AL-Saqer, S. M., Aboukarima, A. M., & Sayedahmed, A. (2013). Artificial neural network model for predicting draft and energy requirements of a disk plow. *The Journal of Animal and Plant Sciences*, *23*(6), 1714 - 1724.

Alimardani, R., Abbaspour-Gilandeh, Y., & Sadati, S. H. (2009). Prediction of draft force and energy of subsoiling operation using ANN model. *Journal of Food, Agriculture and Environment, 7*(34), 537- 542.

Al-Janobi, A. A., Aboukarima, A. M., & Ahmed, K. A. (2001). Prediction of specific draft of different tillage implements using neural network. *Journal of Agricultural Engineering*, *18*(3), 699 – 714.

Al-Janobi, A. A., Al-Hamed, S. A., Aboukarima, A. M., & Almajhadi, Y. (2020). Modeling of draft and energy requirements of a moldboard plough using artificial neural networks based on two novel variables. *Engenharia Agrícola, Jaboticabal, 40*(3), 363 - 373. https://doi.org/10.1590/1809-4430-eng.agric.v40n3p363-373/2020

Al-Janobi, A. A., Wahby, M. F., Aboukarima, A. M., & Al-Hamed, S. A. (2002). Influence of chisel plough shank shape on horizontal and vertical force requirements. *Agricultural Science, Sultan Qaboos University, 7*(1), 13 - 19. https://doi.org/10.24200/jams.vol7iss1pp13-19

Allen, R. R., & Musick, J. T. (2001). Deep ripping and blocked furrow effects on lower 1/3 furrow irrigation infiltration. *Applied Engineering in Agriculture,* 17, 41 – 48. https://doi.org/10.13031/2013.1934

Alletto, L., Coquet, Y., Benoit, P., Heddadj, D., & Barriuso, E. (2010). Tillage management effects on pesticide fate in soils. A review. *Agronomy for Sustainable Development*, 30, 367 – 400. https://doi.org/10.1007/978-94-007-0394-0_35

Al-Shammary, A. A. G., & Al-Sadoon, J. N. A. (2014). Influence of tillage depth, soil mulching systems and fertilizers on some thermal properties of silty clay soil. *Global Journal of Agricultural Rese4rch*, 2, 18 – 32.

Al-Suhaibani, S. A. (2010). Effect of ploughing depth of tillage and forward speed on the performance of a medium size chisel plough operating in a sandy soil. *American Journal of Agricultural and Biological Sciences*. 10, 247 - 255. https://doi.org/10.3844/ajabssp.2010.247.255

Al-Suhaibani, S. A., & Ghaly, A. E. (2013). Comparative study of the kinetic parameters of three chisel plows operating at different depths and forward speed in a sandy soil. *The International Journal of Engineering and Science*, *2*(7), 42 – 59. https://doi.org/10.3844/ajabssp.2010.247.255

Ampoorter, E., Schrijver, A., Nevel, L., Hermy, M., & Verheyen, K., (2012). Impact of mechanized harvesting on compaction of sandy and clayey forest soils: results of a meta-analysis. *Annals of. Forest Science*, 69, 533 – 542. https://doi.org/10.1007/s13595-012-0199-y

Ansorge, D., & Godwin, R. J. (2007). The effect of tyres and a rubber track at high axle loads on soil compaction, Part 1: single axle-studies. *Biosystems Engineering*, 98, 115 – 126. https://doi.org/10.1016/j.biosystemseng.2007.06.005

Ansorge, D., & Godwin, R. J. (2008). The effect of tyres and a rubber track at high axle loads on soil compaction, Part 2, multi-axle machine studies. *Biosystems Engineering*, 99, 338 – 347. https://doi.org/10.1016/j.biosystemseng.2007.11.014

Anwar, S., & Mikami, Y., (2011). Comparing accuracy performance of ANN, MLR, and GARCH Model in predicting time deposit return of Islamic Bank. *International Journal of Trade, Economics and Finance*, *2*(1), 44 - 50. https://doi.org/10.7763/ijtef.2011.v2.77

Arlindo A., Shahgholi, G., Mardani, A., & Chiyaneh, H. (2018). Prediction effect of farmyard manure, multiple passes and moisture content on clay soil compaction using adaptive neuro-fuzzy inference system. *Journal of Terramechanics*, 77, 49 – 57. https://doi.org/10.1016/j.jterra.2018.03.002

Arslan, S., Misiewicz, P., Smith, E., & Godwin, R. J. (2015). The effect of tire tracks on draft force requirements of soil tillage and field traffic systems. 152189648, St. Joseph, Mich., ASABE. https://doi.org/10.13031/aim.20152189648 .

Arvidsson, J., & Keller, T. (2011). Comparing penetrometer and shear vane measurements with measured and predicted mould board plough draft in a range of Swedish soils. *Soil and Tillage Research*, 111, 219 – 223. https://doi.org/10.1016/j.still.2010.10.005.

Arvidsson, J., Keller, T., & Gustafsson, K. (2011). Specific draft for mouldboard plough, chisel plough and disc harrow at different water contents. *Soil and Tillage Research,* 79, 221–231. https://doi.org/10.1016/j.still.2004.07.010 .

ASABE. (2006). Agricultural machinery management data. American Society of Agricultural and Biological Engineers Standard ASAE D497.5, ASABE, St Joseph, MI, USA. 391 – 398.

ASABE. (2006). Procedures for using and reporting data obtained with the soil cone penetrometer. St. Joseph., Mich: ASABE.

ASABE Standards. (2009). ASAE D497.6, Agricultural machinery management data. *ASABE,* St. Joseph, Mich: ASABE.

ASAE., (2004). *Soil cone penetrometer* (49th ed). ASAE.

Asaf, Z., Rubinstein, D., & Shmulevich, I. (2007). Determination of discrete element model parameters required for soil tillage. *Soil and Tillage Research*, *92*(12), 227 - 242. https://doi.org/10.1016/j.still.2006.03.006 .

Askari, M., & Khalifahamzehghasem, S. (2013). Draft force inputs for primary and secondary tillage implements in a clay loam soil. *World Applied Sciences Journal*, *21*(12), 1789 – 1794.

Askari M., Shahgholi G., & Abbaspour-Gilandeh Y., (2017). The effect of tine, wing, operating depth and speed on the draft requirement of subsoil tillage tines. *Research in Agricultural Engineering*, 63, 160 – 167. https://doi.org/10.17221/4/2016-rae .

Augustin, K., Kahwald, M., Brunotte, J., & Duttmann, R. (2020). Wheel load and wheel pass frequency as indicators for soil compaction risk: A four-year analysis of traffic intensity at field scale. *Geosciences 10*(292), 1 – 15. https://doi.org/10.3390/geosciences10080292 .

Bajpal, D., & Mandal, A. (2015). Comparative analysis of T- Sugeno and Mamdani Type fuzzy logic controller for PMSM drives. *International Journal of Engineering Research and General Science, 3*(2), 1 – 15.

Balbuena, R. H., Terminiello, A. M., & Claverie, J. A. (2000). Soil compaction by forestry harvester operation: Evolution of physical properties. *Revista Brasileira,* 4, 453 – 459.

Ball, B. C., Crichton, I., & Horgan, G. W. (2008). Dynamics of upward and downward N_2O and CO_2 fluxes in ploughed or no-tilled soils in relation to water-filled pore space compaction and crop presence. *Soil and Tillage Research*, 101, 20 – 30. https://doi.org/10.1016/j.still.2008.05.012

Ball, B. C., Scott, A., & Parker, J. P. (2000). Soil and residue management effects on cropping conditions and nitrous oxide fluxes under controlled traffic in Scotland. *Revista Brasileira,* 52, 191 – 201.

Bateman, J. C., & Chanasyk, D. S. (2001). Effects of deep ripping and organic matter amendments on Ap horizons of soil reconstructed after coal strip-mining. *Canadian Journal of Soil Science*, 8, 113 – 120. https://doi.org/10.4141/s00-105

Batey, T. (2009). Soil compaction and soil management - A Review. *Soil Use and Management*, *25*(4), 335 - 345. https://doi.org/10.1111/j.1475-2743.2009.00236.x.

Batey, T., & McKenzie, D., (2006). Soil compaction, identification directly in the field. *Soil Use and Management*, 10, 1475 - 2743. https://doi.org/10.1111/j.1475-2743.2006.00017.x

Battiato, A., Diserens, E., Laloui, L., & Sartori, L. (2013). A mechanistic approach to topsoil damage due to slip of tractor tyres. *Journal of. Agricultural Science Applications, 2*(3), 160 – 168. https://doi.org/10.14511/jasa.2013.020305

Bayhan, Y., Kayisoglu, B., & Gonulol, E. (2002). Effect of soil compaction on sunflower growth. *Soil and Tillage Research,* 68, 31 – 38. https://doi.org/10.1016/s0167-1987(02)00078-8

Bengough, A., McKenzie, B., Hallett, P., & Valentine, T. (2011). Root elongation, water stress, and mechanical impedance: a review of limiting stresses and beneficial root tip traits. *Journal of Experimental Botany*, *62*(1), 59 - 68. https://doi.org/10.1093/jxb/erq350

Bergamin, A. S., Vitorino, A. C. T., Souza, F. R., & Venturoso, L. R. (2015). Relationship of soil physical quality parameters and maize yield in a Brazilian Oxisol. *Chilean Journal of Agricultural Research, 75*(3), 357 - 368. https://doi.org/10.4067/s0718-58392015000400013

Berisso, F. E., Schjønning, P., Keller, T., Alakukku, L., & Forkman, J. (2013). Gas transport and subsoil pore characteristics: anisotropy and long-term effects of compaction. *Geoderma,* 195, 184 – 191. https://doi.org/10.1016/j.geoderma.2012.12.002

Berisso, F. E., Schjønning, P., Keller, T., & Forkman, J. (2012). Persistent effects of subsoil compaction on pore size distribution and gas transport in a loamy soil. *Soil and Tillage Research*, 122, 42 - 51. https://doi.org/10.1016/j.still.2012.02.005

Beylich, A., Oberholzer, H., Schrader, S., & Wilke, B. (2010). Evaluation of soil compaction effects on soil biota and soil biological processes in soils. *Soil and Tillage Research*, 109, 133 – 143. https://doi.org/10.1016/j.still.2010.05.010

Blanco-Canqui, H., Gantzer, C. J., Anderson, S. H., & Alberts, E. E. (2004). Tillage and crop influences on soil properties for an Epiaqualf. *Soil Science Society of America Journal*, 68, 567 - 576.

Bluett, C., Tullberg, J. N., McPhee, J. E., & Antille, D. N. (2019). Soil and Tillage Research: Why still focus on soil compaction? Letter to the Editor. *Soil and Tillage Research*, 194 104282 https://doi.org/10.1016/j.still.2019.05.028

Boivin, P., Schäffer, B., Temgoua, E., Gratier, M., & Steinman, G. (2006). Assessment of soil compaction using soil shrinkage modelling: Experimental data and perspectives. *Soil and Tillage Research*, 88, 65 – 79. https://doi.org/10.1016/j.still.2005.04.008

Borghei, A. M., Taghinejad, J., Minaei, S., Karimi, M., & Varnamkhasti, G. M. (2008). Effect of subsoiling on soil bulk density, penetration, and cotton yield in northwest of Iran. *International Journal of Agriculture and Biology*, 10, 120 – 123.

Botta, G. F., Becerra, A. T., & Tourn, F. B. (2009). Effect of the number of tractor passes on soil rut depth and compaction in two tillage regimes. *Soil and Tillage Research*, 103, 381 – 386. https://doi.org/10.1016/j.still.2008.12.002

Botta, G. F, Jorajuria, D., Balbuena, R., & Rosatto, H. (2004). Mechanical and cropping behavior of direct drilled soil under different traffic intensities: effect on soybean (*Glycine max L.*) yields. *Soil and Tillage Research*, 78, 53 - 58. https://doi.org/10.1016/j.still.2004.01.004

Botta, G. F., Jorajuria D., & Draghi, L. (2002). Influence of the axle load, tyre size and configuration, on the compaction of a freshly tilled clayey soil. *Terramechanics*, 39(1), 47-54. https://doi.org/10.1016/s0022-4898(02)00003-4

Botta, G. F., Jorajuria, D., Rosatto, H., & Ferrero, C. (2006). Light tractor traffic frequency on soil compaction in the rolling pampa region of Argentina. *Soil and Tillage Research*, 86, 9 – 14. https://doi.org/10.1016/j.still.2005.01.014

Bouwman, L., & Arts, W. (2000). Effects of soil compaction on the relationships between nematodes, grass production and soil physical properties. *Applied Soil Ecology*, 14, 213 – 222. https://doi.org/10.1016/s0929-1393(00)00055-x

Brus, D. J., & van den Akker, J. J. H. (2018). How serious a problem is subsoil compaction in the Netherlands? A survey based on probability sampling. *Soil*, 4, 37– 45. https://doi.org/10.5194/soil-4-37-2018

Bulinski, J., & Niemczyk, H., (2001). Effect of method of agricultural outfit running on the field on soil properties and sugar beet yielding. *Annals of Warsaw University Agricultural Engineering*, 41, 39 – 44. https://doi.org/10.17221/3579-pse

Buragohain, M. (2008). *Adaptive Network based Fuzzy Inference System (ANFIS) as a tool for system identification with special emphasis on training data minimization* [Doctoral dissertation, Indian Institute of Technology, Guwahati].

Capello, G., Biddoccu, M., & Cavallo, E. (2019). Effects of tractor passes on hydrological and soil erosion processes in tilled and grassed vineyards. *Water*, 11, 1 - 25. https://doi.org/10.3390/w11102118

Carter, E. A., & Shaw, J. N. (2002). Correlations and spatial variability of soil physical properties in harvested piedmont forests. In: *Proceedings of the 6th International Conference on Precision Agriculture and Other Precision Resources Management* (130 – 142). USDA Forest Service.

Casanova, M., Tapia, E., Seguel, O., & Salazar, O. (2016). Direct measurement and prediction of bulk density on alluvial soils of central Chile. *Chilean Journal of Agricultural Research.* 76, 105 – 113. https://doi.org/10.4067/s0718-58392016000100015

Chakraborty, C., & Joseph, A. (2017). *Machine learning at central banks.* Bank of England Working Paper No. 674.

Chamen, W. C. T. (2011). *The effects of low and controlled traffic systems on soil physical properties, yields and the profitability of cereal crops on a range of soil types* [Doctoral dissertation, Cranfield University, Bedfordshire].

Chamen, T. (2015). Controlled traffic farming - from worldwide research to adoption in Europe and its future prospects. *Acta Technologica Agriculturae* 3, *18*(3), 64 – 73. https://doi.org/10.1515/ata-2015-0014

Chamen, T., Alakukku, L., Pires, S., Sommer, C., Spoor, G., Tijink, F., & Weisskopf, P. (2003). Prevention strategies for field traffic-induced subsoil compaction: a review Part 2. Equipment and field practices. *Soil and Tillage Research*, *73*(12), 161 - 174. https://doi.org/10.1016/s0167-1987(03)00108-9

Chamen, T., Moxey, A., Towers, W., & Ballana, D. (2015). Mitigating arable soil compaction: A review and analysis of available cost and benefit data. *Soil and Tillage Research,* 146,10 – 25. https://doi.org/10.1016/s0167-1987(03)00108-9

Chan, K., & Barchia, I. (2007). Soil compaction controls the abundance, biomass and distribution of earthworms in a single dairy farm in south-eastern Australia. *Soil and Tillage Research*, 94, 75 – 82. https://doi.org/10.1016/j.still.2006.07.006

Chapuis, R. P. (2004). Predicting the saturated hydraulic conductivity of sand and gravel using effective diameter and void ratio. *Canadian Geotechnical Journal, 41*(5), 787 - 795. https://doi.org/10.1139/t04-022

Chen, Y., Cavers, C., Tessier, S., & Lobb, D. (2005). Short-term tillage effects on soil cone index and plant development in a poorly drained, heavy clay soil. *Soil and Tillage Research, 82*(2), 161-171. https://doi.org/10.1016/j.still.2004.06.006

Chen, Y., McLaughlin, N. B., & Tessier, S. (2007). Double extended octagonal ring drawbar dynamometer. *Soil and Tillage Research*, 93, 462 - 471. https://doi.org/10.1016/j.still.2006.06.008

Chen, Y., Munkholm, L. J., & Nyord, T, (2013). A discrete element model for soil-sweep interaction in three different soils. *Soil and Tillage Research*, 136, 34 - 41. https://doi.org/10.1016/j.still.2012.08.008

Chen, H., &Yang, Y. (2015). Effect of controlled traffic system on machine fuel saving in annual two crops region in North China Plain. *Soil and Tillage Research,* 153, 137 – 144. https://doi.org/10.1016/j.still.2015.06.001

Chen, H.**,** Yang, Y., & Chen, L. (2010). Effect of wheel traffic on soil water infiltration. *Advanced Materials Research,* 113, 335 – 338. https://doi.org/10.4028/www.scientific.net/amr.113-116.335

Christian, B. (2020). *The Alignment Problem: Machine Learning and Human Values*. New York: WW Norton and Company.

Chyba, J., Kroulik, M., Kristof. K., & Misiewicz, P. A. (2017). The influence of agricultural traffic on soil infiltration rates. *Agronomy Research*, *15*(3), 664 – 673.

Chyba, J. (2012). *The influence of traffic intensity and soil texture on soil water infiltration rate* [Doctoral dissertation. Harper Adams University].

Corti, G., Ugolini, F. C., Agnelli, A., Certini, G., Cuniglio, R., Berna, F., & Fernandez, M. J. (2002). The soil skeleton, a forgotten pool of carbon and nitrogen in soil. *European Journal of Soil Science,* 53, 283 – 298. https://doi.org/10.1046/j.1365-2389.2002.00442.x

Cuttle, S., Shepherd, M., & Goodlass, G. (2003). A review of leguminous fertility building crops, with particular reference to nitrogen fixation and utilizations. Part of DEFRA project of the development of improved guidance on the use of fertility-building crops in organic farming. London, 165.

Dahab, M. H., & Mutwalli, M. D. (2002). Tractor tractive performance as affected by soil moisture content, tires inflation pressure and implement type. *Agricultural Mechanization in Asia, Africa and Latin America*, 33, 29 – 34.

Défossez, P., & Richard, G. (2002). Models of tilled compaction due to traffic and their field evaluation. *Soil and Tillage Research,* 67, 41– 64.

Défossez, P., Richard, G., Boizard, H., & O'Sullivan, M. F. (2003). Modeling change in soil compaction due to agricultural traffic as function of soil water content. *Geoderma*, 116, 89 - 105. https://doi.org/10.1016/s0016-7061(03)00096-x

Demir, M., Makineci, E., & Gungor, B. (2008). Plant species recovery on a compacted skid road. *Sensors*, 8, 3123 – 3133. https://doi.org/10.3390/s8053123

Demuth, H., Beal, M., & Hogan, M. (2009). *Neural Network Toolbox 6 User's Guide with MATLAB.* The Math Works, Inc., USA.

Dexter, A. R. (2004). Soil physical quality. Part I. Theory, effects of soil texture, density, and organic matter, and effects on root growth. *Geoderma*, 120, 201 – 214.

de Wit, A., Boogaard, H., Fumagalli, D., Janssen, S., Knapen, R., van Kraalingen, D. N., Supit, I., van der Wijngaart, R., & van Diepen, K. (2019). Twenty-five years of the WOFOST cropping systems model. *Agricultural Systems*, 168, 154 – 167. https://doi.org/10.1016/j.agsy.2018.06.018

Di, H. J., Cameron, K. C., Milne, J., & Reijnen, B. (2001). A mechanical hoof for simulating animal treading under controlled conditions. *New Zealand Journal of Agricultural Research,* 44, 111 – 116. https://doi.org/10.1080/00288233.2001.9513465

Diaz-Zorita, M., & Grosso, G.A. (2000). Effect of soil texture, organic carbon and water retention on the compactibility of soils from the Argentinian pampas. *Soil and Tillage Research*, 54, 121 – 126. https://doi.org/10.1016/s0167-1987(00)00089-1

Dobbie, K. E., & Smith, K. A. (2003). Nitrous oxide emission factors for agricultural soils in Great Britain: the impact of soil water-filled pore space and other controlling variables. *Global Change Biology,* 9, 204 – 218. https://doi.org/10.1046/j.1365-2486.2003.00563.x

Droutsas, I., Challinor, A. J., Swiderski, M., & Semenov, M. A. (2019). New modelling technique for improving crop model performance-application to the GLAM model. *Environmental Modelling and Software*, 118, 187 – 200. https://doi.org/10.1016/j.envsoft.2019.05.005

Duiker, S. W. (2004). *Avoiding soil compaction*. Penn State University, 1 - 8.

Egaji, O. A., Griffiths, A., Hasan, M. S., & Yu, H. (2015). A comparison of Mamdani and Sugeno Fuzzy based packet scheduler for MANET with a realistic wireless propagation model. *International Journal of Automation and Computing*, 1 - 14. https://doi.org/10.1007/s11633-014-0861-y

Erbach, D. (2006). Farm equipment and soil compaction. *Transactions of the ASAE,* ASAE Paper No: 860730. https://doi.org/10.4271/860730

Ewetola, E. A., Onofua, O. E., & Babatunde, E. I. (2022). Soil compaction effects on soil physical properties and soybean (*Glycine max.)* yield in Ogbomoso, Southwestern Nigeria. *Asian Soil Research Journal*, *6*(2), 47 - 56. https://doi.org/10.9734/asrj/2022/v6i230129

Fabiola, N., Giarola, B., da Silva, A. P., Imhoff, S., & Dexter, A. R. (2003). Contribution of natural soil compaction on hard-setting behavior. *Geoderma*, 113, 95 - 108. https://doi.org/10.1016/s0016-7061(02)00333-6

Folberth, C., Baklanov, A., Balkovič, J., Skalský, R., Khabarov, N., & Obersteiner, M. (2019). Spatio-temporal downscaling of gridded crop model yield estimates based on machine learning. *Agricultural and Forest Meteorology,* 264, 1 – 15. https://doi.org/10.1016/j.agrformet.2018.09.021

Fielke, J., Ucgul, A., & Saunders, C. (2013). Discrete element modeling of soil-implement interaction considering soil plasticity, cohesion and adhesion. ASABE Paper No. 131618800. St. Joseph, MI: ASABE. https://doi.org/10.13031/aim.20131618800

Frey, B., Kremer, J., Rüdt, A., Sciacca, S., Matthies, D., & Lüscher, P. (2009). Compaction of forest soils with heavy logging machinery affects soil bacterial community structure. *European Journal of Soil Biology*, 45, 312 – 320. https://doi.org/10.1016/j.ejsobi.2009.05.006

Gachene, C. K., & Kimaru, G. (2003). *Soil fertility and land productivity*. RELMA/Sida Publication, Nairobi, 30 - 38.

Gao, W. D., Whalley, W. R., & Ren, T. S. (2016). A simple model to predict soil penetrometer resistance as a function of density, drying and depth in the field. *Soil Tillage and Research.* 155, 190 – 198. https://doi.org/10.1016/j.still.2015.08.004

Gao, Q., Chen, Y., Zhou, H., & Sadek, M. A. (2015). Simulation of soil dynamic properties of a seed opener using the discrete element method (DEM). *Agricultural Engineering International: CIGR Journal 17*(3), 72 - 82.

Garcia-Tomillo, A., de Figueiredo, T., & Dafonte, J. D. (2018). Effects of machinery trafficking in an agricultural soil assessed by Electrical Resistivity Tomography (ERT). *Open Agriculture*, 3, 378 – 385. https://doi.org/10.1515/opag-2018-0042

Gasso, V., Sørensen, C. A., Oudshoorn, F. W., & Green, O. (2013). Controlled traffic farming: review of the environmental impacts. *European Journal of Agronomy* 48, 66 – 73. https://doi.org/10.1016/j.eja.2013.02.002

Gitau, A. N. (2004). *Mechanical behaviour of a hardsetting luvisol soil* [Doctoral thesis, University of Nairobi].

Gitau, A. N., Gumbe, L. O., & Biamah, E. K. (2006). Influence of soil water on stress–strain behaviour of a compacting soil in semi-arid Kenya. *Soil and Tillage Research*, 89, 144 – 154.

Gitau, A. N., Gumbe, L. O., & Mwea, S. K. (2008). Mechanical behavior of a hard setting *luvisol* soil as influenced by soil water and effective confining stress. *Agricultural Engineering International: the CIGR Ejournal*, 10, 1 - 13.

Głąb, T. (2014). Effect of soil compaction and Nitrogen fertilization on soil pore characteristics and physical quality of sandy loam soil under red clover/grass sward. *Soil and Tillage Research*, 144, 8 – 19. https://doi.org/10.1016/j.still.2014.05.010

Gliński, J., Horabik, J., & Lipiec, J. (2011). *Encyclopedia of Agrophysics*. Springer Verlag, 767.

Godwin, R. J., O'Dogherty, M. J., Saunders, S., & Balafoutis, A. T. (2007). A force prediction model for mouldboard ploughs incorporating the effects of soil characteristic properties, plough geometric factors and ploughing speed. *Biosystems Engineering*, 97, 117 – 129. https://doi.org/10.1016/j.biosystemseng.2007.02.001

Grigorev, I., Kunickaya, O., Burgonutdinov, A., & Tikhonov, E. (2020). Theoretical studies of dynamic soil compaction by wheeled forestry machines. *Diagnostyka*. *21*(4), 3 - 13. https://doi.org/10.29354/diag/127650

Hagan, M., Demuth, H., & Beale, M. (2002). *Neural Network Design.* PWS Publishing Company, Boston, USA.

Håkansson, L. (2005). Machinery-induced compaction of arable soils–incidence, consequences and counter-measures. Swedish University of Agricultural Sciences, Division of Soil Management. Report no. 109, 153.

Hakansson, I., & Lipiec, J. (2000). A review of the usefulness of relative bulk density values in studies of soil structure and compaction. *Soil and Tillage Research*, 53, 71 – 85. https://doi.org/10.1016/s0167-1987(99)00095-1

Hamza, M. A., & Anderson, W. K. (2005). Soil compaction in cropping systems. A review of the nature causes and possible solutions. *Soil and Tillage Research*, 82, 121 – 145.

Hamza, M. A., & Anderson, W. K. (2003). Responses of soil properties and grain yields to deep ripping and gypsum application in a compacted loamy sand soil contrasted with a sandy clay loam soil in Western Australia. *Australian Journal of Agricultural Research*, 54, 273 – 282. https://doi.org/10.1071/ar02102

Hamza, M. A., & Anderson, W. K. (2002). Improving soil fertility and crop yield on a clay soil in Western Australia. *Australian Journal of Agricultural Research*, 53, 615 – 620.

Hamza, M. A., & Penny, S. (2002). Treatment of compacted soils in the eastern wheatbelt. Department of Agriculture, Western Australia. Farmnote no. 26/2002. https://doi.org/10.1071/ar01099

Han, H. S., Page-Dumroese, D. S., Han, S. K., & Tirocke, J. (2006). Effect of slash, machine passes, and soil moisture on penetration resistance in a cut-to-length harvesting. *International Journal for Engineering*, 17, 11 – 24. https://doi.org/10.1080/14942119.2006.10702532

Hansen, S., Bleken, M., & Sitaula, B. K., (2008). Effect of soil compaction and fertilization practise on N_2O emission and CH_4 oxidation. *Proceedings from the International Conference Organic Agriculture and Climate Change* (11 – 15). Enita of Clermont, France.

Hargreaves, P. J., Baker, K. L., Graceson, A., Bonnett, S., & Balle, B. C. (2019). Soil compaction effects on grassland silage yields and soil structure under different levels of compaction over three years. *European Journal of Agronomy*, 109, 117 - 123. https://doi.org/10.1016/j.eja.2019.125916

Hassan, B. A. Abdullah, Z. M., & Hussein, S. A. (2022). A new family of conjugate gradient methods to solve unconstrained optimization problems. *Journal of Information and Optimization Sciences, 43*(4), 811 – 820.

Hayati, M., Rashidi, A. M., & Rezaei, A. (2011). Prediction of grain size of nanocrystalline nickel coatings using adaptive neuro-fuzzy inference system. *Solid State Sciences*; 13, 163 – 167. https://doi.org/10.1016/j.solidstatesciences.2010.11.007

Hetz, E. J. (2001). Soil compaction potential of tractors and other heavy agricultural machines used in Chile. *Agricultural Mechanization in Asia, Africa and Latin America*, 32, 38 – 42.

Hillel, D. (2009). The mission of soil science in a changing world. *Journal of Plant Nutrition and Soil Science*, 172, 5 – 9. https://doi.org/10.1002/jpln.200800333

Horgan, G., & Ball, B. (2005). Modeling the effect of water distribution and hysteresis on air-filled pore space. *European Journal of Soil Science*, 56, 647 – 654. https://doi.org/10.1111/j.1365-2389.2005.00714.x

Horn, R. (2015). Soil compaction and consequences of soil deformation on changes in soil functions. In: Northcliff, S. (Ed.): Task Force – Solutions under Foot. *Catena Verlag, Reiskirchen*, 28 – 32.

Horn, R., & Fleige, H. (2009). Risk assessment of subsoil compaction for arable soils in Northwest Germany at farm scale. *Soil and Tillage Research*, 102, 201 - 208. https://doi.org/10.1016/j.still.2008.07.015

Horn, R., & Kutilek, M. (2009). The intensity-capacity concept-How far is it possible to predict intensity values with capacity parameters. *Soil and Tillage Research,* 103, 1 - 3. https://doi.org/10.1016/j.still.2008.10.007

Horn, R., Way, T., & Rostek, J. (2003). Effect of repeated tractor wheeling on stress/strain properties and consequences on physical properties in structured arable soils. *Soil and Tillage Research*, 73, 101 – 106. https://doi.org/10.1016/s0167-1987(03)00103-x

Hosseini, S. A., & Karparvarfard, S. H. (2011). Prediction of acting forces on chisel plough tine by dimensional analysis method. *Iranian Journal of Biosystems Engineering*, *43*(1), 93 - 103.

Houshyar, E., Davoodi, M. J., Bahrami, H., Kiani, S., & Houshyar, M. (2010). Energy use forecasting for wheat production utilizing artificial neural network. *Word Applied Science Journal*, *10*(8), 958 - 962.

Jabro, J. D., Sainju, U. M., & Sevens, W. B. (2009). Long-term tillage influences on soil physical properties under dryland conditions in northeastern Montana. *Archives of Agronomy and Soil Science*, *55*(6), 633 – 640. https://doi.org/10.1080/03650340902804316

Jebaraj, S., & Iniyan, S. (2006). A Review of Energy Models. *Renewable and Sustainable Energy Review,* 10, 281 - 311.

Jégou, D., Brunotte, J., Rogasik, H., & Cluzeau, D. (2002). Impact of soil compaction on earthworm burrow systems using X-ray computed tomography: preliminary study. *European Journal of Soil Biology*, 38, 329 – 336. https://doi.org/10.1016/s1164-5563(02)01148-2

Jiang, D., Yang, X. Clinton, N., & Wang, N. (2004). An Artificial Neural Network model for estimating crop yield using remotely sensed information, *International Journal of Remote Sensing*, 25, 1723 - 1732.

Jones, R. J. A., Spoor, G., & Thomasson, A. J. (2003). Vulnerability of subsoils in Europe to compaction: a preliminary analysis. *Soil and Tillage Research,* 73, 131 – 143. https://doi.org/10.1016/s0167-1987(03)00106-5

Jordan, D., Ponder, F., & Hubbard, V. (2003). Effects of soil compaction, forest leaf litter and nitrogen fertilizer on two oak species and microbial activity. *Applied Soil Ecology*, 23, 33 – 41. https://doi.org/10.1016/s0929-1393(03)00003-9

Kabri, H. U., Umar, B., & Tashiwa, Y. (2019). A mathematical model for predicting draft output of an animal-drawn mouldboard ridger. *International Journal of Engineering Inventions*.8(2), 5 - 11.

Kadam, R. F., & Al-Abrahemee, K. M. M. (2022). On convergence of the Levenberg-Marquardt method under local error bound. *Journal of Interdisciplinary Mathematics*. *25*(5), 1495 - 1508.

Kader, K.A. (2008). Effect of some primary tillage implement on soil pulverization and specific energy. *Misr Journal of Agricultural Engineering, 25*(3), 731 - 745.

Karmakar, S. (2005). *Numerical modeling of soil flow and pressure distribution on a simple tillage tool using Computational Fluid Dynamics* [Doctoral dissertation, University of Sasketchewan].

Karmakar, S., & Kushwaha, R. L. (2006). Dynamic modeling of soil–tool interaction: An overview from a fluid flow perspective. *Journal of Terramechanics,* 43, 411 - 425. https://doi.org/10.1016/j.jterra.2005.05.001

Karmakar, S., Ashrafizadeh, S. R., & Kushwaha. R. L. (2009). Experimental validation of Computational Fluid Dynamics modeling for narrow tillage tool draft. *Journal of Terramechanics*, *46*(6), 277 – 283. https://doi.org/10.1016/j.jterra.2009.06.001

Karparvarfard, S. H., & Rahmanian-Koushkaki, H. (2014). Development of a fuel consumption equation: Test case for a tractor chisel-ploughing in a clay loam soil. *Biosystems Engineering*, (30), 23 - 33. https://doi.org/10.1016/j.biosystemseng.2014.11.015

Kathirvel, K., Manian, R., & Balasubramanian, M. (2001). Tractive performance of power tiller tyres. *Agricultural Mechanization in Asia, African and Latin America.* 32(2), 32 - 36.

Kasisira, L. L. (2004). *Force modeling and energy optimization for subsoilers in tandem* [Doctoral dissertation, University of Pretoria].

Kasisira, L. L., & du Plessis, H. L. M. (2006). Energy optimization for subsoilers in tandem in a sandy clay loam soil. *Soil and Tillage Research,* 86, 185–198. https://doi.org/10.1016/j.still.2005.02.031

Kaur, A., & Kaur, A. (2012). Comparison of Mamdani-type and Sugeno-type Fuzzy Inference system for air conditioning system. *International Journal of Soft Computing and Engineering*, *2*(2), 2231 – 2307. https://doi.org/10.11591/ijaas.v5.i4.pp163-167

Kawuyo, U. A. (2011). *Mathematical modeling of draft characteristics of selected animal-drawn implements on the upland soils of Samaru, Nigeria* [Doctoral thesis, Ahmadu Bello University, Zaria].

Kees, G. (2008). Using subsoiling to reduce soil compaction. Technology and Development Program 0834–2828–MTDC. Missoula, MT: U.S. Department of Agriculture.

Keller, T. (2004). *Soil Compaction and Soil Tillage – Studies in Agricultural Soil Mechanics* [Doctoral thesis, Swedish University of Agricultural Sciences, Uppsala].

Keller, T., & Arvidsson, J. (2004). Technical solutions to reduce the risk of subsoil compaction: Effects of dual wheels, tandem wheels and tyre inflation pressure on stress propagation in soil. *Soil and Tillage Research*, 79, 191 – 205. https://doi.org/10.1016/j.still.2004.07.008

Keller, T., Défossez, P., Weisskopf, P., Arvidsson, J., & Richard, G. (2004). SoilFlex: A model for prediction of soil stresses and soil compaction due to agricultural field traffic including a synthesis of analytical approaches. *Soil and Tillage Research*, *93*(2), 391- 411. https://doi.org/10.1016/j.still.2006.05.012

Keller, T., Lamandé, M., Peth, S., & Delenne (2013). An interdisciplinary approach towards improved understanding of soil deformation during compaction. *Soil and Tillage Research*, 12, 61 – 80. https://doi.org/10.1016/j.still.2012.10.004

Keller, T., Sandin, M., Colombi, T., Horn, R., & Or, D. (2019). Historical increase in agricultural machinery weights enhanced soil stress levels and adversely affected soil functioning. *Soil and Tillage Research*, 194, 104293. https://doi.org/10.1016/j.still.2019.104293

Khadr, K. A. (2008). Effect of some primary tillage implement on soil pulverization and specific energy. *Journal of Agricultural Engineering*, *25*(3), 731 - 745. https://doi.org/10.21608/mjae.2008.191017

Khalilian, A., Williamson, R. E., Sullivan, M. J., & Mueller, J. (2002). Injected and broadcast application of composted municipal solid waste in cotton. *Applied Engineering in Agriculture*, 18, 17 – 22. https://doi.org/10.13031/2013.7704

Khan, M. A., Qaisrani, R., & Li. J. Q. (2010). Techniques of reducing adhesion and scouring soil by bionic: Review of literature. *Advances in Natural Science*, *3*(2), 41 - 50.

Kheiralla A. F., Azmi, Y., Zohadie, M., & Ishak, W. (2004). Modeling of power and energy forces for tillage implements operating in Serdang sandy clay loam, Malaysia. *Soil and Tillage Research*, 78, 21–34. https://doi.org/10.1016/j.still.2003.12.011

Khoshnevisan, B., Rafiee, S., Omid, M., & Mousazadeh, H. (2014). Development of an intelligent system based on ANFIS for predicting wheat grain yield on the basis of energy inputs. *Information Processing in Agriculture*, 1, 14 – 22. https://doi.org/10.1016/j.inpa.2014.04.001

Khuntia, S. (2014). *Modeling of geotechnical problems using soft computing* [Master's thesis, National Institute of Technology, Rourkela].

Kingwell, R., & Fuchsbichler, A. (2011). The whole-farm benefits of controlled traffic farming: an Australian appraisal. *Agricultural Systems*, 104, 513 – 521. https://doi.org/10.1016/j.agsy.2011.04.001

Kirby, J., & Bengough, A. (2002). Influence of soil strength on root growth: experiments and analysis using a critical-state model. *European Journal of Soil Science,* 53, 119 – 127. https://doi.org/10.1046/j.1365-2389.2002.00429.x

Koch, H., Heuer, H., Tomanová, O., & Märländer, B. (2008). Cumulative effect of annually repeated passes of heavy agricultural machinery on soil structural properties and sugar beet yield under two tillage systems. *Soil and Tillage Research,* 101, 69 – 77. https://doi.org/10.1016/j.still.2008.07.008

Košutić, S. Filipović, D., Gospodarić, Z., & Čopec, K. (2005). Effects of different soil tillage systems on yield of maize, winter wheat and soybean on Albic uvisol in North-West Slavonia. *Journal of Central European Agriculture, 6*(3), 241 - 248.

Krebstein, K., von Janowsky, K., Kuht, J., & Reintam, E. (2014). The effect of tractor wheeling on the soil properties and root growth of smooth brome. *Plant Soil Environment, 60*(2), 74 – 79. https://doi.org/10.17221/804/2013-pse

Kremers, J., & Boosten, M. (2018). Soil compaction and deformation in forest exploitation. *American Journal for Alternative Agriculture*. *7(*12), 25 – 31.

Kristoffersen, A., & Riley, H. (2005). Effects of soil compaction and moisture regime on the root and shoot growth and phosphorus uptake of barley plants growing on soils with varying phosphorus status. *Nutrient Cycle Agroecosystems*, 72, 135 – 146. https://doi.org/10.1007/s10705-005-0240-8

Kroulík, M., Kumhála, F., Hula, J., & Honzík, I., (2009). The evaluation of agricultural machines field trafficking intensity for different soil tillage technologies. *Soil and Tillage Research*, 105, 171 – 175. https://doi.org/10.1016/j.still.2009.07.004

Kroulik, M., Kviz, Z., Kumhala, F., Hůla, J., & Loch, T. (2011). Procedures of soil farming allowing reduction of compaction. *Precision Agriculture, 12*(3), 317 – 333. https://doi.org/10.1007/s11119-010-9206-1

Kumar, D., Bansal, M. L., & Phogat, V. K. (2009). Compactability in relation to texture and organic matter content on alluvial soils. *Indian Journal of Agricultural Research.* 43, 180 – 186.

Kumar, A., & Thakur, T. C. (2005). *An investigation into comparative test of conventional and winged subsoilers.* ASAE Paper No. 051061. St. Joseph, Mich.: ASAE. https://doi.org/10.13031/2013.19770

Lacey, S.T., Brennan, P. D., & Parekh, J. (2001). Deep may not be meaningful: cost and effectiveness of various ripping tine configurations in a plantation cultivation trial in eastern Australia. *New Forests*, 21, 231 – 248.

Laker, M. C. (2001). Soil compaction: effects and amelioration. *Proceedings of the 75th Annual Congress of the South African Sugar Technologists' Association* (125 – 128). Durban, South Africa.

Lal, R. (2009). Soils and food sufficiency, a review. *Agronomy for Sustainable Development*, 29, 113 – 133. https://doi.org/10.1051/agro:2008044

Lamandé, M., & Schjønning, P. (2014). Transmission of vertical stress in a real soil profile. *Soil and Tillage Research*. 114 (2), 57 - 70. https://doi.org/10.1016/j.still.2010.10.001

Lamandé, M., Schjønning, P., & Tøgersen, F. A. (2007). Mechanical behaviour of an undisturbed soil subjected to loadings: Effects of load and contact area. *Soil and Tillage Research*, 97, 91 – 106. https://doi.org/10.1016/j.still.2007.09.002

Li, B., Xia, R., Liu, F. Y., Chen, J., Han, W. T., & Han, B. (2016). Determination of the draft force for different subsoiler points using discrete element method. *International Journal of Agricultural and Biological Engineering*, *9*(3), 81－87.

Li, H., Gao, H., Chen, J., Li, W., & Li, R. (2000). Study on controlled traffic with conservative tillage. *Transactions of the Chinese Society of Agricultural Engineers,* 16, 73 – 77.

Li, M., & Wang, J. (2019). An empirical comparison of multiple linear regression and artificial neural network for concrete dam deformation modeling. *Mathematical Problems in Engineering*, 1 – 14. https://doi.org/10.1155/2019/7620948

Li, X., & Zhang, L. M. (2009). Characterization of dual-structure pore-size distribution of soil. *Canadian Geotechnical Journal*, 46, 129 – 141. https://doi.org/10.1139/t08-110

Li, Y., Tullberg, J. N., & Freebairn, D.M. (2001). Traffic and residue cover effects on infiltration. *Australian Journal of Soil Research*, 39, 239 – 247.

Lin, H. (2010). Earth's critical zone and hydropedology: concepts, characteristics, and advances, *Hydroloy and Earth System Sciences*, 14, 25 – 45.

Linde, J. (2007). *Discrete Element Modeling of a vibratory subsoiler* [Master's thesis, University of Stellenbosch].

Lipiec, J., Arvidsson, J., & Murer, E. (2003). Review of modeling crop growth, movement of water and chemicals in relation to topsoil and subsoil compaction. *Soil and Tillage Research*, 73, 15 – 29.

Lipiec, J., & Hatano, R. (2003). Quantification of compaction effects on soil physical properties and crop growth. *Geoderma*, 116, 107 – 136. https://doi.org/10.1016/s0016-7061(03)00097-1

Lipiec, J., Giovanetti, V., & Turski, M. (2002). Response of structure to simulated trampling of woodland soil. *Advanced Geoecology*, 35, 133 – 140.

Litta, A. J., Idicula, S. M., & Mohanty, U. C. (2013). Artificial neural network model in prediction of meteorological parameters during pre-monsoon thunderstorms. *International Journal of Atmospheric Sciences*, 1 - 14. https://doi.org/10.1155/2013/525383

Liu, K., Benetti, M., Sozzi, M., Gasparini, F., & Sartori, L. (2022). Soil compaction under different traction resistance conditions - A case study in North Italy. *Agriculture*, 12, 1954. https://doi.org/10.3390/agriculture12111954

Lysych, M. N. (2019). Review of numerical methods for modeling the interaction of soil environments with the tools of soil tillage machines. *Journal of Physics: Conference Series*, 1399, 1 – 9. https://doi.org/10.1088/1742-6596/1399/4/044014

Mac, J., Chen, Y., & Sadek, M. A. (2012). Determining parameters of a discrete element model for soil–tool interaction. *Soil and Tillage Research*, 118, 117 - 122. https://doi.org/10.1016/j.still.2011.10.019

Macrì, G., De Rossi, A., Papandrea, S, Micalizzi, F. Russo, D., & Settineri, G. (2017). Evaluation of soil compaction caused by passages of farm tractor in a forest in Southern Italy. *Agronomy Research, 15*(2), 478 – 489.

Mak**,** J., & Chen, Y. (2014). Simulation of draft forces of a sweep in a loamy sand soil using the discrete element method. *Canadian Biosystems Engineering*, 56, 211 - 217. https://doi.org/10.7451/cbe.2014.56.2.1

Mak, J., Chen, Y., & Sadek, M. A. (2012). Determining parameters of a discrete element model for soil–tool interaction. *Soil and Tillage Research*, 118, 117 – 122. https://doi.org/10.1016/j.still.2011.10.019

Makange, N. R, Ji, C., Nyalala, I., Sunusi, I. I., & Opiyo, S. (2021). Prediction of precise subsoiling based on analytical method, discrete element simulation and experimental data from soil bin. *Springer Nature*, 1 – 12. https://doi.org/10.9734/ajarr/2019/v3i430093

Mamkagh, A. M. (2014). Review of fuel consumption, draft force and ground speed measurements of the agricultural tractor during tillage operations. *Asian Journal of Advanced Research and Reports, 3*(4), 1 - 9.

Manuwa, S. I. (2009). Performance evaluation of tillage tines operating under different depths in a sandy clay loam soil. *Soil and Tillage Research*, 103, 399 – 405. https://doi.org/10.1016/j.still.2008.12.004

Manuwa, S., & Ademosun, O. C. (2007). Draft and soil disturbance of model tillage tines under varying soil parameters. *Agricultural Engineering International: the CIGR Ejournal*, 9, 112 - 129.

Marenya, M. O. (2009). *Performance characteristics of deep tilling rotavator performance characteristics of a deep tilling rotavator* [Doctoral thesis, University of Pretoria]

Mari, G. R., Ji, C., Zhou, J., & Bukhari, F. S. (2006). Effect of tillage machinery traffic on soil properties, corn root development and plant growth. *Agricultural Engineering International: the CIGR Ejournal*, (8), 12 - 20.

Martínez, E., Silva, P., Valle, S., & Acevedo, E. (2008). Soil physical properties and wheat root growth as affected by no-tillage and conventional tillage systems in a Mediterranean environment of Chile. *Soil and Tillage Research*, 99, 232 – 244. https://doi.org/10.1016/j.still.2008.02.001

MathWorks. *Fuzzy logic toolbox user's guide*. (2012). Natick: Inc, 3 Apple Hill Drive, 137–179.

McGarry, D. (2001). Tillage and soil compaction. In: Garcia-Torres, L., Benites, J., Martinez-Vilela, A. (Eds.), First World Congress on Conservation Agriculture, 1 – 5th October 2001, Madrid, Spain, *Natural Resource Sciences*, 281 – 291.

McNabb, D., Startsev, A., & Nguyen, H. (2001). Soil wetness and traffic level effects on bulk density and air-filled porosity of compacted boreal forest soils. *Soil Science Society of America Journal*, 65, 1238 – 1247. https://doi.org/10.2136/sssaj2001.6541238x

Metwalli, S. M., Kabeel, M. H. A., Aboukarima, A. M., & Bader, S. E. (2002). Effect of forward speed, ploughing depth and inflation pressure on tractors performance during tillage I. In clay loam soil. *Misr Journal of Agricultural Engineering*, *19*(3), 597 - 610.

Mileusnic Z. I., Petrovic, D. V., & Devic, M. S. (2010). Comparison of Tillage Systems According to Fuel Consumption. *Energy*, 35, 221 – 2 28. https://doi.org/10.1016/j.energy.2009.09.012

Milne, A. E., Haskard, K. A., Webster, C. P., Truan, I. A., Goulding, K. W. T., & Lark, R.M. (2011). Wavelet analysis of the correlations between soil properties and potential nitrous oxide emission at farm and landscape scales. *European Journal of Soil Science*, 62, 467 – 478. https://doi.org/10.1111/j.1365-2389.2011.01361.x

Miransari, M., Bahrami, H. A., Rejali, F., & Malakouti, M. J. (2009). Effects of soil compaction and arbuscular mycorrhiza on corn (*Zea mays L.*) nutrient uptake. *Soil Tillage and Research*, 103, 282 – 290. https://doi.org/10.1016/j.still.2008.10.015

Mogharreban, N., & DiLalla, L. F. (2006). Comparison of Defuzzification techniques for analysis of non-interval data. In *Proceedings of the Annual Meeting of the North American Fuzzy Information Processing Society* (257 – 260). Montreal, Canada, https://doi.org/10.1109/nafips.2006.365418

Mohammadi, A., Alimardani, R., Akbarnia, A., & Akram, A. (2012). Modeling of draft force variation in a winged share tillage tool using fuzzy table look-up scheme. *Agricultural Engineering International, CIGR Journal*, *14*(4), 262－268.

Moinar, A. M., & Shahgholi, G. (2018). Dimensional analysis of the tractor tractive efficiency parameters. *Acta Technologica Agriculturae*, 3, 94 – 99. https://doi.org/10.2478/ata-2018-0017

Moinar, A. M., & Shahgholi, G. (2019). The effect of tractor driving system type on its slip and rolling resistance and its modeling using ANFIS. *Acta Technologica Agriculturae*, *22*(4), 115 - 121. https://doi.org/10.2478/ata-2019-0021

Moitzi, G., Wagentristl, H., Refenner, K., Weingartmann, H., & Gronaue, A. (2014). Effects of working depth and wheel slip on fuel consumption of selected tillage implements. *Agricultural Engineering International: CIGR Journal*, *16*(1), 182 - 190.

Montgomery, D, C., Peck, E. A., & Vining, G. G. (2007). *Introduction to Linear Regression Analysis, Solutions Manual (Wiley Series in Probability and Statistics)*. Wiley-Interscience, New York, USA: ISBN: 0470125063.

Morvan, X., Verbeke, L., Laratte S., & Schneider A. R. (2018). Impact of recent conversion to organic farming on physical properties and their consequences on runoff, erosion and crusting in a silty soil", *CATENA*, 165, 398 – 407. https://doi.org/10.1016/j.catena.2018.02.024

Mossadeghi-Björklund, M., Arvidsson, J., Keller, T., Koestel, J., Lamandé, M., Larsbo, M., & Jarvis, N. (2016). Effects of subsoil compaction on hydraulic properties and preferential flow in a Swedish clay soil. *Soil and Tillage Research*, 156, 91 – 98. https://doi.org/10.1016/j.still.2015.09.013

Mosaddeghi, M. R., Hajabbasi, M., Hemmat, A., & Afyuni, M. (2000). Soil compactibility as affected by soil moisture content and farmyard manure in Central Iran. *Soil and Tillage Research*, 55, 87 – 97. https://doi.org/10.1016/s0167-1987(00)00102-1

Mouazen, A. B., & Ramon, H. (2002). A numerical–statistical hybrid modelling scheme for evaluation of draft requirements of a subsoiler cutting a sandy loam soil, as affected by moisture content, bulk density and depth. *Soil and Tillage Research*, *63*(3), 155 - 165. https://doi.org/10.1016/s0167-1987(01)00243-4

Mouazen, A. B., & Ramon, H. (2006). Development of on-line measurement system of bulk density based on on-line measured draft, depth and soil moisture content. *Soil and Tillage Research*, 86, 218 – 229. https://doi.org/10.1016/j.still.2005.02.026

Mouazen, A. M., Herman R., & De B. J. (2003). Modeling compaction from on-line measurement of soil properties and sensor draft. *Precision Agriculture*, *4*(2), 203 - 212.

Muhsin, S. J. (2017). Determination of energy requirements, ploughed soil volume rate and soil pulverization ratio of chisel plough under various operating conditions. *Basrah Journal of Agricultural Sciences*, *30*(1), 73 - 84. https://doi.org/10.33762/bagrs.2017.127519

Mujdeci, M., Isildar, A. A., Uygur, V., & Alaboz, P. (2017). Cooperative effects of field traffic and organic matter treatments on some compaction-related soil properties. *Solid Earth*, 8, 189 – 198. https://doi.org/10.5194/se-2016-84-sc1

Murray, S. (2016). *Modeling of soil-tool interactions using the Discrete Element Method (DEM)* [Master's thesis. University of Manitoba, Winnipeg].

Naderi-Boldaji, M., Kazemzadeh, A., & Keller, T., (2018). Changes in soil stress during repeated wheeling: a comparison of measured and simulated values. *Soil Research.* 56, 204 – 214. https://doi.org/10.1071/sr17093

Naderloo, L., Alimadani, R., Akram, A., & Khanghah, H. Z. (2009). Tillage depth and forward speed effects on draft of three primary tillage implements in clay loam soil. *Journal of Food, Agriculture and Environment, 76*(3), 382 – 385.

Naderloo, L., Alimardani, R., Omid, M., Sarmadian, F., Javadikia, P., & Torabi, M. Y. (2012). Application of ANFIS to predict crop yield based on different energy inputs. *Measurement, 45*(6), 1406 – 1413. https://doi.org/10.1016/j.measurement.2012.03.025

Naghdi, R., & Solgi, A. (2014). Effects of skidder passes and slope on soil disturbance in two soil water contents. *Croatian Journal of Forest Engineering*, 35, 73 – 80.

Najafi, A., Solgi, A., & Sadeghi, S. H. (2009). Soil disturbance following four-wheel rubber skidder logging on the steep trail in the north mountainous forest of Iran. *Soil and Tillage Research,* 103, 165 – 169.

Nawaz, M. F., Bourrié, G., & Trolard, F. (2013). Soil compaction impact and modeling. A review *Agronomy for Sustainable Development,* 33, 291 – 309.

Nawaz, M. F. (2010). *Geochemistry of hydromorphic soils and waters under rice culture and forest—continuous measurements, thermodynamic modeling and kinetics* [Doctoral dissertation, Marseille University].

Ndisya, J., Gitau, A. N. Mbuge, D. O., & Hiuhu, A. W. (2016). Investigation of the effect of rake angle on draft requirement for ripping in sandy clay. *Agricultural Engineering International: CIGR Journal*, *18*(4), 52 - 69.

Nikolic, R., Savin, L., Furman, T., Gligoric, R., & Tomic, M., (2001). Research of the problems of soil compaction. *Acta Technologica Agriculturae* 4, 107 – 112.

Nkakini, S. O., Ekemube, R. A., & Igoni, A. H. (2019). Modeling fuel consumption rate for harrowing operations in loamy sand soil. *European Journal of Agriculture and Forestry Research, 7*(2), 1 - 12.

Nkakini, S. O., & Vurasi, N. M. (2015). Effects of moisture content, bulk density and tractor forward speeds on energy requirement of disc plough. *Technology, 6*(7), 69 - 79.

Nyaanga, D. M. (2000). *Prediction of potato bulk temperature during free natural convection storage* [Doctoral dissertation, University of Nairobi].

Nyeki, A., Milics, G., Kovacs, A. J., & Nemenyi, M. (2013). Improving yield advisory models for precision agriculture with special regards to soil compaction in maize production. In: Stafford, J. (Ed.), *Precision Agriculture* (443 – 450).

Obermayr, M., Dressler, K., Vrettos, C., & Eberhard, P. (2011). Prediction of draft forces in cohesionless soil with the Discrete Element Method. *Journal of Terramechanics, 48*(5), 347 - 358. https://doi.org/10.1016/j.jterra.2011.08.003

Odey, S. O., Manuwa, S. I., & Ademosun, O. C. (2014). Effect of tractor traffic and moisture content on cone index in a crop-cultivated land. In *proceedings of the International Soil Tillage Research Organisation (ISTRO) Nigeria Symposium* (135 – 142). Akure.

Odey, S. O., Ovat, F. A., & Okon, O. O. (2018). Drafts, power requirements and soil disruption of subsoilers. *International Journal of Emerging Engineering Research and Technology*. *6*(9), 24 – 38.

Okayasu, T., Morishita, K., Terao, H., Mitsuoka, M., Inoue, E., & Fukami, K. (2012). Modeling and prediction of soil cutting behavior by a plow frictional slider. In *Power and Machinery. International Conference of Agricultural Engineering - CIGR-Ag Eng:* Agriculture and Engineering for a Healthier Life, Valencia: *CIGR-European Journal of Agricultural Engineering.* 1 - 6.

Olatunji, O. M., Akor, A. J., & Davies, R. M. (2009). Modeling the effect of weight and forward speed on the performance of disc plough. *Electronic Journal of Environment and Agriculture, 8*(2), 130 – 149.

Olatunji, O. M., Burubai, W. I., & Davies, R. M. (2009). Effect of weight and draft on the performance of disc plough on sandy loam soil. *Journal of Applied Science, Engineering and Technology, 1*(1), 22 – 26.

Olesen, J. E., & Munkholm, L. J. (2007). Subsoil loosening in a crop rotation for organic farming eliminated plough pan with mixed effects on crop yield. *Soil* and *Tillage Research*, 94, 376 – 385. https://doi.org/10.1016/j.still.2006.08.015

Oluwafemi, I., Laseinde, T., & Dada, D. (2019). Evaluation of saturated hydraulic conductivity at adaptable depths in a sandy loam using the Beerkan Method. *Proceedings of the International Conference on Industrial Engineering and Operations Management*. Pilsen.

Osunbitan, J. A., Oyedele, D. J., & Adekalu, K.O. (2005). Tillage effects on bulk density, hydraulic conductivity and strength of loamy sand soil in southwestern Nigeria. *Soil and Tillage Research*, 82, 57 - 64. https://doi.org/10.1016/j.still.2004.05.007

Pagliai, M., Marsili, A., Servadio, P., Vignozzi, N., & Pellegrini, S. (2003). Changes in some physical properties of a clay soil in Central Italy following the passage of rubber tracked and wheeled tractors of medium power. *Soil and Tillage Research*, 73, 119 - 129. https://doi.org/10.1016/s0167-1987(03)00105-3

Parker, R. T. (2007). Monitoring soil strength conditions resulting from mechanical harvesting in volcanic ash soils of Central Oregon. *Journal of Applied Forestry*, 22, 261 – 268. https://doi.org/10.1093/wjaf/22.4.261

Patel, S. K., & Mani, I. (2011). Effect of multiple passes of tractor with varying normal load on subsoil compaction. *Journal of Terramechanics*, 48, 277 – 284. https://doi.org/10.1016/j.jterra.2011.06.002

Pengthamkeerati, P., Motavalli, P., & Kremer, R. (2011). Soil microbial activity and functional diversity changed by compaction, poultry litter and cropping in a claypan soil. *Applied Soil Ecology*, 48, 71 - 80. https://doi.org/10.1016/j.apsoil.2011.01.005

Petersen, M., Ayers, P., & Westfall, D. (2004). *Managing Soil Compaction*. CSU Cooperative Extension Agriculture, No. 0.519.

Picchio, R., Neri, F., Petrini, E., Verani, S., Marchi, E., & Certini, G. (2012). Machinery-induced soil compaction in thinning two pine stands in central Italy. *Forest Ecology Management*, 285, 38 – 43. https://doi.org/10.1016/j.foreco.2012.08.008

Pitla, S. K., Luck, J. D., Werner, J., Lin, N., & Shearer, S. A. (2016). In-field fuel use and load states of agricultural field machinery. *Computers and Electronics in Agriculture*, 121, 290 – 300. https://doi.org/10.1016/j.compag.2015.12.023

Powers, R. F., Scott, D. A., Sanchez, F. G., Voldseth, R. A., Page-Dumroese, D., Elioff, J. D., & Stone, D. M. (2005). The North American long-term soil productivity experiment: findings from the first decade of research. *Forest Ecology Management*, 220, 31 – 50. https://doi.org/10.1016/j.foreco.2005.08.003

Powlson, D. S., Whitmore, A. P., & Goulding, W. T. (2011). Soil carbon sequestration to mitigate climate change: a critical re-examination to identify the true and the false. *European Journal of Soil Science*, 62, 42 – 55. https://doi.org/10.1111/j.1365-2389.2010.01342.x

Poznyak, A., Chairez, I., & Poznyak, T. (2019). A survey on artificial neural networks application for identification and control in environmental engineering: biological and chemical systems with uncertain models. *Annual Reviews in Control*, 48, 250 – 272. https://doi.org/10.1016/j.arcontrol.2019.07.003

Pulido-Moncada, M., Munkholm, L. J., & Schjønning, P. (2019). Wheel load, repeated wheeling, and traction effects on subsoil compaction in northern Europe. *Soil and Tillage Research*, 186, 300 – 309. https://doi.org/10.1016/j.still.2018.11.005

Pupin, B., Freddi, O., & Nahas, E. (2009). Microbial alterations of the soil influenced by induced compaction. *Rev Bras Cienc Solo*, 33, 1207 – 1213.

Putri, R. S., Purwanto, A., Pramono, R., Asbari, M., Wijayanti, L. M., & Hyun, C. C. (2020). Impact of the COVID-19 pandemic on online home learning: an explorative study of primary schools in Indonesia. *International Journal of Advanced Science and Technology* 29, 4809 – 4818.

Pytka, J., & Szymaniak, G. (2004). *Investigations of stress state in soil under tractor tyres*, Polish Academy of Sciences.

Radford, B. J., Yule, D. F., McGarry, D., & Playford, C. (2001). Crop responses to applied soil compaction and to compaction repair treatments. *Soil and Tillage Research*, 61, 157 – 166. https://doi.org/10.1016/s0167-1987(01)00194-5

Radford, B. J., Yule, D. F., McGarry, D., & Playford, C. (2007). Amelioration of soil compaction can take 5 years on a vertisol under no till in the semi–arid subtropics. *Soil and Tillage Research*, 97, 249 – 255. https://doi.org/10.1016/j.still.2006.01.005

Ramezani, N., Sayyad, G. A., & Barzegar, A. R. (2017). Tractor wheel compaction effect on soil water infiltration, hydraulic conductivity and bulk density. *Malaysian Journal of Soil Science*, 21, 47 - 61.

Raper, R. L. (2005). Agricultural traffic impacts on soil. *Journal of Terramechanics*, 42, 259 – 280. https://doi.org/10.1016/j.jterra.2004.10.010

Raper, R. L., & Bergtold. J. S. (2007). In-row subsoiling: A review and suggestions for reducing cost of this conservation tillage operation. *Applied Engineering in Agriculture*, *23*(4), 463 - 471. https://doi.org/10.13031/2013.23485

Raper, R. L., Grift, T. E., & Tekeste, M. Z. (2004). A portable tillage profiler for measuring subsoiling disruption. *Transactions of the ASAE, 47*(1), 23 - 27. https://doi.org/10.13031/2013.15861

Raper, R. L., & Kirby, J. M. (2006). *Soil compaction: how to do it, undo it, or avoid doing it*. ASABE Distinguished Lecture 30, Agricultural equipment technology conference, ASABE Publication no. 913C0106, 1 - 14.

Raper, R. L., & Sharma. A. K. (2004). Soil moisture effects on energy requirements and soil disruption of subsoiling a coastal plains soil. *Transactions of the ASAE, 47*(6), 1899 - 1905. https://doi.org/10.13031/2013.17799

Ren, L. Q., Tong, J., Li, J. Q., & Chen, B. (2001). Soil adhesion and biometrics of soil engaging components: A review. *Journal of Agricultural Engineering Research*, 79, 239 - 263.

Reynolds, W. D., Drury, C. F., Tan, C. S., Fox, C. A., & Yang, X. M. (2009). Use of indicators and pore volume-function characteristics to quantify soil physical quality. *Geoderma*, 152, 252 – 263. https://doi.org/10.1016/j.geoderma.2009.06.009

Rezaei, M., Seuntjens, P., Shahidi, R., Joris, I., Boënne, W., Al-Barri, B., & Cornelis, W. (2016). The relevance of in-situ and laboratory characterization of sandy soil hydraulic properties for soil water simulations. *Journal of Hydrology*, 534, 251 – 265.

Rosolem, C., Foloni, J., & Tiritan, C. (2002). Root growth and nutrient accumulation in cover crops as affected by soil compaction. *Soil and Tillage Research*, 65, 109 –115. https://doi.org/10.1016/s0167-1987(01)00286-0

Rodriguez, L. A., Valencia, J. J., & Urbano, J. A. (2012). Soil compaction and tires for harvesting and transporting sugarcane. *Journal of Terramechanics*, 49, 183 – 189. https://doi.org/10.1016/j.jterra.2012.04.002

Roul, A.K., Raheman, H., Pansare, M. S., & Machavaram, R. (2009). Predicting the draught requirement of tillage implements in sandy clay loam soil using an artificial neural network. *Biosystems Engineering*, 104, 476 – 485.

https://doi.org/10.1016/j.biosystemseng.2009.09.004

Sadek, M. A., & Chen, Y. (2015). Feasibility of using PFC3D to simulate soil flow resulting from a simple soil engaging tool. *Transactions of the ASABE, 58*(4), 987 - 996. https://doi.org/10.13031/trans.58.10900

Sadek, M. A., Chen, Y., & Liu, J. (2011). Simulating shear behavior of a sandy soil under different soil conditions. *Journal of Terramechanics*, 48, 451 – 458. https://doi.org/10.1016/j.jterra.2011.09.006

Sadek, M. A., Chen, Y., & Zen, Z. (2021). Draft force prediction for a high-speed discimplement using discrete element modelling. *Biosystems Engineering,* 202, 133 – 141. https://doi.org/10.1016/j.biosystemseng.2020.12.009

Safa, M., & Samarasinghe, S. (2011). Determination and modeling of energy consumption in wheat production using neural networks: A case study in Canterbury province, New Zealand. *Energy, 36* (8), 5140 – 5147. https://doi.org/10.1016/j.energy.2011.06.016

Saffih-Hdadi, K., Défossez, P., Richard, G., & Chaplain, V. (2009). A method for predicting soil susceptibility to the compaction of surface layers as a function of water content and bulk density. *Soil and Tillage Research,* 105, 96 – 103. https://doi.org/10.1016/j.still.2009.05.012

Sahay, J. (2008). *Elements of Agricultural Engineering*. Standard Publishers Distributors. 224 – 225.

Saleh, B., & Ayman A. A. (2013). Artificial neural network model for evaluation of the ploughing process performance. *International Journal of Control, Automation and System*, *2*(2), 1 - 11.

Sahu, R. K., & Raheman, H. (2006). Draft prediction of agricultural implements using reference tillage tools in sandy clay loam soils. *Biosystems Engineering*, 94, 275 - 284. https://doi.org/10.1016/j.biosystemseng.2006.01.015

Sahu, R. K., & Raheman, H. (2008). A decision support system on matching and field performance prediction of tractor-implement system. *Computers and Electronics in Agriculture*, *60*(1), 76 – 86. https://doi.org/10.1016/j.compag.2007.07.001

Sainju, U. M., Schomberg, H. H., Singh, B. P., Tillman, P. G., & Lachnicht, S. L. (2007). Cover crop effect on soil carbon fractions under conservation tillage cotton. *Soil and Tillage Research,* 96, 205 – 218. https://doi.org/10.1016/j.still.2007.06.006

Saqib, M., Akhtar, J., & Qureshi, R. (2004a). Pot study on wheat growth in saline and waterlogged compacted soil I. Grain yield and yield components. *Soil and Tillage Research*, 77, 169 – 177. https://doi.org/10.1016/j.still.2003.12.004

Saqib, M., Akhtar, J., & Qureshi, R. (2004b). Pot study on wheat growth in saline and waterlogged compacted soil II. Root growth and leaf ionic relations. *Soil and Tillage Research*, 77, 179 – 187. https://doi.org/10.1016/j.still.2003.12.005

Satomi, T., Haruya N., & Takahashi, H. (2012). Investigation on characteristics of soil adhesion to metallic material surface and soil animal's cuticle. *Proceedings of the 15th International Conference on Experimental Mechanics* (1 – 9). Porto.

Schäffer, B., Schulin, R., & Boivin, P. (2008). Changes in shrinkage of restored soil caused by compaction beneath heavy agricultural machinery. *European Journal of Soil Science* 59, 771 – 783. https://doi.org/10.1111/j.1365-2389.2008.01024.x

Schäffer, B., Attinger, W., & Schulin, R. (2007). Compaction of restored soil by heavy agricultural machinery - Soil physical and mechanical aspects. *Soil and Tillage Research*, 93, 28 – 43. https://doi.org/10.1016/j.still.2006.03.007

Schäfer-Landefeld, L., Brandhuber, R., & Stockfisch, N. (2004). Effects of agricultural machinery with high axle load on soil properties of normally managed fields. *Soil and Tillage Research*, 75, 75 – 86. https://doi.org/10.1016/s0167-1987(03)00154-5

Schnurr-Putz, S., Guggenberger, G., & Kusell, K. (2006). Compaction of forest soil by logging machinery favours occurrence of prokaryotes. FEMS *Microbiology and Ecology*, 58, 503 – 516. https://doi.org/10.1111/j.1574-6941.2006.00175.x

Schwen, A., Ramirez, G. H., Clothier, B. E., Buchan, G. D., & Loiskandl, W. (2011). Hydraulic properties and the water-conducting porosity as affected by subsurface compaction using tension infiltrometers. *Soil Science Society of America Journal*, 75, 822 - 831. https://doi.org/10.2136/sssaj2010.0257

Schjønning, P., Lamandé, M., Keller, T., Pedersen, J., & Stettler, M. (2012). Rules of thumb for minimizing subsoil compaction. *Soil Use Management*. 28, 378 – 393. https://doi.org/10.1111/j.1475-2743.2012.00411.x

Schjønning, P., van den Akker, J., Keller, T., Stettler, M., Arvidsson, J., & Breuning-Madsen., H. (2015). *Soil compaction* in: Soil threats in Europe - Status, methods, drivers and effects on ecosystem services, EU Joint Research Centre, 69 - 78.

Secco, D., Reinert, D. J., Reichert, J. M., Ferreira, F. P., & Silva, V. D. (2013). Shear parameters associated with compaction states and degrees of water saturation in two Hapludox. *African Journal of Agricultural Research, 8*(10), 112 - 119.

Sekhar, C., & Meghana, P. S. (2020). A study on backpropagation in Artificial Neural Networks. *Asia-Pacific Journal of Neural Networks and Its Applications, 4*(1), 21 – 28.

Servadio, P., Marsili, A., Vignozzi, N., & Pagliai, M. (2005). Effects on some soil qualities in central Italy following the passage of four-wheel drive tractor fitted with single and dual tires. *Soil and Tillage Research*, 84, 87 – 100. https://doi.org/10.1016/j.still.2004.09.018

Shafaei, S. M., Loghavi, M., & Kamgar, S. (2018a). A comparative study between mathematical models and the ANN data mining technique in draft force prediction of disk plough implement in clay loam soil. *Agricultural Engineering International: CIGR Journal, 20*(2), 71 – 79.

Shafaei, S. M., Loghavi, M., & Kamgar, S. (2018b). Appraisal of Takagi-Sugeno-Kang type of adaptive neuro-fuzzy inference system for draft force prediction of chisel plow implement. *Computers and Electronics in Agriculture,* 142, 406 - 415. https://doi.org/10.1016/j.compag.2017.09.023

Shah, A. N., Tanveer, N., & Hafeez, A. (2015). Soil compaction effects on soil health and crop productivity: an overview. *Environment, Science and Pollution Research*, 4, 7 – 10.

Shaheb, M. R., Venkatesh, R., & Shearer, S. A. (2021). A review on the effect of soil compaction and its management for sustainable crop production. *Journal of Biosystems Engineering* 46, 417– 439. https://doi.org/10.1007/s42853-021-00117-7

Shahgoli, G., & Jannatkhah. J. (2018). Investigation of the effects of organic matter application on soil compaction. *Journal of Agricultural Science*, *28*(2), 175 - 185.

Shahgholi, G., Kanyawi, N., & Kalantari, D. (2019). Modeling the effects of narrow blade geometry on soil failure draft and vertical forces using discrete element method. *Journal of Agricultural Sciences*, *29*(1), 24 - 33.

Sharifat, K., & Kushwaha, R. L. (2000). Modeling soil movement by tillage tools. *Canadian Agricultural Engineering*, 42, 165 - 172.

Sheehy, J. E., Mitchell, P. L., & Ferrer, A. B. (2006). Decline in rice grain yields with temperature: Models and correlations can give different estimates. *Field Crop Research*. *98*(23), 151 – 156. https://doi.org/10.1016/j.fcr.2006.01.001

Shestak, C., & Busse, M. (2005). Compaction alters physical but not biological indices of soil health. *Soil Science Society of America Journal*, 69, 236 – 246. https://doi.org/10.2136/sssaj2005.0236

Shmulevich, I., Asaf, Z., & Rubinstein, D. (2007). Interaction between soil and a wide cutting blade using the discrete element method. *Soil and Tillage Research, 97*(1), 37 - 50. https://doi.org/10.1016/j.still.2007.08.009

Smith, C. W., Johnston, M. A., & Lorentz, S. (2000). Assessing the compaction susceptibility of South African forestry soils. I. The effect of soil type, water content and applied pressure on uni-axial compaction. *Soil and Tillage Research*, 41, 53 – 73. https://doi.org/10.1016/s0167-1987(96)01084-7

Srivastava, A. K., Goering, C. E., Rohrbach, R. P., & Buckmaster, D. R. (2006). *Engineering principles of agricultural machines* (2nd ed.). USA: American Society of Agricultural and Biological Engineers.

Silva, S., Barros, N., Costa, L., & Leite, F. (2008). Soil compaction and eucalyptus growth in response to forwarder traffic intensity and load. *Revista Brasileira de Ciência do Solo*, 32, 921–932. https://doi.org/10.1590/s0100-06832008000300002

Silva, V. R., Reinert, D. J., & Reichert, J. M. (2000). Soil density, chemical attributes and maize root distribution as affected by grazing and soil management. *Revista Brasileira de Ciencia do Solo*, 24, 191 – 199.

Silveira, M., Comerford, N., Reddy, K., Prenger, J., & De Busk, W. (2010). Influence of military land uses on soil carbon dynamics in forest ecosystems of Georgia, USA. *Ecological Indicators*, 10, 905 – 909. https://doi.org/10.1016/j.ecolind.2010.01.009

Simonyan, K., Yiljep, Y. D., & Mudiare, O. J. (2006). Modeling the grain cleaning process of a stationary sorghum thresher. *Agricultural Engineering International: The CIGR Ejournal.* Manuscript PM 06-012. 8.

Solgi, A., & Najafi, A. (2014). The impacts of ground-based logging equipment on forest soil. *Journal of Forestry Science*, 60, 28–34. https://doi.org/10.17221/76/2013-jfs

Solyali, D. (2020). A comparative analysis of machine learning approaches for short-/long-term electricity load forecasting in Cyprus. *Sustainability, 12*(3), 1 - 34. https://doi.org/10.3390/su12093612

Songül, G. (2021). Soil compaction due to increased machinery intensity in agricultural production: Its main causes, effects and management. *Technology in Agriculture*. https://doi.org/10.5772/intechopen.98564

Stalham, M. A., Allen, E. J., & Herry, F. X. (2005). Effects of soil compaction on potato growth and its removal by cultivation. *Research review*, R261 British Potato Council, Oxford.

Stenitzer, E., & Murer, E. (2003). Impact of soil compaction upon soil water balance and maize yield estimated by the SIMWASER model. *Soil and Tillage Research*, 73, 43 – 56. https://doi.org/10.1016/s0167-1987(03)00098-9

Spoor, G. (2006). Alleviation of soil compaction: requirements, equipment and techniques. *Soil Use Management*, 22, 113 – 122. https://doi.org/10.1111/j.1475-2743.2006.00015.x

Spoor, G., Tijink, F. G. J., & Weisskopf, P. (2003). Subsoil compaction: risk, avoidance, identification and alleviation. *Soil and Tillage Research*, 73, 175 – 182. https://doi.org/10.1016/s0167-1987(03)00109-0

Sun, Y., Meng, F., Buescher, W., & Cheng, Q. (2012). A study to identify and correct friction-induced error of penetration measurement for agricultural materials. *Measurement: Journal of the International Measurement Confederation, 45*(5), 89 - 835. https://doi.org/10.1016/j.measurement.2012.02.017

Taghavifar, H., & Mardani, A. (2014a). Effect of velocity, wheel load and multipass on soil compaction. *Journal of the Saudi Society of Agricultural Sciences*, 13, 57 – 66. https://doi.org/10.1016/j.jssas.2013.01.004

Taghavifar, H., & Mardani, A. (2014b). On the modeling of energy efficiency indices of agricultural tractor driving wheels applying adaptive neuro-fuzzy inference system. In *Journal of Terramechanics*, 56, 37 – 47. https://doi.org/10.1016/j.jterra.2014.08.002

Tajik, S, Ayoubi, S., & Nourbakhsh, F. (2012). Prediction of soil enzymes activity by digital terrain analysis: comparing artificial neural network and multiple linear regression models. *Environmental Engineering Science, 29*(8), 798 - 806. https://doi.org/10.1089/ees.2011.0313

Tamás, K., Jóri, I. J., & Mouazen. A. M. (2013). Modelling soil–sweep interaction with discrete element method. *Soil and Tillage Research, 134*(11), 223 – 231. https://doi.org/10.1016/j.still.2013.09.001

Tanaka, H., Oida, A. Daikoku, M. Inooku, K. Sumikawa, O. Nagasaki Y., & Miyazaki. M. (2007). DEM simulation of soil loosening process caused by a vibrating subsoiler. *Agricultural Engineering International: the CIGR Ejournal 9*, Manuscript PM 05 010s.

Tanveera, A., Tasawoor, A., Parvaiz, A., & Mehrajuddin, N. (2016). Relation of soil bulk density with texture. total organic matter content and porosity in the soils of Kandi Area of Kashmir valley, India. *International Research Journal of Earth Sciences,* 4, 1 – 6.

Tenu, I., Carlescu, P., Cojocariu, P., & Rosca, R. (2012). Impact of agricultural traffic and tillage technologies on the properties of soil. *Resource Management for Sustainable Agriculture*, 263 - 296. https://doi.org/10.5772/47746

Thuku, S. M. (2018*). Effect of chisel ploughing on physical and mechanical soil properties: Case of a clay soil* [Master's thesis, University of Nairobi].

Tong, J., & Moayad, B. Z. (2006). Effects of rake angle of chisel plough on soil cutting factors and power requirements: A computer simulation. *Soil and Tillage Research, 88*(12), 55 – 64. https://doi.org/10.1016/j.still.2005.04.007

Torella, J. L., Ceriani, J. C., Introcaso, R. M., Guecaimburu, J., & Wasinger, E. (2001). Tillage, liming and sunflowers. *Agrochimica,* 45, 14 – 23.

Tracy, S. R., Black, C. R., Roberts, J. A., & Mooney, S. J. (2011). Soil compaction: a review of past and present techniques for investigating effects on root growth. *Journal of Food Science and Agriculture*, 91, 1528 – 1537. https://doi.org/10.1002/jsfa.4424

Tullberg, J., Yule, D. F., & McGarry, D. (2003). 'On track' to sustainable cropping systems in Australia. *Proceedings of the International Soil Tillage Research Organization 16th Triennial Conference* (1271 – 1285). Brisbane.

Tullberg, J. N., (2000). Wheel traffic effects on tillage draft. *Journal of Agricultural Engineering Research,* 75, 375 – 382.

Ucgul, M. (2014). *Simulation of sweep tillage using discrete element modeling* [Doctoral thesis, Barbara Hardy Institute, University of South Australia].

United Nations. (2015). Transforming our world: the 2030 agenda for sustainable development. Resolution adopted by the General Assembly, 3 - 35.

United States Department of Defense. (2009). Modeling and Simulation: verification, validation and accreditation. DoD. Instruction 5000.61.

Urbán, M., Kotrocz, K., & Kerényi, G. (2002). Investigation of the soil - tool interaction by SPH (Smooth Particle Hydrodynamics) based simulation. *American Transactions on Engineering and Applied Sciences*, 1 – 6.

Van Camp, L., Bujarrabal, B., Gentile, A. R., & Selvaradjou, S. K. (2004). Soil thematic strategy, in: Reports of the Technical Working Groups. Luxembourg. 872.

Van den Akker, J. J. H. (2008). Chapter 7: Soil compaction, in: Environmental assessment of soil for monitoring: Volume I, Indicators and Criteria, EUR 23490 EN/1. Luxembourg, 339.

Van den Akker, J. J. H., & Schjønning, P., (2004). Subsoil compaction and ways to prevent it. In: Schjønning, P., Elmholt, S., Christensen, B.T. (Eds.) *Managing Soil Quality Challenges in Modern Agriculture*. https://doi.org/10.1079/9780851996714.0163

van der Linde, J. (2007). *Discrete element modelling of a vibratory subsoiler Matieland, South Africa* [Master's thesis, University of Stellenbosch].

Varga, F., Tkáč, Z., Kosiba, J., & Uhrinová, D. (2014). Measurement of soil resistance by using a horizontal penetrometer working with the two–argument comparative method. *Agronomy Research,* 12, 187 – 196.

Vaz, C. M. P., Manieri, J. M., De Maria, I. C., & Tuller, M. (2011). Modeling and correction of soil penetration resistance for varying soil water content. *Geoderma*, *166*(1), 92 – 101. https://doi.org/10.1016/j.geoderma.2011.07.016

Veiga, M., Horn, R., Reinert, D. J., & Reichert, J. M. (2007). Soil compressibility and penetrability of an Oxisol from southern Brazil, as affected by long-term tillage systems. *Soil and Tillage Research, 92*(2), 104 - 113. https://doi.org/10.1016/j.still.2006.01.008

Vermeulen, G. D., & Mosquera, J. (2009). Soil, crop and emission responses to seasonal controlled traffic in organic vegetable farming on loam soil. *Soil and Tillage Research*, 102, 126 – 134. https://doi.org/10.1016/j.still.2008.08.008

Wamalwa, P. W. (2022). *Optimization of design parameters and performance of a portable common beans (Phaseolus vulgaris L) thresher* [Doctoral dissertation, Jomo Kenya University of Agriculture and Technology].

Wang, X., He, J., Bai, M., Liu, L., Gao, S., Chen, K., & Zhuang, H. (2022). The impact of traffic-induced compaction on soil bulk density, soil stress distribution and key growth indicators of maize in North China Plain. *Agriculture*, 12, 1220. https://doi.org/10.3390/agriculture12081220

Wang, Q., & Leng, F. (2016). A soft computing approach to prediction of wheel induced rut depth: Appraisal of Artificial Neural Network. *Journal of Advances in Vehicle Engineering, 2*(2), 116 - 123.

Webb, R. (2002). Recovery of severely compacted soils in the Mojave Desert, California, USA. *Arid Land Resource Management,* 16, 291 – 305. https://doi.org/10.1080/153249802760284829

Whalley, W. R., Watts, C. W., Gregory, A. S., Mooney, S. J., Clark, L. J., & Whitmore, A. P. (2008). The effect of soil strength on the yield of wheat. *Plant Soil,* 306, 237 – 247.

Whitmore, A. P., Whalley, W. R., Bird, N. R. A., Watts, C. W., & Gregory, A. S. (2010). Estimating soil strength in the rooting zone of wheat. *Plant Soil,* 339, 363 – 375. https://doi.org/10.1007/s11104-010-0588-7

Williamson, J. R., & Neilsen, W. A. (2000). The influence of forest site on rate and extent of soil compaction and profile disturbance of skid trails during ground-based harvesting. *Canadian Journal of Forestry Research,* 30, 1196 – 1205. https://doi.org/10.1139/x00-041

Xue, L., Li, L., Zeng, J., Huang, B., Zeng, Y., Liu, M., & Li, J. (2022). The Measurement of Shear Characteristics of Paddy Soil in Poyang Lake Area. *Sustainability*, *14* (11960), 1 - 10. doi.org/10.3390/su141911960

Yalcin H., Cakir, E., & Aykas, E. (2005). Tillage parameters and economic analysis on direct seeding, minimum and conventional tillage in wheat. *Journal of Agronomy*, *4*(4), 329 - 332. https://doi.org/10.3923/ja.2005.329.332

Yang, P., Dong, W., Heinen, M., Qin, W., & Oenema, O. (2022). Soil compaction prevention, amelioration and alleviation measures are effective in mechanized and smallholder agriculture: A Meta-Analysis. *Land, 11*(645), 1 – 18. https://doi.org/10.3390/land11050645

Yavuzcan, H. G., Matthies, D., & Auernhammer, H. (2005). Vulnerability of Bavarian silty loam soil to compaction under heavy wheel traffic: Impacts of tillage method and soil water content. *Soil and Tillage Research*, 84, 200 – 215. https://doi.org/10.1016/j.still.2004.11.003

Yusuf, A. O. (2015). *Modeling of energy requirement demand for tillage operations in maize production* [Doctoral thesis. Ahmadu Bello University, Zaria].

Zadeh, S. R. (2006). *Modeling of energy requirements by a narrow tillage tool* [Doctoral dissertation. University of Saskatchewan, Saskatoon].

Zaki, D. H., Khorasani, M. E., Nategh, N. A., Sheikhdavoodi, M., & Andekaiezadeh. K. (2022). Specific draft modeling for combined and simple tillage implements. *Agricultural Engineering International: CIGR Journal*, *24*(4), 41- 56.

Zenner, E., & Berger, A. (2008) Influence of skidder traffic and canopy removal intensities on the ground flora in a clearcut-with-reserves northern hardwood stand in Minnesota, USA. *Forest Ecology Management*, 256, 1785 – 1794. https://doi.org/10.1016/j.foreco.2008.05.030

Zenner, E., Kabrick, J., Jensen, R., Peck, J., & Grabner, J. (2006) Responses of ground flora to a gradient of harvest intensity in the Missouri Ozarks. *Forestry*, *222* (13), 326 – 334. https://doi.org/10.1016/j.foreco.2005.10.027

Zhang, S., Grip, H., & Lövdahl, L. (2006). Effect of soil compaction on hydraulic properties of two loess soils in China. *Soil and Tillage Research*, 90, 117 – 125. https://doi.org/10.1016/j.still.2005.08.012

Zink, A., Fleige, H., & Horn, R., (2011). Verification of harmful subsoil compaction in loess soils. *Soil and Tillage Research*, 114, 127 – 134.

APPENDICES

Appendix A: Results of experiments to determine soil properties

A1 Sample raw data for bulk density, porosity and moisture content determination

No wheel pass									
Depth (cm)	**0 – 20**			**20 – 30**			**30 – 40**		
Sample	1	**2**	**3**	**1**	**2**	**3**	**1**	**2**	**3**
Wt. of ring (g)	104.23	102.11	106.2	101.35	99.89	106.20	100.23	101.23	106.20
Wt. of wet soil + ring (g)	290.39	281.13	292.62	302.83	282.13	298.42	293.09	302.43	300.72
Wt. of dry soil+ ring (g)	236.97	229.01	233.09	236.85	232.55	241.80	236.68	241.70	243.80
Wt. of dry soil (g)	132.74	126.9	126.89	135.50	132.66	135.60	136.45	140.47	137.60
Wt. of moisture (g)	53.42	52.12	59.53	65.98	49.58	56.62	56.41	60.73	56.92
MC (%)	40.24	41.07	46.91	48.69	37.37	41.76	41.34	43.23	41.37
Volume of can (m^3)	101	99.19	99	98.19	99.19	100.19	98.19	99.19	100.19
Bulk Density (g/cm^3)	1.31	1.28	1.28	1.38	1.34	1.35	1.39	1.42	1.37
Porosity (%)	50.41	51.72	51.63	47.93	49.53	48.93	47.56	46.56	48.17

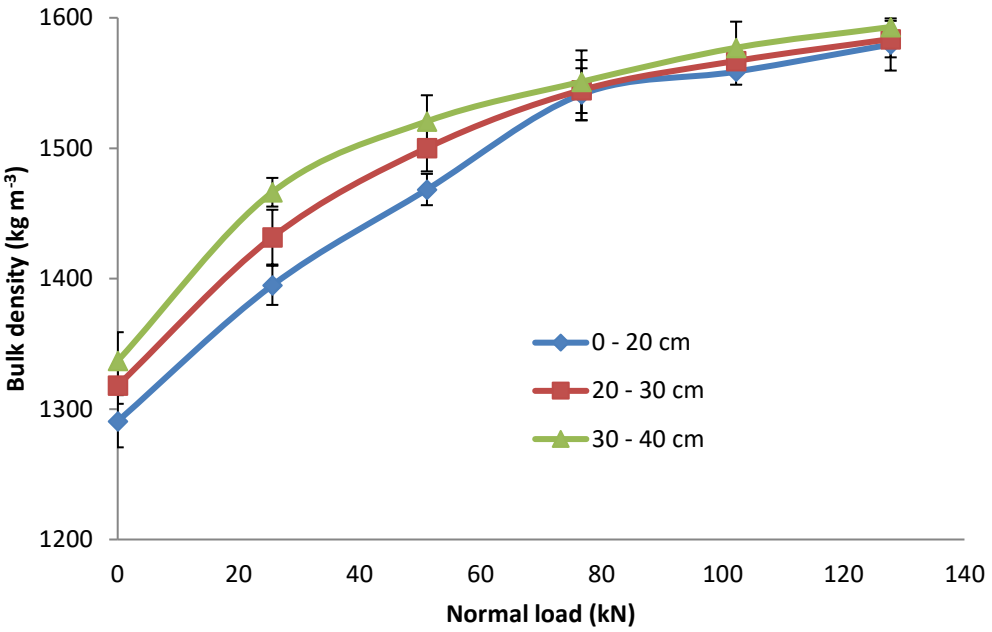

Figure A1.1: Effect of vertical load and depth on bulk density

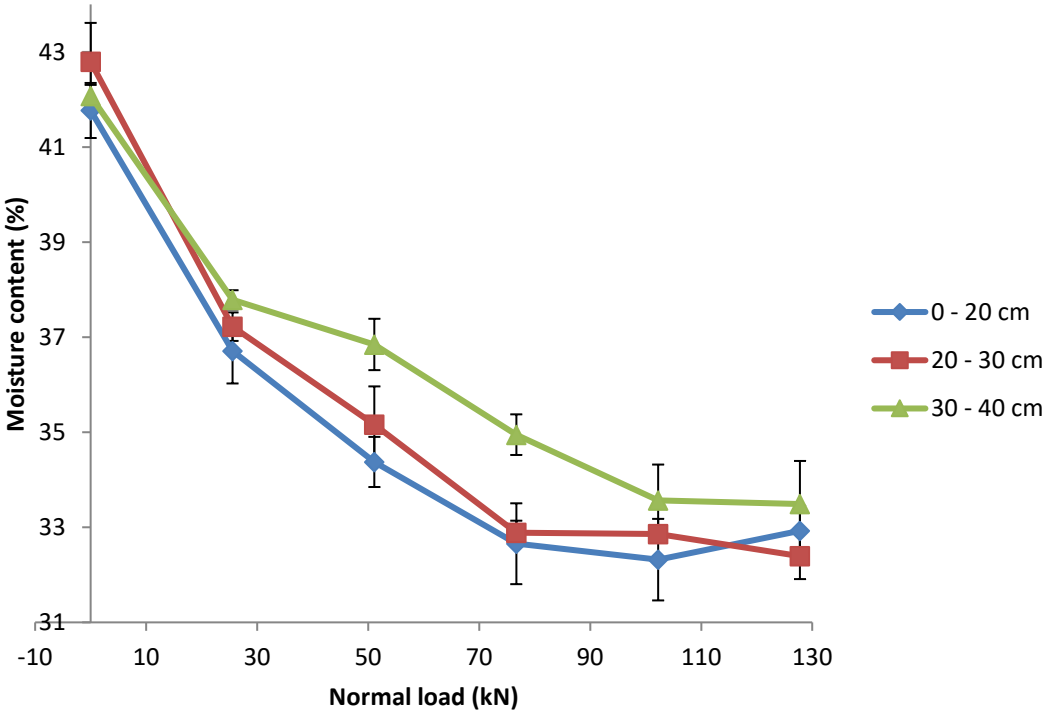

Figure A1.2: Soil moisture content variation with normal load and soil depth

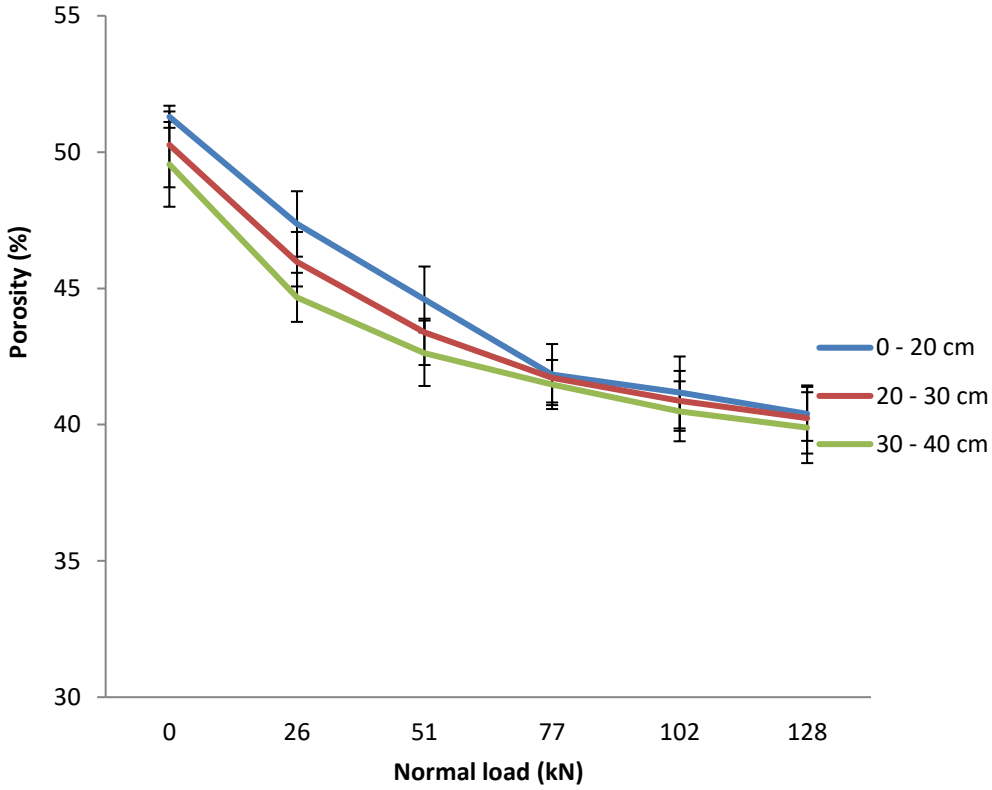

Figure A1.3: Variation of porosity with wheel passes and depth

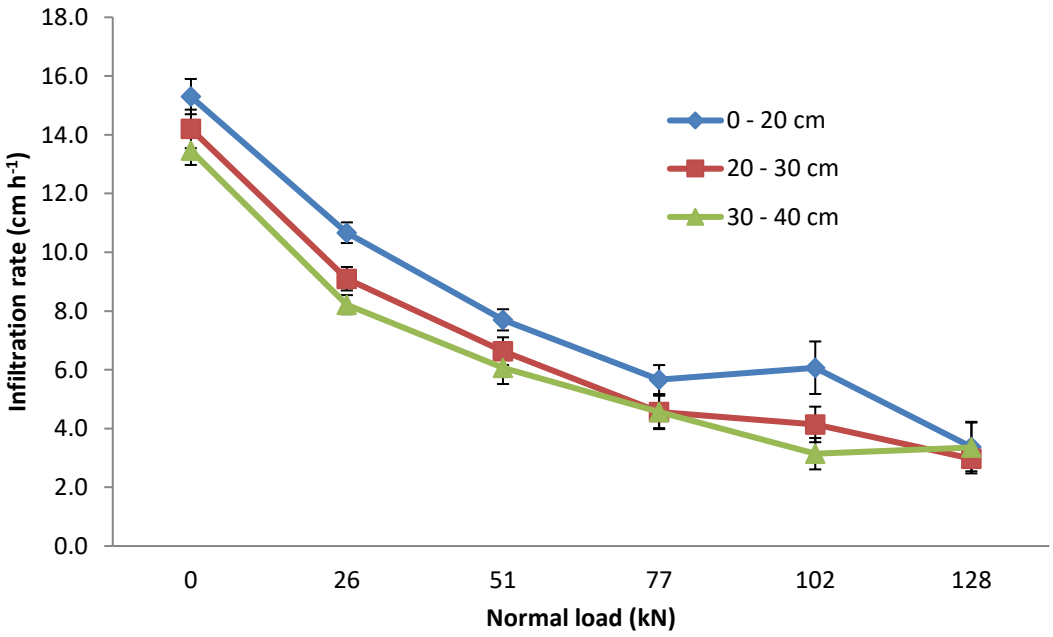

Figure A1.4: Variation of infiltration rate with normal load and soil depth

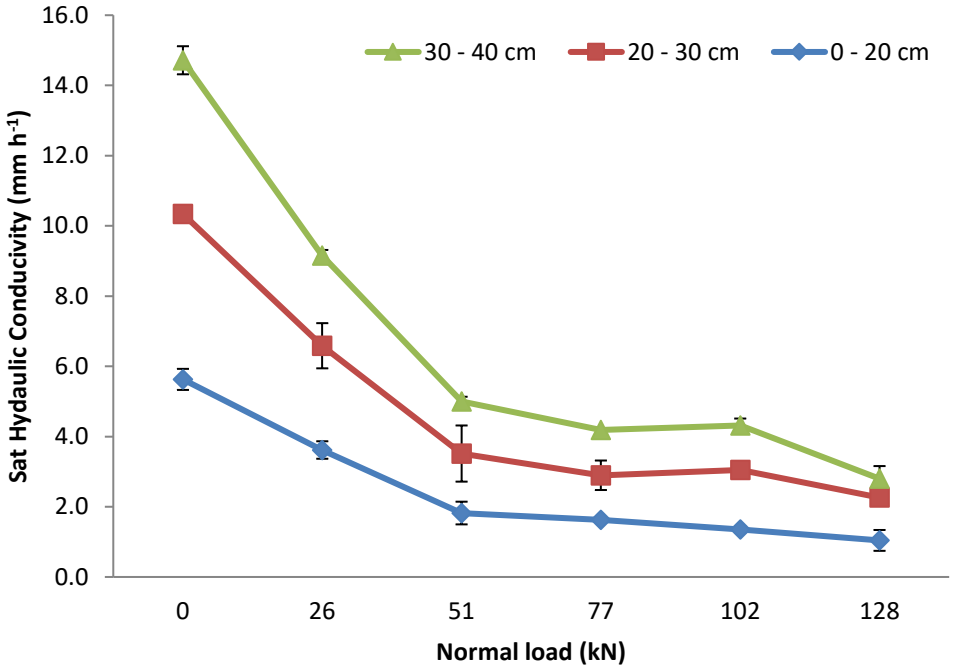

Figure A1.5: Effect of vertical load and depth on saturated hydraulic conductivity

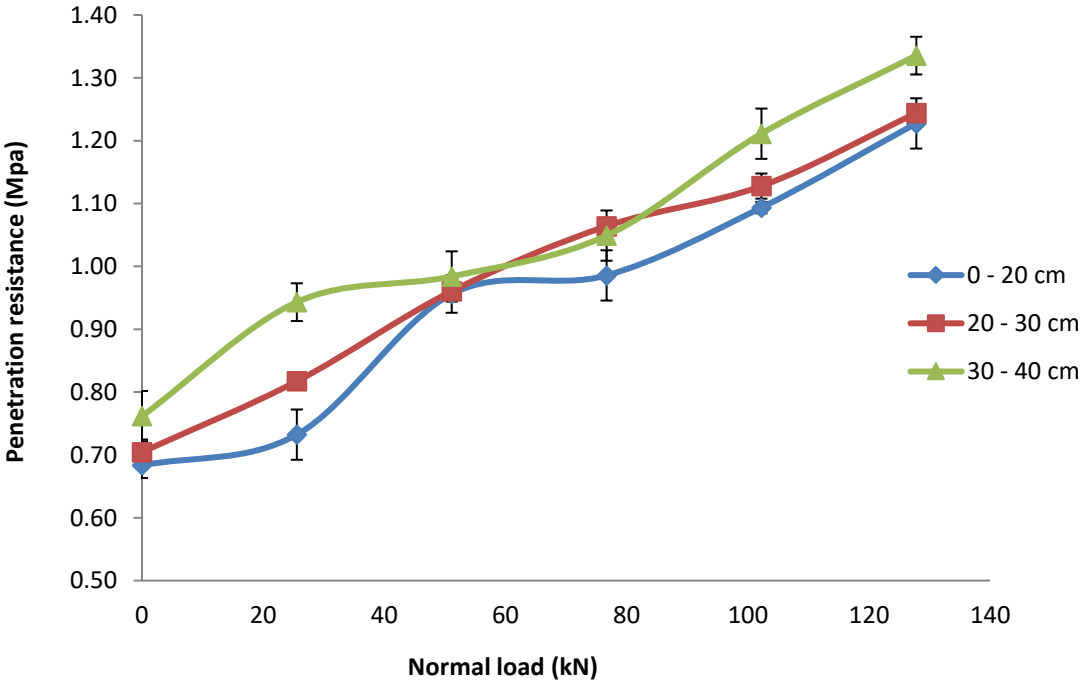

Figure A1.6: Effect of vertical load and depth on penetration resistance

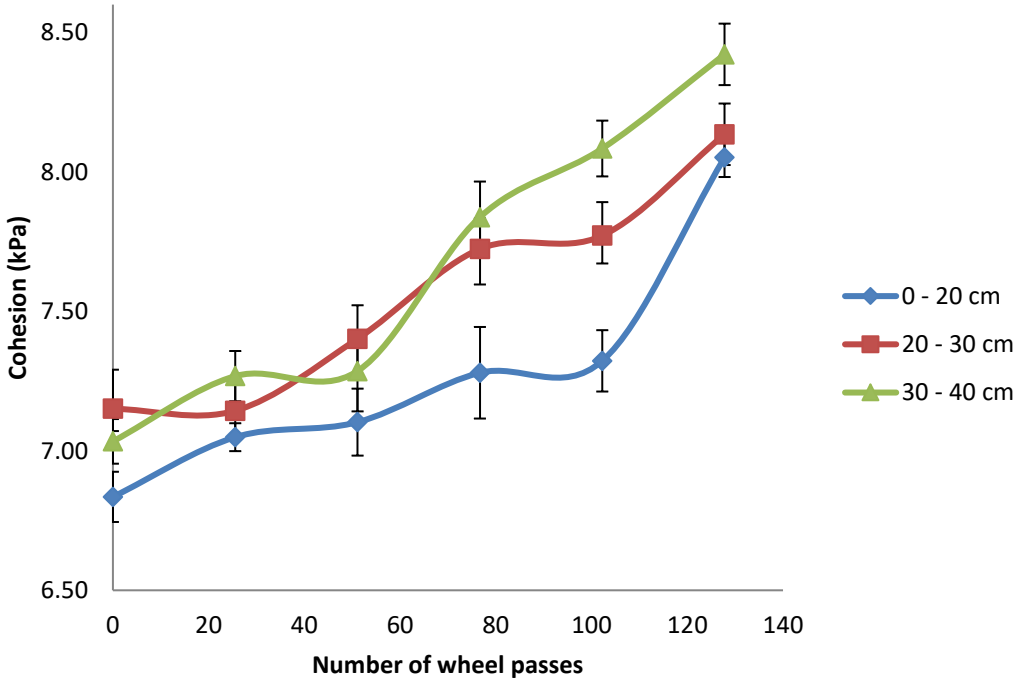

Figure A1.7: Effect of vertical load and depth on cohesion

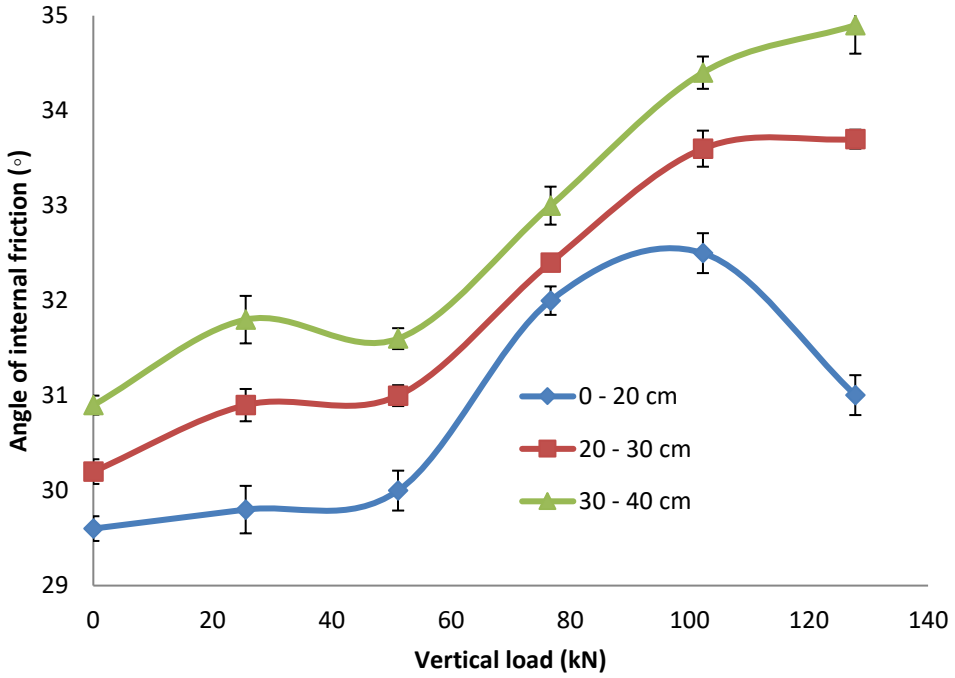

Figure A1.8: Effect of vertical load and depth on angle of internal friction

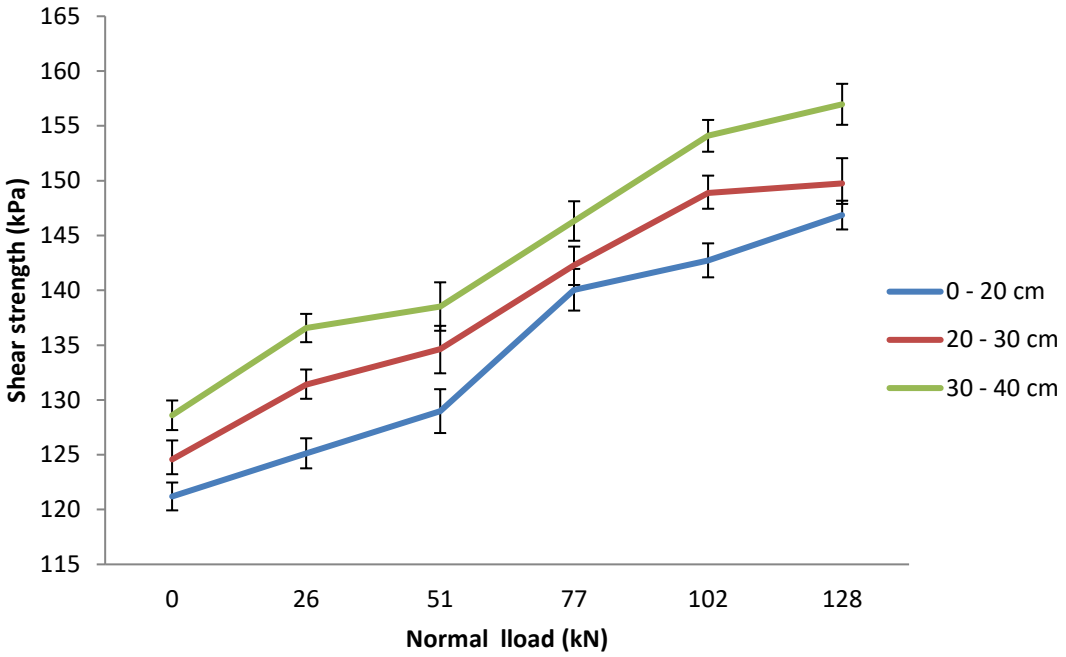

Figure A1.9: Effect of vertical load and depth on shear strength

Table A3.1: Summary of experimental results for modeled variables

MEASURED DATA								
Exp. No.	**Depth (cm)**	**Bulk density (kg m^{-3})**	**Penetration Resistance (kPa)**	**Moisture content (%)**	**Cohesion (kPa)**	**tan φ**	**Shear strength kPa)**	**Measured Draft (kN)**
1	0 - 20	1256.8590	642.3356	41.7684	6.8350	0.5681	121.1971	1.40
2	20 - 30	1318.0277	704.4444	42.7926	7.1510	0.5820	124.5766	2.83
3	30 - 40	1336.9555	761.6498	42.0729	7.0340	0.5985	128.6008	4.99
4	0 - 20	1394.8678	732.2299	47.3635	7.0490	0.5727	125.1311	2.35
5	20 - 30	1431.8107	817.2208	45.9694	7.1440	0.5985	131.3948	5.19
6	30 - 40	1466.2407	943.0728	44.6702	7.2680	0.6200	136.5591	6.00
7	0 - 20	1468.3291	1468.3291	44.5914	7.1030	0.5774	128.9802	3.38
8	20 - 30	1529.9689	1529.9689	42.2653	7.4020	0.6009	134.6402	5.73
9	30 - 40	1538.5439	1538.5439	41.9417	7.2860	0.6152	138.5208	7.22
10	0 - 20	1526.7414	985.5683	42.3871	7.2800	0.6249	140.0508	4.60
11	20 - 30	1540.1385	1064.0215	41.8816	7.7240	0.6346	142.2884	6.08
12	30 - 40	1550.9950	1048.9847	41.4719	7.8380	0.6494	146.3233	8.53
13	0 - 20	1558.7122	1093.4415	41.1807	7.3227	0.6371	142.7357	5.12
14	20 - 30	1579.1722	1127.7648	40.4086	7.7718	0.6644	148.8925	7.96
15	30 - 40	1577.0423	1211.1213	40.4890	8.0840	0.6847	154.0933	9.83
16	0 - 20	1556.0835	1227.4657	41.2799	8.0518	0.6475	146.8631	6.43
17	20 - 30	1583.6779	1243.8101	40.2386	8.1350	0.6344	149.7536	8.09

Exp. No.	Depth (cm)	Bulk density (kg m^{-3})	Penetration Resistance (kPa)	Moisture content (%)	Cohesion (kPa)	tan φ	Shear strength kPa)	Measured Draft (kN)
18	30 – 40	1592.9394	1335.3388	39.8891	8.4216	0.6616	156.9680	10.68
19	0 – 20	1256.7590	642.2356	41.6684	6.7350	0.4681	121.0971	1.30
20	20 – 30	1317.9277	704.3444	42.6926	7.0510	0.4820	124.4766	2.73
21	30 – 40	1336.8555	761.5498	41.9729	6.9340	0.4985	128.5008	4.89
22	0 – 20	1394.7678	732.1299	47.2635	6.9490	0.4727	125.0311	2.25
23	20 – 30	1431.7107	817.1208	45.8694	7.0440	0.4985	131.2948	5.09
24	30 – 40	1466.1407	942.9728	44.5702	7.1680	0.5200	136.4591	5.90
25	0 – 20	1468.2291	1468.2291	44.4914	7.0030	0.4774	128.8802	3.28
26	20 – 30	1529.8689	1529.8689	42.1653	7.3020	0.5009	134.5402	5.63
27	30 – 40	1538.4439	1538.4439	41.8417	7.1860	0.5152	138.4208	7.12
28	0 – 20	1526.6414	985.4683	42.2871	7.1800	0.5249	139.9508	4.50
29	20 – 30	1540.0385	1063.9215	41.7816	7.6240	0.5346	142.1884	5.98
30	30 – 40	1550.8950	1048.8847	41.3719	7.7380	0.5494	146.2233	8.43
31	0 – 20	1558.6122	1093.3415	41.0807	7.2227	0.5371	142.6357	5.02
32	20 – 30	1579.0722	1127.6648	40.3086	7.6718	0.5644	148.7925	7.86
33	30 – 40	1576.9423	1211.0213	40.3890	7.9840	0.5847	153.9933	9.73
34	0 – 20	1555.9835	1227.3657	41.1799	7.9518	0.5475	146.7631	6.33
35	20 – 30	1583.5779	1243.7101	40.1386	8.0350	0.5344	149.6536	7.99
36	30 – 40	1592.8394	1335.2388	39.7891	8.3216	0.5616	156.8680	10.58
37	0 – 20	1256.9590	642.4356	41.8684	6.9350	0.6681	121.2971	1.50

Exp. No.	Depth (cm)	**Bulk density (kg m^{-3})**	**Penetration Resistance (kPa)**	**Moisture content (%)**	**Cohesion (kPa)**	**tan φ**	**Shear strength kPa)**	**Measured Draft (kN)**
38	20 – 30	1318.1277	704.5444	42.8926	7.2510	0.6820	124.6766	2.93
39	30 – 40	1337.0555	761.7498	42.1729	7.1340	0.6985	128.7008	5.09
40	0 – 20	1394.9678	732.3299	47.4635	7.1490	0.6727	125.2311	2.45
41	20 – 30	1431.9107	817.3208	46.0694	7.2440	0.6985	131.4948	5.29
42	30 – 40	1466.3407	943.1728	44.7702	7.3680	0.7200	136.6591	6.10
43	0 – 20	1468.4291	1468.4291	44.6914	7.2030	0.6774	129.0802	3.48
44	20 – 30	1530.0689	1530.0689	42.3653	7.5020	0.7009	134.7402	5.83
45	30 – 40	1538.6439	1538.6439	42.0417	7.3860	0.7152	138.6208	7.32
46	0 – 20	1526.8414	985.6683	42.4871	7.3800	0.7249	140.1508	4.70
47	20 – 30	1540.2385	1064.1215	41.9816	7.8240	0.7346	142.3884	6.18
48	30 – 40	1551.0950	1049.0847	41.5719	7.9380	0.7494	146.4233	8.63
49	0 – 20	1558.8122	1093.5415	41.2807	7.4227	0.7371	142.8357	5.22
50	20 – 30	1579.2722	1127.8648	40.5086	7.8718	0.7644	148.9925	8.06
54	30 – 40	1577.1423	1211.2213	40.5890	8.1840	0.7847	154.1933	9.93
52	0 – 20	1556.1835	1227.5657	41.3799	8.1518	0.7475	146.9631	6.53
53	20 – 30	1583.7779	1243.9101	40.3386	8.2350	0.7344	149.8536	8.19
54	30 – 40	1593.0394	1335.4388	39.9891	8.5216	0.7616	157.0680	10.78

Table A3.2 Measured versus predicted draft by the models

Exp. No	Measured draft (kN)	Predicted draft (kN)			
		MLR	Empirical	ANN	ANFIS
1	1.40	1.19	1.41	1.39	1.14
2	2.83	3.19	2.43	2.83	3.42
3	4.99	4.88	4.03	4.90	6.97
4	2.35	2.47	2.17	2.35	1.19
5	5.19	4.63	3.98	5.19	3.61
6	6.00	6.69	7.43	6.00	7.96
7	3.38	3.20	3.53	3.38	1.32
8	5.73	5.37	4.92	5.81	3.54
9	7.22	7.02	7.11	7.22	7.05
10	4.60	4.80	2.98	4.60	1.35
11	6.08	6.69	5.43	6.13	4.31
12	8.53	8.49	7.25	8.53	8.60
13	5.12	5.27	3.68	5.16	1.42
14	7.96	7.63	5.79	7.96	4.42
15	9.83	9.79	9.41	9.83	10.25
16	6.43	6.45	1.41	1.39	1.87
17	8.09	8.11	2.43	2.83	5.11
18	10.68	10.52	4.03	4.90	11.66
19	1.30	1.10	1.39	1.30	1.11
20	2.73	3.10	2.42	2.73	3.35
21	4.89	4.79	4.02	4.78	6.82
22	2.25	2.42	2.57	2.21	1.16
23	5.09	4.54	3.98	5.01	3.53
24	5.90	6.60	7.42	5.90	7.79
25	3.28	3.11	3.53	3.28	1.29
26	5.63	5.28	4.91	5.63	3.46

Exp. No	Measured draft (kN)	Predicted draft (kN)			
		MLR	Empirical	ANN	ANFIS
27	7.12	6.93	7.09	7.12	7.12
28	4.50	4.71	3.01	4.35	4.50
29	5.98	6.60	5.42	5.98	6.01
30	8.43	8.40	7.23	8.28	8.43
31	5.02	5.18	3.67	5.02	5.03
32	7.86	7.54	5.78	7.84	7.86
33	9.73	9.70	9.39	9.73	9.75
34	6.33	6.36	4.40	6.33	6.33
35	7.99	8.01	6.92	7.99	7.99
36	10.58	10.43	11.21	10.58	10.48
37	1.50	1.28	1.39	1.46	1.50
38	2.93	3.28	2.43	2.93	2.93
39	5.09	4.97	4.04	5.09	5.09
40	2.45	2.60	2.58	2.45	2.45
41	5.29	4.72	3.99	5.29	5.31
42	6.10	6.78	7.44	6.10	6.10
43	3.48	3.30	3.54	3.36	3.48
44	5.83	5.46	4.93	5.83	5.83
45	7.32	7.11	7.12	7.32	7.32
46	4.70	4.90	3.02	4.70	4.70
47	6.18	6.78	5.44	6.18	6.23
48	8.63	8.58	7.26	8.63	8.62
49	5.22	5.36	3.69	5.22	5.24
50	8.06	7.72	5.80	8.06	8.09
51	9.93	9.88	9.44	9.93	9.73
52	6.53	6.54	4.42	6.53	6.55

Exp. No	Measured draft (kN)	Predicted draft (kN)			
		MLR	Empirical	ANN	ANFIS
53	8.19	8.20	6.96	8.19	8.20
54	10.78	10.62	11.27	10.77	10.81

Table A3.3: Table of π- terms

Exp. No.	π_1	π_2	π_3
1	0.00002309	44.264	0.0013
2	0.00000712	47.426	0.0013
3	0.00000632	49.701	0.0013
4	0.00003494	51.556	0.0011
5	0.00001203	54.406	0.0012
6	0.00000693	59.578	0.0012
7	0.00004768	92.465	0.0011
8	0.00001243	87.641	0.0011
9	0.00000794	86.970	0.0011
10	0.00006253	56.739	0.0012
11	0.00001310	59.998	0.0013
12	0.00000931	58.162	0.0013
13	0.00006807	59.903	0.0012
14	0.00001673	59.839	0.0013
15	0.00001055	64.477	0.0015
16	0.00008571	67.521	0.0014
17	0.00001695	65.532	0.0013
18	0.00001135	69.338	0.0015
19	0.00002145	44.154	0.0010
20	0.00000686	47.312	0.0010
21	0.00000619	49.580	0.0011
22	0.00003346	51.444	0.0009
23	0.00001180	54.285	0.0010
24	0.00000681	59.442	0.0010
25	0.00004627	92.257	0.0009
26	0.00001222	87.434	0.0009
27	0.00000783	86.763	0.0009
28	0.00006117	56.603	0.0010

Exp No.	π_1	π_2	π_3
29	0.00001288	59.853	0.0011
30	0.00000920	58.020	0.0011
31	0.00006674	59.756	0.0010
32	0.00001652	59.690	0.0011
33	0.00001044	64.317	0.0012
34	0.00008438	67.356	0.0011
35	0.00001674	65.368	0.0011
36	0.00001124	69.163	0.0012
37	0.00002474	44.373	0.0015
38	0.00000737	47.540	0.0015
39	0.00000644	49.822	0.0015
40	0.00003643	51.669	0.0013
41	0.00001227	54.527	0.0014
42	0.00000704	59.713	0.0014
43	0.00004908	92.672	0.0013
44	0.00001265	87.849	0.0013
45	0.00000805	87.178	0.0013
46	0.00006388	56.875	0.0014
47	0.00001331	60.143	0.0015
48	0.00000942	58.304	0.0016
49	0.00006939	60.050	0.0014
50	0.00001694	59.989	0.0015
51	0.00001065	64.638	0.0017
52	0.00008704	67.686	0.0016
53	0.00001716	65.696	0.0016
54	0.00001145	69.513	0.0017

Appendix B: Plates

Plate 4.1 Taking soil samples

Plate 4.2: In situ determination of penetration resistance

Plate 4.3: Laboratory measurement

Plate 4.4: The experimental plots at Egerton University Agroforestry Research Field

Plate 4.5: Connecting the dynamometer

Plate 4.6: Subsoiling draft determination

Plate 4.8: Subsoiling

Plate 4.9: Taking measurements on trafficked soil

Effect of soil compaction on physico-mechanical properties of silt loam soils of Njoro, Kenya

S. O. Abich[1*], A. N. Gitau[2], D. M. Nyaanga[1]

(1. Department of Agricultural Engineering, Egerton University, 536 20115, Egerton;
2. Department of Biosystems and Environmental Engineering, University of Nairobi, 30197, GPO Nairobi)

Abstract: In order to cope with the demand for more food for the continuously growing world population, it has become necessary to intensify farming leading to increased mechanization. The repeated movement of agricultural machines across the field has led to increased incidences of soil compaction. Although more studies undertaken on the effect of wheel traffic on soil compaction have used bulk density and penetration resistance as indicators, not much has been done on the effect of wheel traffic on mechanical properties of soil. The objective of this study was to establish the effects of soil compaction on selected soil physico-mechanical properties. A tractor of 4070 kg with an engine of 74.6 kW was used and the effect of repeated wheel passes on bulk density, penetration resistance, soil cohesion, angle of internal friction and soil strength studied. A factorial experiment in a completely randomized block design was used. Tests were conducted on 18 plots to investigate the effect of five tractor wheel pass treatments (1, 2, 3, 4 and 5) and a no wheel pass treatment on the soil properties at three depths (0 - 20, 20 - 30 and 30 - 40 cm) with three replications per plot. The results showed that increasing the intensity of traffic wheel passes and depth resulted in significant increase in bulk density (1291 to 1593 kg m^{-3}), penetration resistance (from 640 to 1340 kPa), soil strength (from 121.20 to 156.97 kPa), angle of internal friction (from 29 ° to 35 °) and soil cohesion (from 6.84 to 8.42 kPa) at 5% level of confidence. It was concluded that although wheel passes subsequent to the first had a smaller effect on the studied properties, it is cautioned that additional passes may lead to increased tillage draft requirements.

Keywords: bulk density. cohesion, compaction, strength, tractor, wheel traffic

Citation: Abich, S. O., A. N. Gitau, and D. M. Nyaanga. 2022. Effect of soil compaction on physico-mechanical properties of silt loam soils of Njoro, Kenya. Agricultural Engineering International: CIGR Journal, 24(4): 20-29.

1 Introduction

Farming has been intensified in recent days to cope with the demand for more food for the growing world population. This has resulted in increased mechanized farm operations. The increase of soil degradation by compaction has resulted from the intensive use of these machinery (Orzech et al., 2021). Soil compaction is an invisible form of soil degradation that is not easily detected on the soil surface (Ramazan et al., 2012).

Compaction of the soil occurs when an external stress applied on the soil surface exceeds the mechanical stability of the soil (Gürsoy, 2021). The applied stress alters the soil structure by pushing particles closer together. This reduces the volume of

Received date: 2022-02-12 **Accepted date:** 2022-07-18
***Corresponding author: S. O. Abich,** PhD candidate, Department of Agricultural Engineering, Egerton University, Egerton. Tel: +254 716 809 201.
Email: otienoabich@gmail.com.

MODELING SUBSOILING DRAFT REQUIREMENTS USING DIMENSIONAL ANALYSIS

S. O. Abich[1], A.N. Gitau.[2], D.M. Nyaanga [1]

1. Department of Agricultural Engineering, Egerton University, P.O Box 536 20115 Egerton

2. Department of Biosystems and Environmental Engineering, University of Nairobi, P.O. Box 30197 GPO Nairobi

DOI:https://doi.org/10.37017/jeae-volume8-no2.2022-4

Publication Date:11 May 2022

ABSTRACT:

Increased conventional tillage of farming operations has increased soil compaction. The objective of this study was to model the effects of soil compaction on draft force of sub soiling silt loam soils using dimensional analysis. A factorial experiment in a Completely Randomized Block design was used in the study. Experiments were conducted on 18 plots to investigate the effect of five-wheel pass (1, 2, 3, 4, 5) and control treatments on soil mechanico-physical properties at 0 - 20, 20 - 20 and 30 - 40 cm depths with three replications. The data obtained from the experiments were subjected to analysis of variance and the student t-test. Dimensional analysis was investigated for its draft prediction accuracy. It was concluded that the prediction ability of the model was satisfactory since its R^2 value and RMSE were 0.8722 and 2.256 kN repectively.

Keywords: *Compaction, Dimensions, Draft Requirement, Pi term.*

1.0. INTRODUCTION

Agricultural traffic causes the majority of soil compaction because of the increased mechanization of tillage operations to meet the demand for food (Songül, 2021). Wheel traffic increases soil strength, resulting in higher tillage draft requirement (Keller et al., 2004). Soil compaction is a sub-surface phenomenon and so is difficult to locate (Garcia-Tomillo, 2018). The higher energy consumption in

REPUBLIC OF KENYA

NATIONAL COMMISSION FOR SCIENCE,TECHNOLOGY & INNOVATION

Ref No: **932971**

Date of Issue: **21/August/2020**

RESEARCH LICENSE

This is to Certify that Mr.. SAMUEL Otieno ABICH of Egerton University, has been licensed to conduct research in Nakuru on the topic: Moddeling wheel traffic effects on tillage draught- case of subsoiling for the period ending : 21/August/2021.

License No: **NACOSTI/P/20/6323**

932971

Applicant Identification Number

Director General
NATIONAL COMMISSION FOR SCIENCE,TECHNOLOGY & INNOVATION

Verification QR Code

NOTE: This is a computer generated License. To verify the authenticity of this document, Scan the QR Code using QR scanner application.